PB80-177413

Pilot Scale Combustion Evaluation of Waste and Alternate Fuels: Phase III Final Report

Acurex Corp.
Mountain View, CA

Prepared for

Industrial Environmental Research
Lab.-Cincinnati, OH

Mar 80

U.S. Department of Commerce
National Technical Information Service
NTIS

PB80-177413

United States
Environmental Protection
Agency

Industrial Environmental Research
Laboratory
Research Triangle Park NC 27711

EPA-600/7-80-043
March 1980

EPA

Pilot Scale Combustion Evaluation of Waste and Alternate Fuels:
Phase III Final Report

Interagency Energy/Environment R&D Program Report

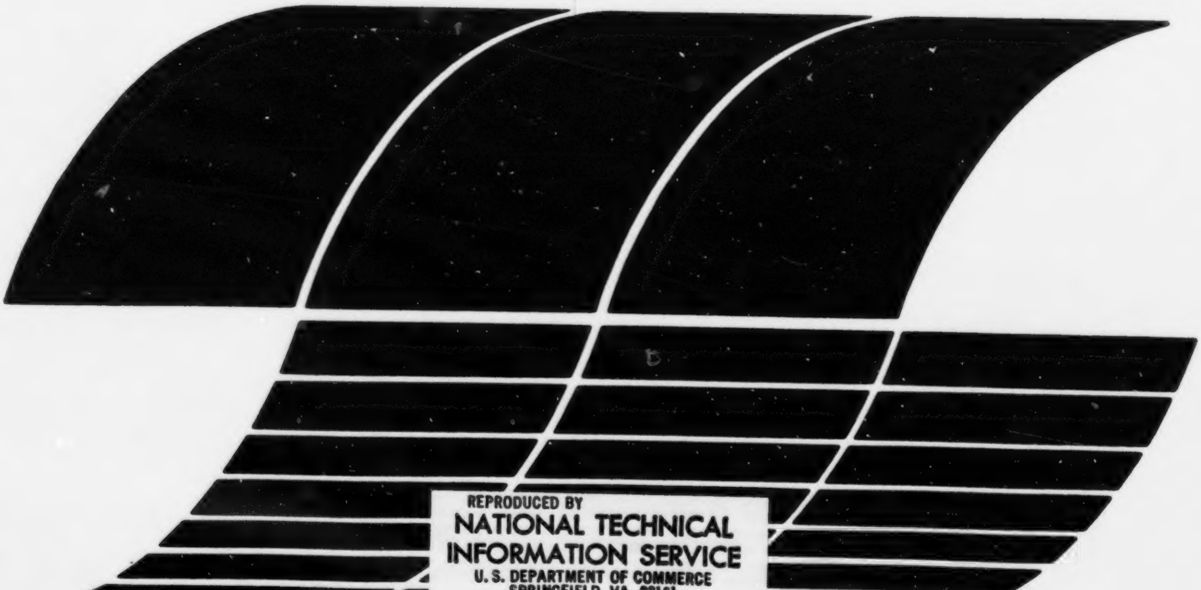

REPRODUCED BY
NATIONAL TECHNICAL
INFORMATION SERVICE
U. S. DEPARTMENT OF COMMERCE
SPRINGFIELD, VA. 22161

RESEARCH REPORTING SERIES

Research reports of the Office of Research and Development, U.S. Environmental Protection Agency, have been grouped into nine series. These nine broad categories were established to facilitate further development and application of environmental technology. Elimination of traditional grouping was consciously planned to foster technology transfer and a maximum interface in related fields. The nine series are:

1. Environmental Health Effects Research
2. Environmental Protection Technology
3. Ecological Research
4. Environmental Monitoring
5. Socioeconomic Environmental Studies
6. Scientific and Technical Assessment Reports (STAR)
7. Interagency Energy-Environment Research and Development
8. "Special" Reports
9. Miscellaneous Reports

This report has been assigned to the INTERAGENCY ENERGY-ENVIRONMENT RESEARCH AND DEVELOPMENT series. Reports in this series result from the effort funded under the 17-agency Federal Energy/Environment Research and Development Program. These studies relate to EPA's mission to protect the public health and welfare from adverse effects of pollutants associated with energy systems. The goal of the Program is to assure the rapid development of domestic energy supplies in an environmentally-compatible manner by providing the necessary environmental data and control technology. Investigations include analyses of the transport of energy-related pollutants and their health and ecological effects; assessments of, and development of, control technologies for energy systems; and integrated assessments of a wide range of energy-related environmental issues.

EPA REVIEW NOTICE

This report has been reviewed by the participating Federal Agencies, and approved for publication. Approval does not signify that the contents necessarily reflect the views and policies of the Government, nor does mention of trade names or commercial products constitute endorsement or recommendation for use.

This document is available to the public through the National Technical Information Service, Springfield, Virginia 22161.

TECHNICAL REPORT DATA

(Please read Instructions on the reverse before completing)

1. REPORT NO. EPA-600/7-80-043	2.	3. RECIPIENT'S ACCESSION NO.
4. TITLE AND SUBTITLE Pilot Scale Combustion Evaluation of Waste and Alternate Fuels: Phase III Final Report		5. REPORT DATE March 1980 6. PERFORMING ORGANIZATION CODE
7. AUTHOR(S) R.A. Brown and C.F. Busch		8. PERFORMING ORGANIZATION REPORT NO.
9. PERFORMING ORGANIZATION NAME AND ADDRESS Acurex Corporation Energy and Environmental Division 485 Clyde Avenue Mountain View, California 94042		10. PROGRAM ELEMENT NO. EHE624A 11. CONTRACT/GRANT NO. 68-02-1885
12. SPONSORING AGENCY NAME AND ADDRESS EPA, Office of Research and Development Industrial Environmental Research Laboratory Research Triangle Park, NC 27711		13. TYPE OF REPORT AND PERIOD COVERED Phase III Final; 2-8/78 14. SPONSORING AGENCY CODE EPA/600/13

15. SUPPLEMENTARY NOTES IERL-RTP project officer is David G. Lachapelle, Mail Drop 65, 919/541-2236. EPA-600/7-79-132 was the Phase II final report; there was no Phase I final report.

16. ABSTRACT The report gives results of three studies at EPA's Multifuel Test Facility. The first evaluated a distributed-air staging concept for NOx control in pulverized-coal-fired systems. The results showed that minimum NO levels of 140 ppm were achieved at overall residence times similar to those used during conventional staging tests. However, the NO levels achieved with the distributed-air concept were no lower than those achievable with conventional staging. The second evaluated combustion control techniques and NO emissions when firing coal/oil mixtures. NO emissions for a given burner and nozzle were generally proportional to the fuel-nitrogen content of the fuel. Additionally, combustion control technology currently used for NOx control from pulverized coal was found to be effective with coal/oil mixtures, but to differing degrees, depending on the coal/oil mixture ratios and compositions. The third evaluated emissions and combustion characteristics of refuse-derived fuel (RDF) co-fired with either natural gas or pulverized coal. Four RDF materials were evaluated for gaseous, particulate, trace metal, and organic emissions. In general: CO and UHC emissions were low; NOx and SOx emissions decreased with increasing RDF content when co-fired with coal; particulate levels did not substantially increase with the RDF; and no trace metal emissions correlation was found.

17. KEY WORDS AND DOCUMENT ANALYSIS

a. DESCRIPTORS		b. IDENTIFIERS/OPEN ENDED TERMS	c. COSATI Field/Group
Pollution	Fuel Oil	Pollution Control	13B
Nitrogen Oxides		Stationary Sources	07B
Combustion Control		Staged Combustion	21B
Refuse		Refuse-derived Fuel	
Wastes		Coal/Oil Mixtures	
Coal		Alternate Fuels	21D

18. DISTRIBUTION STATEMENT Release to Public	19. SECURITY CLASS *(This Report)* Unclassified	21. NO. OF PAGES 227
	20. SECURITY CLASS *(This page)* Unclassified	22. PRICE

EPA Form 2220-1 (9-73)

EPA-600/7-80-043
March 1980

Pilot Scale Combustion Evaluation of Waste and Alternate Fuels:
Phase III Final Report

by

R.A. Brown and C.F. Busch

Acurex Corporation
Energy and Environmental Division
485 Clyde Avenue
Mountain View, California 94042

Contract No. 68-02-1885
Program Element No. EHE624A

EPA Project Officer: David G. Lachapelle

Industrial Environmental Research Laboratory
Office of Environmental Engineering and Technology
Research Triangle Park, NC 27711

Prepared for

U.S. ENVIRONMENTAL PROTECTION AGENCY
Office of Research and Development
Washington, DC 20460

ABSTRACT

This report gives results of three studies at EPA's Multifuel Test Facility. The first evaluated a distributed-air staging concept for NO_x control in pulverized-coal-fired systems. The results showed that minimum NO levels of 140 ppm were achieved at overall residence times similar to those used during conventional staging tests. However, the NO levels achieved with the distributed-air concept were no lower than those achievable with conventional staging. The second evaluated combustion control techniques and NO emissions when firing coal/oil mixtures. NO emissions for a given burner and nozzle were generally proportional to the fuel-nitrogen content of the fuel. Additionally, combustion control technology currently used for NO_x control from pulverized coal was found to be effective with coal/oil mixtures, but to differing degrees, depending on the coal/oil mixture ratios and compositions. The third evaluated emissions and combustion characteristics of refuse-derived fuel (RDF) co-fired with either natural gas or pulverized coal. Four RDF materials were evaluated for gaseous, particulate, trace metal, and organic emissions. In general: CO and UHC emissions were low; NO_x and SO_x emissions decreased with increasing RDF content when co-fired with coal; particulate levels did not substantially increase with the RDF; and no trace metal emissions correlation was found.

CONTENTS

Abstract iii
Figures vi
Tables vii
Conversion Table xii

1. Overview and Summary 1
2. Distributed Air Tests 7
    2.1 Special experimental hardware 9
    2.2 Test plan 15
    2.3 Experimental data 18
    2.4 Conclusions 35
3. Coal/Oil Mixture Tests 37
    3.1 Test plan 50
    3.2 Test data 54
    3.3 Baseline tests 56
    3.4 Control technology tests. 60
    3.5 Fuel nitrogen studies 69
    3.6 Burner nozzle comparison 71
    3.7 Previous testing data 71
    3.8 Summary and conclusions 71
    3.9 Recommendation. 75
4. Refuse-Derived Fuel Tests 76
    4.1 Objectives. 77
    4.2 RDF experimental hardware 78
    4.3 Test theory and plan. 101
    4.4 Analytical procedures 106
    4.5 Experimental data 114

References. 166

Appendices

A. Data summary – distributed air; coal/oil mixture; RDF testing; COM/DOE report 169

FIGURES

Number Page

Distributed Air Tests

2-1 Distributed air concept as per Pershing 8

2-2 Distributed air arrangement in the horizontal extension . . . 10

2-3 IFRF burner 12

2-4 B&W-type coal spreader 13

2-5 Baffle detail 14

2-6 Residence time in section 1b 20

2-7 Distribured air configurations 21

2-8 Effect of SR_{1a} 24

2-9 Effect of SR_{1a} 25

2-10 Effect of SR_{1b} 27

2-11 Effect of 1a stage residence time 28

2-12 Effect of 1a stage residence time 29

2-13 Effect of 1b stage residence time 31

2-14 Effect of 1b stage residence time 32

Coal/Oil Mixture Tests

3-1 EPA/Acurex multifuel furnace. 39

3-2 Facility modifications. 40

3-3 Delavan swirl-air nozzle. 41

3-4 Sonic Corporation Sonicore nozzle 42

FIGURES (CONTINUED)

Number Page

3-5 Coal/oil delivery system 49

3-6 Baseline emissions 58

3-7 Boiling point curves 59

3-8 Nitrogen evolution curves 61

3-9 Staging emissions 62

3-10 Burner air distribution 64

3-11 Burner air distribution 65

3-12 Air distribution tests 66

3-13 Effect of firing rate and residence time 68

3-14 Effect of fuel nitrogen. 70

3-15 Nozzle comparison 72

3-16 Date from earlier work 73

Refuse-Derived Fuel Tests

4-1 Furnace cross section 79

4-2 Tangential configuration, aerodynamic patterns 80

4-3 Corner-fired burner. 81

4-4 RDF nozzle 82

4-5 Modified corner-burner assembly 84

4-6 Fuel delivery schematic 85

4-7 RDF feed system design 87

4-8 Pneumatic transport system 88

4-9 Safety system 90

4-10 Sampling system online at experimental multiburner furnace . 95

4-11 Aerotherm high volume stack sampler 96

FIGURES (CONTINUED)

Number		Page
4-12	Source assessment sampling system (SASS)	97
4-13	Ash deposition	102
4-14	Test matrix for baseline emissions characterization	104
4-15	Test matrix for emissions control through theoretical air variation	105
4-16	Test matrix for baseline emissions characterization	107
4-17	Test matrix for emissions control through theoretical air variation	108
4-18	Photographs of fuel samples	117
4-19	NO emissions during baseline testing (Ames)	120
4-20	NO emissions during baseline testing (Richmond)	121
4-21	NO emissions during baseline testing (Americology)	122
4-22	NO emissions during baseline testing (San Diego)	123
4-23	Thermal NO (previous work)	124
4-24	NO emissions during baseline testing (all RDF's)	126
4-25	SO_2 data (all RDF's)	127
4-26	NO emissions during detailed testing (Richmond RDF/Pittsburgh coal	129
4-27	Fuel nitrogen contribution	130
4-28	Stack gas particle size vs. cumulative percent less than diameter	137
4-29	Particulate loading results	138
4-30	Stack gas particulate size vs. cumulative percent less than diameter – trace metal Cu	149
4-31	Stack gas particle size vs. cumulative percent less than diameter – trace metal Zn	150

FIGURES (CONCLUDED)

Number Page

4-32 Stack gas particle size vs. cumulative percent less than diameter — trace metal Mn 151

4-33 Stack gas particle size vs. cumulative percent less than diameter — trace metal Pb 152

4-34 Stack gas particle size vs. cumulative percent less than diameter — trace metal Cd 153

4-35 Stack gas particle size vs. cumulative percent less than diameter — trace metal Be 154

4-36 Stack gas particle size vs. cumulative percent less than diameter — trace metal Ti 155

4-37 Stack gas particle size vs. cumulative percent less than diameter — trace metal Sb 156

4-38 Stack gas particle size vs. cumulative percent less than diameter — trace metal Sn 157

4-39 Stack gas particle size vs. cumulative percent less than diameter — trace metal Hg 158

4-40 Stack gas particle size vs. cumulative percent less than diameter — trace metal As 159

TABLES

Number Page

Distributed Air Tests

2-1 Optimum Staging Parameters (Pershing) 9

2-2 Range of Parameters of Interest 16

2-3 Revised Distributed Air Studies Matrix 17

2-4 Residence Times in 1a Stage 19

2-5 Distributed Air Versus Conventional Staging 34

2-6 Facility Characteristics. 35

Coal/Oil Mixture Tests

3-1 Emission Monitoring Equipment 44

3-2 Fuel Oil Analyses 45

3-3 Coal Analyses, As-Received Basis 46

3-4 Coal/Oil Mixture Analyses, As-Received Basis, 30% Coal by Weight 47

3-5 Baseline Matrix 51

3-6 Effect of Load and Residence Time 52

3-7 Distributed Air Burner Tests 53

3-8 Effect of Fuel Nitrogen 55

Refuse-Derived Fuel Tests

4-1 Emission Monitoring Equipment 94

4-2 Fuel Analysis 106

TABLES (CONCLUDED)

Number Page

4-3 Metals Which Were Analyzed 109

4-4 Liquid Chromatography Elution Sequence 110

4-5 Distribution of Compound Classes in Liquid Chromatographic Fractions of Organic Extracts 111

4-6 Test Matrix. 115

4-7 Fuel Analyses 116

4-8 Particulate Analyses: Effect of RDF Type 131

4-9 Particulate Analyses: Effect of Excess Air 133

4-10 Particulate Analyses: Effect of Percent RDF 135

4-11 Particulate Analyses: Coal vs. 10% RDF + Coal vs. 10% RDF + Gas. 136

4-13 Total Trace Metal Loadings — Coal Cofiring 142

4-14 Trace Metal Concentrations as Vapor — Coal Cofiring 144

4-15 Total Trace Metal Loadings — Gas Cofiring 145

4-16 Trace Metal Concentrations as Vapor — Coal Cofiring 146

4-17 Trace Metal Concentrations — Pilot vs. Full Scale — Particulate Only 148

4-18 Organics Found 161

4-19 LC Column Data 163

4-20 LC Column Data 164

4-21 Possible Compounds in LC Fractions not Analyzed 165

CONVERSION TABLE

ENGLISH TO SI METRIC CONVERSION FACTORS

To convert from	To	Multiply by
inch	m	2.540 000 E-02
foot	m	3.048 000 E-01
scfm	m^3/s	4.719 474 E-04
gr/ft^3	g/m^3	2.288 352 E+00
gallon	m^3	3.785 412 E-03
gph	m^3/s	1.051 503 E-06
Btu/hr	W_t	2.930 711 E-01
lb/hr	kg/s	1.259 979 E-04
Btu/lb	kJ/kg	2.326 000 E+00
$Btu/hr{\cdot}ft^3$	W_t/m^3	1.034 971 E+01
lb	kg	4.535 924 E-01
psig	kPa	6.894 757 E+03
μg/Btu	μg/J	9.478 170 E-01
°F	°C	t°C = (t°F-32)/1.8

---

scfm = standard cubic feet per hour

gr/ft^3 = grains per cubic foot

gph = gallons per hour

Btu = British thermal unit

hr = hour

lb = pound

ft^3 = cubic foot

psig = pounds per square inch (gauge)

μg = micrograms

m = metre

m^3 = cubic meter

s = second

g/m^3 = grams per cubic meter

W_t = thermal watt

kg = kilogram

kJ = kilojoule

kPa = kilopascal

SECTION 1

OVERVIEW AND SUMMARY

The work summarized in this report was performed during the period October 1977 to July 1978 as Phase III of the Pilot Scale Evaluation of NO_x Combustion Control Techniques, EPA Contract 68-02-1885. This report discusses

- Advanced NO_x Control Techniques for Pulverized Coal Through Distributed Air
- Emissions and NO_x Control Technology Evaluation of Coal/Oil Mixtures (COMs)
- Evaluation of Emissions on Co-firing of Four Refuse-Derived Fuels (RDF) with Natural Gas and Pulverized Coal

A brief summary of the scope and results from each of these tasks follows.

Distributed Air Tests

Tests at the University of Arizona in a bench-scale coal-fired furnace suggested that low NO levels could be achieved in relatively overall short residence time by sequencing the air into the burner in three stages. The primary zones include the primary air conveying coal and some secondary air. The stoichiometric ratio of this first stage would be in the range of 0.3 to 0.6 and a residence time of 0.3 to 0.75 seconds. Tertiary air

---

It is the EPA policy to use SI metric units; however, in this report English units are occasionally used for convenience. See attached conversion table.

was then added through four ports at 90° to the flow of combustion products. This second stage is held at a stoichiometric ratio of 0.75 to 0.95, and staging air is then added through four additional ports.

This series of tests explored a range of stoichiometric ratios and residence times for each stage. Unfortunately, the results from these tests could not duplicate the Arizona tests. What was found was that even with the distributed air approach, NO levels increase with decreasing SR below an SR of about 0.6. In addition, NO always decayed with increasing residence time in both the first and second stages. Minimum NO levels of about 140 ppm were achieved in overall residence times similar to the conventional staging results. Thus, no advantage over conventional staging was achieved. These results may be partially explained by the fact that a diffusion burner was used in a relatively low L/D firebox as compared to a premixed burner in a high L/D firebox in the Arizona tests.

Coal/Oil Mixture Tests

In order to utilize coal in the near term, it has been proposed to fire oil or gas boilers with a slurried mixture of coal and oil. Although the feasibility has been demonstrated in a number of small and larger scale demonstrations, there is a need to determine the environmental problems associated with COMs. Because of the generally higher fuel-N content of the mixture as compared to oil, it seems likely that the NO_x levels would also be higher. Therefore, the purpose of this study was as follows:

- Obtain emission data for coal/oil combustion in an environment closely simulating an industrial package boiler
- Determine if emissions levels were affected by the fuel composition
- Determine if conventional control technology developed for coal

is effective in reducing emissions levels produced by coal/oil combustion

- Investigate the effect of burner modification on emission levels produced by coal/oil combustion.

During this study, two oils and three coals were fired in a package boiler simulator. Baseline emissions of the parent fuels and the fuel combinations were determined. Control technology tests were run on the COMs as follows:

- Baseline NO emissions from COM were, in general, proportional to the fuel-N for a given burner and nozzle type.
- The burner settings and fuel nozzle type have a strong effect on NO emissions.
- Conventional control technology currently utilized for pulverized fuel combustion is effective in reducing NO emissions, but to different degrees, depending on fuel composition
- NO emissions increase in proportion to the amount of coal in the coal-oil mixture, but fall between the parent fuel oil and coal baseline emissions.

If there is to be significant utilization of COM in industry, and if NO levels are to be controlled, much additional work is needed to understand the mechanisms which control NO_x formation in COMs for different fuel combinations.

Refuse-Derived Fuels Testing

It is necessary that investigations regarding the environmental compatibility of RDF be conducted before this vast, untapped energy source can be considered a viable supplement to present energy resources. It has thus been suggested that such investigations can be carried out most cost effectively in a pilot-scale facility. To determine the feasibility of such pilot-scale testing, the IERL of EPA/Cincinnati funded a study as part of the Phase III activity. The goals of this study were as follows:

- To design, fabricate, and operate a system for combustion testing of RDF in a laboratory scale facility
- To characterize RDF emissions of several types of material presently available for use as fuel
- To evaluate the combustion efficiency of fuels consisting of conventional clean and dirty fossil fuels (natural gas and coal) mixed with varying percentages of refuse
- To evaluate the effects of combustion parameters on emissions from RDF/conventional fuel mixtures
- To provide direction for future investigations on refuse-derived fuel to insure solutions to problems associated with its use.

A feed system was designed to control and measure from 10 to 60 lb/hr of a variety of "fluff" refuse-derived materials. This was accomplished using a rotating drum hopper depositing on an internal moving belt conveyor. The conveyor, in turn, deposits the material into a tube where it is conveyed by air into the top port of a tangential burner. The pilot-scale facility was tangentially-fired at 1.5 x 10^6 Btu/hr with RDF fed to two of the four corners. The test program was designed to determine the gaseous, particulate, trace metal, and organic emissions of four sources of RDF. The four materials were from San Diego, California; Richmond, California; the Americology Facility in Milwaukee, Wisconsin; and from the Ames, Iowa Plant. NO emissions increased with both percent RDF and percent excess air when fired with natural gas. NO emissions also varied for the four fuel types in approximate proportion to the fuel-N content of the RDF. When co-fired with coal, the NO emissions decreased with increasing percent RDF, even though the percent N available increased. This may be attributed to shielding of the coal by the RDF from the oxygen, flame/flame processing or locally fuel-rich zones in the coal stream caused by redistribution of the combustion air during the RDF firing.

Particulate levels did not substantially increase with the RDF, but a higher concentration was found in the less than 1μ size range. No correlations were found with trace metal emissions, either with respect to percent RDF or percent excess air. It is believed that, due to the great variability in the feed from minute to minute and the problems with holdup in the heat exchanger sections, a valid trace metal evaluation is not possible from a single test. Many tests will be necessary to form a statistically reliable number. Lastly, few poly-organic materials (POMs) were found and no poly-chlorinated biphenyls (PCBs).

Combustion efficiency of these pilot-scale tests was perhaps better than full-scale tests due to higher combustion temperatures. Additional tests are needed to better determine the variability of gaseous, trace metal, and organic emissions from a single source and from a variety of sources.

In the sections that follow, the results from each of these test programs will be explained in more detail. In all cases they were performed in EPA's multifuel, multiburner test facility located at Acurex Corporation in Mountain View, California. The facility was either used in its normal utility boiler configuration (main firebox only) or with the horizontal extensions which can simulate a package boiler configuration or serve as an asymmetric flow combustion system. Details of this facility may be found in the Phase II report (Reference 1). A description of the special equipment required for each of the test programs and details of the configurations for those tests are included within the section on that program.

SECTION 2

DISTRIBUTED AIR TESTS

The conventional staging studies performed in the main firebox and horizontal extensions (Reference 1) of the EPA Multiburner Test Facility revealed that low NO_x levels could be achieved with a sufficiently long residence time under fuel-rich conditions. However, this approach necessitates an exceptionally long residence time under fuel-rich conditions with potential for corrosion and slagging problems. Thus, an alternate approach was sought.

Tests run on a subscale premixed combustor at the University of Arizona (Reference 2) indicated that a three-stage approach would be able to achieve low NO_x levels in an overall residence time of less than 1.5 seconds.

The approach is illustrated for the Arizona facility in Figure 2-1. In this arrangement premixed coal, primary air, and secondary air enter the top of the furnace at a stoichiometric ratio SR_{1a}. This stoichiometry is held for a residence time τ_{1a} seconds, whereuopon tertiary air is introduced. The second part of the first stage is held at a stoichiometric ratio of SR_{1b} for τ_{1b} seconds. The second-stage air is then introduced for final burnout under excess air conditions for a residence time of τ_2 seconds. Pershing found that for his facility a unique combination of

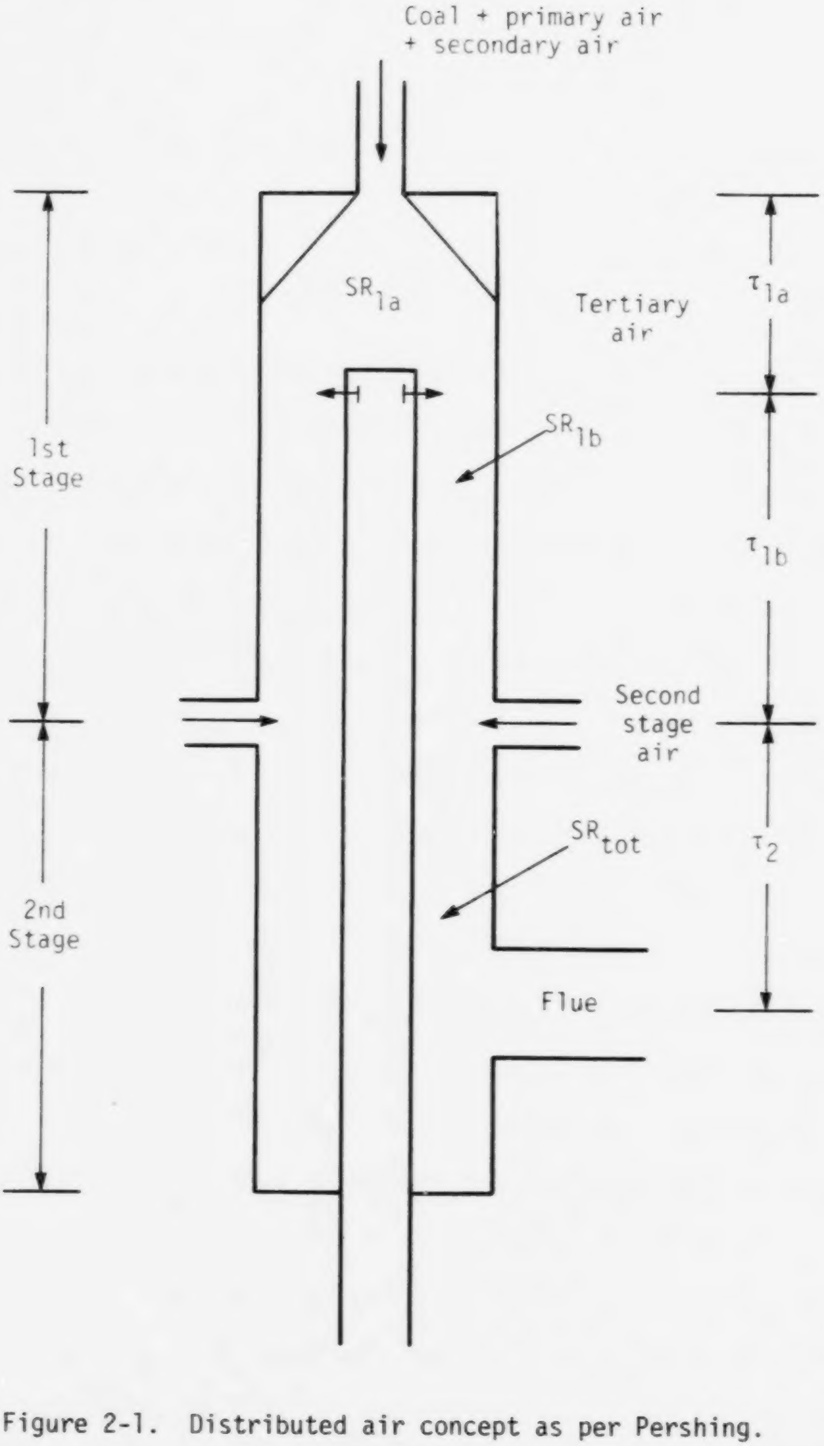
Coal + primary air
+ secondary air
SR_{1a}
Tertiary air
τ_{1a}
SR_{1b}
1st Stage
τ_{1b}
Second stage air
SR_{tot}
τ_2
2nd Stage
Flue

Figure 2-1. Distributed air concept as per Pershing.

SR_{1a}, τ_{1a}, SR_{1b}, and τ_{1b} achieved the lowest NO_x level. The optimum conditions for the Pershing experiment are tabulated in Table 2-1. In summary he found the following:

- Stack NO_x decreased with decreasing SR_{1a} until an SR_{1a} = 0.5. Below an SR_{1a} = 0.5, stack NO did not decrease further for constant conditions downstream
- An optimum τ_{1a} was necessary to achieve minimum NO_x. On either side of the optimum, NO_x would increase.
- NO_x decreased with decreasing SR_{1b}
- NO_x increased with decreasing τ_{1b}
- τ_2 residence time had no effect on the stack NO_x

TABLE 2-1. OPTIMUM STAGING PARAMETERS (PERSHING)

SR_{1a}	0.4 - 0.5
SR_{1b}	0.85
τ_{1a}	0.4 sec
τ_{1b}	1-1.5 sec (not varied)

This approach was thus investigated using the EPA multiburner-horizontal extension test facility.

2.1 SPECIAL EXPERIMENTAL HARDWARE

It was decided that the horizontal extensions would be the best equipment to perform these tests. The horizontal extensions were set up as shown in Figure 2-2. Each horizontal extension is 33-inch inside diameter, refractory lined, and two feet long. Up to five sections may be

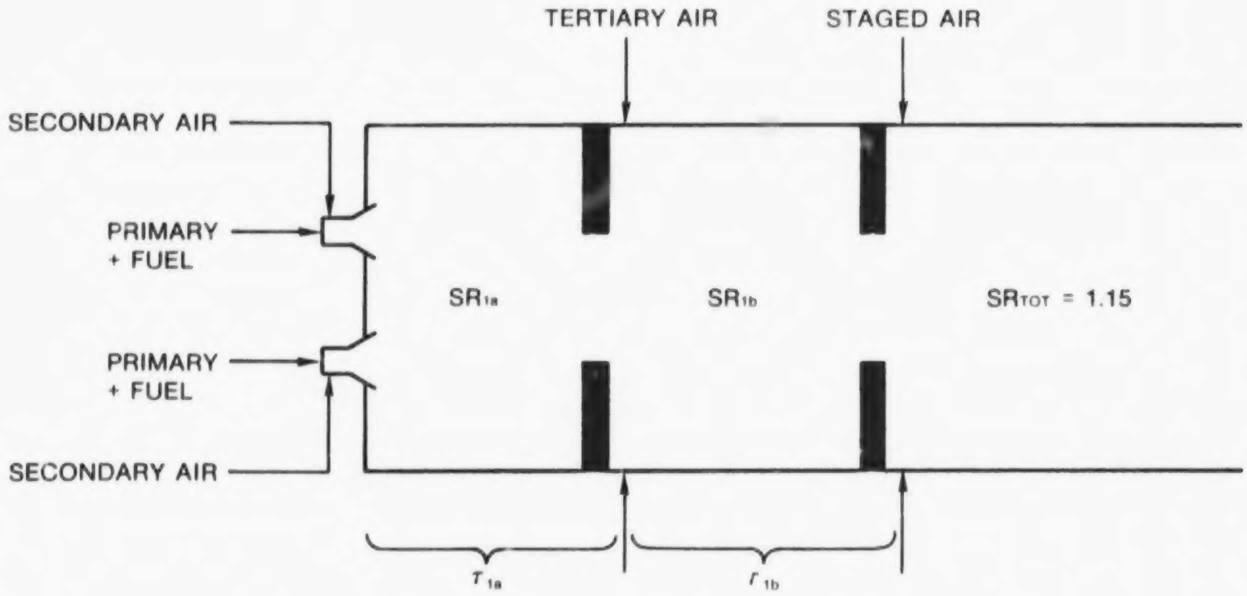
TERTIARY AIR
STAGED AIR
SECONDARY AIR
PRIMARY + FUEL
PRIMARY + FUEL
SECONDARY AIR
SR_{1a}
SR_{1b}
$SR_{TOT} = 1.15$
τ_{1a}
τ_{1b}

Figure 2-2. Distributed air arrangement in the horizontal extension.

joined together to form an overall length of 10 feet. A transition section connects to the main firebox where the flue gases are then quenched by the closed loop Dowtherm® heat exchange sections. Gaseous emissions are sampled just downstream of the heat exchange section. On the other end of the horizontal extensions, either a single burner or up to five burners may be mounted. For this test, four of the nominal 300,000 Btu/hr IFRF variable swirl block burners were chosen. These burners were fitted with a 2-inch diameter sleeve in the air throat to achieve reasonable velocities under very fuel-rich conditions. The burner is illustrated in Figure 2-3. The burners also used the B&W-type coal spreader illustrated in Figure 2-4, and the swirl was set at a mid-position of four. Part of the objective for utilizing these four burners in this configuration was to achieve a well-mixed first stage. To further enhance the mixing in each stage, baffles were used whenever possible at the end of the 1a stage and 1b stage, as was illustrated in Figure 2-3. These baffles also served to separate the stages and prevent backmixing into the first stage. The baffle or choke was made from a high temperature refractory in four sections as shown in Figure 2-5. This arrangement made it relatively easy to move the baffle to any desired location within the tunnel. At the first tertiary air position, it was not possible to install the baffle due to the close proximity to the burners. The baffle opening was 16 inches in diameter. The tertiary air was introduced just downstream of the first baffle in four locations 90 degrees apart. This air was introduced through 2-inch diameter ports perpendicular to the main flow. The horizontal extensions have four ports 90 degrees apart every foot along the length of the furnace. The first four locations, 1 foot apart, were chosen to vary the tertiary air residence

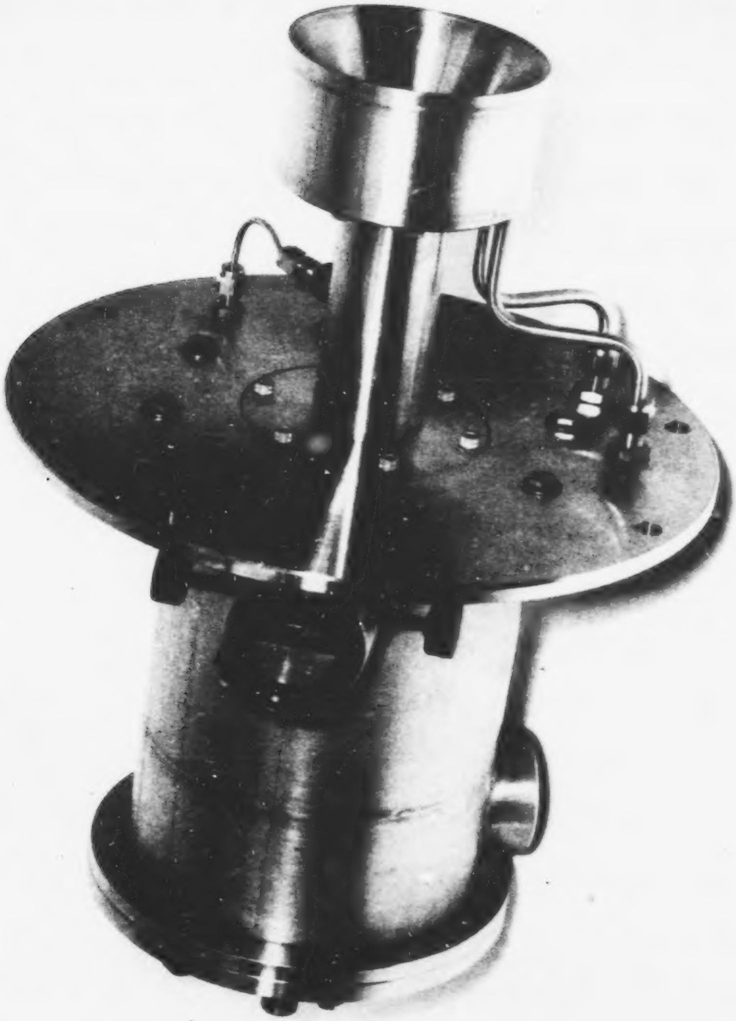

Figure 2-4. IFRF burner.

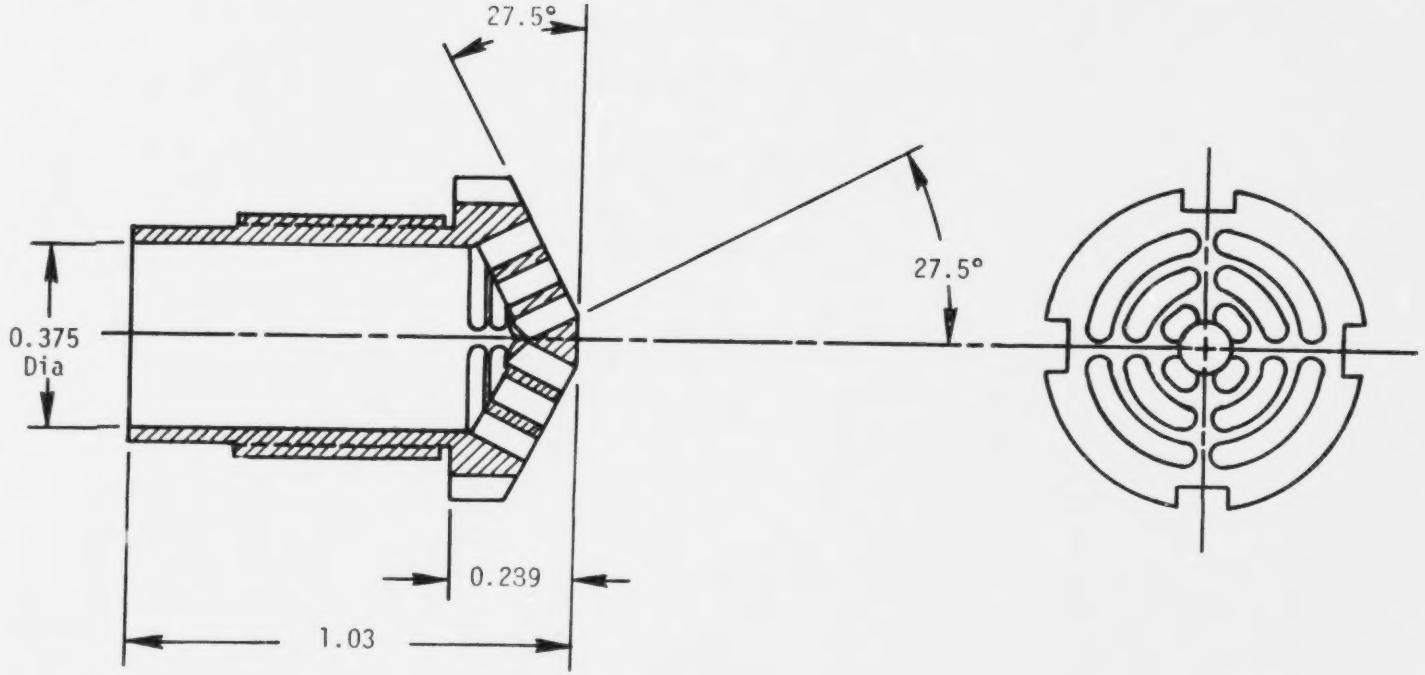
27.5°
27.5°
0.375
Dia
0.239
1.03

Figure 2-4. B&W-type coal spreader.

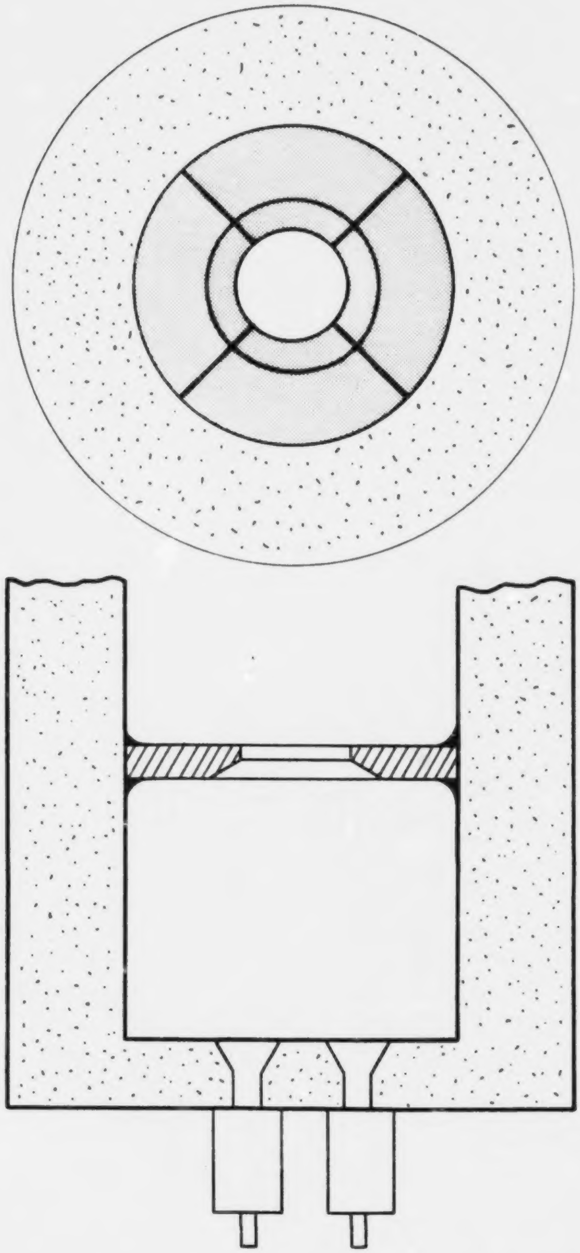

Figure 2-5. Baffle detail.

time t_{1a}. This enabled the 1a stage residence time to be varied from less than 0.5 second to over 2 seconds. The τ_{1b} residence time was then varied by positioning the staging air ports from 2 to 7 feet downstream of the tertiary air position. No attempt was made to control the second-stage residence time, but it was always sufficient to complete combustion.

Temperature of the secondary and tertiary air was maintained at about 600°F and the stage air at 300°F. Bare platinum-platinum/rhodium thermocouple measurements were made in the 1a stage and 1b stage.

2.2 TEST PLAN

The tests were structured to explore the following variables in the distributed air concept:

- 1a stage residence time τ_{1a}
- 1b stage residence time τ_{1b}
- 1a stage stoichiometric ratio SR_{1a}
- 1b stage stoichiometric ratio SR_{1b}
- Firing rate
- Temperature

The range of each parameter of interest is given in Table 2-2. Table 2-3 shows the matrix that was run. This matrix is the matrix which was developed during the course of the testing as the results redirected the effort. It was found, for instance, that a fairly dense matrix was needed to truly see the effects of the various parameters. In general two to three 1a stage residence times and two 1b residence times were selected for each tertiary air position. The 1a stage stoichiometric ratio was varied from 0.3 to 0.7, and two 1b stoichiometries of 0.85 and 0.95 were selected. The firing rate changes not only effect early mixing, but the

TABLE 2-2. RANGE OF PARAMETERS OF INTEREST

Parameter	Range
SR_{1a}	0.3 – 0.7
SR_{1b}	0.8 – 0.95
τ_{1a}	0.5 – 3.0
τ_{1b}	0.5 – 1.5
Firing Rate	0.85 – 1.7 x 10^6 Btu/hr
Temperature	Ambient – 600°F

TABLE 2-3. REVISED DISTRIBUTED AIR STUDIES MATRIX[a]

Distributed Air Studies Matrix			Position #1 – τ_{1a}						Position #2 – τ_{1a}						Position #3 – τ_{1a}						Position #4 – τ_{1a}			
			τ_{1b} – Short			τ – Long			τ_{1b} – Short			τ_{1b} – Long			τ_{1b} – Short			τ_{1b} – Long			τ_{1b} – Short		τ_{1b} – Long	
			SR_{1a}			SR_{1a}			SR_{1a}			SR_{1a}			SR_{1a}			SR_{1a}						
			0.3	0.45	0.6	0.3	0.45	0.6	0.3	0.45	0.6	0.3	0.45	0.6	0.3	0.45	0.6	0.3	0.45	0.6	0.6	0.7	0.6	0.7
Load (10^6 Btu/hr) 1.7	Preheat 600°F	SR_{1b} 0.95							213x (f)	213v (f)	213w (f)				212ℓ (k)	212k (k)	212j (k)	210b (j)	210a (j)	210c (j)	214a (m)	214b (m)	214g (n)	214h (n)
		0.8							213u (f)	213s (f)	213t (f)				211b (k)	211a (k)	211c (k)	210f (j)	210e (j)	210d (j)	214c (m)	214d (m)	214f (n)	214e (n)
	AMB	SR_{1b} 0.95																						
		0.8																						
1.3	Preheat 600°F	SR_{1b} 0.95							213i (e)	213h (e)	213g (e)	213p (f)	213q (f)	213r (f)	212g (h)	212h (h)	212i (h)	211i (k)	211g (k)	211h (k)				
		0.8							213j (e)	213k (e)	213ℓ (e)	213o (f)	213n (f)	213m (f)	211j (h)	211k (h)	211ℓ (h)	211f (k)	211d (k)	211e (k)				
	AMB	SR_{1b} 0.95																						
		0.8																						
0.85	Preheat 600°F	SR_{1b} 0.95					209i (a)								212f (h)	212e (h)	212d (h)							
		0.8				209j (a)	209k (a)	209ℓ (a)							212b (h)	212a (h)	212c (h)							
	AMB	SR_{1b} 0.95					209h (a)		213d (e)	213e (e)	213f (e)													
		0.8	209b (b)	209a (b)	209c (b)	209g 209t (a)	209e (a)	209d (a)	213c (e)	213a (e)	213b (e)													

---

[a] Letters in parentheses refer to the configuration designation (Figure 2-7). Numbers with letters are test designations

residence time between any two points in the furnace and the temperature at any point. A few tests were also run with no preheat and the lowest firing rate to further enhance any temperature effect. When no effect was seen at this lowest load, further tests of temperature were exchanged for a more complete matrix in other regions.

To aid in estimating the effect of residence time, a plot and tables were prepared to determine the residence time for a given staging position, firing rate, and stoichiometric ratio. Table 2-4 presents this data for the 1a residence time as a function of tertiary air position, stoichiometric ratio, and firing rate. Figure 2-6 presents residence time plots for the 1b stage as a function of firing rate and SR_{1b}. The absissa of this plot is the distance between the tertiary air position and the stage air position. Also shown on this plot are the various configuration letters associated with each test point. The matrix in Table 2-3 gives the configuration letter for each test number, and the configurations are depicted in Figure 2-7. Thus, by referring to the matrix, the configuration letter can be determined and seen schematically in Figure 2-7. By referring to Figure 2-6 and knowing the firing rate and SR_{1b}, the residence time in the 1b stage may be determined. This procedure together with the table for τ_{1a} were used to reduce the data to common residence times. Thus, the true effect of the stoichiometric ratios and, conversely, the effect of residence time at consistent stoichiometric ratio could be determined.

2.3 EXPERIMENTAL DATA

The data have been compiled in this section in its reduced form. First, all data were reduced to an air-free (0 percent O_2) basis. Then cross plots were made so that the true effect of any parameter could be

TABLE 2-4. RESIDENCE TIMES IN 1a STAGE

(τ_{1a} – seconds)

Load (10^6 Btu/hr)		Position 1 SR_{1a}			Position 2 SR_{1a}			Position 3 SR_{1a}			Position 4 SR_{1a}	
		0.3	0.45	0.6	0.3	0.45	0.6	0.3	0.45	0.6	0.6	0.7
	1.7	0.487	0.354	0.280	0.885	0.644	0.509	1.47	1.06	0.84	1.17	1.10
	1.3	0.637	0.464	0.366	1.16	0.84	0.67	1.93	1.39	1.11	--	--
	0.85	0.974	0.711	0.560	1.77	1.29	1.02	2.94	2.14	1.69	--	--

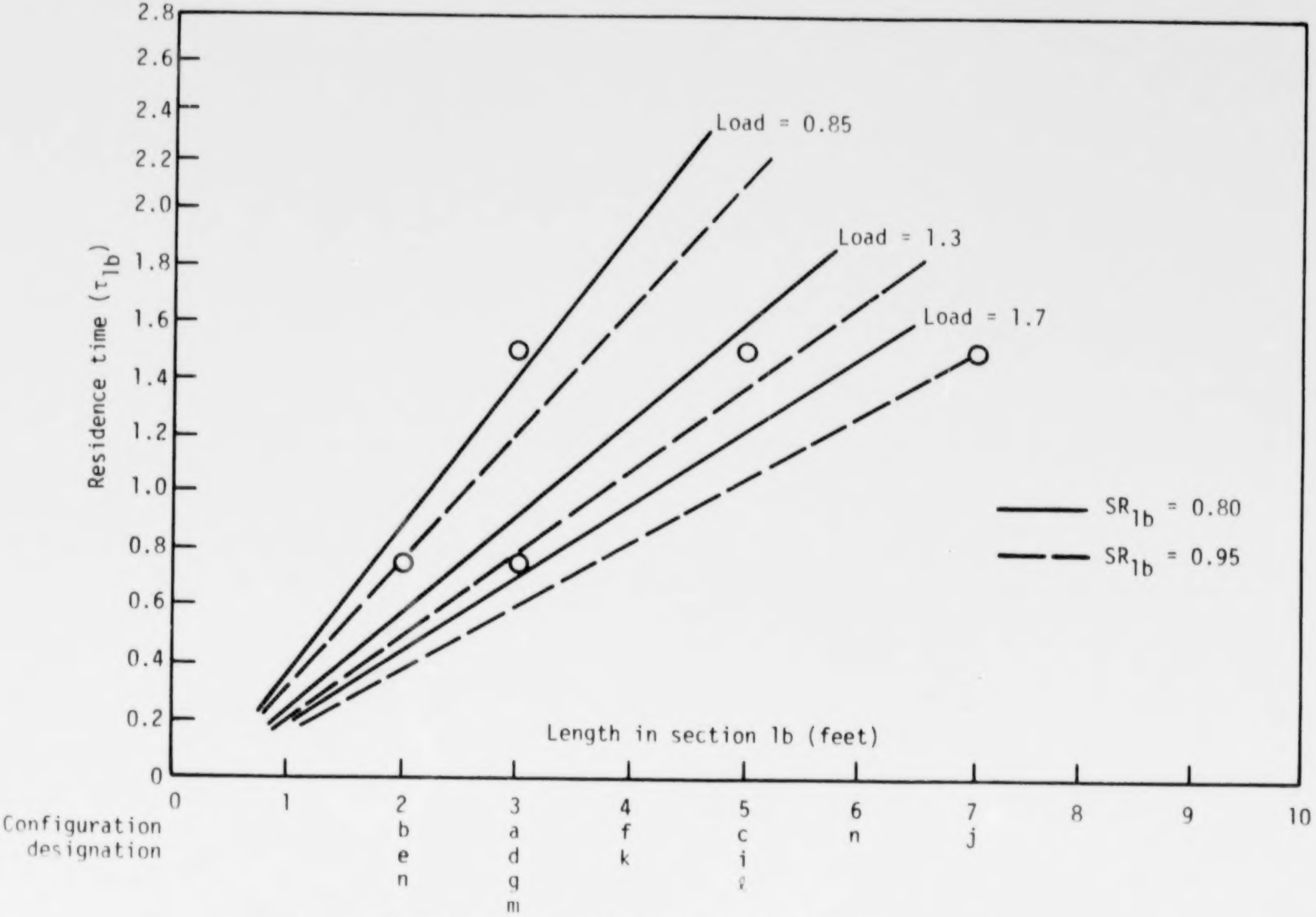

Figure 2-6. Residence time in section 1b.

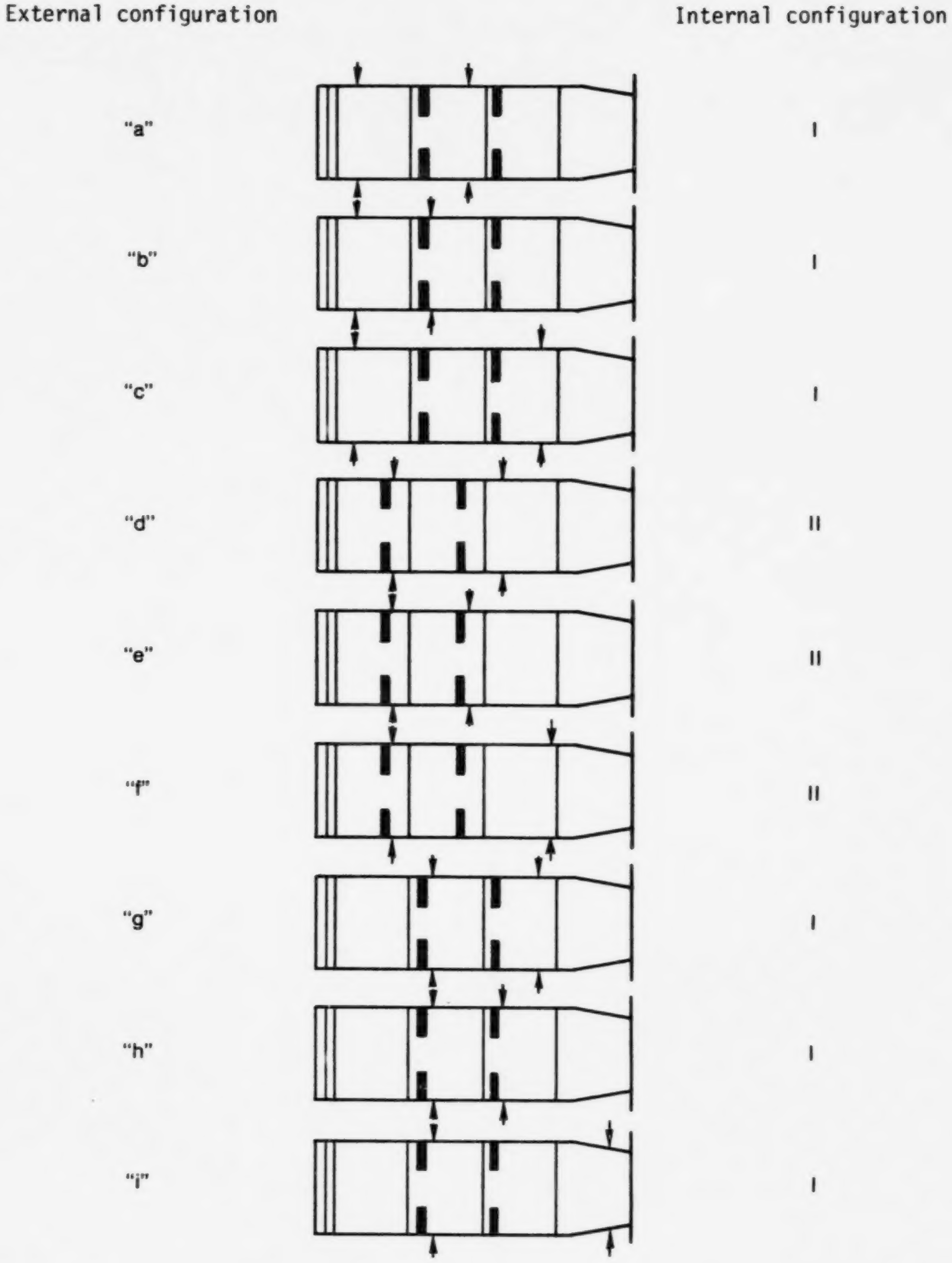
External configuration
Internal configuration
"a"
I
"b"
I
"c"
I
"d"
II
"e"
II
"f"
II
"g"
I
"h"
I
"i"
I

Figure 2-7. Distributed air configurations.

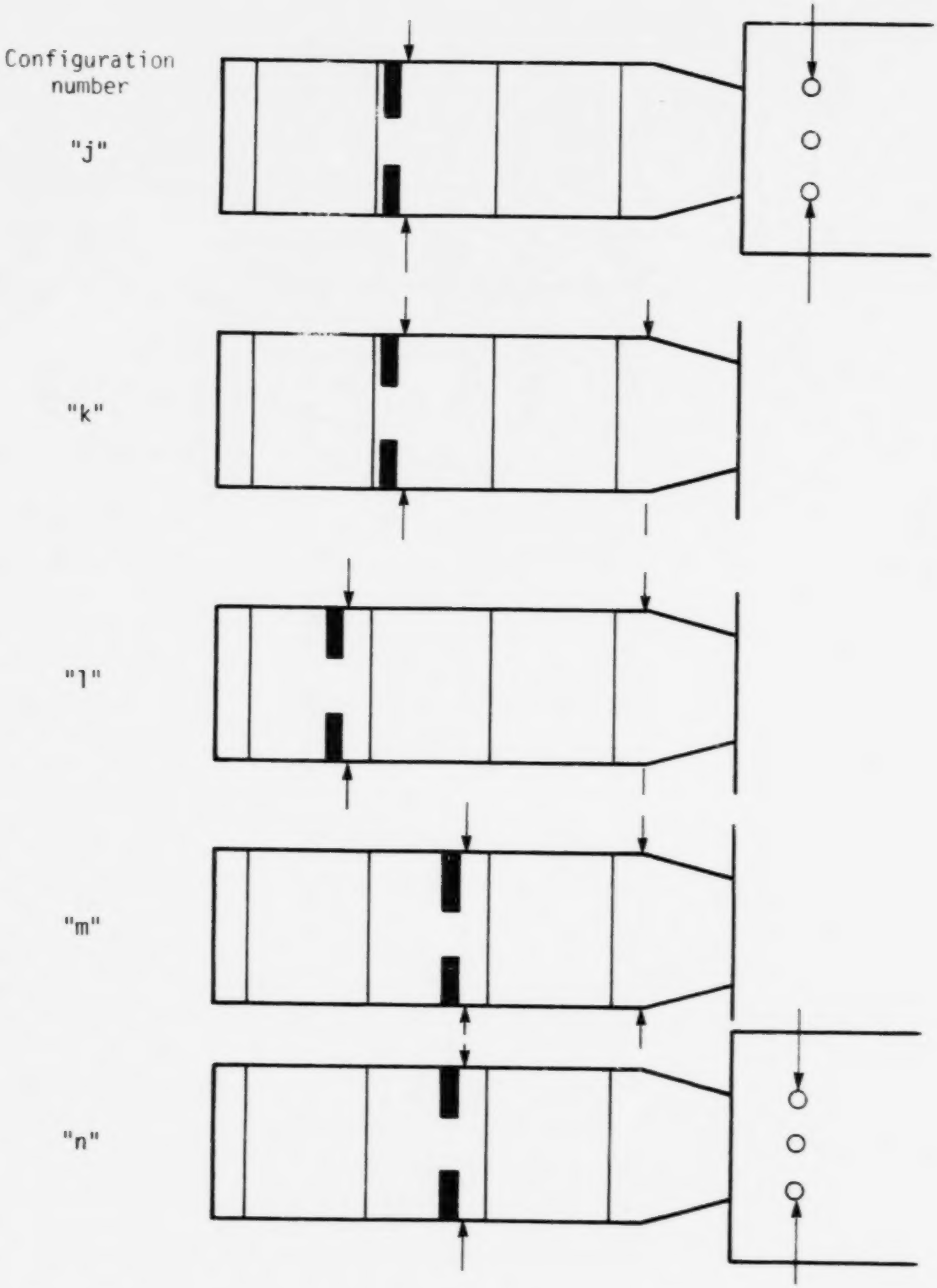
Configuration number
"j"
"k"
"l"
"m"
"n"

Figure 2-7. Distributed air configurations (concluded).

determined. Each of the various parameters will be discussed in the subsections that follow.

2.3.1 1a Stage Stoichiometric Ratio

Figure 2-8 shows the effect of the 1a stage stoichiometric ratio at a constant SR_{1b} of 0.80, 1a stage residence time of 1.00 seconds, and τ_{ib} residence time of 0.97 seconds. As can be seen on the plot, the effect was fairly pronounced with NO decreasing with increasing SR_{1a}. Previous tests indicated that above an SR of 0.7-0.8, the NO levels would again increase. This result is in contrast to the Pershing result which indicated that there was no effect of SR_{1a} below a level of SR_{1a} 0.50. Actually, this data is consistent with the data taken previously in this facility with conventional staging. It was suggested in that previous work that this increase in NO at low stoichiometric ratios was due to the formation of second-stage NO.

A similar trend was found at an SR_{1b} = 0.95 as seen in Figure 2-9. There is some question as to the validity of the points at 1.7 x 10^6 Btu/hr, particularly at the lower SR_{1a}'s because the baffle collapsed during these tests. Nevertheless, the data still indicate that NO increases with decreasing stoichiometric ratio. The NO levels are about 100 ppm higher, however, at an SR_{1b} of 0.95 than at an SR_{1b} of 0.80. This suggests that some second-stage NO is being formed and is either dependent on the stoichiometric ratio in the 1b stage or on a dependent variable of the stoichiometric ratio. Recent tests (Reference 3), for example, have shown that second-stage NO is strongly dependent on the initial flame temperature in the second stage, provided this temperature is below 2200°F. However, if it was an effect of temperature, in this case we would expect to see an increase of NO with firing tate. In both plots this is true at an SR_{1a}

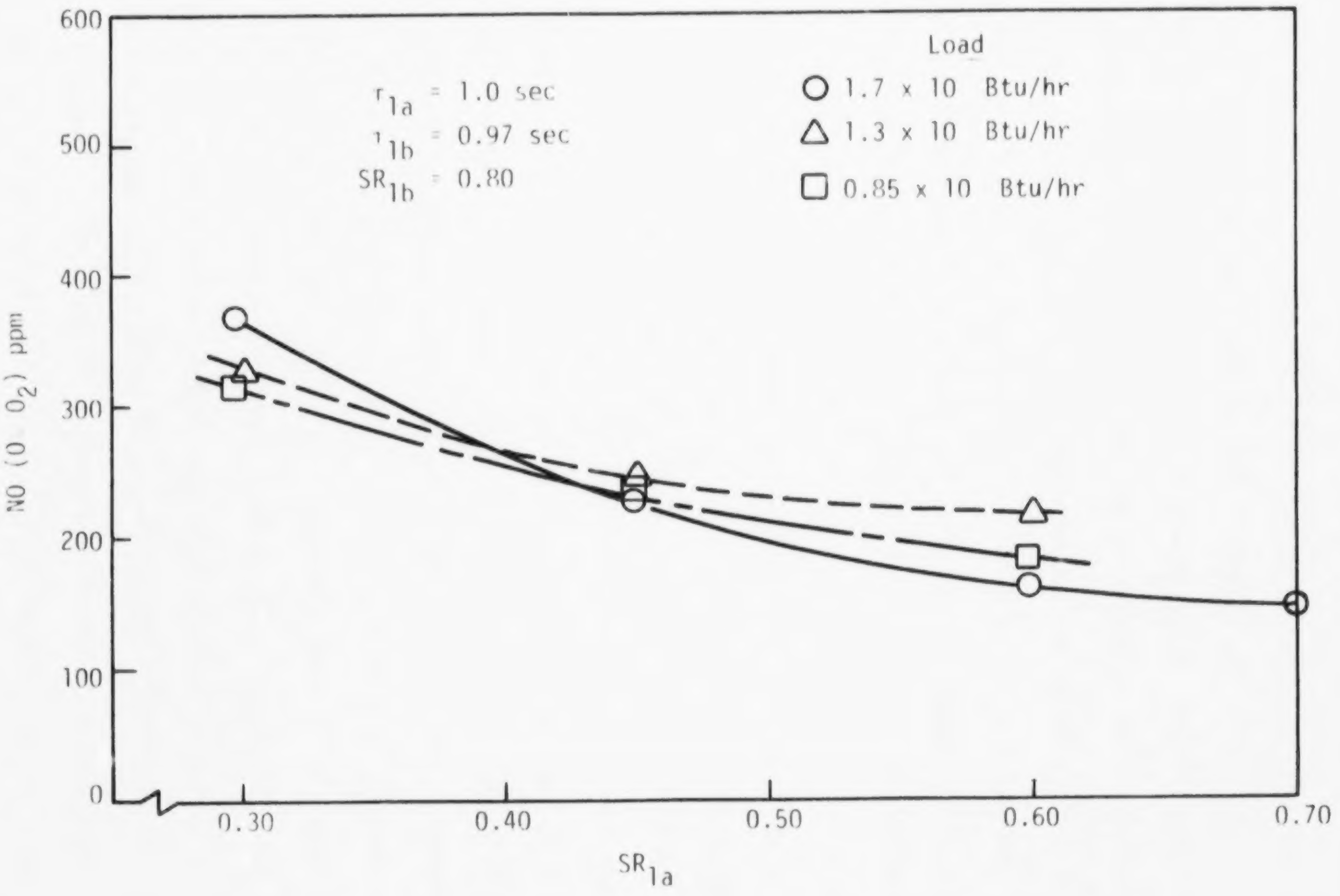

Figure 2-8. Effect of SR_{1a}.

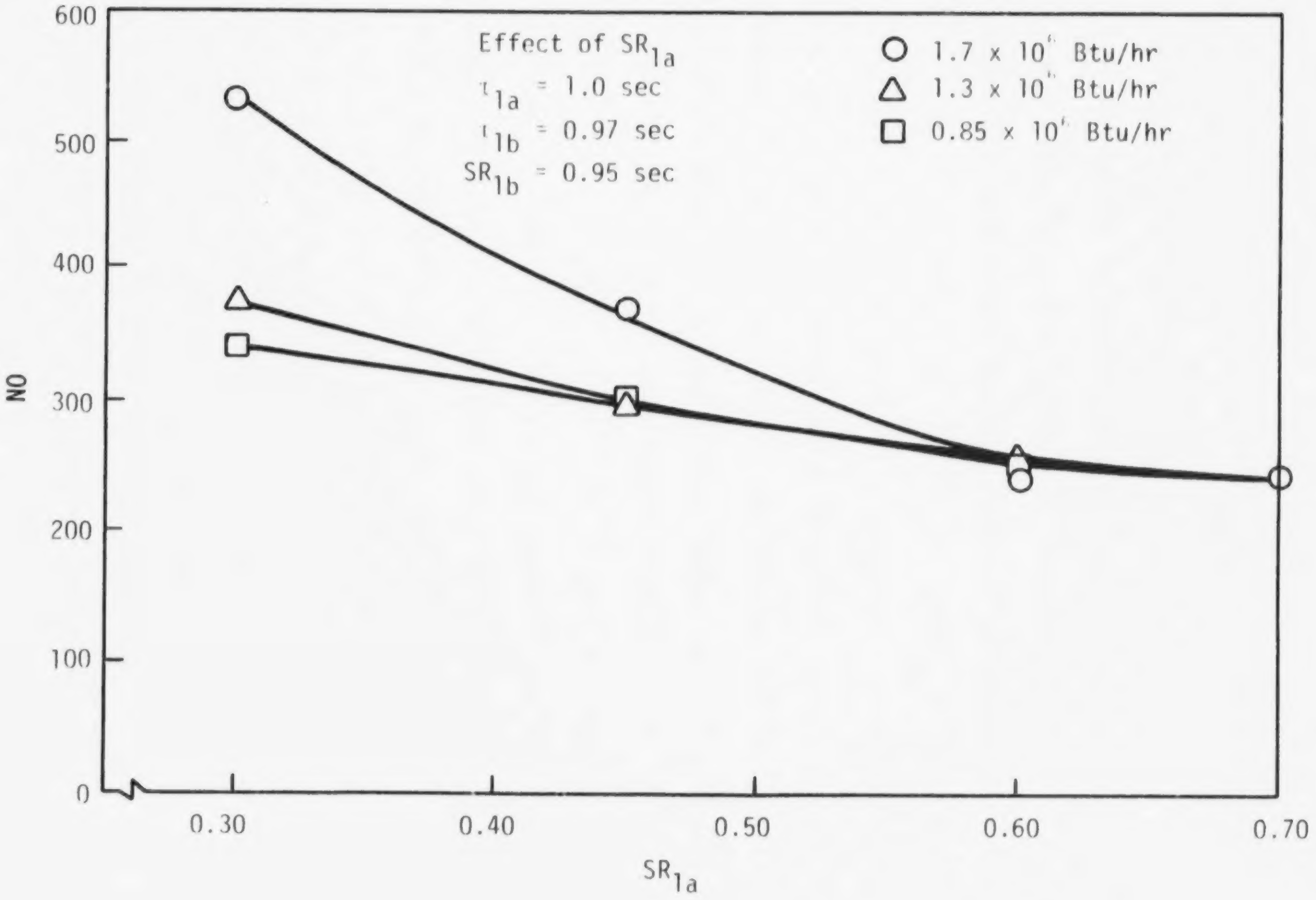

Figure 2-9. Effect of SR_{1a}.

of 0.3, but not at 0.6. Previous data (Reference 1) indicated the higher the first-stage temperature, the greater the decay rate in the first stage. Thus, it is possible that there are competing effects with an optimum decay at the high load and 0.6 stoichiometric ratio, while at the 0.3 SR_{1a} greater heat release is experienced in the second stage causing the second-stage NO to increase. In fact, this is a possible explanation for the decrease of NO with increasing stoichiometric ratio up to an SR_{1a} of 0.7. (It is known from previous work that the NO will again increase beyond an SR of 0.7).

2.3.2 1b Stage Stoichiometric Ratio

The effect of SR_{1b} is shown in Figure 2-10 for an SR_{1a} of 0.3 and 0.6. As can be seen, NO always increased with an increase in SR_{1b}. Again, this may be either due to the greater degree of oxygen availability or may reflect an increase in flame temperature in the 1b stage. This data is also interpolated data at constant residence times in the 1a and 1b stages.

2.3.3 Residence Time, 1a stage

The effect of the 1a stage residence time is shown in Figure 2-11 and 2-12 for an SR_{1b} of 0.80 and 0.95, respectively, and an SR_{1a} of 0.6 (the point at which minimum NO occurred). The data for the three firing rates is also included on these plots. These data are stack emisions at an overall excess air level of 15 percent. The data indicates a strong decay between 0.5 to 1.0 second at all loads and then a decrease in the decay rate following 1.0 second. The data also suggest that at the higher load the initial NO levels are higher, but the decay rate is also higher resulting in lower NO levels after a τ_{1a} of 1.0 second. This is consistent with previous results which show lower NO levels at higher load or first-stage temperatures. The main conclusion from this curve is that little

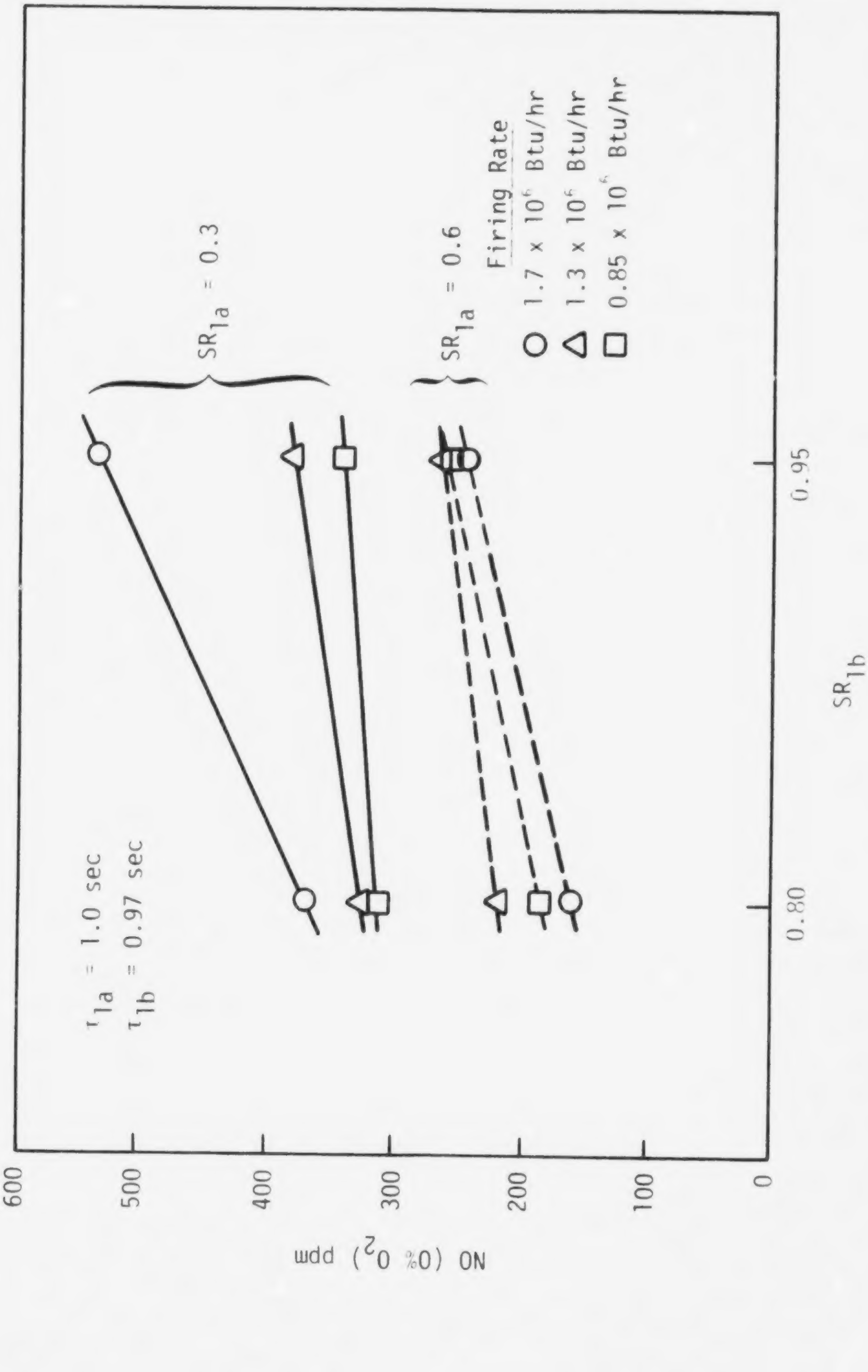

Figure 2-10. Effect of SR_{1b}.

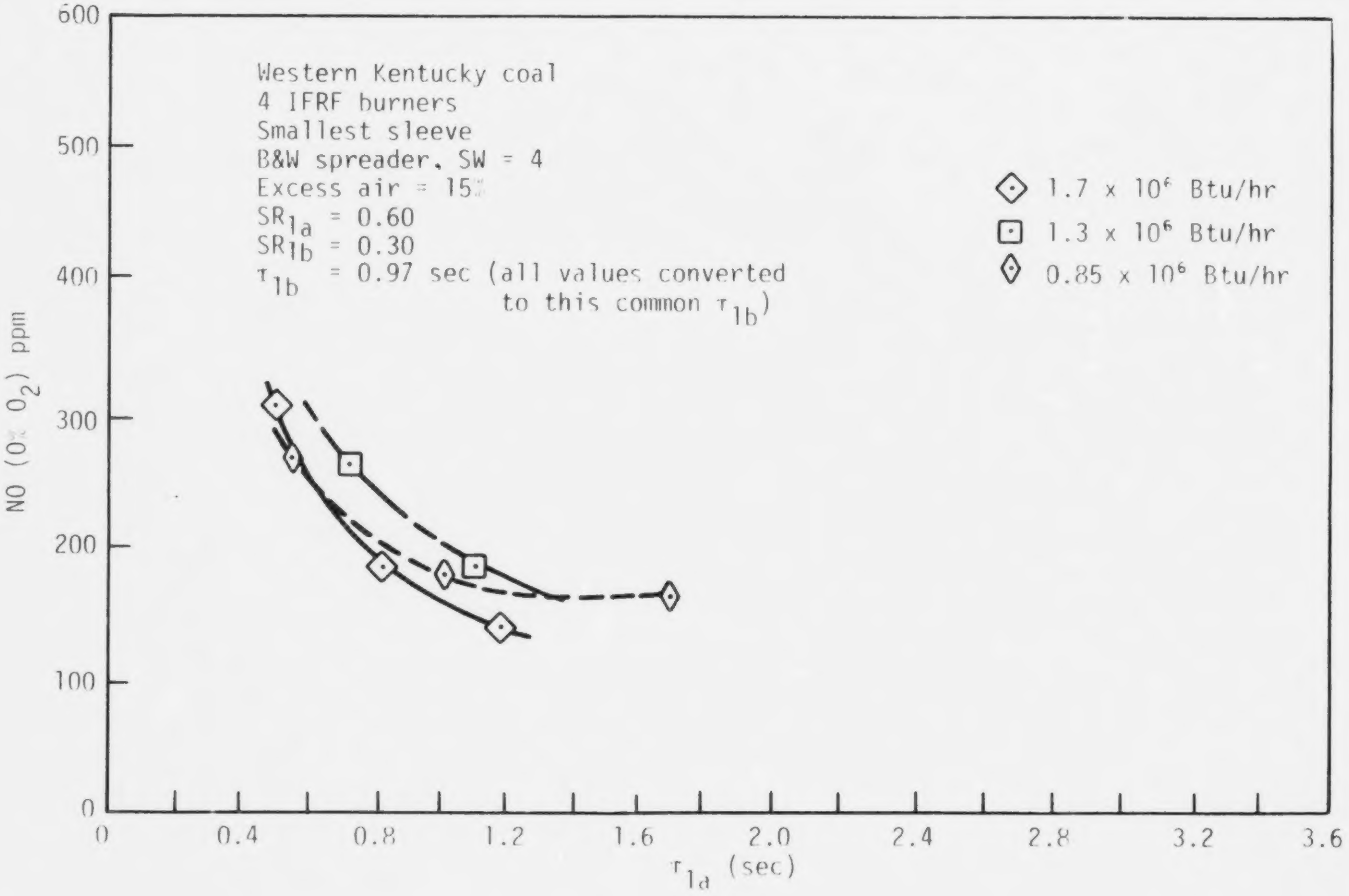

Figure 2-11. Effect of 1a stage residence time.

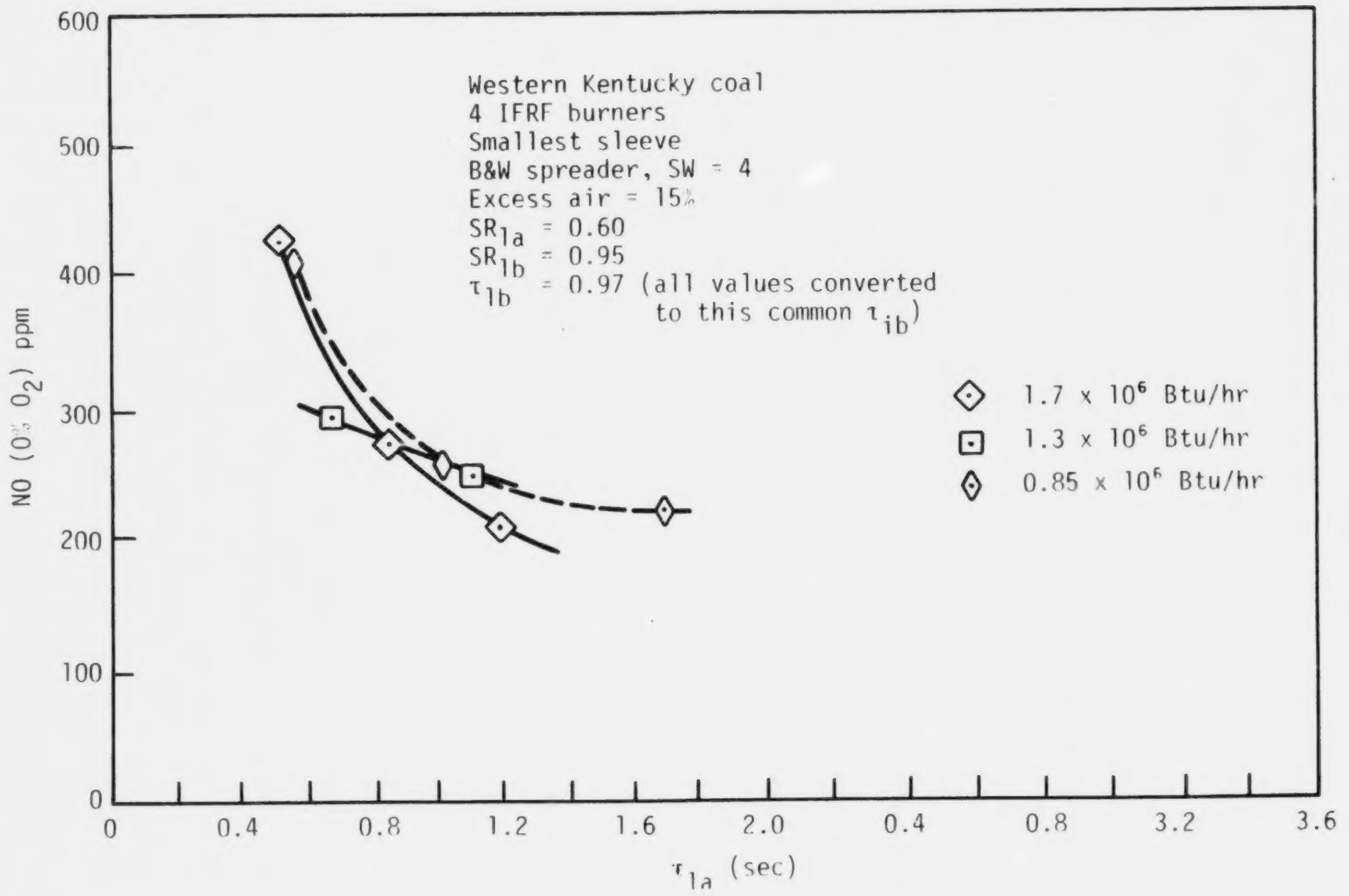

Figure 2-12. Effect of la stage residence time.

additional benefit is gained past a residence time of about 1 second. Similar curves were made for lower SR_{1a}'s and the general trend is the same as at this stochiometry. These curves were used to determine the real effect of the 1a stage stoichiometry at a constant τ_{1a} presented earlier.

2.3.4 Residence Time, 1b Stage

The slow decay experienced in the 1a stage past a residence time of 1 second appears to continue in the 1b stage as shown in Figure 2-13 at an SR_{1b} of 0.80. This data is at a constant injection position so that τ_{1a} will be varying with SR_{1a} and firing rate. However, at the third tertiary air position, the residence time for most SR_{1a}'s and firing rates is sufficiently long (>1.0) that the 1a stage residence time should not seriously effect the results. It is thus interesting to note that the data at a firing rate of 1.3 and 1.7 x 10^6 Btu/hr coincides at the same 1a stage stoichiometric rato. However, at the lower firing rate of 0.85 x 10^6 Btu/hr, the NO levels appear to be a bit lower. This could possibly be due to the longer residence time in the 1a stage and/or due to a lower temperature environment. In the 1b stage at an SR_{1b} of 0.95, the decay rate was generally less than at an SR_{1b} = 0.80 as illustrated in Figure 2-14.

In summary then, stack NO levels decayed both in the 1a stage and the 1b stage. The decay appears to be fairly rapid in the initial 1 second in the 1a stage, then drops off to a relatively slow decay in the 1b stage.

2.3.5 Firing Rate

In the previous sections on the effects of SR_{1a}, SR_{1b}, τ_{1a} and τ_{1b}, the effect of firing rate has been discussed. Since firing rate effects both local mixing, temperature and residence time between two given points, it is often difficult to determine which of these effects is is predominant.

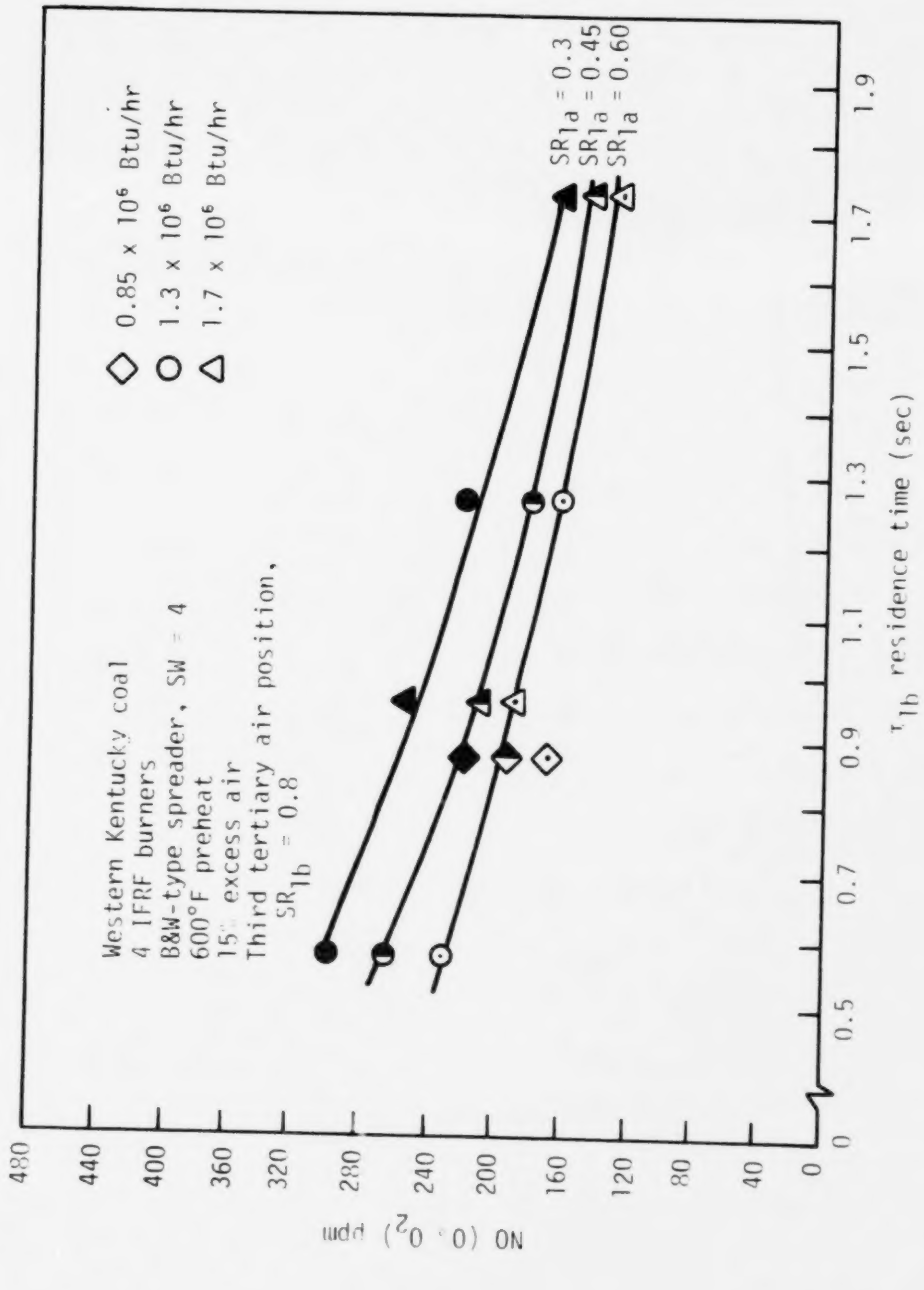

Figure 2-13. Effect of 1b stage residence time.

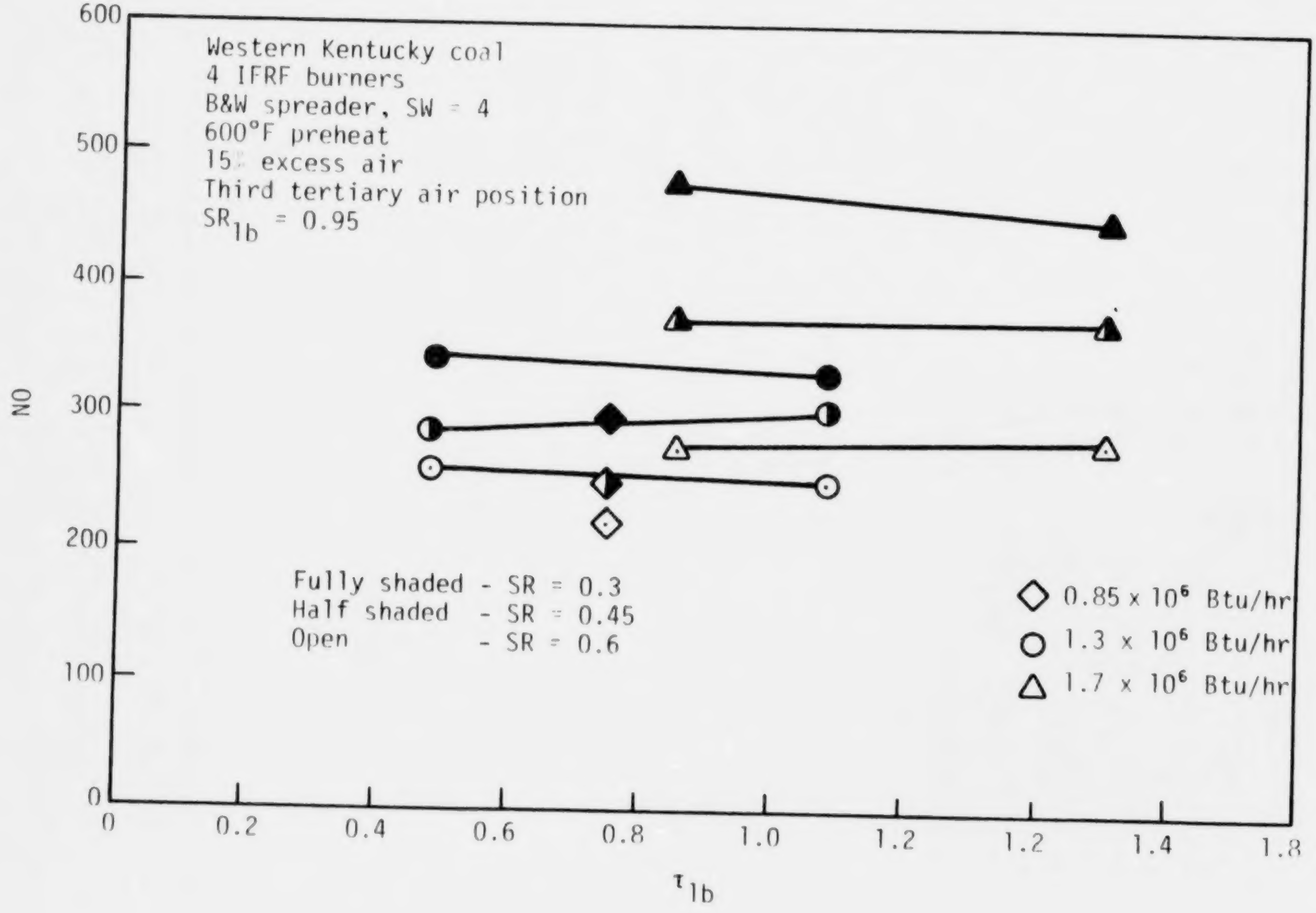

Figure 2-14. Effect of 1b stage residence time.

Thus, we see different effects depending on SR_{1a} and SR_{1b}, or τ_{1a}. However, in summary, the only area where the attributes of firing rate are beneficial is at the optimum SR_{1a} of 0.6 and a $\tau_{1a} > 1.0$ seconds with either an SR_{1b} of 0.80 or 0.95. It is believed this is primarily due to a more rapid decay rate in the 1a stage associated with higher temperature.

2.3.6 Effect of Temperature

Except for the resultant effect of temperature noted in the previous section due to firing rate, only a few tests were run with no preheat to the secondary air. These tests run at a firing rate of 0.85 x 10^6 Btu/hr showed no significant effect. It is possible that the change in secondary air temperature was not significant enough to change the combustion temperatures.

2.3.7 Comparison with Conventional Staging

The question may be asked: Has anything really been gained by going to this more complex staging arrangement? Table 2-5 will aid in answering this question. Let's consider the optimum $SR_{1a} = \sim 0.6$ seconds in the 1a stage with an SR_{1b} of 0.95 at a residence time of 0.97 seconds. This yields a stack NO level of about 400 ppm. The average stoichiometric ratio over this time period is about 0.82. Now conventional staging at an SR = 0.95 yields an NO level of about 700 ppm. However, at an SR close to the average for the total residence time of 1.57 seconds, 400 ppm is also achieved. Thus, it appears that the distributed air concept has not really improved upon the conventional staging result unless it is better to be at a very low SR for a brief period followed by a higher SR for another time element as opposed to being at the average stoichiometric ratio for the total time period. A similar conclusion is drawn at an SR_{1a} of 0.6 and SR_{1b} of 0.80. In fact, it

TABLE 2-5. DISTRIBUTED AIR VERSUS CONVENTIONAL STAGING

Arrangement Stage	SR	τ (sec)	NO (0% O_2) ppm
Case 1			
Distr. air 1a	0.6	0.6	
1b	0.95	0.95	
	avg. 0.82	Total 1.57	400
Conventional staging	0.95	1.57	700
Conventional staging	0.85	1.57	400
Case 2			
Distr. air 1a	0.6	0.5	
1b	0.8	0.97	
	avg. 0.73	Total 1.57	300
Conventional staging	0.75	1.57	250

appears the conventional staging produces even lower NO levels than the distributed arrangement for the same time period for this particular combination.

2.4 CONCLUSIONS

In summary, a number of tests were conceived to explore a distributed air concept to achieve low NO_x emissions in a relatively short overall residence time. This concept had proven successful in a premixed, small-scale facility. Unfortunately, the results of the current study did not achieve any improvement in the NO_x time to staging results achieved with conventional staging. This may be explained partly by the fact that a diffusion flame was utilized in this experiment as opposed to a premixed flame in the smaller scale experiment. Attempts were made to achieve as premix a situation as possible by utilizing four burners and increasing the burner exit velocity to effect a high mixing rate near the burner. However, the diameter of the firebox (33 inches) results in a relatively low L/D for any given residence time, especially compared to the Pershing facility (Reference 2). Table 2-6 compares these two facilities.

TABLE 2-6. FACILITY CHARACTERISTICS

Parameters	EPA Hor. Ext.	Pershing
Diameters (in.)	33	6
Length (in.) for ~1 sec residence time	12	54
L/D	0.364	9

Thus, at the shorter bulk residence times in the EPA facility, it will be difficult to achieve a real bulk residence time. That is, the real residence time, for residence times under 1 second, will be much less than the bulk residence time due to a nonuniform velocity profile across the diameter of the firebox.

It was found that with the distributed air approach, NO levels increase with decreasing SR below an SR of about 0.6. In addition, NO always decayed with increasing residence time in both the 1a and 1b stages.

In conclusion, no advantage was found for the distributed air concept as applied to the diffusion burner arrangement in the EPA Multiburner Facility.

SECTION 3

COAL/OIL MIXTURE TESTS

As part of the Phase III alternate fuels testing, an emissions evaluation test program was developed to look at coal/oil mixtures (COMs) fired in a simulated package boiler configuration. Supplementing industrial oil supplies with coal in the form of coal/oil mixtures has been investigated for nearly 100 years (Reference 4). Over this period, the feasibility of coal/oil technology has been demonstrated in both small-scale testing and practical application.

With new interest in this technology, it is necessary to determine if technology developed to minimize the environmental effects of coal combustion is applicable to coal/oil systems or if further work is necessary to ensure that pollution standards can be met.

OBJECTIVE

The purpose of this study was:

1. To obtain emission data for coal/oil combustion in an environment closely simulating an industrial package boiler
2. To determine if emission levels were affected by the fuel composition
3. To determine if conventional control technology developed for coal is effective in reducing emission levels produced by coal/oil combustion

4. To investigate the effect of burner modification on emission levels produced by coal/oil combustion

Facility

This study was conducted in the EPA Multifuel Furnace Facility. The experimental facility, as shown in Figure 3-1 and described in detail elsewhere (Reference 1), was designed to simulate the aerodynamics of either a front-wall fired or tangentially-fired boiler.

In order to simulate the heat release and temperature profiles consistent with typical industrial package boilers, the additional modifications, as shown in Figure 3-2, were made. This configuration uses horizontal extension sections that can be attached to the main firebox. These 33-inch inside diameter by 6' long refractory-lined sections allowed the simulation of a tunnel-fired unit and staging of combustion air at residence times typical of what would be available in a package boiler. Additional hardware included water tubes placed in the horizontal extension sections for additional heat absorption in the radiant section, and a heat exchanger placed between the firebox and the horizontal extensions to achieve a gas temperature profile consistent with the radiant and convective sections in a typical industrial package boiler.

The burner used for the study was an IFRF 1.5 x 10^6 Btu/hr wall-mounted unit. This burner is a versatile experimental swirl block burner patterned after that developed by Beér (Reference 5). During baseline tests on the parent coals, a Babcock and Wilcox-type coal spreader was used to achieve a turbulent flame condition. Two commercial fuel oil atomization nozzles were tested with the coal/oil mixture. These were the Delavan Corporation swirl-air nozzle, shown in Figure 3-3, and the Sonic Development Corporation Sonicore nozzle, shown in Figure 3-4. The burner was modified

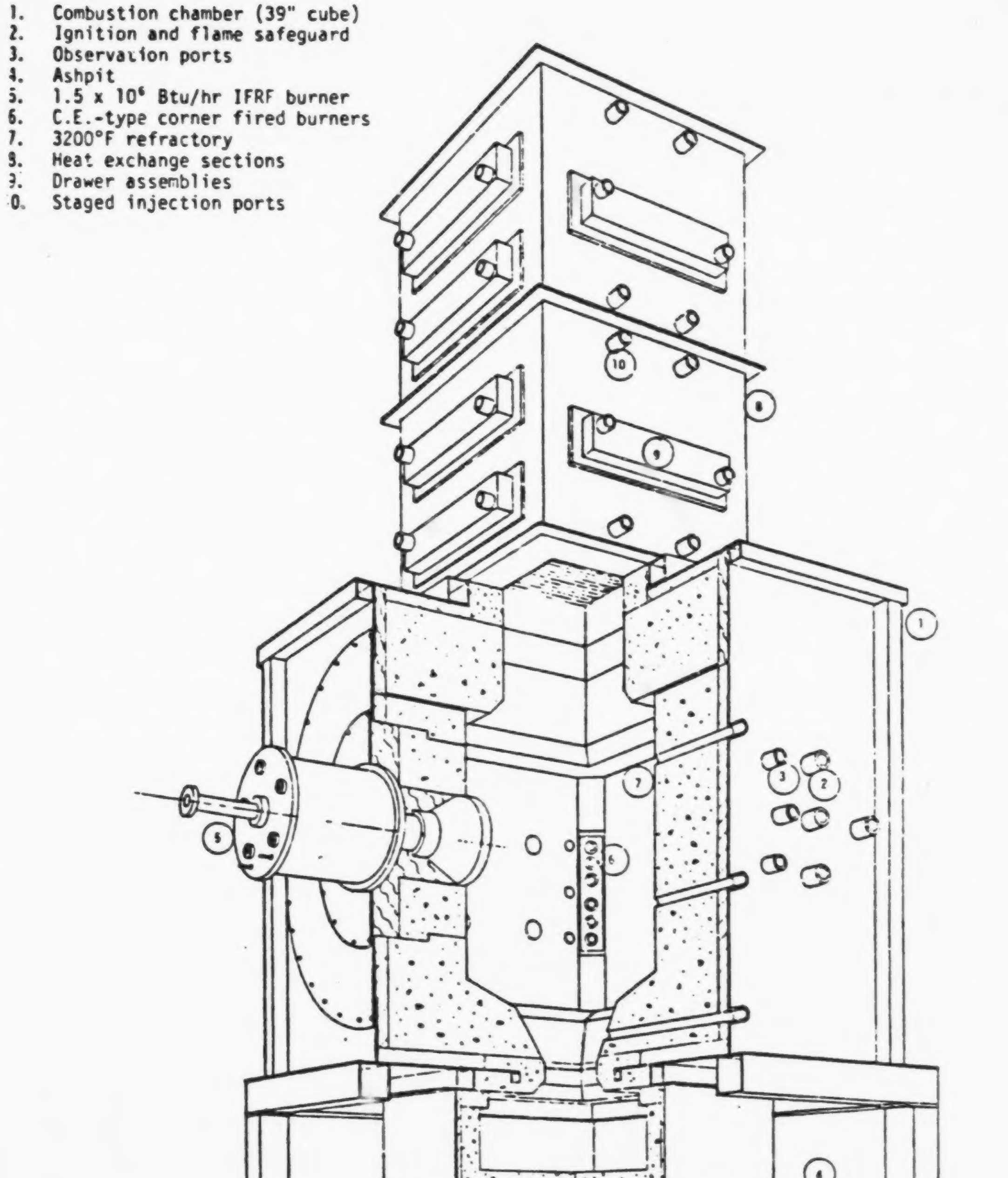

1. Combustion chamber (39" cube)
2. Ignition and flame safeguard
3. Observation ports
4. Ashpit
5. 1.5×10^6 Btu/hr IFRF burner
6. C.E.-type corner fired burners
7. 3200°F refractory
8. Heat exchange sections
9. Drawer assemblies
10. Staged injection ports

Figure 3-1. Acurex/EPA multifuel furnace.

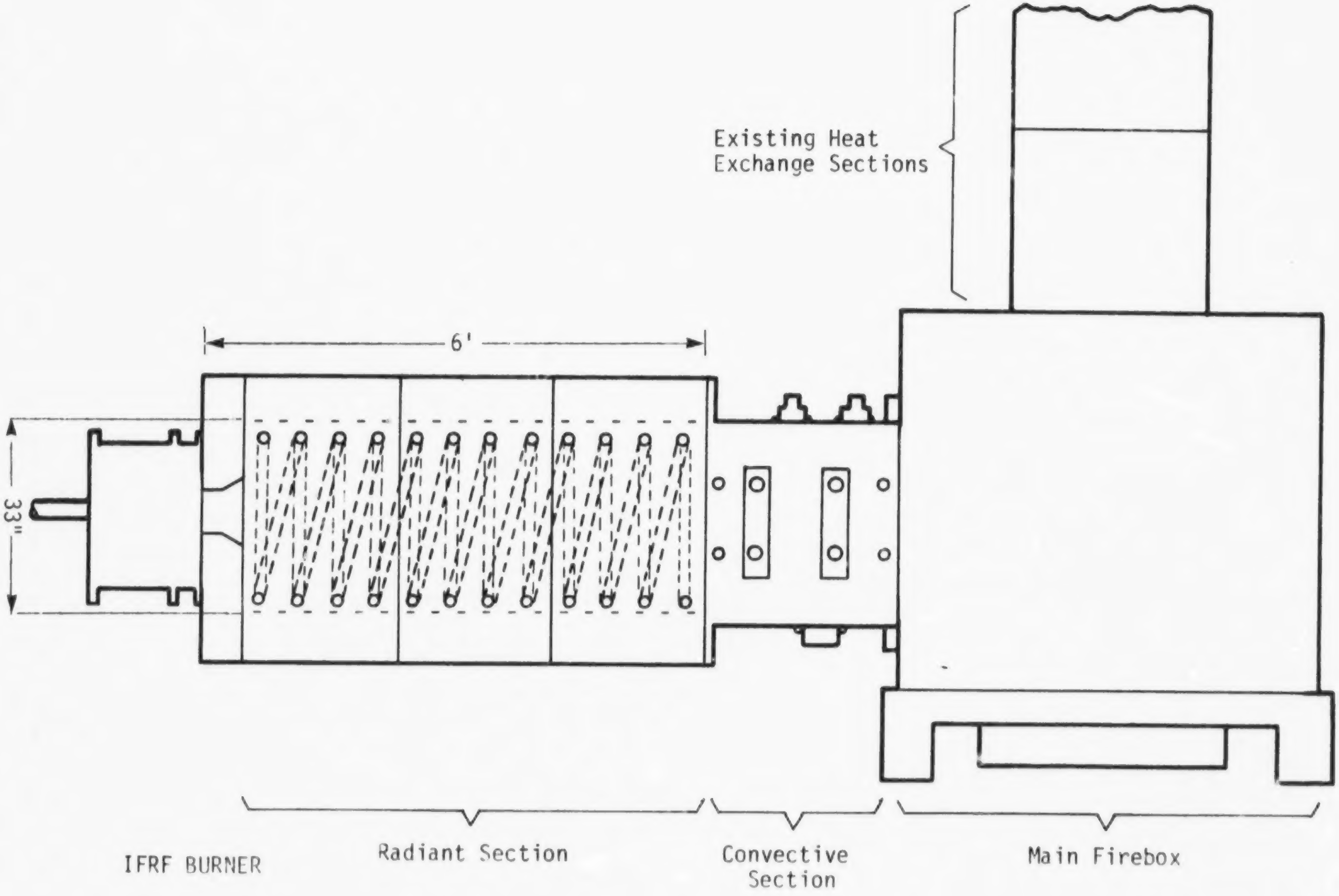
Existing Heat
Exchange Sections
6'
33"
IFRF BURNER
Radiant Section
Convective
Section
Main Firebox

Figure 3-2. Facility modifications.

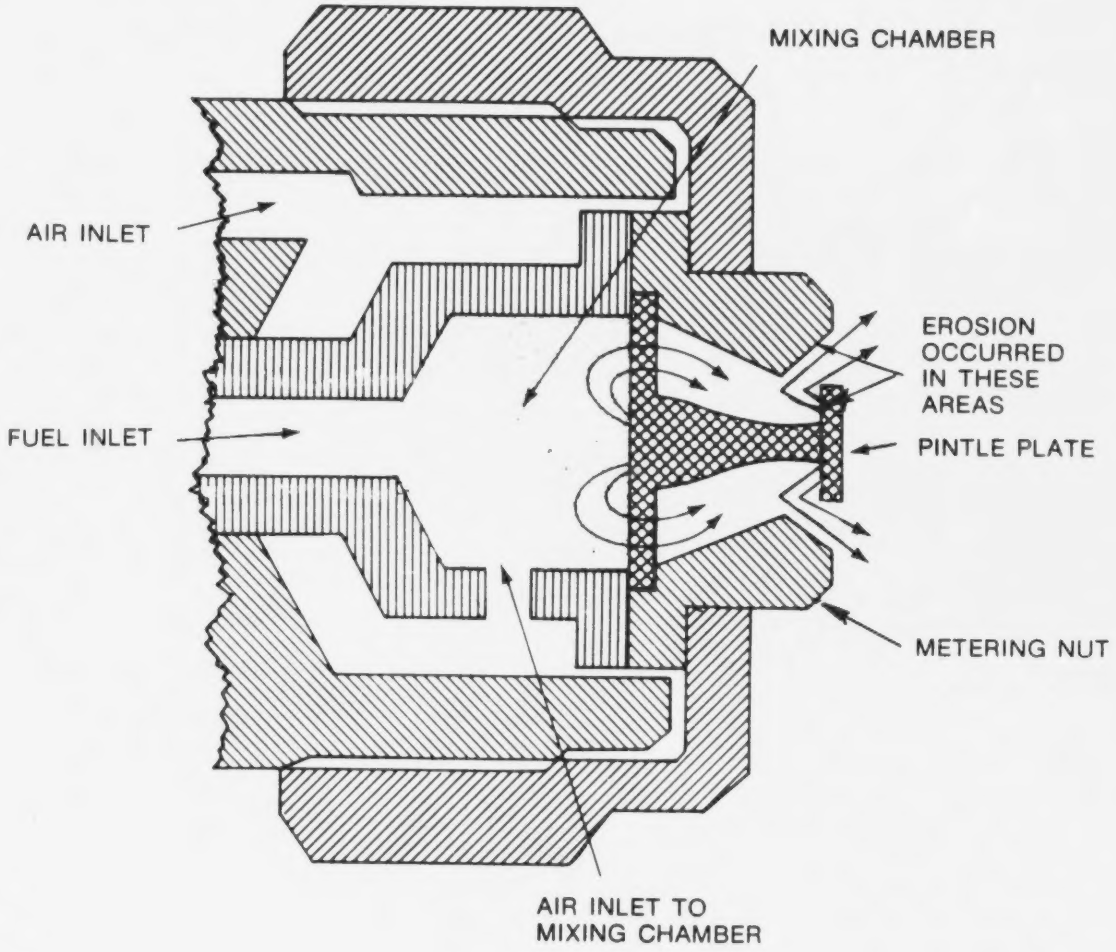
MIXING CHAMBER
AIR INLET
EROSION OCCURRED IN THESE AREAS
FUEL INLET
PINTLE PLATE
METERING NUT
AIR INLET TO MIXING CHAMBER

Figure 3-3. Delavan swirl-air nozzle, 33373-1, 60 gph, 70° spray angle, mild steel construction.

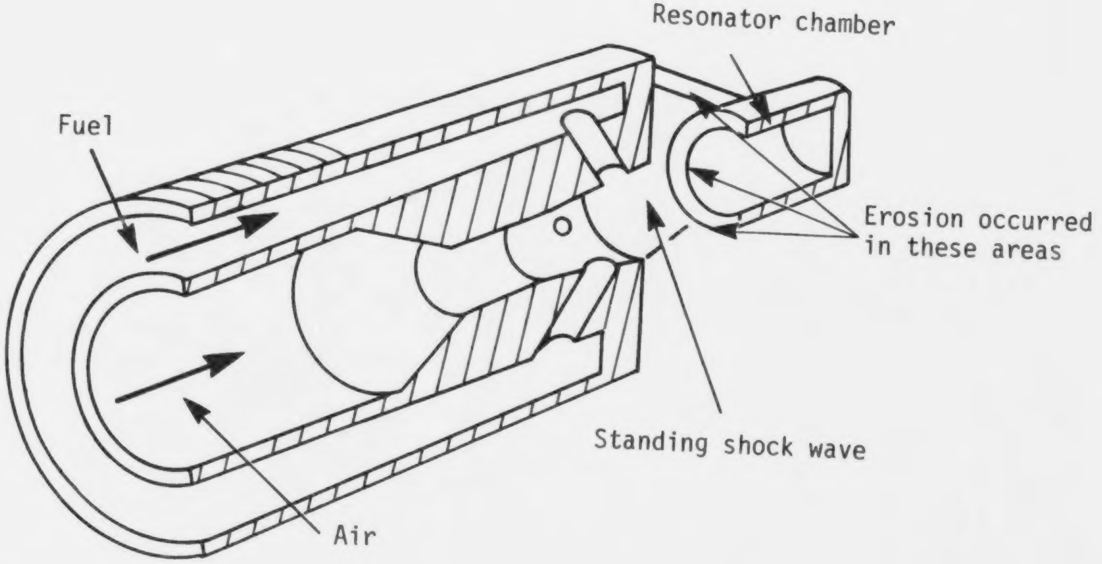
Resonator chamber
Fuel
Erosion occurred in these areas
Standing shock wave
Air

Figure 3-4. Sonic Corporation Sonicore nozzle, 281T-B-11 with stellite resonator chamber.

for a low NO_x configuration by placing an annulus of tertiary air around the diffusor. This will be described later.

Emissions Monitoring Equipment

Continuous monitoring equipment was utilized to collect and record data during this study. Table 3-1 lists the instrumentation used and the principle of operation for each unit.

Fuel Preparation

The coal/oil mixtures examined in this study were prepared from parent fuels which represent a broad range of classifications and fuel compositions. The compositional analyses of the parent fuel oils are listed in Table 3-2 and that of the parent coals in Table 3-3. From these parent fuels, four mixtures of 30 percent by weight coal to oil were prepared. Table 3-4 lists the mixtures and their compositional analyses.

The coals, pulverized to 70 percent through 200 mesh, were blended with the fuel oils in a high turbulence batch mixer supplied by Littleford Brothers. A suspension additive, supplied by Carbonoyl Co., was added to ensure a homogeneous mixture. The additive was prepared as a 5-percent aqueous solution and constituted a 3.75-percent by weight of the total mixture. The mixture was prepared on a batch basis and 55-gallon drums were used to store the fuel. The mixtures were stored at ambient temperatures (50 to 60°F) for up to 21 days before they were fired.

Approximately 4 hours prior to use, each drum was wrapped with heating blankets, and a mixer with a 6-inch propeller was immersed in the mixture. The propeller was located approximately 6 inches from the drum bottom. The mixture was heated and agitated utilizing a pump recirculation system until the mixture temperature reached 150 to 170°F. The mixture was then pumped

TABLE 3-1. EMISSION MONITORING EQUIPMENT

Pollutant	Principal of Operation	Manufacturer	Models	Instrument Range
NO	Chemiluminescence	Ethyl Intertech	Air Monitoring	0-5 ppm 0-10 0-100 0-250 0-1000 0-5000
SO_2	Pulsed Fluorescent	Thermoelectron	Teco Model 40	0-50 ppm 0-100 0-500 0-1000 0-5000
CO	Nondispersive Infrared (NDIR)	Ethyl Intertech	Uras 2T	0-500 ppm 0-2000
CO_2	Nondispersive Infrared (NDIR)	Ethyl Intertech	Uras 2T	0-5% 0-20%
O_2	Paramagnetic	Ethyl Intertech	Magnos 5A	0-5% 0-21%
Particulate Loading	Cyclone and Filtration	Acurex Corp	HVSS	0-3 μm Minimum

TABLE 3-2. FUEL OIL ANALYSES

Specifications Fuel Oil	Amerada Hess #6	Chevron #6
API Gravity	15.3	12.3
Flashpoint, COC°F	204.0	182.0
Viscosity, SSU at 100°F	2,500.0	4,900.0
Heat of Combustion Btu/lb	19,867.0	18,292.0
Ultimate Analysis (% Wt)		
Carbon	84.71	85.57
Hydrogen	10.75	10.52
Nitrogen	0.36	0.81
Oxygen	1.93	2.08
Sulfur	2.22	0.93
Ash	0.03	0.09

TABLE 3-3. COAL ANALYSES, AS-RECEIVED BASIS

Proximate (% Wt) Coal	Montana	Virginia	W. Kentucky
Moisture	21.23	0.31	5.0
Volatiles	35.16	31.9	36.55
Fixed Carbon	34.27	51.4	50.98
Ash	9.34	16.5	7.47
Rank	Sub-bit.C.	High-Vol. A	High-Vol. B
Ultimate (% Wt)			
Carbon	53.26	71.11	69.79
Hydrogen	3.35	4.46	4.79
Nitrogen	0.87	1.68	1.34
Oxygen	11.16	4.24	8.65
Sulfur	0.78	2.02	2.95
Ash	9.34	16.5	7.47
Heat of Combustion, Btu/lb	8,972	14,079	12,349

TABLE 3-4. COAL/OIL MIXTURE ANALYSES, AS-RECEIVED BASIS, 30% COAL BY WEIGHT

Mixture 30% (Wt) Coal / Analysis	W. Kentucky/ Amerada	Montana/ Amerada	Montana/ Chevron	Virginia/ Chevron
Carbon	80.23	75.27	75.88	81.23
Hydrogen	9.00	8.57	8.37	8.70
Nitrogen	0.63	0.49	0.83	1.07
Oxygen	3.92	4.67	4.77	2.73
Sulfur	2.44	1.79	0.89	1.26
Ash	2.26	2.82	2.87	4.95
Moisture	1.52	6.39	6.37	0.09
Heat of Combustion, Btu/lb	17,600	16,600	15,500	17,000

into the coal/oil mixture delivery system, shown schematically in Figure 3-5. After each drum was emptied, the drums were inspected for settling of solids. In all cases, little or no deposits were noted. The delivery system consists of a 120-gallon capacity heated storage tank with an agitation system similar to the one described above. The fuel was kept well agitated and at 180 to 200°F. The mixture was delivered to the burner, through heat traced lines and an electrical heater, via a Viking C-32 rotary pump with a varispeed control. A recirculation loop ensured that a homogeneous mixture was maintained between periods of mixture firing.

A summary of the problem areas associated with this flow system include the following:

- Coal settled out over a period of time in the bottom outlet of the fuel holding tank causing complete plugging.
- Plugging of lines in any low section of piping. Adequate velocities must be maintained to keep the material entrained.
- Shorting of electrical heat tape elements on piping and drums. It is recommended that steam tracing be used if at all possible in future tests.
- Deterioration of pump performance due to wear at the seals and increased clearances. Special seals for handling this very abrasive mixture should be considered when pumping COM
- An immersion heating element was used in the drums for initial heating of the mixture before transfer to the holding tank. If the mixture had settled these elements would not heat the mixture uniformly and fires could easily develop. Also the tanks could

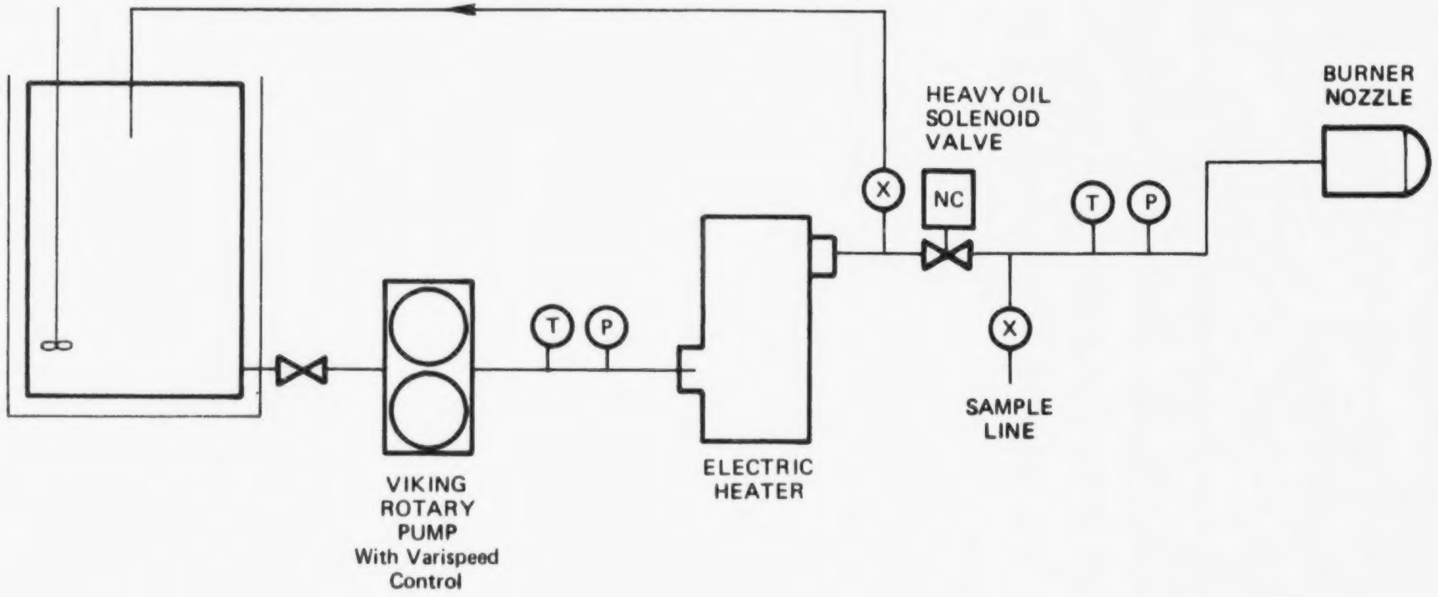
HEAVY OIL SOLENOID VALVE
BURNER NOZZLE
NC
X
T
P
X
T
P
SAMPLE LINE
VIKING ROTARY PUMP With Varispeed Control
ELECTRIC HEATER

Fuel 3-5. Coal/oil delivery system.

not be mixed successfully until they were thoroughly heated. Thus it was found to be quite difficult to get these drums reheated and well mixed after they had been setting for several days.

- The most difficult task was pumping the mixture from the drums to the holding tank. The pump performance frequently deteriorated to the point where it would not draw from the drum. This was of course hampered by reheating the drum and getting the material well entrained.

3.1 TEST PLAN

The tests were planned around a range of fuel types, three coals and two oils, to determine if emission levels both under baseline and incorporating NO_x control technologies are dependent on fuel types. Table 3-5 lists the baseline test matrix for the fuel combinations of interest. Initially a 50 percent mixture of the various fuels was to be tested but because of budget constraints and the mixing/handling problems encountered, it was decided, with the project officer's concurrence, to limit the testing to 30 percent concentration of coal. The baseline tests were run at 20, 30, and 40 percent excess air levels at a firing rate of 1.8×10^6 Btu/hr. This firing rate gave a heat release per unit volume of about 50,000 Btu/hr-ft^3 which is typical of package boilers. The coal tests were run with a B&W-type coal spreader with 15 percent primary air, and the coal and oil tests were run with the Sonicore nozzle.

Table 3-6 shows the matrix for the effect of load and the effect of residence time with staging as the NO_x control technique. All of these tests were run at 20 percent excess air and 30 percent COM. Table 3-7 lists the

TABLE 3-5. BASELINE MATRIX

				Pure Fuels					Coal/Oil Mixtures					
				Western Kentucky Coal	Montana Coal	Virginia Coal	Chevron Oil	Pennsylvania Oil	Coals					
									Western Kentucky		Montana		Virginia	
									Fuel Oils					
									Chev	PA	Chev	PA	Chev	PA
Pure Coal	100%	Excess Air	40	225d	226c	226g								
			30	225c	226b	226f								
			20	225b	226a	226e								
Coal/Oil Mixture	30%		40							217d	221b	221r	218b	
			30							217e	221a	221q	218a	
			20							217f	221c	221n	218c	
Pure Oil	0%		40				217c	222g						
			30				217a	222f						
			20				217b	222e						

TABLE 3-6. EFFECT OF LOAD AND RESIDENCE TIME

Stage	Tertiary Distribution	Primary SR_{1a}	Coal/Oil Mixture 30%					
			Mont/Chev		WKC/PA		VA/Chev	
			Load x 10^6 Btu/hr					
			1.2	1.8	1.2	1.8	1.2	1.8
Residence Time – Short	SR_1 – 1.20	0.85		223f		217k		220g
		0.75		223g		127ℓ		220h
		0.65	224ℓ	223h		217n		220i
		0.55	224j	223i		219o		220j
	SR_1 – 0.95	0.85		223o		219a		221f
		0.75		223m		219b		220j
		0.65		223k		219c		220k
		0.55		223j		219d		220ℓ
Residence Time – Long	SR_1 – 0.95	0.85						
		0.75						
		0.65						
		0.45						

TABLE 3-7. DISTRIBUTED AIR BURNER TESTS

Stage	1st stage SR_1	Large IFRF Burner 20% Excess Air					
		30% COM					
		Mont/Chev		WKC/PA		VA/Chev	
		Load x 10^6 Btu/hr					
		1.2	1.8	1.2	1.8	1.2	1.8
Residence Time—Long	0.95	224c	222c	222c			
	0.85	224d	223b	223b			
	0.75	224g	221h	221h			
	0.65	224h	223e	223e			
Residence Time—Short	0.95	224b	221d		217g		218f
	0.85	224e	221e		217h		218g
	0.75	224f	221g		217i		218h
	0.45	224i	222d		217j		218i

tests for the low NO_x burner and combined low NO_x burner and staging configurations. The purpose of this matrix was to look at the effect of these control technilogies on three fuel combinations. A range of the control core stoichiometric ratios were tried with and without staging. Finally a few tests were run by doping the fuels with pyridine and/or thiophene to increase the nitrogen and sulfur levels appropriately. These tests are shown in Table 3-8. A comparison of stack emissions with these dopants or with fuels that naturally had these levels would then be possible. On all of these matrices the test number has been given so that reference to the emission levels may be determined from the listing in the appendix.

3.2 TEST DATA

The testing was divided into three phases. In Phase I the combustion stability of each fuel was evaluated and delivery conditions were adjusted for optimization of flame stability and combustion.

In Phase II of the study, some of the established combustion control technologies for pulverized fuel were applied to the coal/oil mixtures. These included staging of combustion air (Reference 6) and burner air distribution (Reference 7). Flue gas recirculation, which has been found to be effective in reducing thermal NO (Reference 6), was not applied due to equipment problems.

The last phase of the program was to evaluate fuel nitrogen conversion by addition of dopant to the feed system. Results from each of these phases will be discussed in the following sections. In addition, comparison will be made with data taken during a previous DOE-supported test in this same facility. Details of the DOE tests may be found in the appendix.

TABLE 3-8. EFFECT OF FUEL NITROGEN

		% Sulfur (DMMF)*			
		0.9 1.2	1.96	2.2 2.6	3.4
% Nitrogen (DMMF)	1.9 2.1			Virg. Coal 226e	
	1.4 1.6				W. Kent Coal 225b
	1.0 1.3	Montana Coal 226a Virginia/Chev 218c	Mont/Amer + N 221o	Va/Chev + S 221k Va/Chev + S 221m	
	0.7 1.0	Chevron Oil 217b Mont/Chevron 221c	Mont/Amer + N 221p		
	0.5 0.7		Mont/Amerada 221n	W. Kent/ Amerada 217f	
	0. 0.5			Amerada Oil 222e	

*DMMF: Dry, mineral matter free

3.3 BASELINE TESTS

The baseline tests were designed to determine the optimum burner conditions for each fuel and then the NO emissions as a function of excess air for each parent fuel and fuel combinations. Initially the burner was adjusted (swirl, axial fuel tube position and nozzle atomization rate) for maximum flame stability for each fuel. In all cases, the nozzle position was virtually the same relative to the IFRF burner, i.e., 2 inches forward of the burner throat. However, atomizing air pressure had to be optimized for each of the fuel mixtures. This was due to carbonaecous deposition or "clinkering" on the water-cooled quarl in cases of poor atomization. In general, the atomization pressure ranged from 12.0 to 22.0 psig depending on the fuel. In most cases, this was 2.0 to 4.0 psig greater than the fuel delivery pressure. Throughout the tests, secondary air was preheated to 300°F to enhance solids ignition in the relatively cold environment of the radiant section. Burner swirl was optimized on the parent fuels and on the coal/oil mixtures. A swirl of 5 on a scale of 8 was used for the baseline coal tests, and a swirl of 0 (of 8) was used for both the oil and the coal/oil mixtures throughout the testing. (A zero setting implies no swirl.) Tests conducted earlier at the EPA/Acurex facility for design support of the full scale DOE/Lorillard, Danville, Virginia, COM facility yielded a comparison of the two commercial nozzles described above. After approximately 3 hours of testing on 30-percent coal/oil mixture, utilizing the 440 hardened stainless steel Delavan nozzle, significant erosion was observed. Areas of erosion are shown in Figure 3-3. Equivalent testing with the stellite Sonicore nozzle revealed similar erosion rates in the areas shown on Figure 3-4. However, the erosion had less impact on the atomization characteristics, flame stability and emission levels for the Sonicore nozzle. On this basis, all subsequent coal/oil mixture tests were conducted with the Sonicore nozzle.

Figure 3-6 illustrates the results of the baseline emissions tests. While CO, CO_2, SO_2, and NO data were taken during testing, NO data were considered primarily and will be discussed here. Problems with the SO_2 analysis unit during testing rendered the data useful only on a relative basis. Generally, CO and CO_2 levels which are quantitatively valid reflected good combustion burnout in all cases except during staged combustion tests at long first-stage residence times (1.5 to 2.0 seconds). During these tests, CO levels rose to as high as 800 ppm (0-percent O_2). Detailed emission levels for each test condition may be found in the appendix.

Figure 3-6(a) illustrates NO emission levels from the Chevron No. 6 oil base mixtures along with levels from the parent fuels. As is expected, the NO levels for the mixtures fall in an intermediate range between the parent fuels. The same data for the Amerada-based mixtures are illustrated in Figure 3-6(b). In this case, though, emission levels for the mixtures are very near those of the parent oil. Little contribution from the coal is evidenced. Certainly, there are several possible mechanisms to which this may be attributed. These mechanisms include effects due to sulfur in the fuel, atomization characteristics of the oil, and the manner in which the particular oil and coal volatilize. The volatilization rate of the particular oil surrounding the coal particles may also effect the fate of the fuel nitrogen coming out of the coal. For example, Figure 3-7 shows the boiling point curve for the Chevron and Amerada oils. This shows that the Amerada has a much higher boiling point curve than the Chevron oil. The rate at which the fuel N comes off the oil can also influence these results.

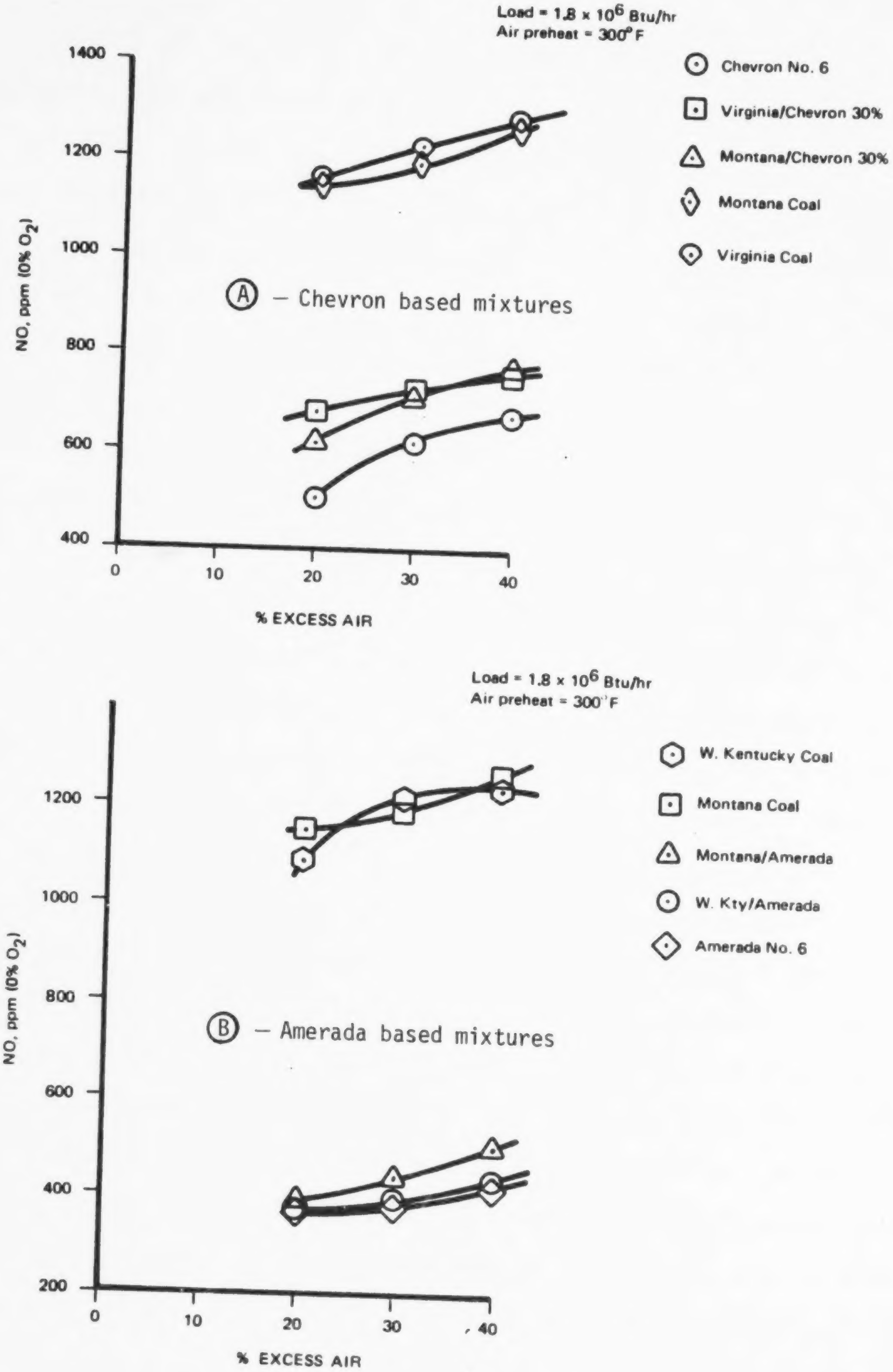

Figure 3-6. Baseline emissions.

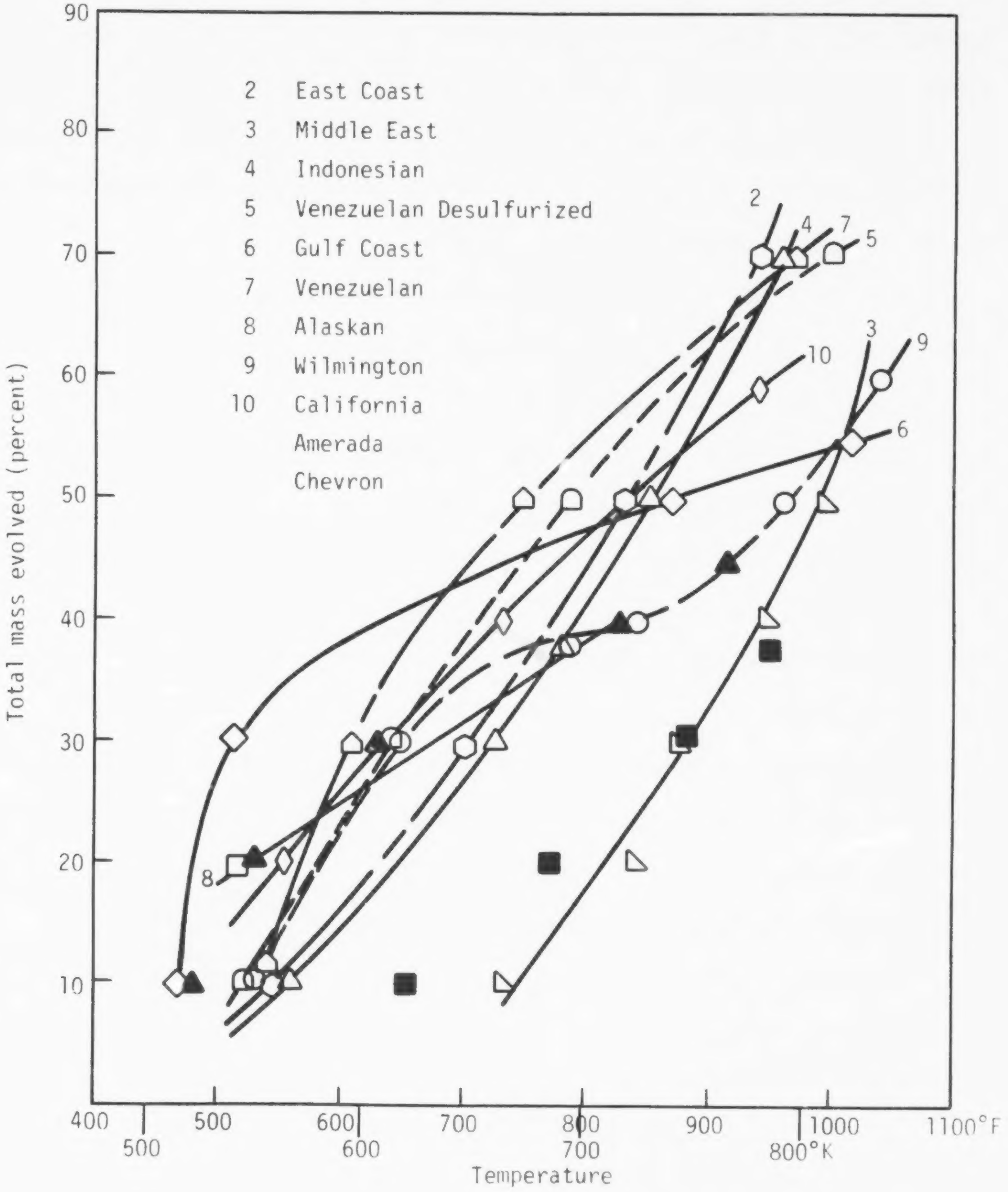

Figure 3-7. Boiling point curves (Reference 8).

Figure 3-8 shows the percent nitrogen evolved as a function of temperature. These curves are shown compared to a variety of other oils (Reference 8). As can be seen from the curve the Amerada oil is one of the more "refractory" as far as N evolution is concerned. These mass and nitrogen evolution rates could indeed play a role in performance of the various fuel combinations to the NO_x control strategies.

At this point there is insufficient data to ascertain which of the various mechanisms is causing this effect. But it is important to note that all fuel combinations do not necessarily behave in the same manner. With regard to the coal baseline tests, the differences between the Montana and Western Kentucky coals are quite minimal and are probably within the error band of the data. The Virginia coal, which consistently showed a higher NO level than the Montana coal, is probably a real effect due to the higher fuel nitrogen in the coal. The comparison of the Montana and Western Kentucky coals differs from previous data (Reference 9). The previous data showed the Montana coal to be consistently above the Western Kentucky coal by about 5 to 10 percent. The main difference between the tests is that in this test the temperatures are 300 to 400°F cooler. It is possible that the volatilization rate of the Montana coal changes with the temperature, and the Montana coal may have had a higher fuel nitrogen evolution rate in the previous tests.

3.4 CONTROL TECHNOLOGY TESTS

The results of staged combustion of the coal-oil mixtures are illustrated in Figure 3-9. As is illustrated, the two Chevron no. 6 oil-based mixtures responded almost identically to the removal of combustion air in the first stage. However, the Amerada-based mixture showed little response

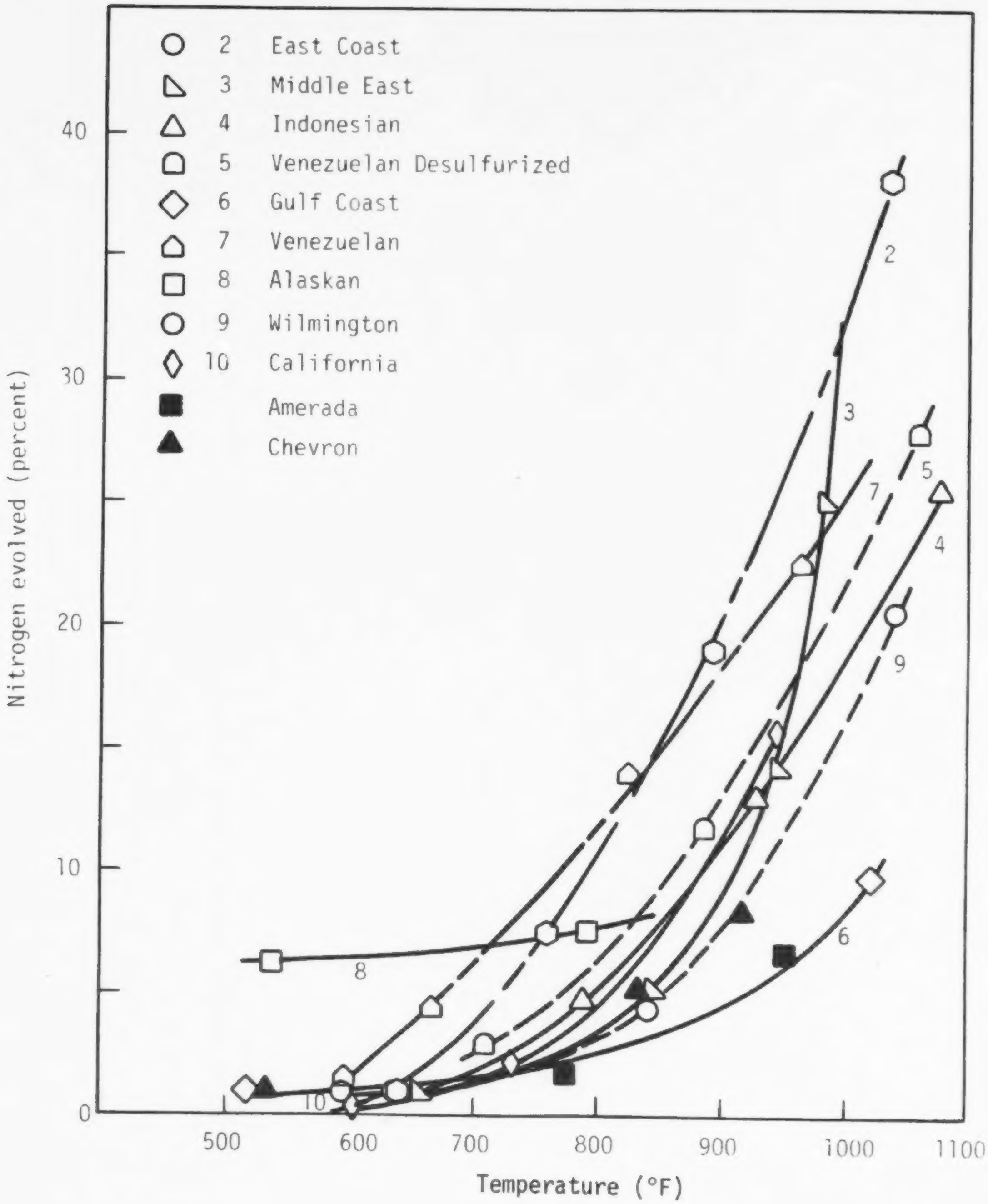

Figure 3-8. Nitrogen evolution curves (Reference 8).

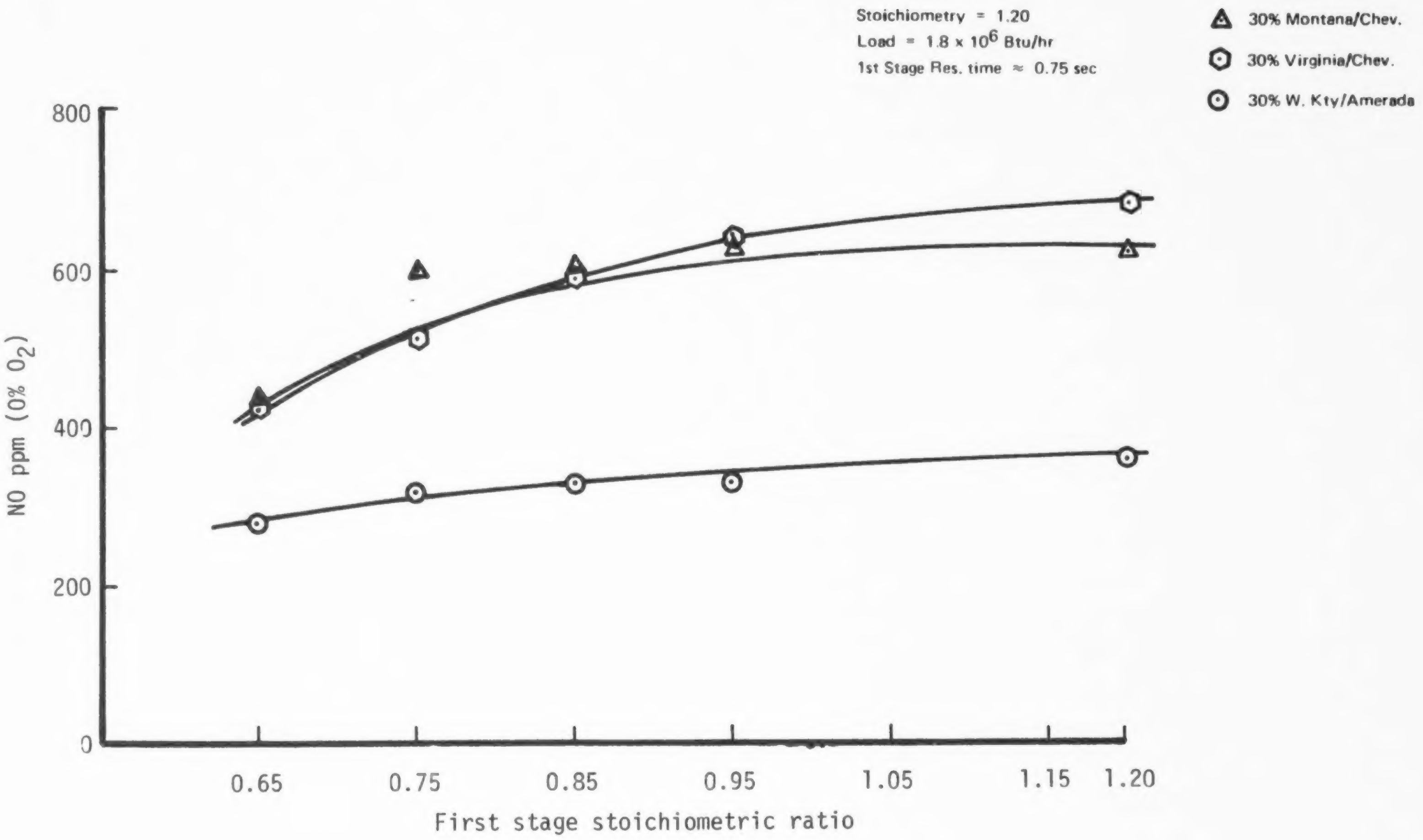

Figure 3-9. Staging emissions.

(10 percent) in emissions reduction. It should be noted from Table 2, that the Amerada no. 6 oil has a very high sulfur content relative to the Chevron parent oil. This compositional difference could possibly have contributed to the ineffectiveness of staging on the Amerada-based mixture NO emissions (References 10 and 11) or it could again be due to the volatilization character of the fuels.

Following the staging tests, distribution of burner air was applied to the mixtures. Figure 3-10 shows the distribution scheme schematically. In these tests air which normally makes up a percentage of the secondary air was injected through an annulus 7 inches radially from the burner throat centerline. This was done in order to enrich the flame core where fuel-bound nitrogen is evolved. The results of this testing are illustrated in Figure 3-11. Each mixture responded favorably to the air distribution, but it is evident that the composition of each mixture leads to a unique emissions curve under these conditions. In this case the Amerada oil-based mixture performed about the same as conventional staging, that is showing little effect to the control technique except when the core was made very fuel-rich. A moderate effect is seen with the Virginia coal/Chevron oil and is again very similar to the conventional staging result. However the Montana/Chevron mixture shows a much more dramatic effect compared to conventional staging, reducing the NO levels by a factor of three. The Montana coal also yielded the lowest NO levels during staging tests in the main firebox during earlier testing (Reference 1).

The curves in Figure 3-12 illustrate the results of applying burner air distribution plus staging vs. straight burner air distribution. The purpose of this comparison was to evaluate the mixture responses to further

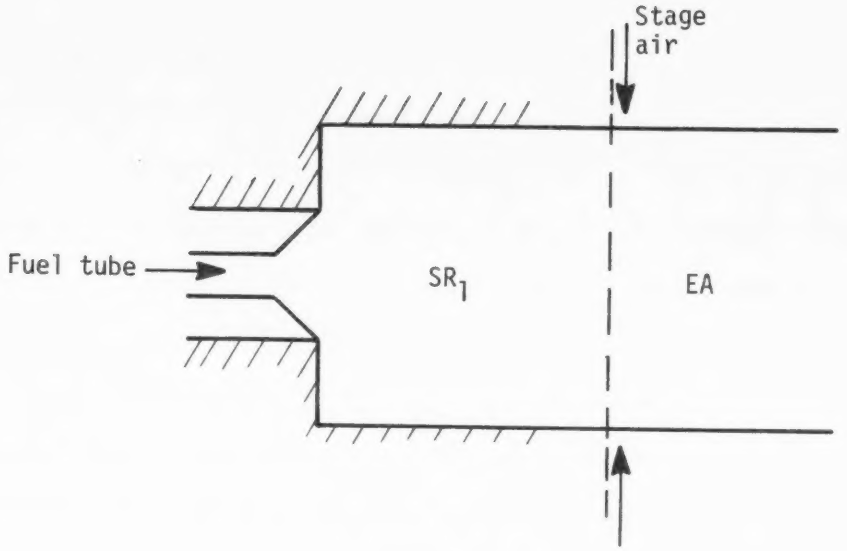
Stage air
Fuel tube
SR_1
EA

Present IFRF burner with staging

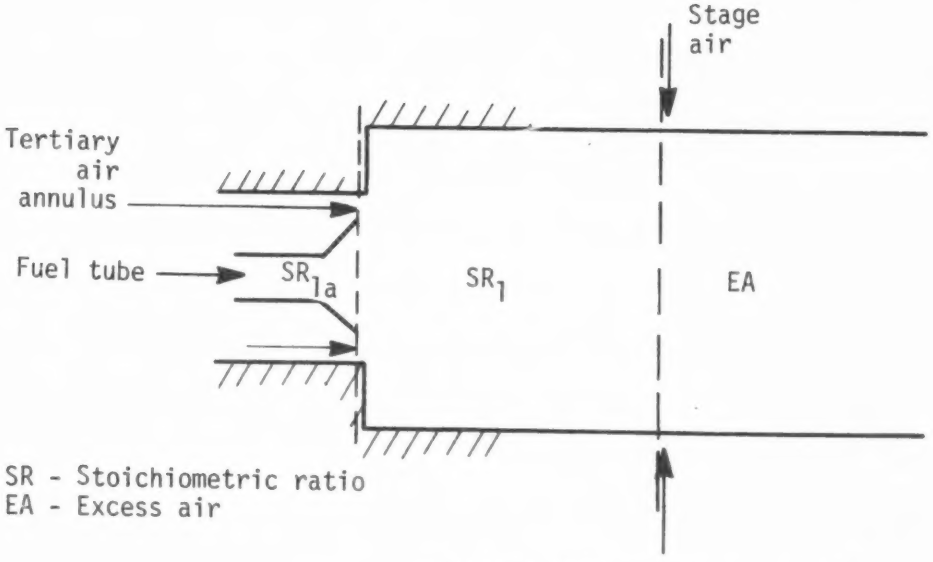
Stage air
Tertiary air annulus
Fuel tube
SR_{1a}
SR_1
EA
SR - Stoichiometric ratio
EA - Excess air

Modified IFRF burner for low NO_x

Figure 3-10. Burner air distribution.

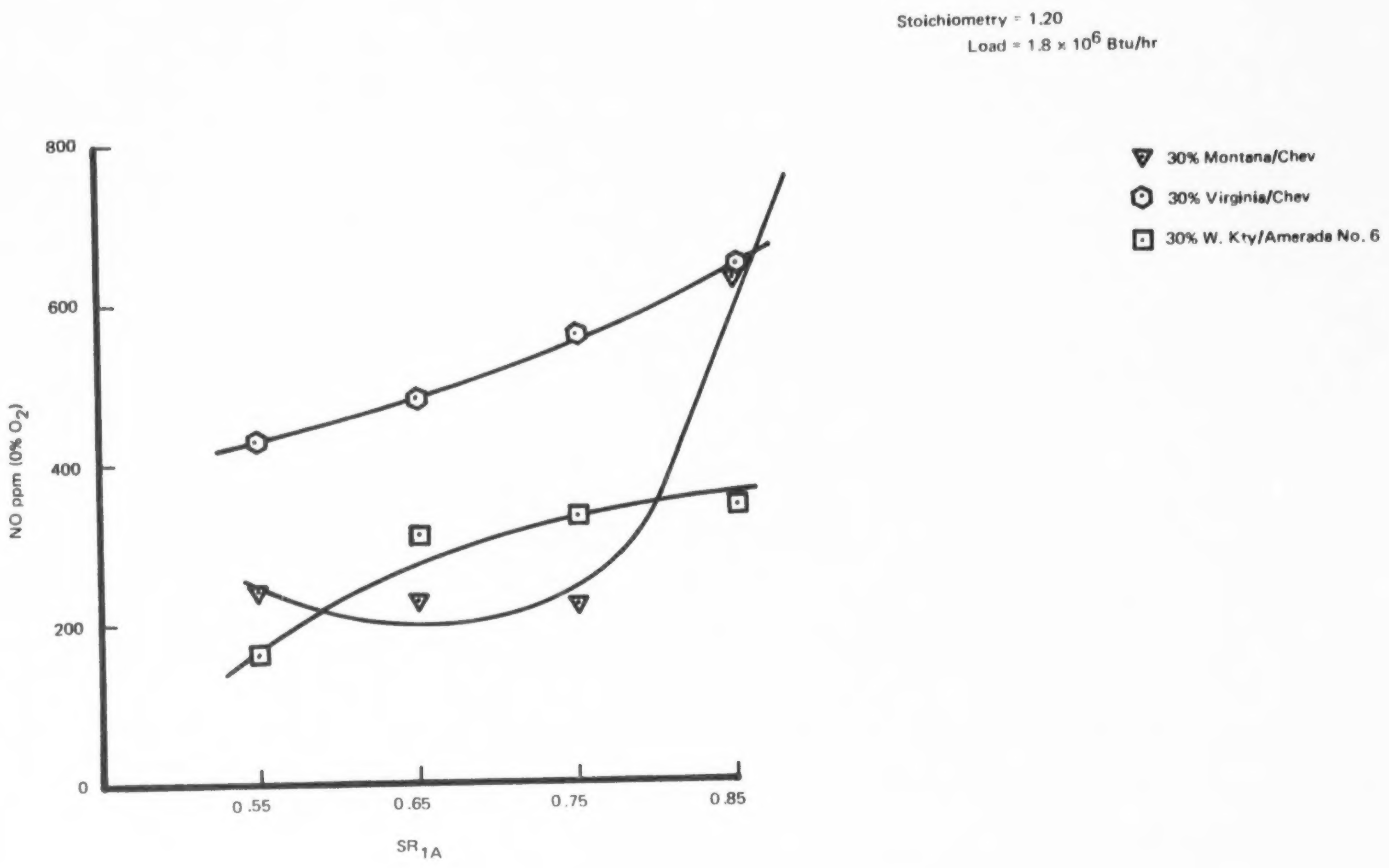

Figure 3-11. Burner air distribution.

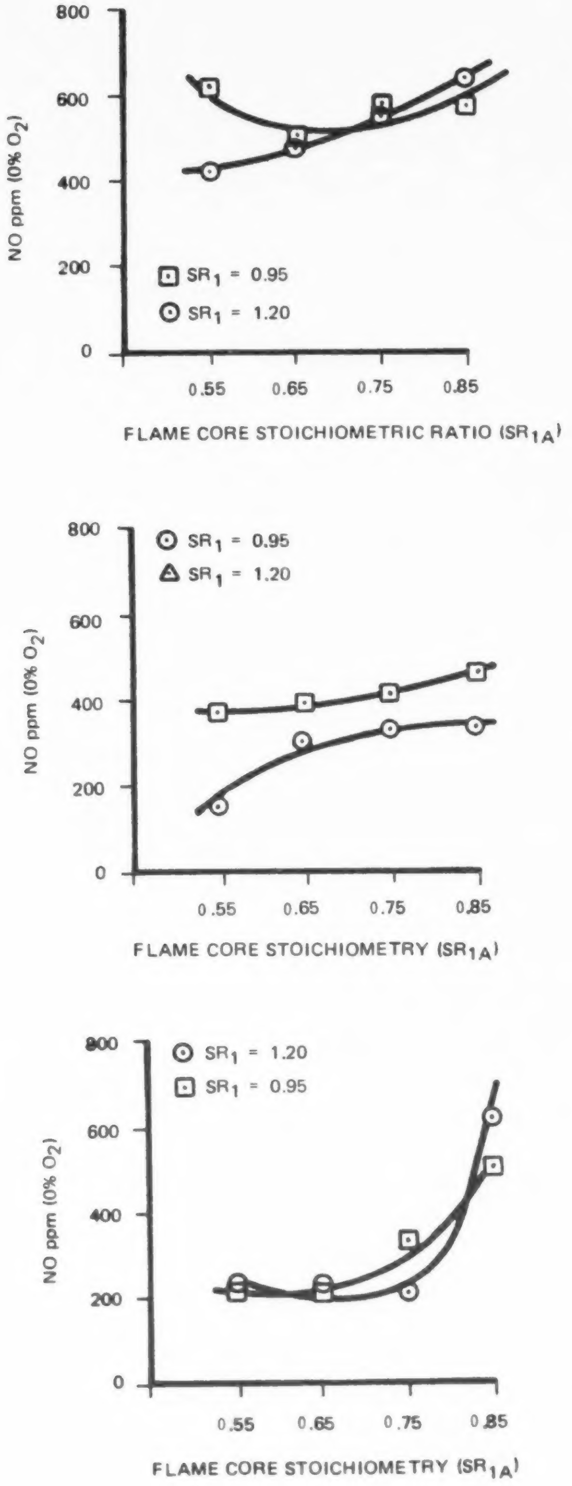

30% Virginia/Chev.
1st Stage Res. time ≈ 0.75 sec.
1.8×10^6 Btu/hr
SR_1 = 1st Stage Stoichiometry

30% W. Kty/Amerada
1st Stage Res. time ≈ 0.75 sec.
SR_1 = 1st Stage Stoichiometry

30% Montana/Chev.
1st Stage Res. time ≈ 0.75 sec.
1.8×10^6 Btu/hr
SR_1 = 1st Stage Stoichiometry

Figure 3-12. Air distribution tests.

enrich the flame zone. In Figure 12(b), for the Western Kentucky/Amerada mixture, the further enriching of the flame zone resulted in higher NO levels. This result, possibly, further illustrates the response of the Amerada high-sulfur parent oil for fuel-rich conditions. The Montana/Chevron mixture results are illustrated in Figure 12(c). This comparison validates the interesting way in which each mixture reacted to the same combustion conditions.

Again, we see little effect of the Amerada-based fuels, a moderate effect on the Virginia/Chevron mixture and a strong effect on the Montana/Chevron mixture. It is interesting to note, however, that there was very little difference between the air distribution or low NO_x burner tests and the stated low NO_x burner tests on the Chevron-based mixtures. This may indicate that with the short residence time staging there is considerable backmixing of the stage air into the first stage. This backmixing would result in a higher overall stoichiometric ratio in the first stage. However, the fact that the Amerada-based fuel reacted differently may indicate there is more a dependence on the N and mass evolution rate and that the timing of the distributed air may be unique for each fuel in order to achieve an optimum low NO_x condition.

The effect of firing rate and residence time on NO emissions during staged combustion is illustrated in Figure 3-13. Figure 3-13(a) represents staging combustion air with a first-stage residence time of approximately 0.75 seconds. A first-stage residence time of approximately 1.50 seconds is applicable to Figure 3-13(b). As expected in both cases, NO emission levels decreased at the lower firing rate of 1.20 x 10^6 Btu/hr. NO levels dropped to about one-half the baseline levels by increasing the residence

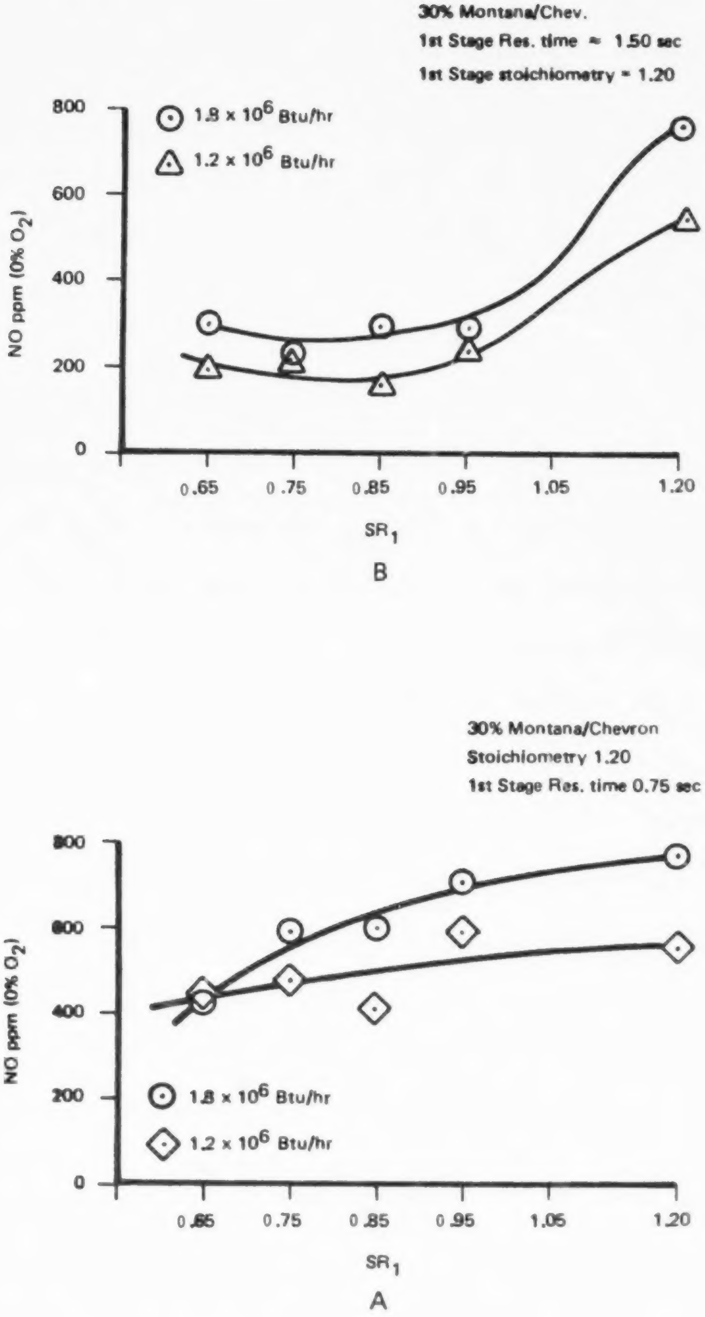

Figure 3-13. Effect of firing rate and residence time.

time. This result of residence time is coincident with earlier tests on coal only that showed marked decreases in NO with residence time during staged combustion. The levels at the longer residence time are similar to the low NO_x burner tests on the COM. However, CO levels during the long residence time tests rose to 800 to 1000 ppm (0-percent O_2) at times.

It should also be noted that the differences in NO at the two loads decrease with decreasing first-stage stoichiometric ratio. This is again consistent with previous coal data.

3.5 FUEL NITROGEN STUDIES

The last phase of the study was a limited evaluation of fuel nitrogen converion in COMs. This involved addition of a dopant to the feed system to evaluate the conversion of fuel bound nitrogen. Pyridine, C_5H_5N, was added to the Montana/Amerada mixture upstream of the fuel tube during two tests, and the percent conversion of nitrogen to NO was calculated based on the emissions levels obtained. These data, along with the emissions levels of all the mixtures and parent fuels under baseline conditions, are plotted against fuel nitrogen content in Figure 3-14. This plot exhibits a definite trend. In both cases, the fuel nitrogen conversion to NO was 30 to 35 percent which is typical of bound-nitrogen conversion during coal combustion. The pyridine dopant points fall slightly below the line, and we have no definitive explanation for this. It is possible that the pyridine volatilizes earlier than the oil or coal/oil mixtures, but this preliminary screening test did not develop sufficient data to draw any definitive conclusions. No correlation with fuel nitrogen was seen with the coal data. This result is consistent with published data (Reference 8). It appears that the COMs behave more like the oil with regard to fuel nitrogen than to coal.

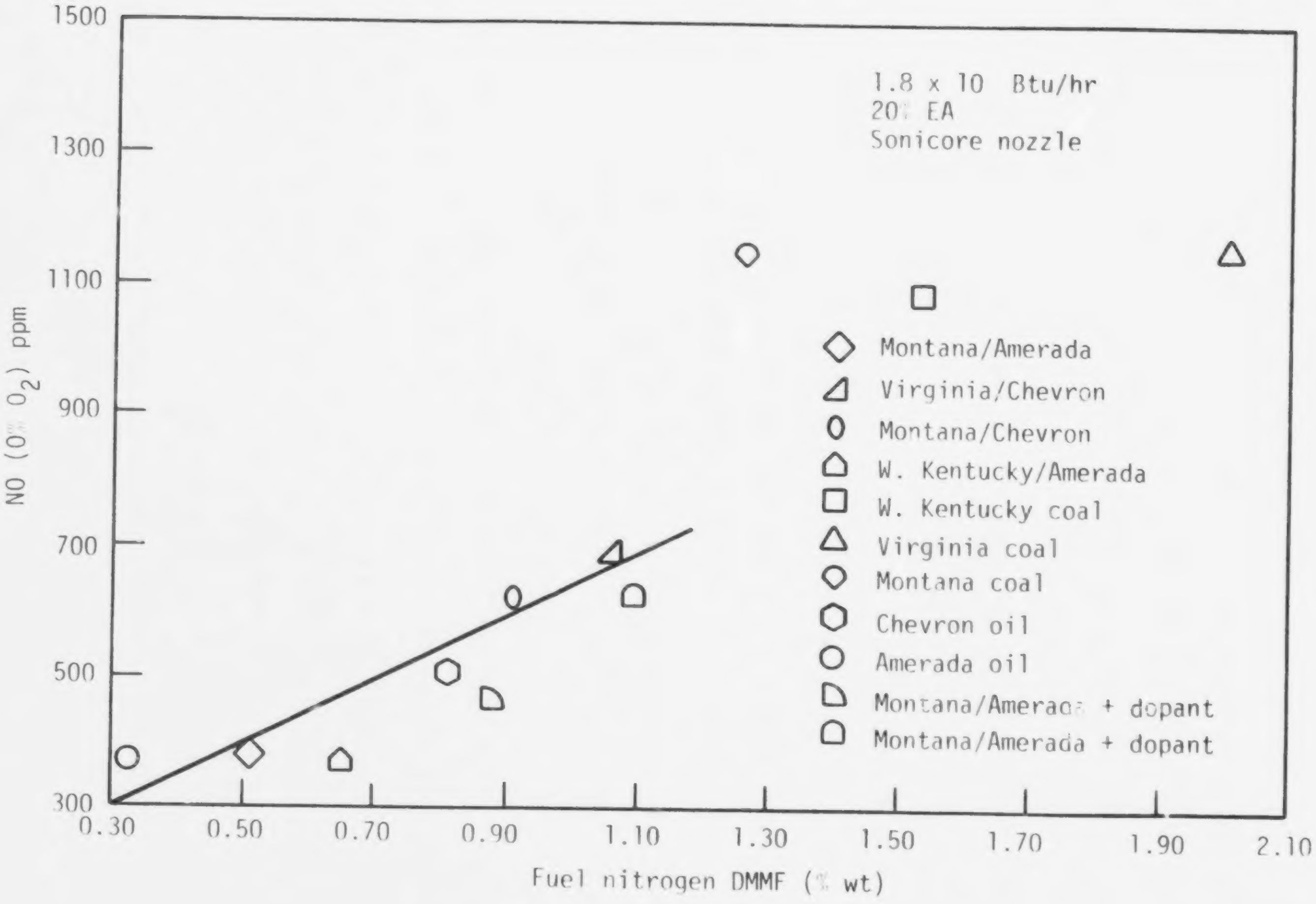

Figure 3-14. Effect of fuel nitrogen.

3.6 BURNER NOZZLE COMPARISON

NO emissions data were obtained with both commercial nozzles described earlier on the parent oils. Figure 3-15 illustrates the results of this comparison. Emissions data obtained earlier during the DOE tests (see appendix for report on these tests) using the Delavan nozzle are also included.

In all cases the Sonicore nozzle gave higher NO levels than the Delavan nozzle. This result is attributable to the way the fuel is atomized and mixed with the region. How a nozzle atomizes any given fuel can also affect the NO levels. For example, the Chevron oil showed a more marked difference between the two nozzles than did the Amerada oil. This again shows the difficulty in trying to predict the NO levels for a given oil and/or nozzle.

3.7 PREVIOUS TESTING DATA

During previous testing NO emission levels were obtained as a function of the percentage of coal in the mixture. These data are illustrated in Figure 3-16. These data were obtained under baseline conditions with the Delavan nozzle (hardened stainless steel) at a firing rate of 1.8×10^6 Btu/hr using the Virginia coal and Amerada parent oil. The results are not too surprising for a given fuel and nozzle. They indicate that as the percentage of coal increases, the NO levels increase, although not quite linearly.

3.8 SUMMARY AND CONCLUSIONS

The following conclusions can be drawn based on this study:

- Baseline NO emissions from COM were, in general, linearly related to the fuel-N for a given burner and nozzle type

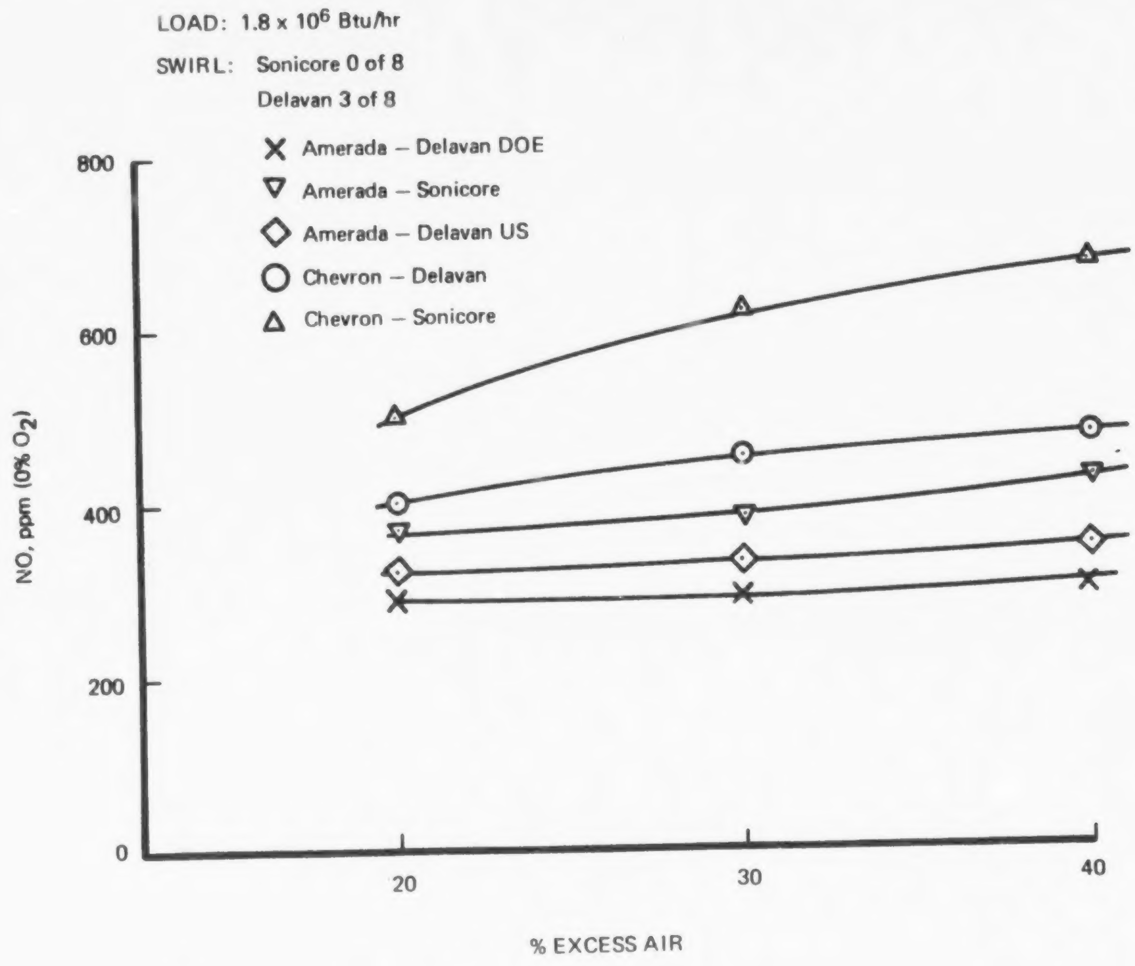

Figure 3-15. Nozzle comparison.

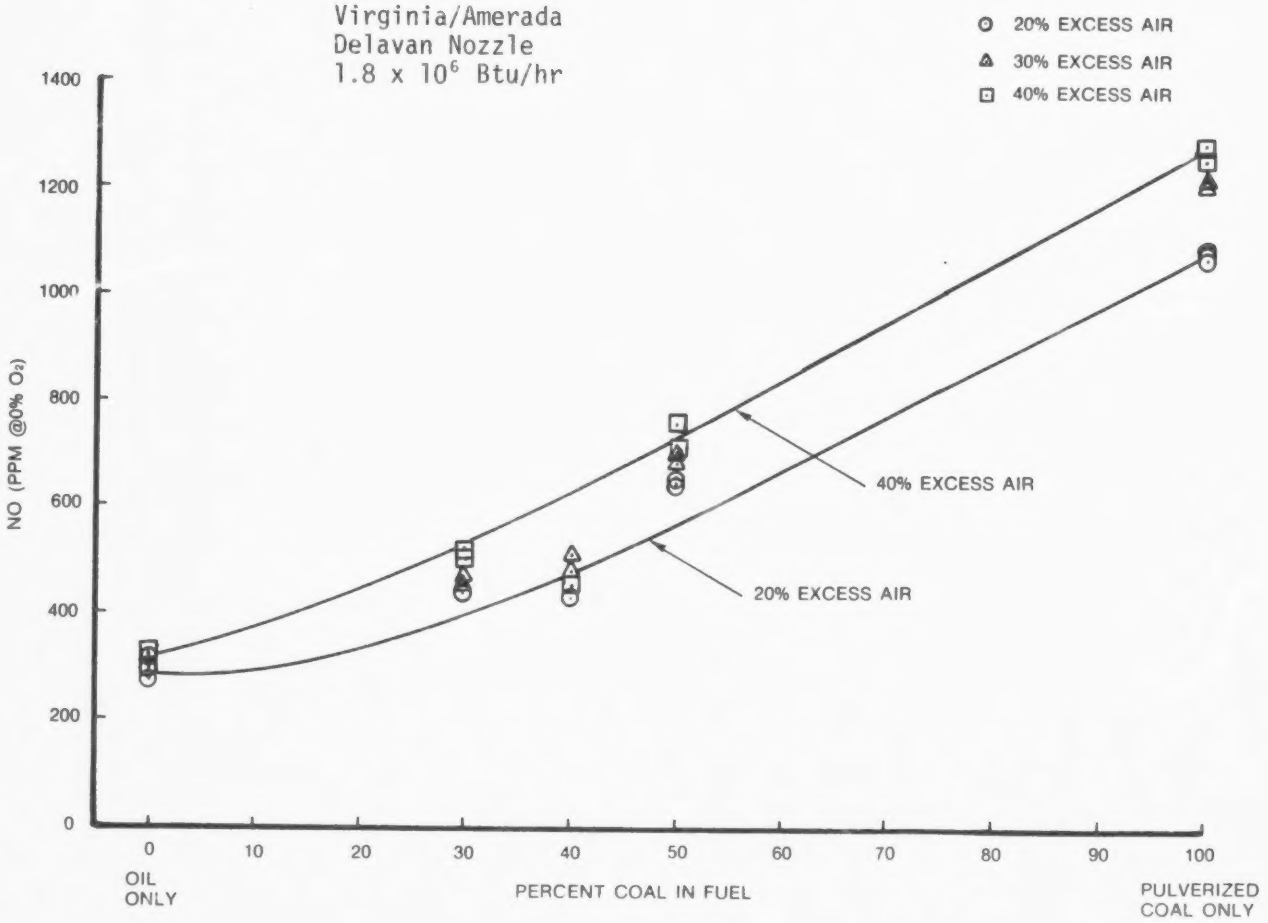

Figure 3-16. Data from earlier work.

- The burner settings and fuel nozzle type have a strong effect on NO emissions.
- Conventional control technology utilized presently for pulverized coal combustion is effective in reducing NO emissions but to different degrees dependent on fuel composition.
    - It was difficult to achieve low NO_x emissions with the Amerada based COMs.
    - Moderate effects were obtained by NO_x control technologies with the Virginia/Chevron mix.
    - Strong effects were obtained by NO_x control technologies with the Montana/Chevron. These were obtained with the low NO_x burner, low NO_x burner plus staging, and staging at long residence times. However, CO levels are excessively high at long residence times.
- NO emissions increase in proportion to the amount of coal in the coal/oil mixture but fall between the parent fuel oil and coal baseline emissions.
- Care must be exercised in designing the pumping systems for coal/oil mixtures to avoid regions where coal may settle out and eventually plug the lines.
- Flow control in small scale combustion tests of COM are quite difficult due to the necessity of small orifices which can either erode or become plugged.
- Fuel nozzles which rely on impingement of solid surfaces by high velocity fluid jets will be subject to high erosion rates. Judicious selection of materials may help to overcome the problem.

- Pumps must be selected which can handle this highly abrasive mixture.

3.9 RECOMMENDATION

In order to analyze and understand the complex process of coal-oil mixture combustion, we must obtain a better understanding of the combustion processes of each parent fuel. Also, the combustion of coal/oil mixture needs detailed examination to determine if it is merely a combination of the two individual processes or if the interaction of these processes results in a completely different complexity of physical and chemical phenomena.

Future work should examine the role of fuel-bound nitrogen utilizing flue gas recirculation and nitrogen evolution studies of the parent oils. Also the effect of the physical presence that each fuel exerts on the other, such as shielding or physical separation in the droplets, should be examined.

SECTION 4

REFUSE-DERIVED FUEL TESTS

During the last decade, it has become apparent that the growing demand for energy and the resulting scarcity of clean, readily available sources to meet that demand have increased the need to use our energy resources wisely and efficiently. The search for new fuels to supplement present energy sources is taking on a new importance.

Commercial and municipal refuse has long been recognized as a vast, untapped source of energy. However, the logistics of efficiently extracting this energy has prevented its serious consideration as a viable source. Dwindling supplies of clean fossil fuels have resulted in higher costs along with restrictions in their use. While dirty fossil fuels are becoming attractive alternatives, environmental considerations dictate that a balance must exist in their use while new technology is developed to reduce their harmful environmental effects. Alternative energy sources such as atomic and solar are considered valuable but distant energy sources due to technological and environmental considerations.

In light of these considerations, fuel derived from refuse is a practical energy source that is becoming increasingly attractive as technological advances overcome the problems inherent with its use. Fuel which is derived from refuse by removal of noncombustible material has a nominal heating value of 4000 to 7000 Btu/lb. A significant number of investigations in which refuse-derived fuel (RDF) has been used to generate steam in full-scale facilities have answered many questions regarding technological problems associated with the use of this fuel. However, gaseous, trace metal, and organic emissions data which can provide answers to environmentally related questions are currently sparse.

It is necessary that investigations regarding the environmental compatibility of refuse derived fuel be conducted before this vast, untapped energy source can be considered a viable supplement to present energy resources. These investigations can be carried out most cost effectively in a laboratory-scale facility.

4.1 OBJECTIVES

The objectives in this investigation were:

1. To design, fabricate and operate a system for combustion testing of RDF in a laboratory-scale facility
2. To characterize RDF emissions of several types of material presently available for use as fuel
3. To evaluate the combustion efficiency of fuels consisting of conventional clean and dirty fossil fuels (natural gas and coal) mixed with varying percentages of RDF
4. To evaluate the effects of combustion parameters on emissions from RDF/conventional fuel mixtures
5. To provide direction for future investigations on RDF to insure solutions to problems associated with its use.

4.2 RDF EXPERIMENTAL HARDWARE

In view of the fact that the majority of the U.S. steam-electric capacity is produced by tangentially-fired boilers, all tests were conducted in the tangential configuration. The EPA/Acurex multifuel facility, shown in Figure 4-1, is capable of simulating several types of industrial and utility boilers. For this investigation, the C.E.-type corner mounted burners, shown in Figure 4-2, were utilized. The aerodynamic pattern developed in this configuration is shown schematically in Figure 4-3. The corner-type axial diffusion burner shown in Figure 4-2 allows for gradual mixing of the fuel and oxidant. In standard operation, fuel and primary transport air are injected through the fuel tube of the center gun. A portion of the secondary combustion air is injected through an annulus surrounding the fuel tube. The balance of the secondary combustion air is injected through annular exits in the upper and lower guns. Secondary fuel tubes, located in the upper and lower guns, are used for system preheating with natural gas.

4.2.1 Burner Modifications

For this investigation, a fuel gun was designed to inject refuse into the combustor and be aerodynamically consistent with the corner-type burners. A modified gun, shown in Figure 4-4, was used for the injections of the refuse material. The forward end of the nozzles includes an actively cooled section to protect against preignition of the refuse. A thermocouple was also installed on the nozzle outlet surface and connected to an over-temperature alarm system.

The end of the nozzle was designed for a venturi effect to ensure material transport velocities. An air injection port was installed at the

1. Combustion chamber (39" cube)
2. Ignition and flame safeguard
3. Observation ports
4. Ashpit
5. 1.5 x 10^6 Btu/hr IFRF burner
6. C.E.-type corner fired burners
7. 3200°F refractory
8. Heat exchange sections
9. Drawer assemblies
10. Staged injection ports

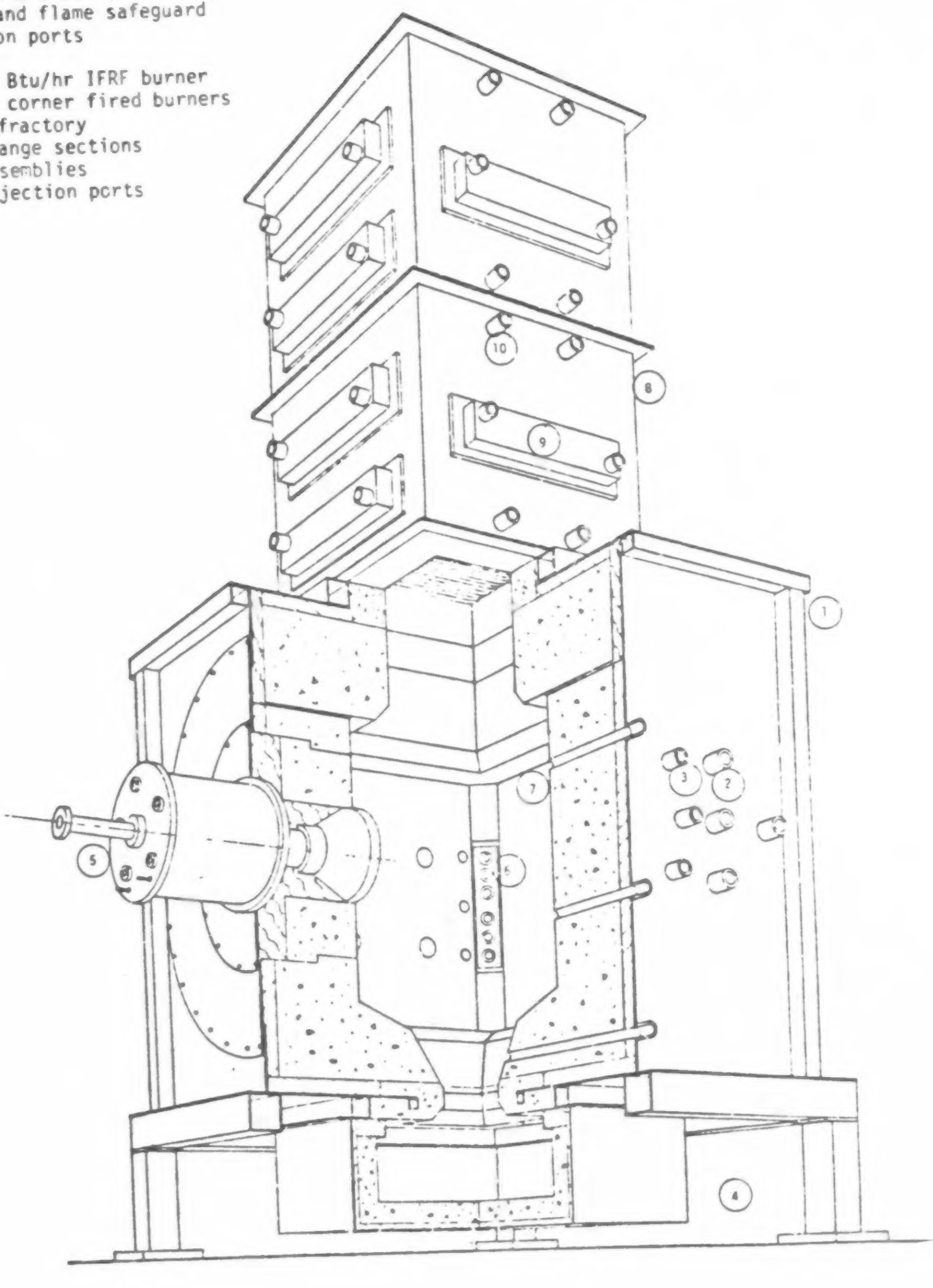

Figure 4-1. Furnace cross section.

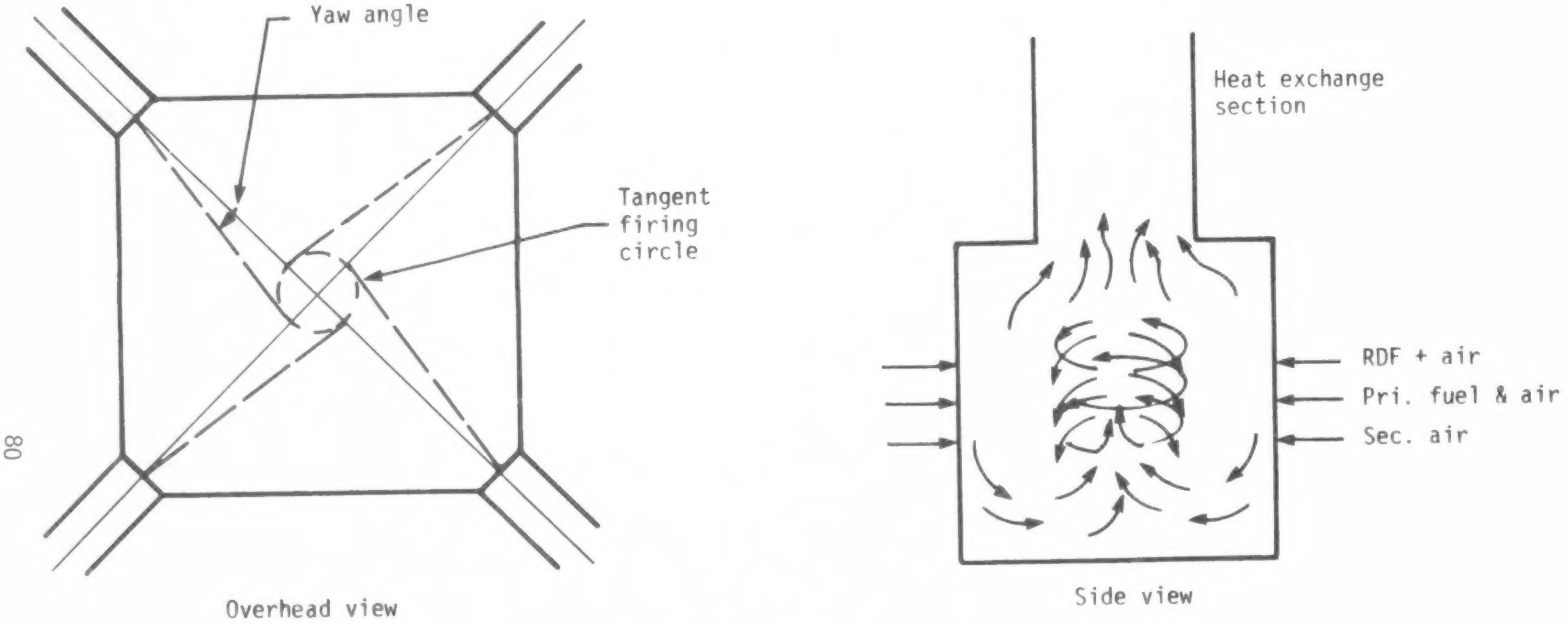
Yaw angle
Tangent
firing
circle
Heat exchange
section
RDF + air
Pri. fuel & air
Sec. air

Overhead view

Side view

Figure 4-2. Tangential configuration, aerodynamic patterns.

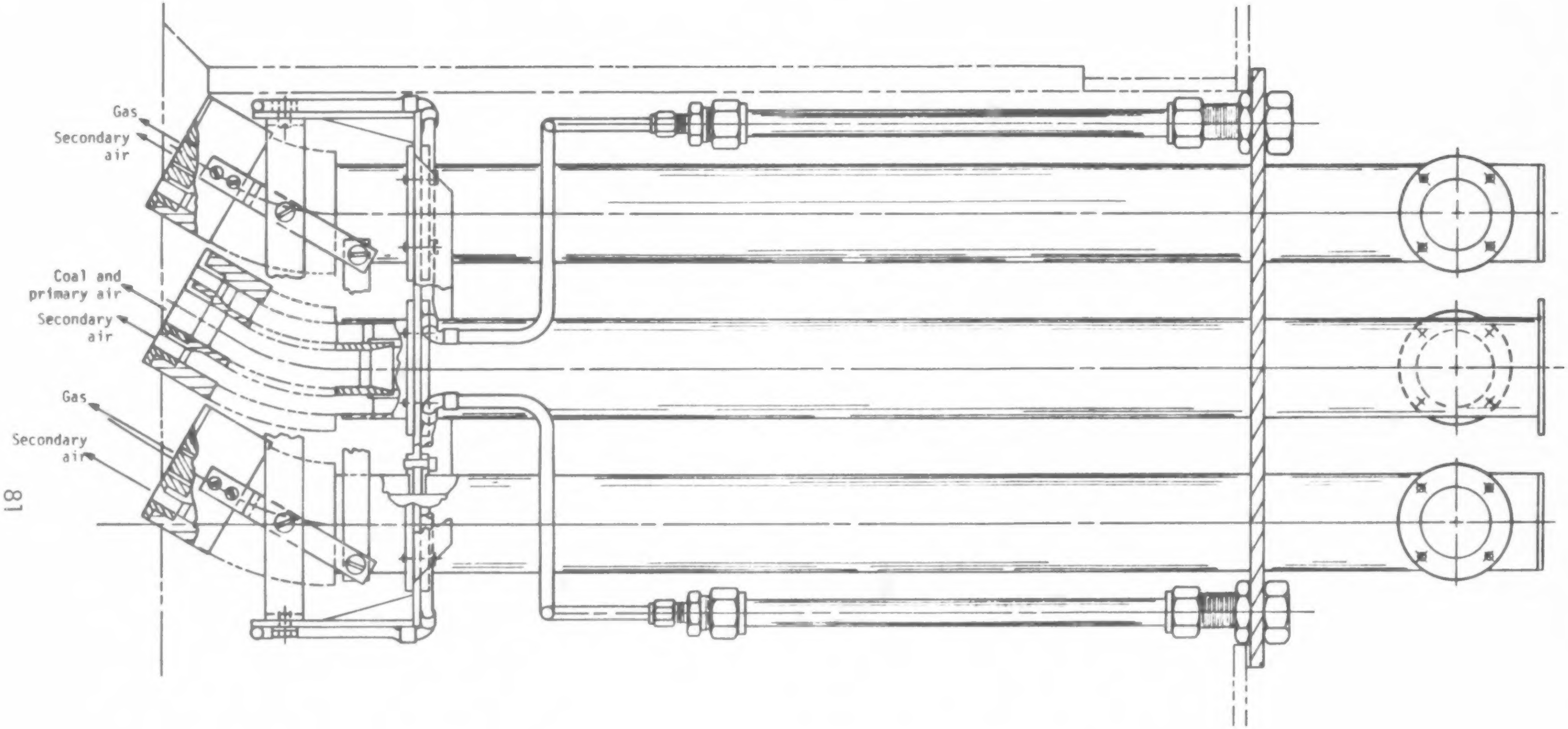
Gas
Secondary air
Coal and primary air
Secondary air
Gas
Secondary air

Figure 4-3. Corner-fired burner.

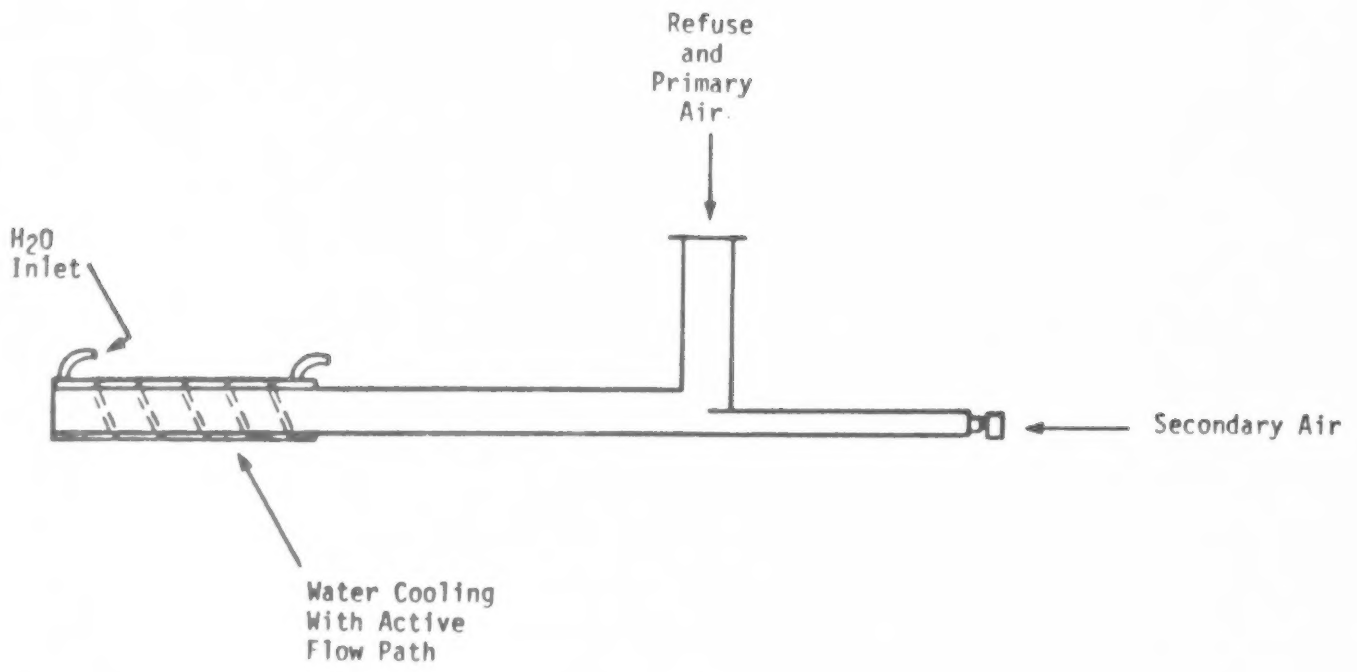
Refuse
and
Primary
Air
H2O
Inlet
Secondary Air
Water Cooling
With Active
Flow Path

Figure 4-4. RDF nozzle.

end to supply a portion of the combustion air. An access port was also installed to permit manual sweeping of material clogs with a rod if needed.

The modified gun assembly is shown in Figure 4-5. In the tangential configuration, two modified burner assemblies were installed in opposite corners, while two of the standard burner assemblies were installed in the remaining opposite corners. This configuration is illustrated schematically in Figure 4-6.

4.2.2 RDF Feed System

A feed system specifically designed to eliminate problems associated with the pneumatic transport of refuse material was fabricated for this investigation. Handling problems, due to the nominal size of municipal refuse (1/8" x 0 to 5.0" x 0), were significant at this scale of operation (1.5×10^6 Btu/hr). A separate feed system was fabricated for each RDF burner. Each unit was specifically designed to meter from 10 to 50 lbs/hr of RDF into the refuse nozzles described in the previous section. Significant design effort was required to overcome many of the inherent problems with feed refuse at these low flowrates. The system is shown schematically in Figure 4-7. A review of the system follows.

The refuse feed system is made up of three main components which were each designed to overcome specific handling problems involved with refuse transport. These are:

- Fluidized system
- Belt transport system
- Pneumatic transport system

Collectively, they result in a consistent feedrate of refuse into the combustor.

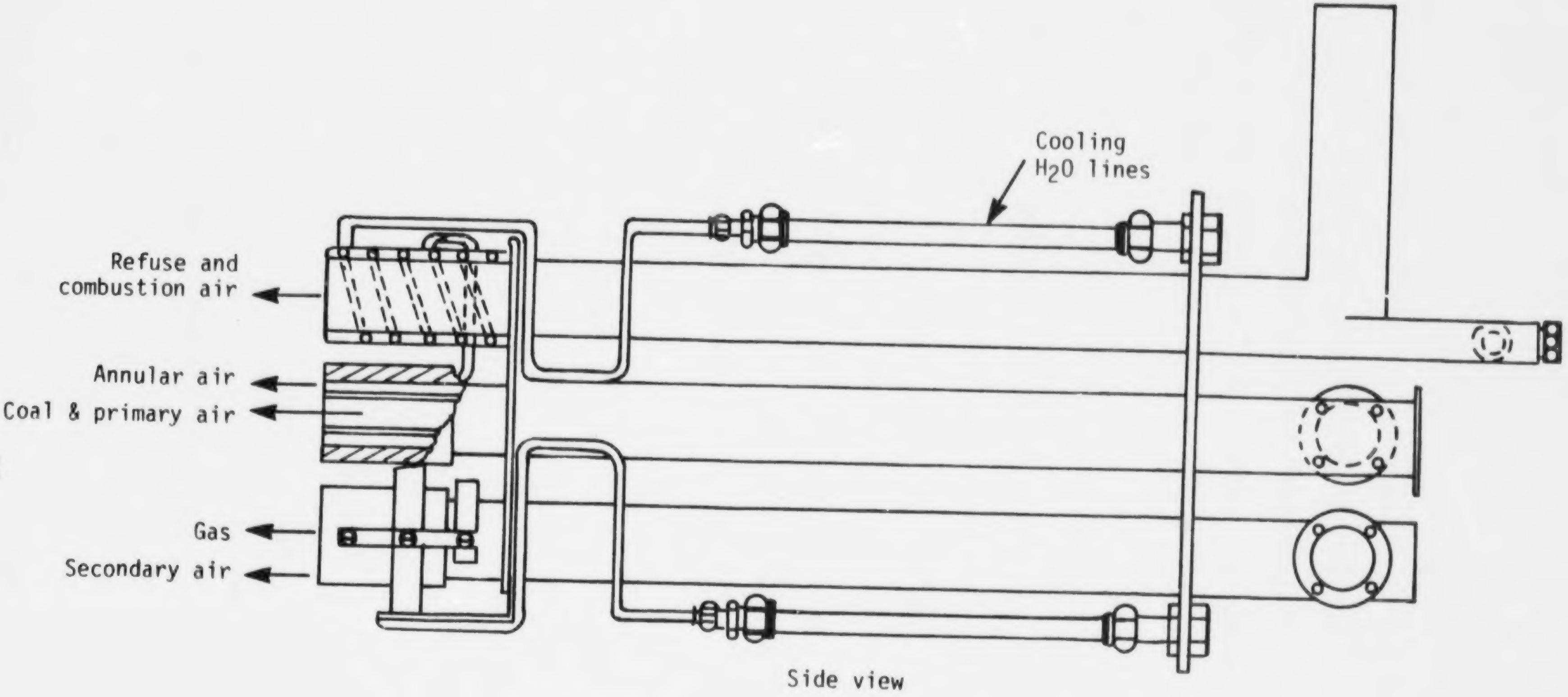
Cooling
H_2O lines
Refuse and
combustion air
Annular air
Coal & primary air
Gas
Secondary air
Side view

Figure 4-5. Modified corner-burner assembly.

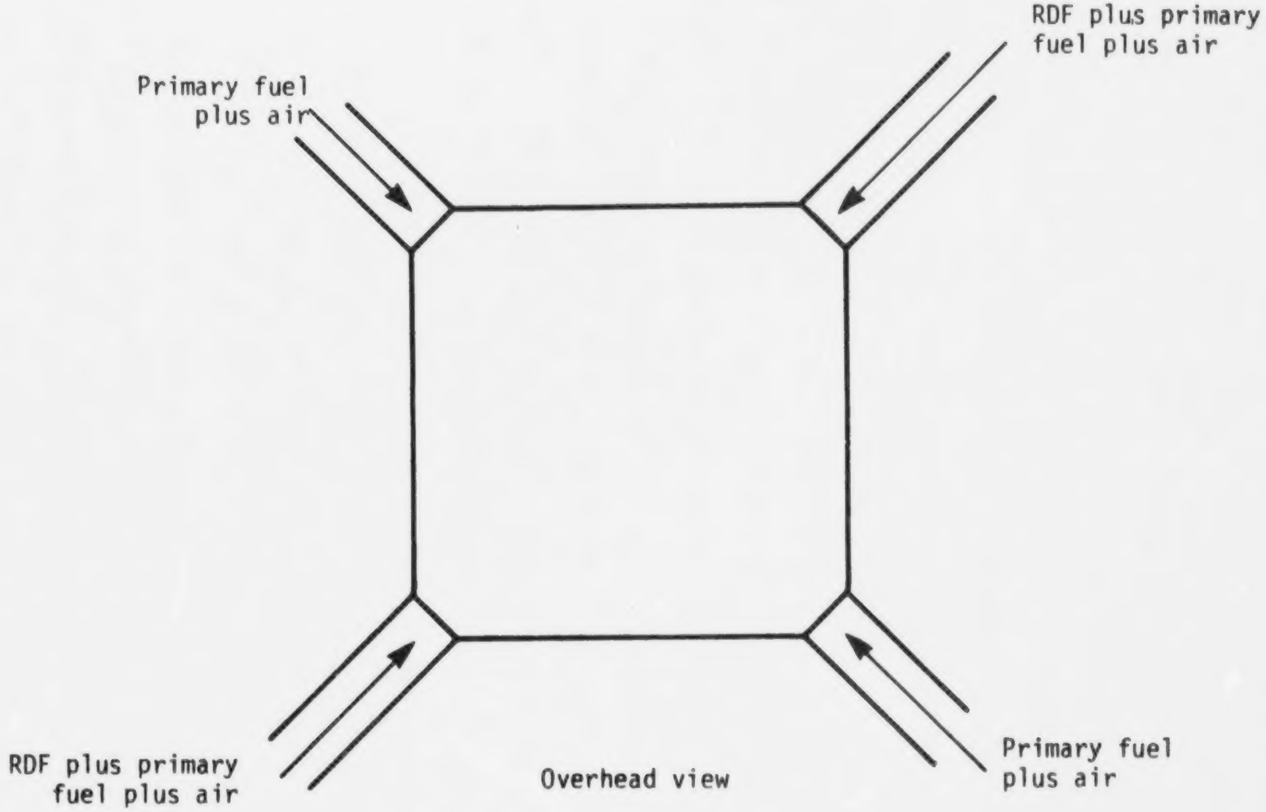
RDF plus primary fuel plus air
Primary fuel plus air
RDF plus primary fuel plus air
Primary fuel plus air
Overhead view

Figure 4-6. Fuel delivery schematic.

- Fluidization System. This system is made up of the refuse supply drum, support frame, and a chain-driven motor system. Refuse is placed into the chamber through a sealable door. An electric motor is used to rotate the drum by way of a chain drive/clutch system. The drum is rotated at a rate which effectively fills the drum with refuse in suspension, at steady state conditions. This system results in an even distribution of fluffy material which can easily be transported to the burners.
- Belt Transport System. An electric-motor-driven conveyor belt system is located axially along the centerline of the drum. As fluffed material falls along the moving belt, it is collected by 1.0 inch metal stand-offs which are evenly distributed along the belt surface area. The refuse layer thickness is controlled by a pointed knife edge at the drum exit. The speed of the belt is controlled at 0 to 1750 rpm by a varispeed motor.
- Pneumatic Transport System. As the belt revolves around the forward roller, the material is stripped off the belt using air jets. The angle of these jets is such that they run tangent to the roller, thereby effectively sweeping the belt clean of material. This system also gives the material momentum into the burner tube. The air used is part of the total combustion air required for the refuse. The material is conveyed into the furnace pneumatically through the RDF nozzle described previously. A schematic of this system is shown in Figure 4-8.

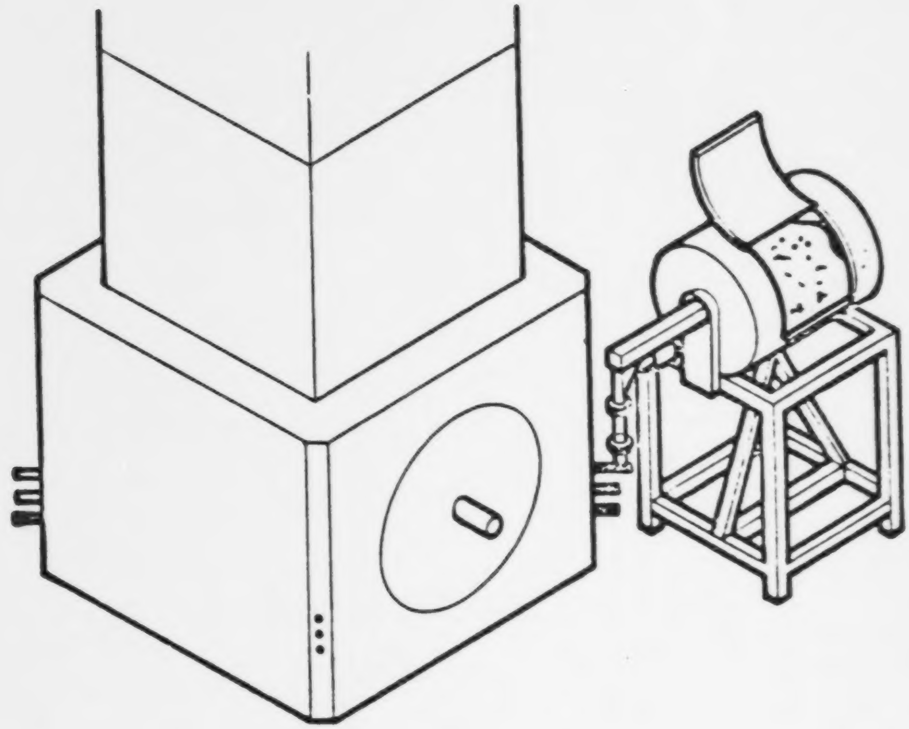

RDF feed system and firebox.

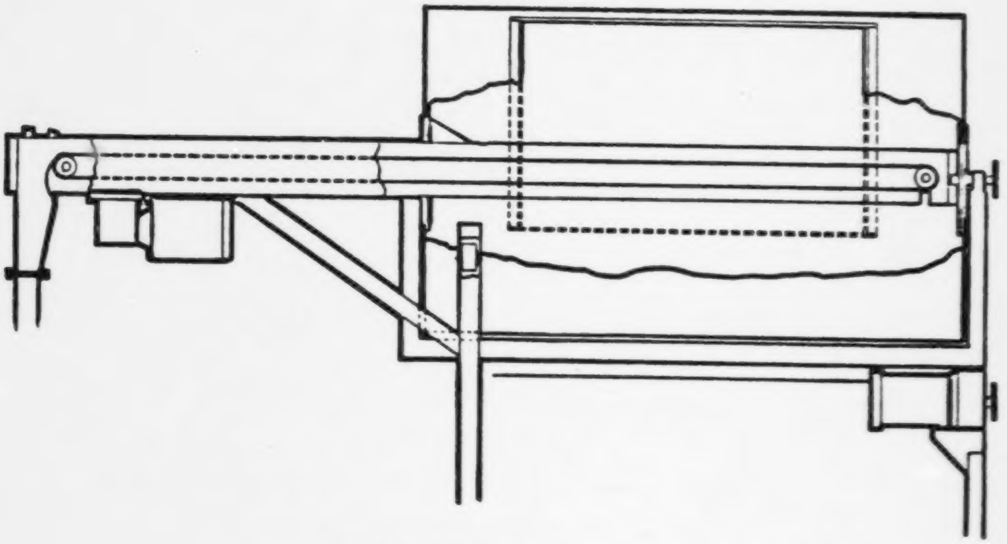

RDF feed system.

Figure 4-7. RDF feed system design.

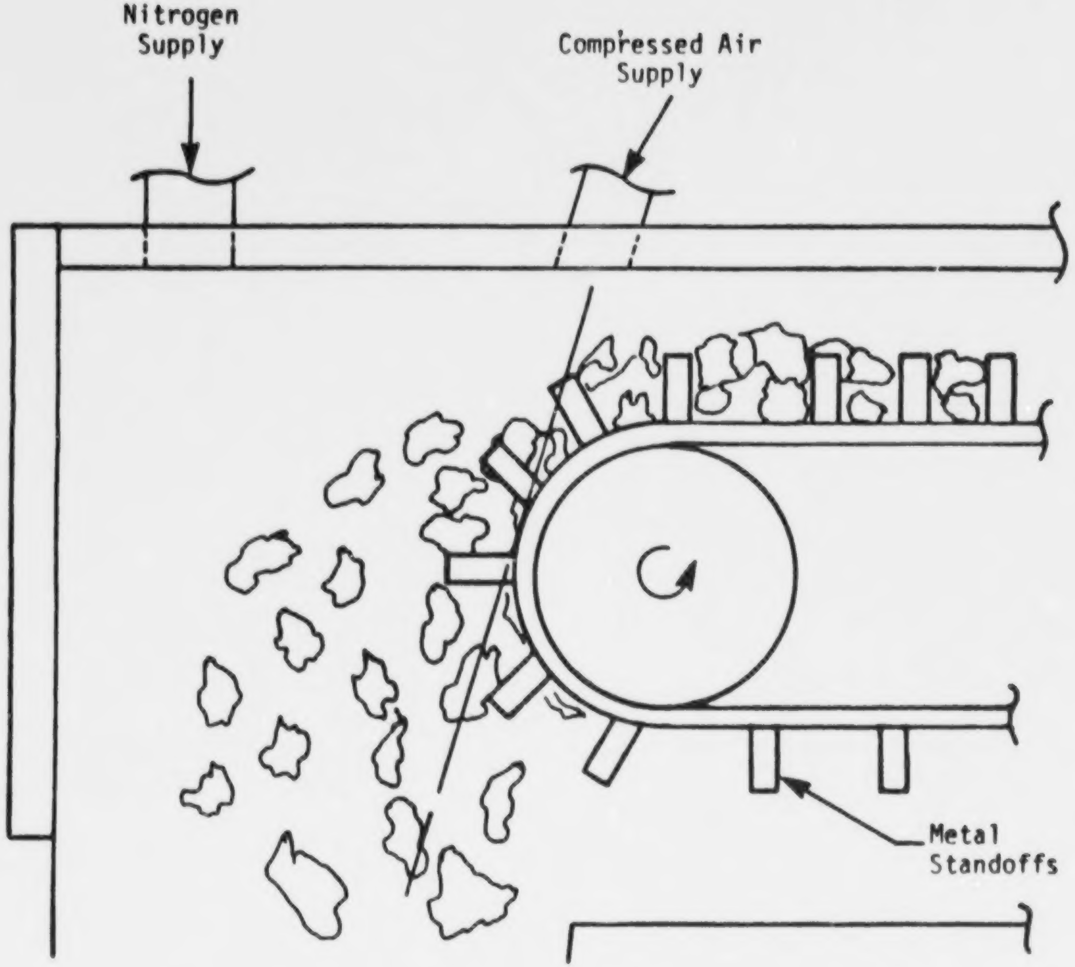
Nitrogen Supply
Compressed Air Supply
Metal Standoffs

Figure 4-8. Pneumatic transport system.

Safety System

The flame safeguard system is designed to prevent flash-back or propagation of refuse flames up the refuse injection tube and onto the belt system. This possibility results from the positive pressure in the furnace and the combustible mixture of air, refuse and dust in suspension in the downcomer tubes. The system is shown schematically in Figure 4-9.

As shown, a Honeywell UV flame detector is positioned with a clear line of sight into the burner tube. A flame signal from the detector is sent to a control panel where three steps are taken automatically:

1. Refuse belt is shut off
2. Refuse air supply is shut off
3. Nitrogen purge is started

These steps ensure immediate loss of combustion essentials in the downcomer and burner tubes. The activated nitrogen purge duration was set for 10 to 30 seconds.

4.2.3 Materials Acquisition and Handling

As stated in the Objectives section, one of the purposes of this investigation was to better characterize combustion efficiency and emissions as a function of refuse type. Therefore, material had to be transported from several locations to the Acurex research facility. In order to assure that the procedures used in obtaining this type of material complied with state and federal regulations, coordination with local, state, and federal authorities was required. In particular, coordination with the State of California Department of Food and Agriculture was necessary because of the potential entomological dangers of shipping RDF from various parts of the country into the state. In order to protect against these dangers,

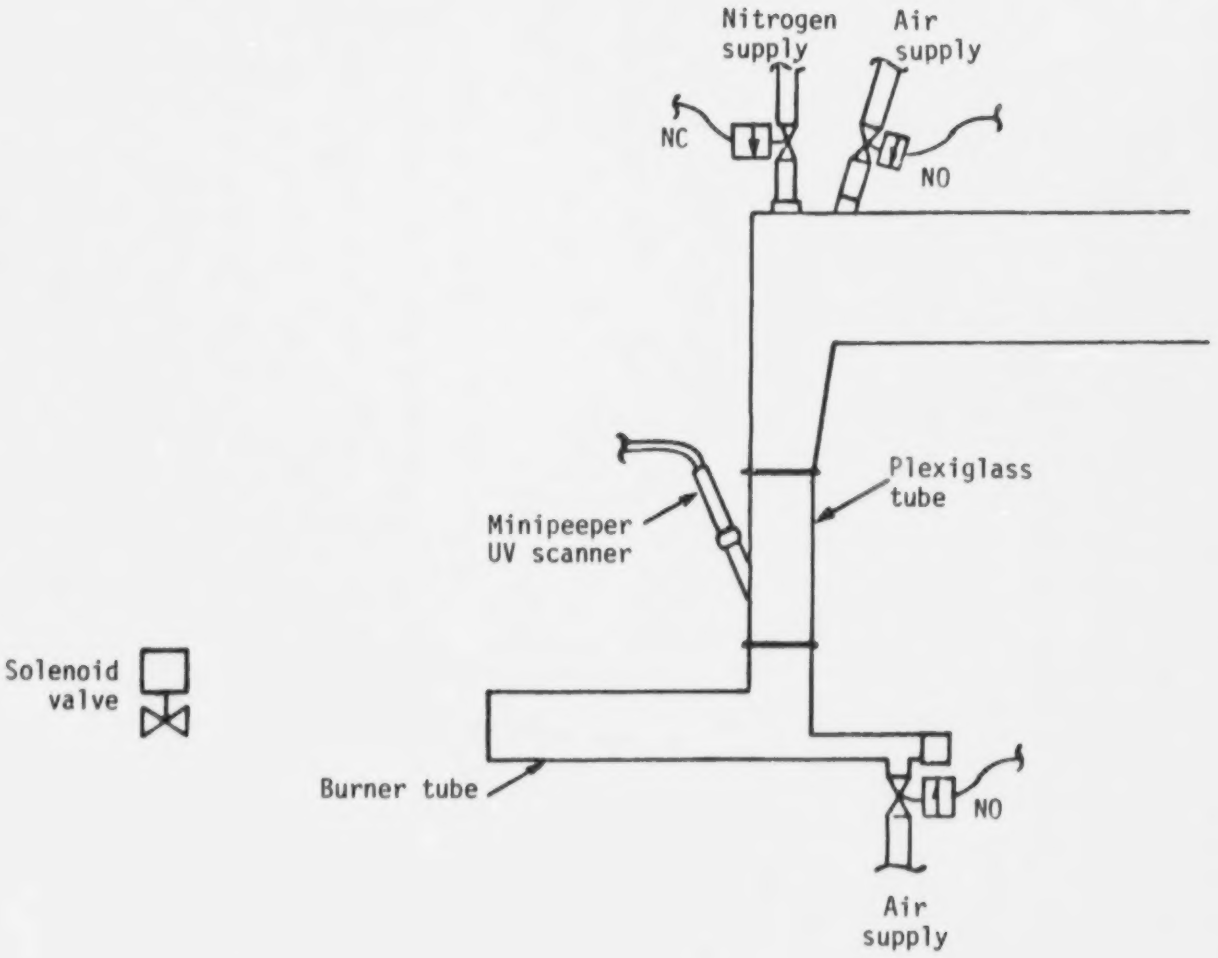
Nitrogen supply
Air supply
NC
NO
Plexiglass tube
Minipeeper UV scanner
Solenoid valve
Burner tube
NO
Air supply

Figure 4-9. Safety system.

the State of California Department of Food and Agriculture, the Santa Clara County Department of Agriculture, and Acurex agreed upon the following packing, shipping and inspection procedures. The RDF material was:

- Fumigated outside of the State of California using the procedure recommended in the U.S. Department of Agriculture Plant Protection and Quarantine Manual, T403 (e)-(2), section 6, page 6. This treatment is methylbromide fumigation under a tarpaulin using 10 pounds of methylbromide per 1000 ft^3 of RDF at atmospheric pressure for 48 hours at 40°F or above.
- Certified in writing by a state or federal agricultural agent as to compliance with the fumigation procedure described above.
- Sealed and shipped in a sturdy container with a rigid, insect-proof frame and a leak-proof plastic liner. Wooden boxes, 44 inches x 48 inches x 100 inches, were constructed and fitted with plastic liners for shipping the 2000-pound lots of RDF from each each of the facilities.
- Received and unopened until notification was given to the County of Santa Clara Department of Agriculture so that a Santa Clara County Agricultural agent could inspect the containers and the written fumigation certification and agree to unloading.

After inspection and approval, the RDF was stored on the Acurex premises in its shipping containers on an outdoor concrete pad and fully covered by a tarpaulin. This protected the RDF from any degradation or attrition from rain and wind during storage and testing.

Emphasis was placed upon safety during all RDF test operations. All of the test personnel in contact with the RDF received tetanus, typhoid, and diphtheria series of vaccinations, and personnel in direct contact with the RDF were required to wear respiratory filtermasks. In addition, daily changes of clothing and footwear were required of test personnel in contact with the RDF so that no contamination was carried around the workplace or to the home. In addition, cleanliness of the test facility was maintained. Floors and equipment were cleaned daily to insure a safe and hygenic workplace.

The as-received RDF was not compatible with the test facility feed system. Early calibration tests revealed that some of the large particles in the RDF plugged the feeding mechanisms and interrupted testing. In order to uniformly feed the RDF into the combustion test unit, the RDF had to be reduced in size. Early testing with the test feeder system proved that RDF particles of 1 inch or less were suitable for controlled combustion testing.

Therefore, the RDF was passed through a commercial garbage composter and reduced to 1 inch or less with no other alteration in the RDF composition. This size reduction process was conducted at the test site during the combustion tests.

At the end of testing, any RDF which was unused was hauled to a landfill area for disposal. The major consideration was to dispose of the unused RDF as soon as possible to prevent insect infestation or putrefaction of the RDF.

4.2.4 Sampling Equipment and Procedures

The sampling required for this project included collection of gaseous emissions by continuous monitoring equipment, collection of flue particulate and gases for trace metal, organic and anion analysis, collection of residual ash for detailed analysis, and sampling of the input fuel. The methods and equipment for each of these sampling tasks are discussed in the following sections.

4.2.4.1 Gaseous Emissions Measurement

Table 4-1 lists the continuous monitoring equipments utilized at the Acurex Energy Laboratory. Figure 4-10 shows a schematic of the gaseous sampling and analysis system. The system is designed for accurate analysis of NO, CO, O_2, CO_2, SO_2, and unburned hydrocarbons.

4.2.4.2 Stack Sampling Equipment

Two stack sampling systems were used during the course of testing. The high volume stack sampling system as shown in Figure 4-11 was used to determine the particulate grain loadings and size distribution. This system meets or exceeds the EPA Method 5 requirements. The second system was the Source Assessment Sampling System (SASS) shown schematically in Figure 4-12. The SASS is used for both sampling of particulates and organics. The sample is drawn through a glass-lined sampling probe and routed through a series of three cyclones and a filter which separates the particulate into four size fractions. Both the probe and particulate removal system are in a 400°F oven to prevent condensation. The gaseous sample then passes through an organic module where it is cooled and the organics are trapped on a polymer adsorbent. Condensate from the module is also collected for analysis. Finally, the sample is routed through an impinger train where oxidizing solutions retain any remaining sample. The sample is then drawn through the control unit where pressures, temperatures, and gas volume are monitored and controlled. An S-type pitot is used to measure gas velocity for the purpose of determining isokinetic sampling rates.

TABLE 4-1. EMISSION MONITORING EQUIPMENT

Pollutant	Principal of Operation	Manufacturer	Models	Instrument Range
NO	Chemiluminescence	Ethyl Intertech	Air Monitoring	0-5 ppm 0-10 0-100 0-250 0-1000 0-5000
SO_2	Pulsed Fluorescent	Thermoelectron	Teco Model 40	0-50 ppm 0-100 0-500 0-1000 0-5000
CO	Nondispersive Infrared (NDIR)	Ethyl Intertech	Uras 2T	0-500 ppm 0-2000
CO_2	Nondispersive Infrared (NDIR)	Ethyl Intertech	Uras 2T	0-5% 0-20%
O_2	Paramagnetic	Ethyl Intertech	Magnos 5A	0-5% 0-21%
UHC	Flame Ionization	Ethyl Intertech	FID	0-100 ppm 0-300 ppm 0-1000 ppm
Particulate Loading	Cyclone and Filtration	Acurex Corp	HVSS	0-3 µm Minimum

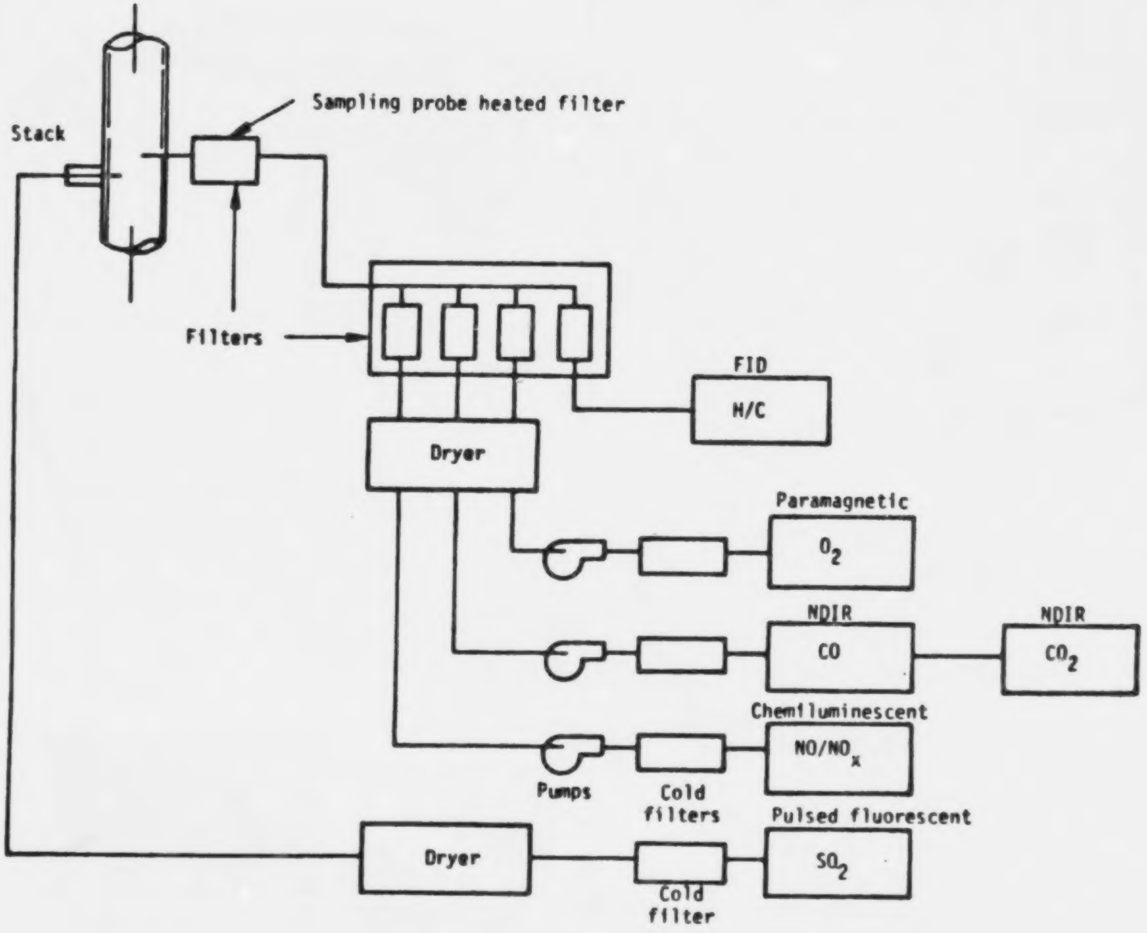
Sampling probe heated filter
Stack
Filters
FID
H/C
Dryer
Paramagnetic
O_2
NDIR
CO
NDIR
CO_2
Chemiluminescent
NO/NO_x
Pumps
Cold filters
Pulsed fluorescent
Dryer
SO_2
Cold filter

Figure 4-10. Sampling system online at experimental multiburner furnace.

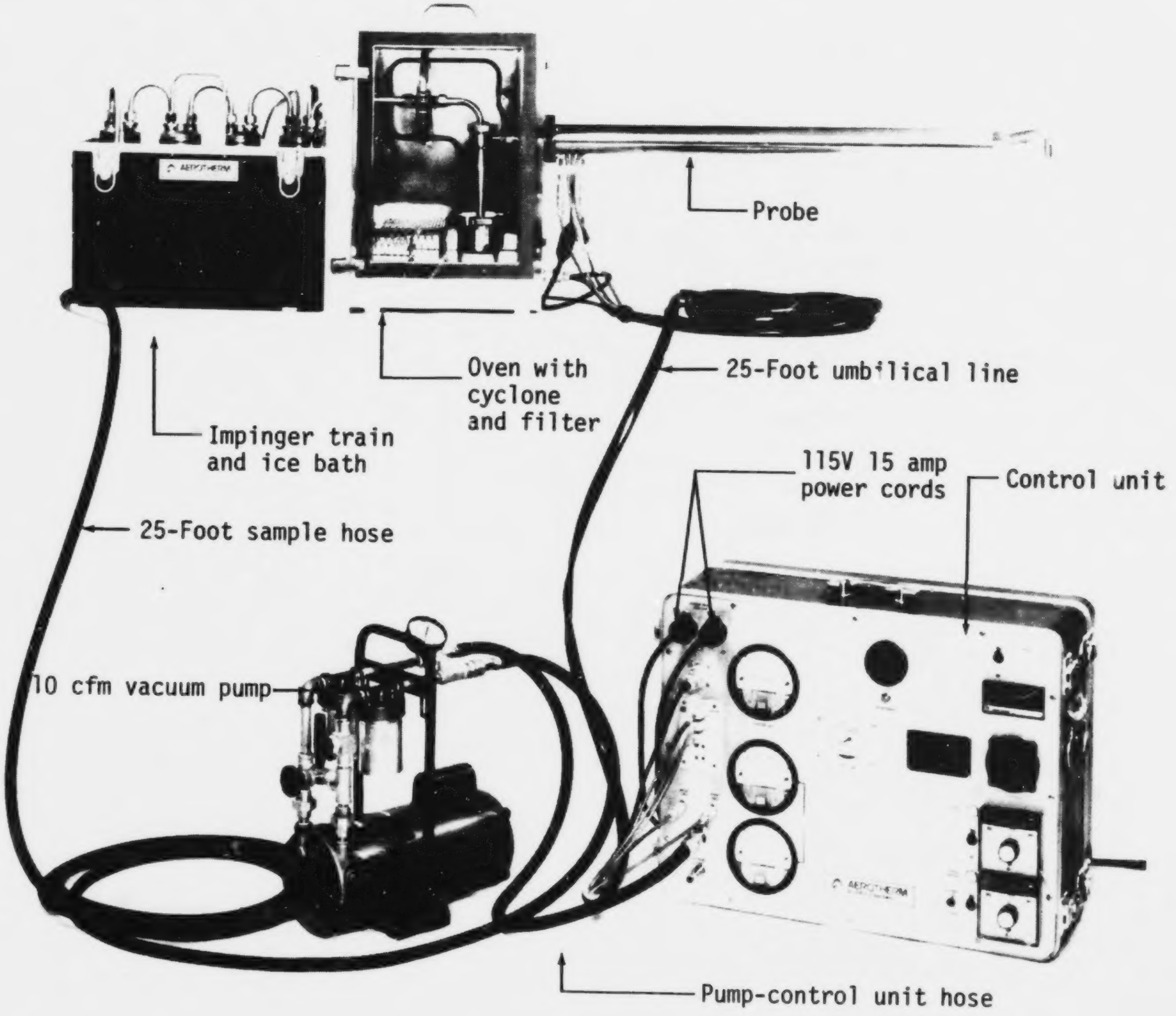
Probe
Oven with cyclone and filter
25-Foot umbilical line
Impinger train and ice bath
115V 15 amp power cords
Control unit
25-Foot sample hose
10 cfm vacuum pump
Pump-control unit hose

Figure 4-11. Aerotherm high volume stack sampler.

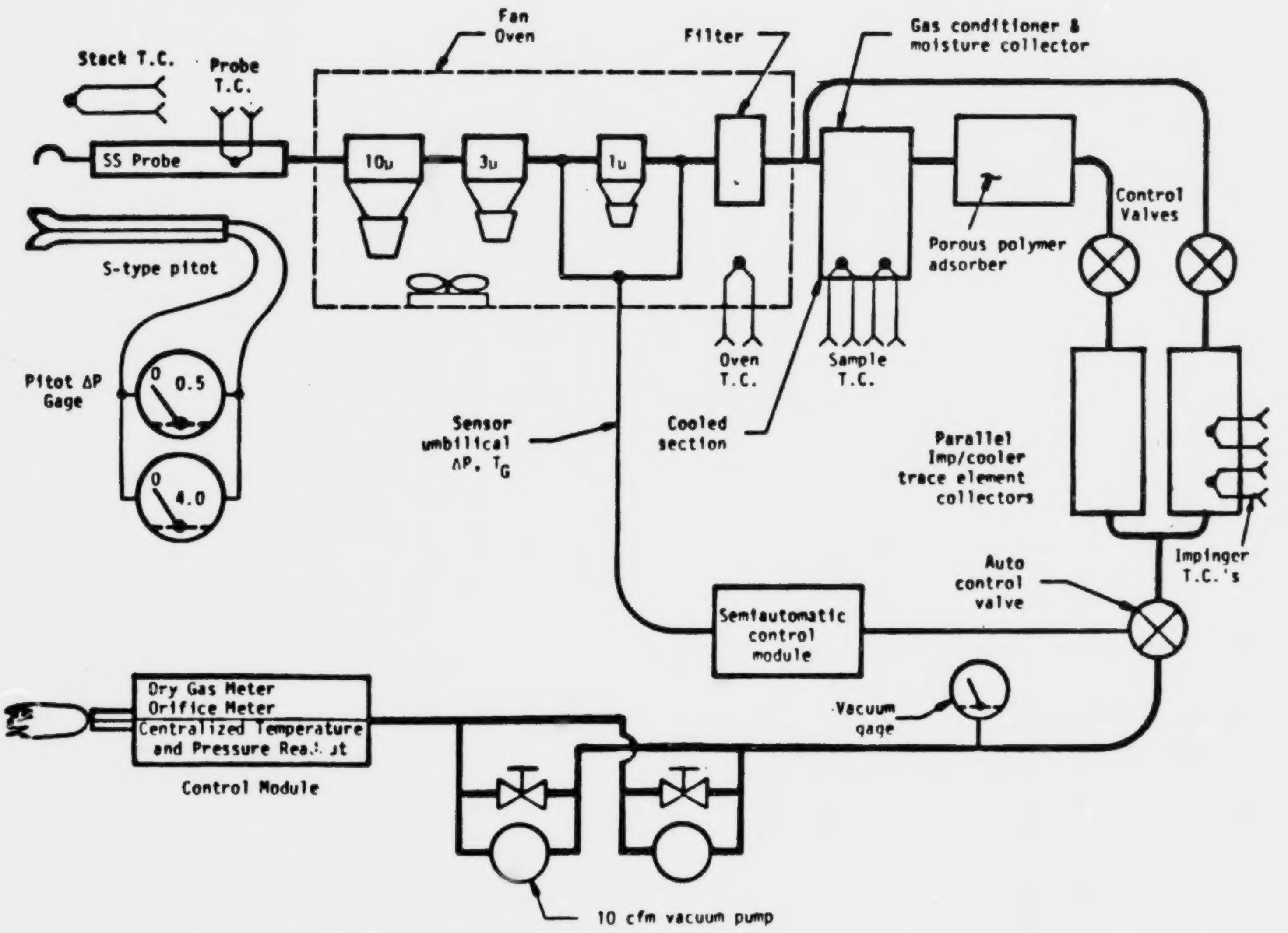
Fan Oven
Filter
Gas conditioner & moisture collector
Stack T.C.
Probe T.C.
SS Probe
10μ
3μ
1μ
S-type pitot
Porous polymer adsorber
Control Valves
Pitot ΔP Gage
0
0.5
0
4.0
Oven T.C.
Sample T.C.
Sensor umbilical ΔP, T_G
Cooled section
Parallel Imp/cooler trace element collectors
Impinger T.C.'s
Auto control valve
Semiautomatic control module
Dry Gas Meter
Orifice Meter
Centralized Temperature and Pressure Readout
Control Module
Vacuum gage
10 cfm vacuum pump

Figure 4-12. Source assessment sampling system (SASS).

4.2.5 Problem Area Summary

As was discussed earlier, one of the objectives of this investigation was to design, fabricate, operate, and evaluate a laboratory-scale system for combustion testing of RDF. Since, to our knowledge, no other refuse investigation had been performed on this scale, it is our intention to fully document the areas where problems occurred during this investigation.

Since the investigation was conducted in the suspension fired, tangential configuration, as descrbed in Section 4.2.2, two complete refuse systems were required for opposed refuse input. The complexity of each system alone required careful monitoring along with the primary fuel systems. The RDF feed systems were evaluated as follows.

Drum System

The mechanical fluidization system performed very well throughout testing, although there were several times the system went down on one side or the other. Problems resulting in downtime were:

1. The weight of the drum system caused compression of the forward cam system and resulted in binding at the teflon bearing-space interface. This problem occurred six to eight times during the 3-week test period and was quickly corrected each time by adjusting the cam vertical position. This problem may be averted altogether by utilizing a noncompressing material for the cam.
2. The nature of the refuse was such that small pieces of paper, glass, etc., being fluidized in the rotating drum found their way into the space between the nylon bearing seals in the forward drum. This resulted in binding at least three times during

testing. The problem was resolved by removing the seal cover and cleaning the entire surface. This required 1 to 1-1/2 hours to complete.

Fluidization of the material was excellent throughout testing as long as the material was in a fluffy, dry condition.

Belt System

As was mentioned earlier, fluidization of the material was poor when it was moist or packed prior to loading in the drums. This resulted in clumping on the belt system which caused inconsistent input to the burners. The drum exit was such that material agglomeration resulted in build up at the exit. This periodically stopped the belt or caused the belt to be stripped of material at that point.

A more efficient deflector design could solve this problem, but more important is providing a properly conditioned feed consistently.

The feed was determined by calibrating the belt rpm against mass delivered. While this system was somewhat accurate initially, as testing on each fuel continued, it became apparent that the calibrations weren't holding. Therefore, the RDF input was determined by back calculating from the flue gas analysis. The errors resulted from the differences in refuse density from layer to layer in the storage bins. Visible differences of the refuse characteristics were evident from day to day on the same fuel types.

Belt to Burner Transition

Most of the plugging problems incurred in this area were due to inconsistency in the refuse sizing. When plugs occurred, sweeping the tube clean was easy and quick, if approached properly. After initial trial and error, elimination of refuse plugs was a secondary problem. However, if material flow sensors allowed buildup on top of the plug to occur, the tube had to be removed in order to sweep the plug.

Generally, a coated or more scratch resistent tube is the only improvement that could have been made.

Plugging in the gun occurred when compacted material from the downcomer was forced into the gun. Other plugs resulted from foreign objects such as wire becoming lodged within the system.

Material Preparation

Generally, a great deal of the handling problems would be eliminated if a material preparation system yielded the same type product each batch. The problems resulting from this are probably nonexistent on a large scale, but become relevant on this small scale. The material is very absorbent in this state and should be guarded from heat and humidity.

Stack Sampling

The physical nature of the particulate product of RDF/gas cofiring resulted in extended sampling periods to collect the required volume of flue gas sample. As shown in Figure 4-12, all particles less than 1.0 micron sizing were collected in a fiberglass filter upstream of the gas conditioner. In all cases with RDF/gas cofiring, all solids collected were smaller than 1.0 micron. Therefore, frequent filter changes were required to complete sampling.

During RDF/coal cofiring tests, the small particulate apparently adhered to the larger coal ash particles and were captured in the cyclones. This eliminated 80 percent of the sample and were captured in the cofired tests.

Ash Deposition

During RDF/gas cofiring, bottom ash deposition was minimal, although after approximately 20 hours of testing at concentrations of 30 percent refuse, on a heat input basis, some ash deposits were removed from the ashpit.

The ash deposition during RDF/coal cofiring displayed characteristics unique to that mixture. Daily ash collection was necessary for all ratios of coal/RDF. However, during approximately 25 hours of testing at a refuse concentration of 30 percent, on a heat input basis, a bridging of ash occurred across the ashpit entrance. This occurrence is illustrated schematically in Figure 4-13. The fused ash material recovered weighed approximately 100 pounds.

This problem has never occurred at this facility before during over 3 years of coal testing at somewhat higher ash input rates.

4.3 TEST THEORY AND PLAN

In order to achieve the objectives noted in Section 4.1, the experimental program consisted of two basic elements:

- Baseline tests -- Evaluation of feed systems and characterization of emissions during gas/refuse cofiring.
- Detailed tests -- Evaluation of combustion efficiency and conventional emissions controls during coal/refuse cofiring.

4.3.1 Baseline Tests

As stated above, the purpose of the baseline tests was to evaluate the refuse feed systems, using all four types of refuse, and characterize the combustion performance and emission levels from each of the materials cofired with gas. Based on the results of these tests, one of the refuse materials was selected for use as the detail test fuel. Also, modifications

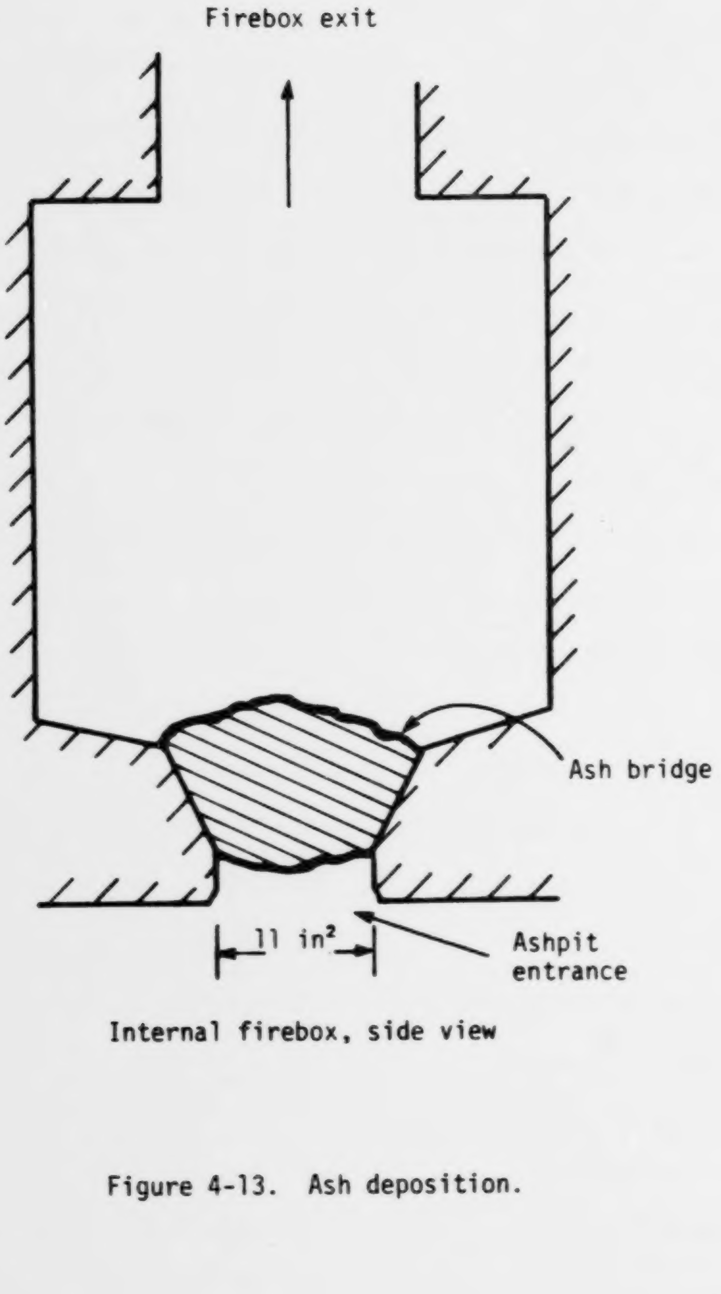
Firebox exit
Ash bridge
11 in²
Ashpit entrance
Internal firebox, side view

Figure 4-13. Ash deposition.

and adjustments of the refuse feed system could be made in order to assure consistent fuel input during the lengthy detailed test points. The emissions produced by each of the refuse types were used to illustrate the uniqueness of each refuse and to obtain background values for the chosen detail test fuel.

The test matrix developed for the baseline testing is shown in Figure 4-14. As noted on all the matrices, sampling is divided in three levels of detail. Level 1 consisted of gaseous emissions sampling only. Level 2 sampling included gaseous emissions and stack particulate loading tests. The Level 3 sampling included tests under Levels 1 and 2 plus detailed stack sampling for trace metals and organic compounds in the stack flue gas.

As indicated in Figure 4-14, the bulk of the testing was completed at 20 percent excess air conditions at a heat input rate of 1.5×10^6 Btu/hr. Tests at other conditions were necessary for background levels to be used with the detailed test results.

4.3.2 Detailed Tests

After completion of the baseline tests and selection of the detail test refuse, the detailed test matrix, shown in Figure 4-15, was addressed. As noted, the purpose of these tests was to evaluate the combustion efficiency of a refuse/coal fuel mixture and to evaluate conventional emissions control, i.e., theoretical air, on the resulting emissions. Sampling test nomenclature was consistent with that used during the baseline tests.

As noted in Section 4.2.5, the particle size of the stack particulate produced during the gas cofired points was such that sampling time required for both Level 2 and 3 tests was increased by a factor of 2. This resulted

4 RDF Types

1) Gas cofire
2) Theoretical air 105%, 110%, 120%, 130%
3) % RDF 5%, 10%, 20%
4) Residence time to convective section (short, long)
5) Firing rate 1.0 x 10^6 and 1.5 x 10^6 Btu/hr

TA — theoretical air; LRT — long residence time; SRT — short residence time;

1. Gaseous emissions sampling only
2. Gaseous emissions plus flue gas particulate loading and size distribution
3. Detailed emissions sampling

		105% TA		110% TA		120% TA		130% TA	
		1.0 x 10^6 Btu/hr	1.5 x 10^6 Btu/hr	1.0 x 10^6 Btu/hr	1.5 x 10^6 Btu/hr	1.0 x 10^6 Btu/hr	1.5 x 10^6 Btu/hr	1.0 x 10^6 Btu/hr	1.5 x 10^6 Btu/hr
5% RDF	SRT								
	LRT		1		1		2		1
10% RDF	SRT								
	LRT		1		1	1	3		1
20% RDF	SRT								
	LRT		1		1		2		1

Figure 4-14. Test matrix for baseline emissions characterization.

1) Cofire RDF with coal
2) Firing rate 1.5 x 10^6 Btu/hr and 1.0 x 10^6 Btu/hr
3) Vary residence time to convective section
4) U.C. RDF, variable %
5) Vary theoretical air

		105% TA		110%		120% TA		130% TA	
		1.0 $\frac{MBtu}{hr}$	1.5 $\frac{MBtu}{hr}$	1.0 $\frac{MBtu}{hr}$	1.5 $\frac{MBtu}{hr}$	1.0 $\frac{MBtu}{hr}$	1.5 $\frac{MBtu}{hr}$	1.0 $\frac{MBtu}{hr}$	1.5 $\frac{MBtu}{hr}$
5% RDF	Long Resid. Time		1		1	1	2		1
	Short Resid. Time								
10% RDF	Long Resid. Time	1	1	1	3	2	3	1	3
	Short Resid. Time								
20% RDF	Long Resid. Time		3	1	2	2	3	3	1
	Short Resid. Time								
30% RDF	Long Resid. Time		2	1	1	1	2		2
	Short Resid. Time								

1. Gaseous emissions sampling only
2. Gaseous emissions sampling plus flue gas particulate loading and size distribution
3. Detailed emissions sampling

Figure 4-15. Test matrix for emissions control through theoretical air variation.

in a loss of sampling points during the detail testing. Figures 4-16 and 4-17 illustrate the completed test matrices. The detailed testing was focused on Level 2 and 3 points as indicated.

4.4 ANALYTICAL PROCEDURES

This investigation required detailed chemical analyses of fuel samples, and gaseous and solid stack product samples. All of these analyses were completed at the Acurex Analytical Laboratory with the exception of analysis of fuel samples.

The methodology of these analyses is outlined below.

4.4.1 Fuel Sample Analysis

Representative samples of all fuels tested during this investigation were submitted to a certified commercial laboratory for ASTM standard analyses listed in Table 4-2.

TABLE 4-2. FUEL ANALYSES

Proximate Analysis	Ultimate Analysis
Moisture	Carbon
Ash	Hydrogen
Fixed Carbon	Nitrogen
Volatile Matter	Oxygen
	Sulfur
	Chlorine
	Heating Value

4.4.2 Trace Metal Analysis

Trace analyses of metals were conducted using atomic absorption spectroscopy by standard EPA and ASTM methods. The metals which were analyzed are listed in Table 4-3. Particulate fractions from the sampling train

4 RDF Types

1)	Gas cofire	
2)	Theoretical air	105%, 110%, 120%, 130%
3)	% RDF	5%, 10%, 20%
4)	Residence time to convective section	(short, long)
5)	Firing rate	1.0 x 10⁶ and 1.5 x 10⁶ Btu/hr

TA – theoretical air; LRT – long residence time; SRT – short residence time;

1. Gaseous emissions sampling only
2. Gaseous emissions plus flue gas particulate loading and size distribution
3. Detailed emissions sampling

		105% TA		110% TA		120% TA		130% TA	
		1.0 x 10⁶ Btu/hr	1.5 x 10⁶ Btu/hr	1.0 x 10⁶ Btu/hr	1.5 x 10⁶ Btu/hr	1.0 x 10⁶ Btu/hr	1.5 x 10⁶ Btu/hr	1.0 x 10⁶ Btu/hr	1.5 x 10⁶ Btu/hr
5% RDF	SRT								
	LRT		①		①		②		①
10% RDF	SRT								
	LRT		①		①	①	③		①
20% RDF	SRT								
	LRT		①		①		②		①

○ Completed tests

Figure 4-16. Test matrix for baseline emissions characterization.

1) Cofire RDF with coal
2) Firing rate 1.5 x 10^6 Btu/hr and 1.0 x 10^6 Btu/hr
3) Vary residence time to convective section
4) U.C. RDF, variable %
5) Vary theoretical air

Reproduced from best available copy.

		105% TA		110%		120% TA		130% TA	
		1.0 $\frac{\text{MBtu}}{\text{hr}}$	1.5 $\frac{\text{MBtu}}{\text{hr}}$	1.0 $\frac{\text{MBtu}}{\text{hr}}$	1.5 $\frac{\text{MBtu}}{\text{hr}}$	1.0 $\frac{\text{MBtu}}{\text{hr}}$	1.5 $\frac{\text{MBtu}}{\text{hr}}$	1.0 $\frac{\text{MBtu}}{\text{hr}}$	1.5 $\frac{\text{MBtu}}{\text{hr}}$
5% RDF	Long Resid. Time		①		①	1	2		1
	Short Resid. Time								
10% RDF	Long Resid. Time	1	①	1	③	2	③	1	3
	Short Resid. Time								
20% RDF	Long Resid. Time		3	1	②	2	③	3	①
	Short Resid. Time								
30% RDF	Long Resid. Time		2	1	①	1	②		②
	Short Resid. Time								

1. Gaseous emissions sampling only
2. Gaseous emissions sampling plus flue gas particulate loading and size distribution
3. Detailed emissions sampling

○ Completed tests

Figure 4-17. Test matrix for emissions control through theoretical air variation.

were analyzed after acid or Parr digestion. For each SASS train, at least three samples were analyzed -- a proportionally combined representative particulate sample, a sample of the XAD-2 resin, and combined aqueous condensate and first impinger solutions after extraction, and the combined second and third impinger solutions. However, only antimony, mercury, and arsenic were analyzed in the second and third impinger samples.

TABLE 4-3. METALS WHICH WERE ANALYZED

Trace Metals	
As	Sb
Be	Sn
Cd	Pb
Hg	Cu
Ti	Mn

4.4.3 Organic Analysis

Organic species were analyzed by a modified Level 1 analysis scheme (Level 1 Environmental Assessment, IERL-RTP Procedures Manual, June 1978). Basically, this scheme involves the separation of a sample extract into broad classes based on liquid chromatography fractionation and gravimetric analysis. An organic extract is placed on a column of silica gel and fractionated by elution with increasingly polar solvents. Table 4-4 lists the solvents which are used in the Level 1 scheme. Each fraction after solvent removal is weighed to yield a rough estimate of material present. This separation scheme yields seven fractions which will contain the compound classes outlined in Table 4-5.

Selected fractions from the liquid chromatography separation were then scrutinized for specific chemical species. For this investigation,

TABLE 4-4. LIQUID CHROMATOGRAPHY ELUTION SEQUENCE

Fraction	Solvent Composition	Volume
1	Pentane	25 ml
2	20 percent methylene chloride in pentane	10 ml
3	50 percent methylene chloride in pentane	10 ml
4	Methylene chloride	10 ml
5	5 percent methanol in methylene chloride	10 ml
6	20 percent methanol in methylene chloride	10 ml
7	50 percent methanol in methylene chloride	10 ml

TABLE 4-5. DISTRIBUTION OF COMPOUND CLASSES IN LIQUID CHROMATOGRAPHIC FRACTIONS OF ORGANIC EXTRACTS

Fraction	Compound Class
1	Aliphatic hydrocarbons Halogenated aliphatics
2,3	Aromatic hydrocarbons Halogenated aromatics (PCB's)
4,5	Nonpolar oxygen or nitrogen containing species
6,7	Polar compounds - phenols, alcohols, amines, etc.

the organic compounds of interest are prevalent only in the LC fractions 2 and 3. Therefore, samples were collected only from these fractions. The sample was then analyzed by gas chromatographic/mass spectrometry methods. During this analysis the level of investigation was determined quantitatively utilizing the threshold level for nearly all the most toxic species as defined by OSHA, that level being 0.10 mg/m^3 of sample gas. All peaks above this level were analyzed for the following groups or species:

1. POM's (polycyclic organic materials)
2. PCB's (polychlorinated biphenals)
3. Four other groups or species

The other groups or species were selected based on the largest quantities of materials which did not fall into the two groups specifically selected above.

4.4.4 Quality Assurance and Control

To assure the quality of the analytical data, a program used to control contamination, calibrate instrument response, and verify qualitative and quantitative data is presented below.

Glassware

All glassware used in the extraction and analysis of the samples was cleaned by one of two methods. Separatory funnels and volumetric glassware were cleaned in a dichromate acid bath, rinsed with deionized water, rinsed with acetone, hexane and methylene chloride, and sealed with muffled aluminum foil. All other glassware was washed with soap and water, rinsed with deionized water, rinsed with acetone and muffled at 450°C to 500°C for approximately 6 hours. Although not adopted as a standard procedure, this procedure has been used by Acurex and EPA labs to produce glassware totally free of detectable organic contaminants for several years.

Solvents and Standards

Only Burdick and Jackson "Distilled in Glass" solvents were used in this program. Acurex purchsed all solvents in lot quantities to assure uniform quality throughout the entire study. A quality check was performed on each solvent to insure the absence of any interfering substances prior to the start of the program.

All standards were purchased from commercial supply houses or from EPA. Each standard was verified by GC/MS prior to its use.

Blanks and Spikes

Two types of blanks were taken: (1) a sampling train blank for each test and (2) method blanks for the solvent extractions. For each series of test runs, a blank train was set up in the same manner as the actual operating train. The blank train was capped off at the nozzle and impinger exit with aluminum foil. The train remained assembled at the test location for the duration of the test period. Sample recovery and analysis proceeded as described for the sampling train. Method blanks using the same glassware and solvents as for the actual samples were taken every 10 samples and analyzed as described earlier.

Metals Analysis

Trace metal analysis requires a careful adherence to good analytical techniques and the measurement of spiked samples. To this end, each sample was spiked to give an increase in the initial concentration greater than 10 percent but less than 100 percent. The recovery was calculated from these data and applied to the values found.

Standards were diluted from stock each day and a standard curve plotted at the beginning and end of each analysis for that element. The standard curve was selected in such a way as to bracket all of the sample concentrations for the run. After each 10 samples, at least one standard was rerun at the level that approximated most of the sample concentrations. Replicates were run at regular intervals to establish precision of the method and spike, and recovery for the accuracy data.

4.5 EXPERIMENTAL DATA

In this section, the experimental results for completed tests will be presented. This will include data on the fuel samples, gaseous emissions, particulate emissions, trace metals, and the organic emissions. Table 4-6 lists the test point designations and their corresponding test conditions for referral from the test data.

4.5.1 Fuel Samples

During the testing phase of this investigation, the fuels were being continually sampled to better characterize the inputs. At the completion of the testing, these gross samples were combined and sent to a commercial laboratory. Representative samples were drawn and analyzed as discussed in the previous section. The results of those analyses are listed in Table 4-7. Photos of the fuel samples are shown in Figure 4-18.

4.5.2 Gaseous Emissions

While the objective of this investigation was primarily to characterize organic and trace metal emissions from conventional fuel/refuse fuel mixtures, gaseous emissions were also fully documented. Discussion of gaseous emissions will be limited to oxides of nitrogen and sulfur dioxide primarily, due to their importance in environmental considerations. Full gaseous data are documented in the appendix.

TABLE 4-6. TEST MATRIX

Test Point	Fuel	RDF Conc*	Combustion Conditions	
11A	Gas/Ames	10%	1.5 x 10^6 Btu/hr	20% EA
B	Gas/Richmond			
C	Gas/Americology			
D	Gas/San Diego	10%		
13A	Gas/Ames	20%		
B	Gas/Richmond			
C	Gas/Americology			
D	Gas/San Diego	20%		
40	Pitts Coal	---		20% EA
15	Coal/Richmond	5%		10% EA
37		10%		10% EA
38		10%		20% EA
32		20%		10% EA
31		20%		20% EA
19		30%		10% EA
35				20% EA
34	Coal/Richmond	30%	1.5 x 10^6 Btu/hr	30% EA

*Heat input basis

TABLE 4-7. FUEL ANALYSES

Ultimate Analysis*	Fuel Type				
	Pittsburg No. 8 coal	Richmond refuse	Ames refuse	Americology refuse	San Diego refuse
Carbon %	75.23	42.60	40.49	40.29	38.01
Hydrogen %	5.15	6.26	6.01	5.88	5.64
Oxyen %	8.12	37.90	30.04	25.20	17.40
Nitrogen %	1.49	0.83	0.73	0.91	0.69
Sulfur %	2.51	0.16	0.35	0.17	0.21
Ash %	7.50	12.25	22.38	27.55	38.05
Moisture % (as received)	0.93	23.8	15.2	24.4	26.3
Chlorine %	0.14	.46	.43	.72	.79
Heating Value Btu/lb	13,545	7696	7831	7164	7146

*Dry basis

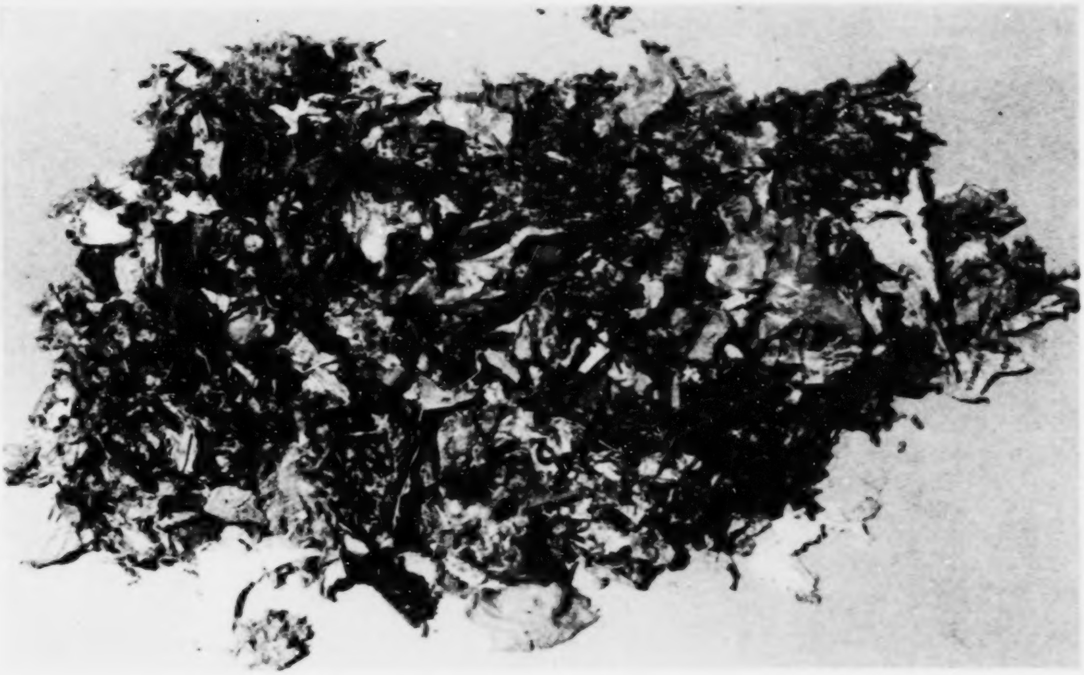

Ames

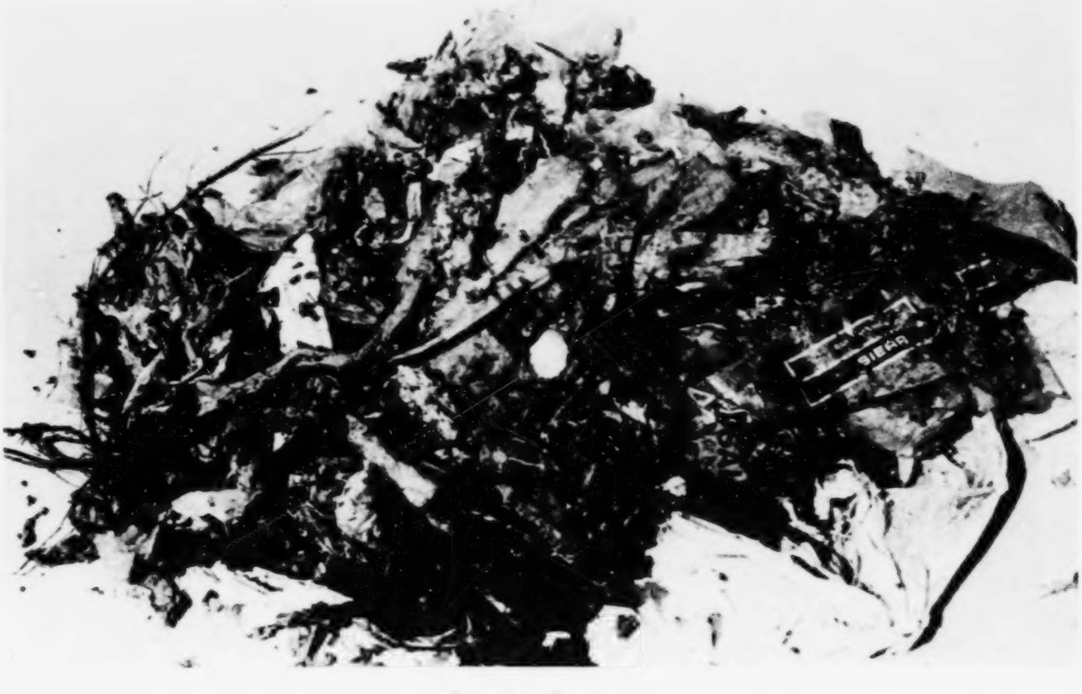

Americology

Figure 4-18. Photographs of fuel samples

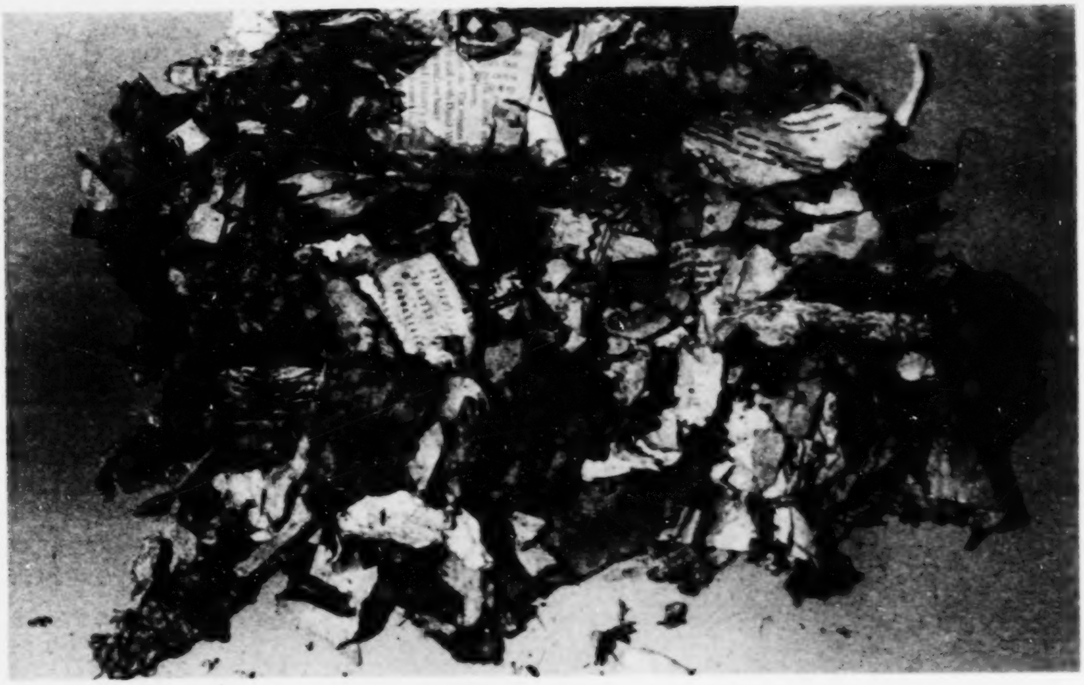

Richmond

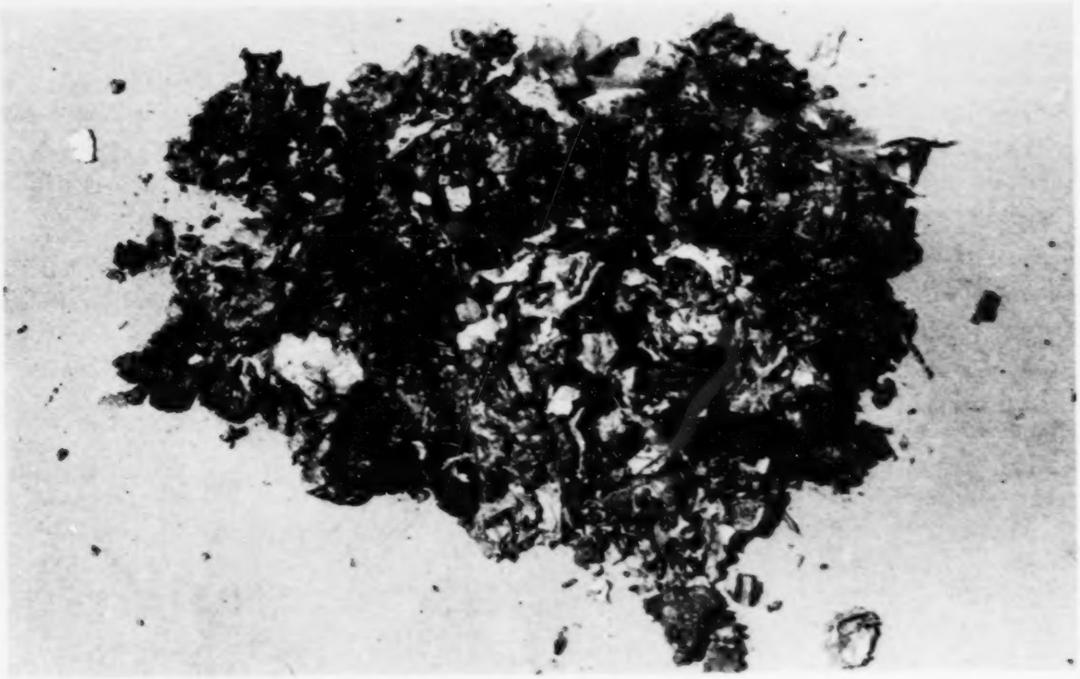

San Diego

Figure 4-18. Concluded.

It should be noted that during this and a previous investigation, sulfur dioxide emissions data were inconsistent. Following this investigation, the Pulsed Florescent SO_2 Analyzer was returned to the manufacturer for evaluation. The source of the inconsistent data was determined to be a photomultiplier tube which rendered the SO_2 data during this investigation invalid on a quantitative basis. However, the data is valid on a relative basis and should be regarded as such.

As discussed in the test plan, baseline testing to characterize the combustion of refuse was conducted first. This was accomplished by co-firing each of the four refuse types with natural gas and by examining several variables. These variables included excess air and concentration of refuse on a heat input basis. All other combustion parameters were held constant.

The results of this baseline testing are illustrated in Figures 4-19 through 4-22 where NO is plotted as a function of excess air percentage for each of the four refuse types. The refuse concentration effects are also illustrated. In each figure, a baseline point is plotted. This point, taken with natural gas as the fuel, represents NO formed through thermal fixation of the atmospheric bound nitrogen. Figure 4-23 represents data taken during previous work on natural gas. The baseline point taken during this investigation is plotted to demonstrate the validity of the NO level. Using this as a baseline illustrates qualitatively the contribution of fuel bound nitrogen to the total NO emission.

It should be noted in Figure 4-20 that the 20 percent Richmond curve falls below the curve representing 10 percent Richmond fuel. This is

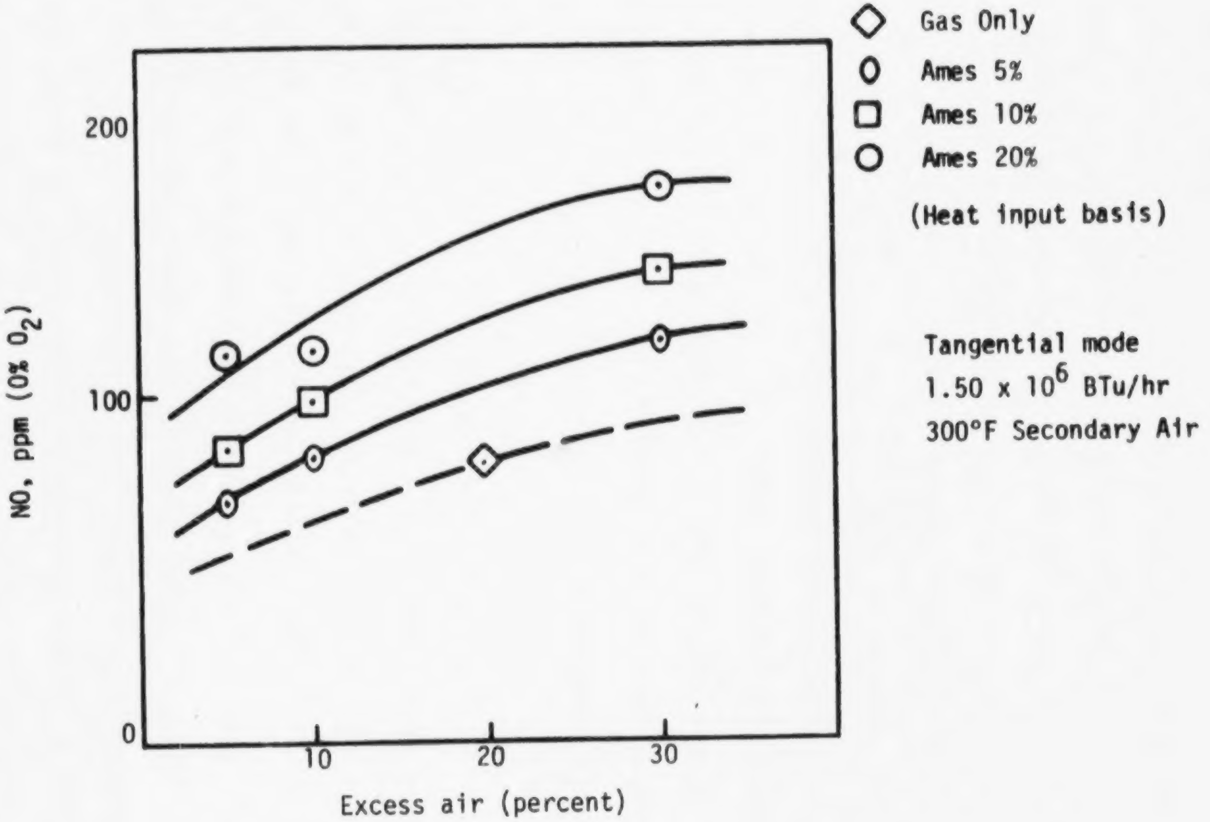

Figure 4-19. NO emissions during baseline testing (Ames).

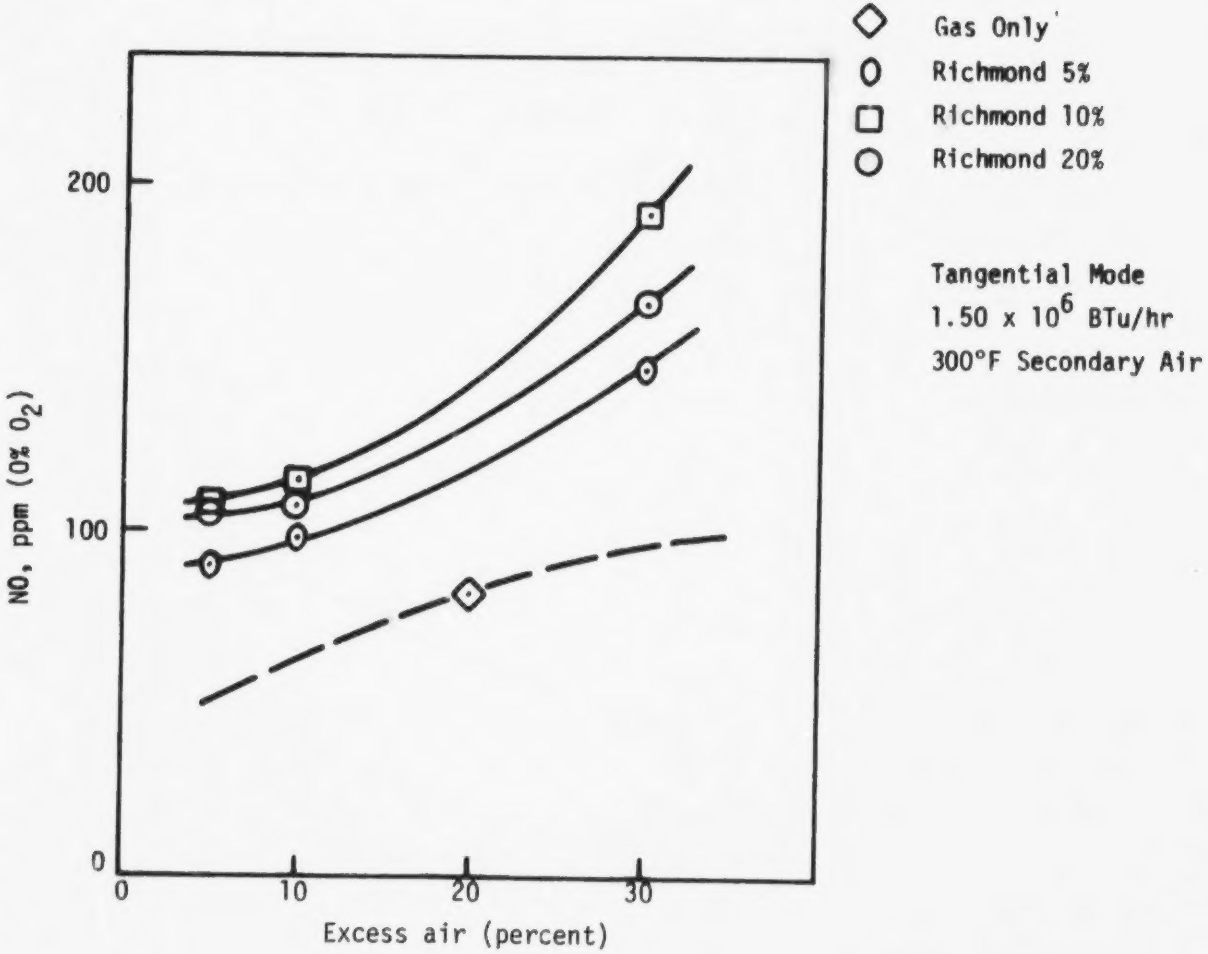

Figure 4-20. NO emissions during baseline testing (Richmond).

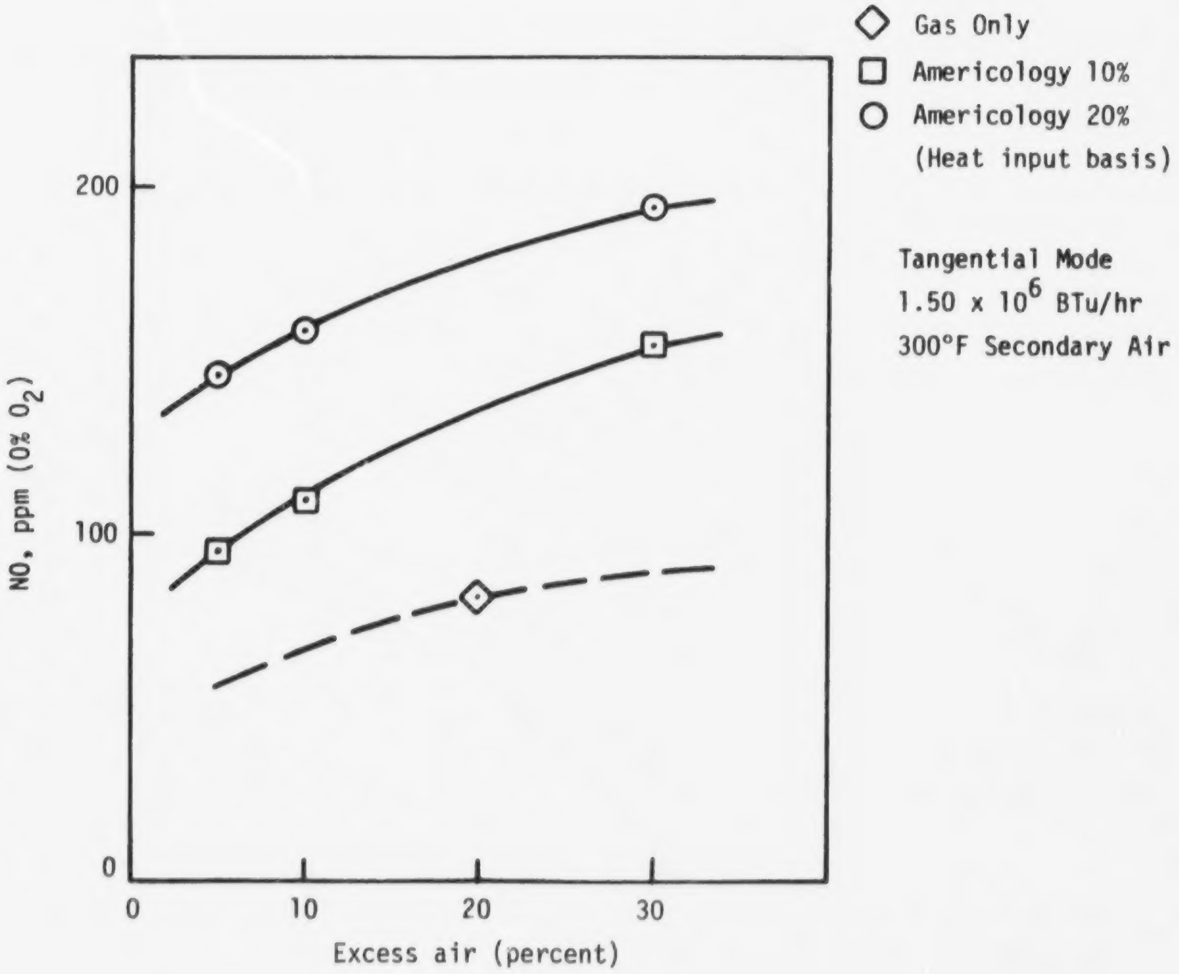

Figure 4-21. NO emissions during baseline testing (Americology).

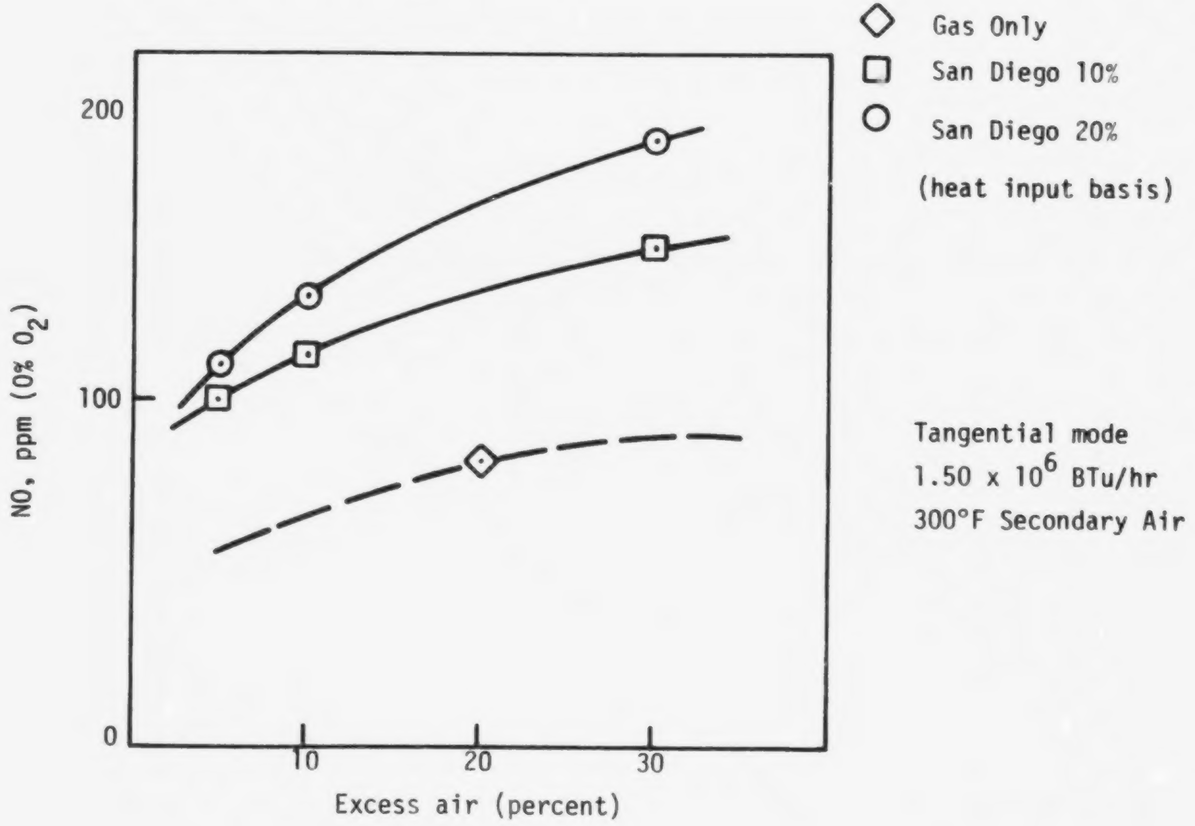

Figure 4-22. NO emissions during baseline testing (San Diego).

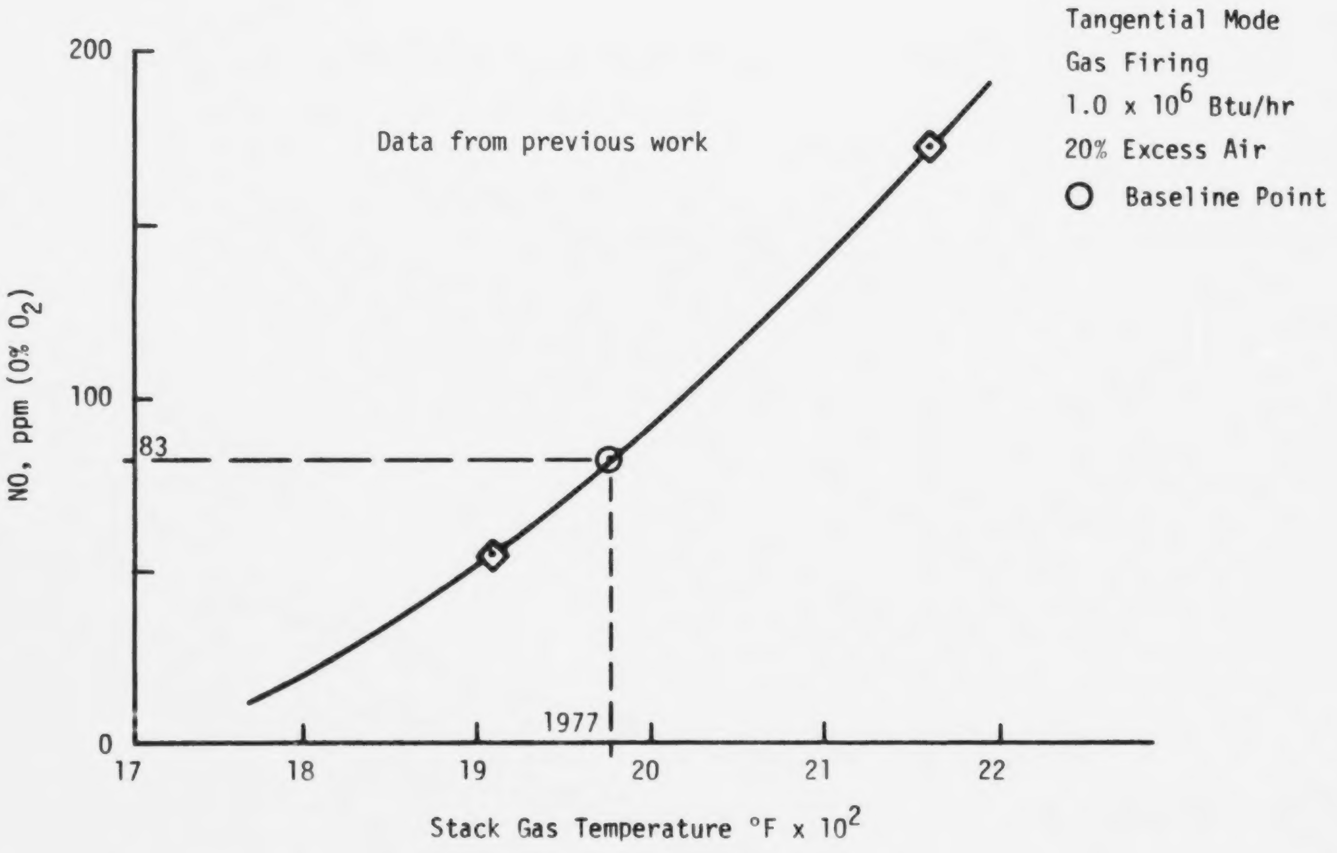

Figure 4-23. Thermal NO (previous work).

believed to be the result of lower thermal NO contributions resulting from cooler flame temperatures. The 20 percent Richmond/gas flame was extremely luminous which resulted in higher radiation losses from the flame and an overall cooler flame. It is well documented that thermal NO is very sensitive to temperature.

Note that neither the Americology nor the San Diego fuel curves contain 5 percent by heat input refuse concentration fuel mixtures. This is due to the density of these two fuels. The feed systems were not capable of delivering a consistent feed at the required low flowrates.

A comparative analysis of the combustion characteristics of each of the individual fuel types is illustrated in Figure 4-24. Shown in this figure are curves representing a constant fuel mixture consisting of natural gas and each of the refuse types with all the other parameters held constant. The fuel nitrogen content of each mixture is listed in the legend. The order of the curves in Figure 4-24 demonstrates the fact that each refuse contributed to the overall NO level in a unique manner. While the curves representing the Ames and San Diego source mixtures are consistent with the chemical relationship, the Richmond source fuel is clearly varying in fuel nitrogen concentration.

As noted earlier, all sulfur dioxide data is valid only on a relative basis. However, a good comparison of fuel types is illustrated in Figure 4-25, where curves for each refuse type cofired with gas at 30 percent excess air are plotted. The sulfur analysis of each fuel is also listed. These curves demonstrate the unique characteristics which each refuse exhibits in a combustion environment.

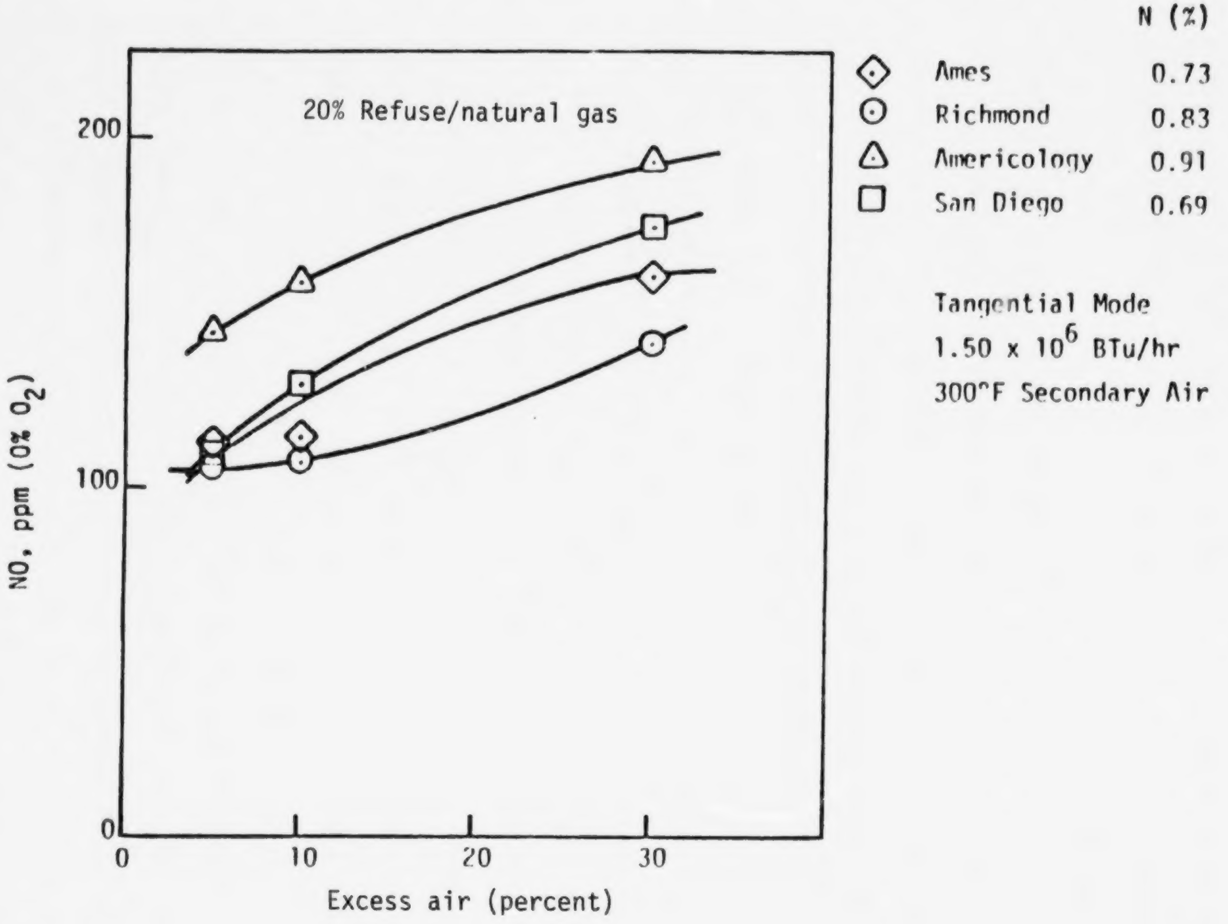

Figure 4-24. NO emissions during baseline testing (all RDF's).

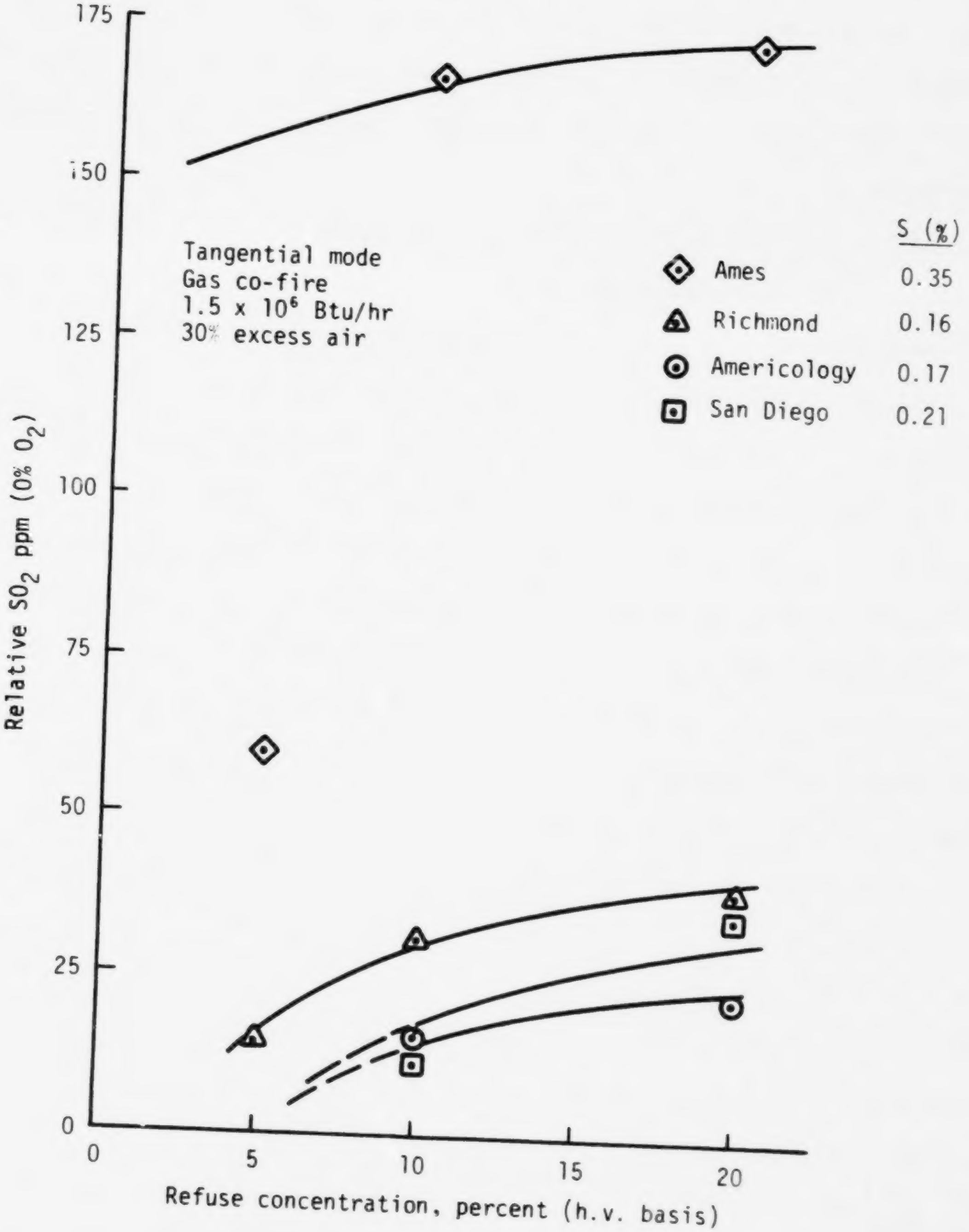

Figure 4-25. SO_2 data (all RDF's).

All gaseous emission data for natural gas testing is listed in the appendix for completeness. In general, however, carbon monoxide, carbon dioxide and unburned hydrocarbon measurements were consistently low throughout the baseline tests.

The refuse/coal cofired tests were focused on obtaining stack gas analyses other than gaseous emissions. However, gaseous emissions were recorded and are presented in the appendix for completeness. The NO emissions for coal cofiring are summarized in Figure 4-26 where the effect of excess air percentage and refuse concentration in the fuel mixture are illustrated. As is shown, a general downward trend is exhibited as refuse concentration is increased. This trend was first believed to be the result of cooler flame temperatures reducing the thermal NO and a reduction in the amount of fuel N available. However, an examination of the fuel nitrogen availability using thermal NO data taken from Figure 4-23 as a function of temperature indicates that a reduction in fuel nitrogen conversion is the likely source of lower NO levels. This data is shown schematically in Figure 4-27 where fuel nitrogen conversion and fuel nitrogen availability is plotted.

4.5.3 Particulate Analyses

The results of the particulate analyses are presented according to variation of combustion conditions.

4.5.3.1 Refuse Type

Table 4-8 lists the results as a function of refuse type for the gas cofired tests. Each point is also expressed as percent of total mass to illustrate where the bulk of the loading lies, according to size. As noted

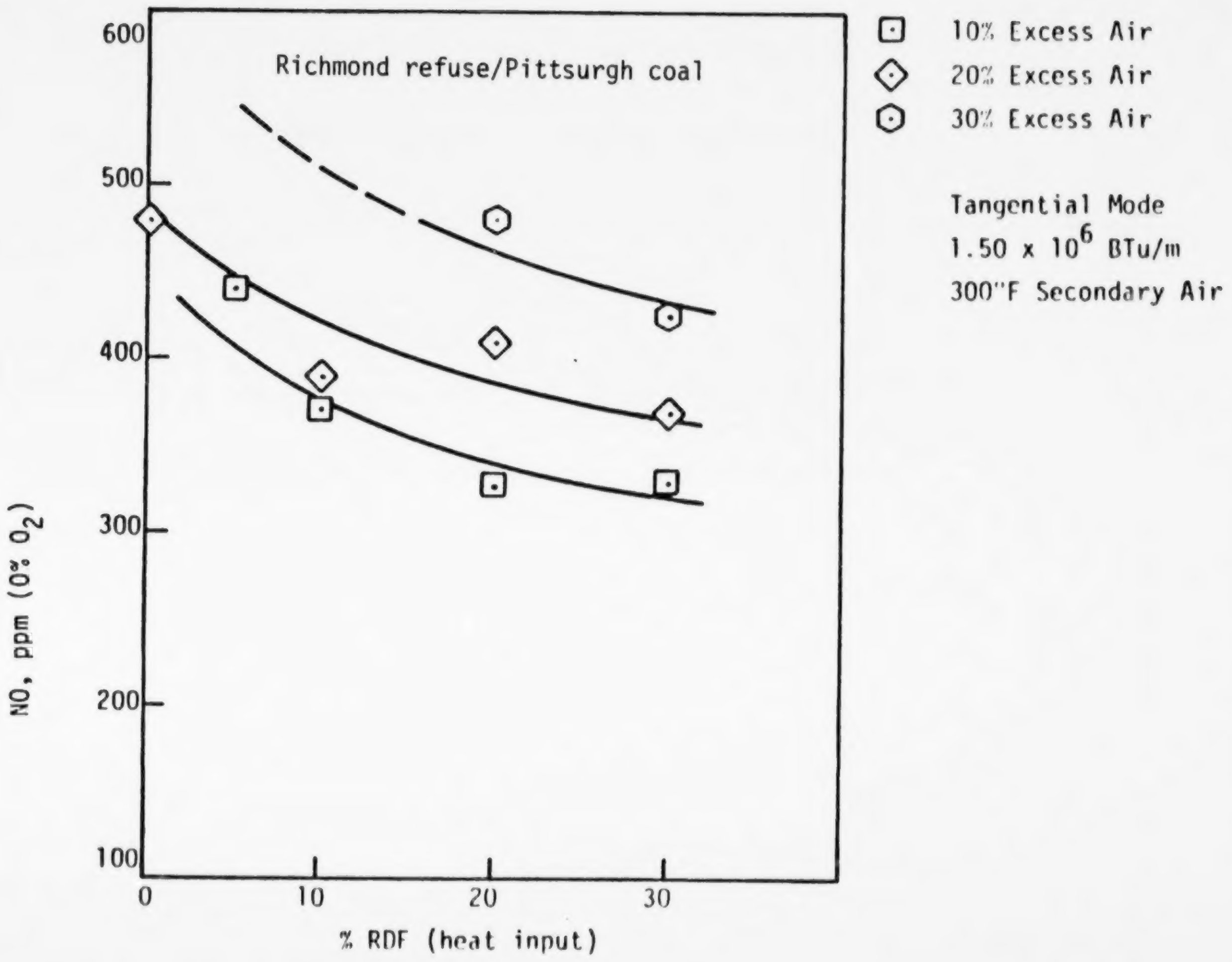

Figure 4-26. NO emissions during detailed testing (Richmond RDF/Pittsburg coal).

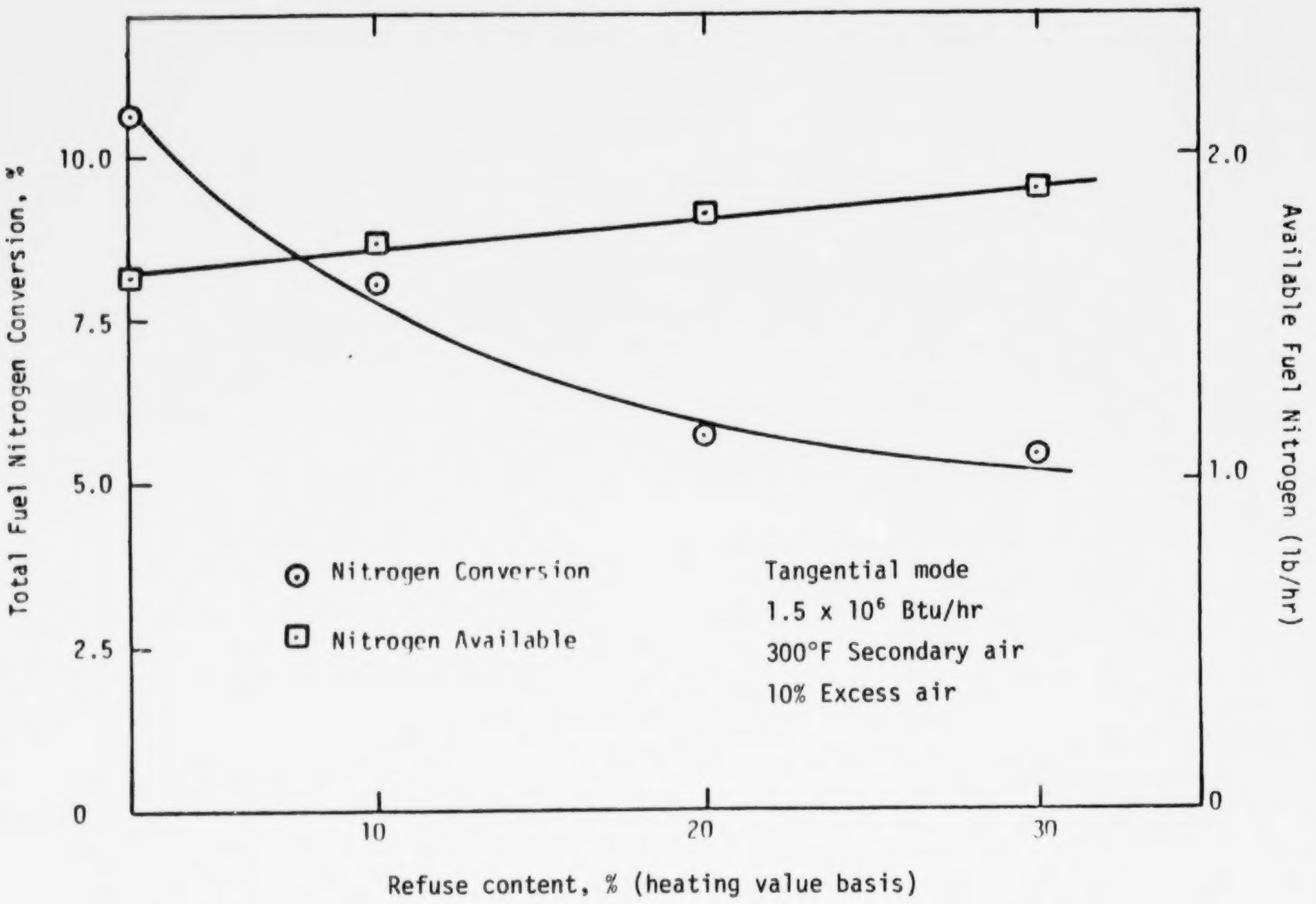

Figure 4-27. Fuel nitrogen contribution.

TABLE 4-8. PARTICULATE ANALYSES: EFFECT OF RDF TYPE

Type/ % RDF	Test* No.	Excess Air (%)	Filter (gr/ft^3)	>10 (gr/ft^3)	>3μ (gr/ft^3)	>1μ (gr/ft^3)	Total (gr/ft^3)	% Ash
Ames/ 20%	13A	20	0.03912	0.01067	0.00343	0.00351	0.05673	22.38
	% of Total		68.96	18.81	6.05	6.19		
Richmond/ 20%	13B		0.03223	0.00044	0.00042	0.00235	0.03544	12.25
	% of Total		90.94	1.24	1.19	6.63		
Americology/ 20%	13C		0.04063	0.00233	0.00232	0.00217	0.04744	27.55
	% of Total		85.65	4.91	4.89	4.57		
San Diego/ 20%	13D		0.06158	0.00732	0.00245	0.00601	0.07737	38.05
	% of Total		79.59	9.46	3.17	7.77		
Ames/ 10%	11A		0.03165	0.00317	0.00213	0.00169	0.03883	22.38
	% of Total		81.51	8.16	5.49	4.35		
Richmond/ 10%	11B		0.02445	0.00095	0.00036	0.00023	0.02600	12.25
	% of Total		94.04	3.65	1.38	0.88		
Americology/ 10%	11C		0.06330	0.00283	0.00288	0.00370	0.07272	27.55
	% of Total		87.05	3.89	3.96	5.09		
San Diego/ 10%	11D		0.06684	0.00354	0.00137	0.00391	0.07568	38.05
	% of Total		88.32	4.68	1.81	5.17		

---

*Fired with natural gas

in Section 4.2.5, the highest percentage loading consistently occurred in the less than 10 micron (μ) range which was trapped in the filters. As can be noted from the table, the grain loading corresponds roughly to the percent ash in the fuel. It can also be observed that the Richmond fuel consistently had the highest percentage of particules in the less than 1 μ size cut. Similarly, the Ames fuel consistently had the lowest percentage in this range size cut.

4.5.3.2 Excess Air

Table 4-9 shows the effect of excess air for the coal cofired tests. Both 10 percent and 20 percent refuse concentration points are shown. Note that in the coal cofired tests, the majority of the loadings were evenly distributed in the size ranges larger than 1.0 micron (μ). Several additional comments can be made regarding Table 4-9.

- The percent material in the less than 1 μ size cut increases with excess air. If the particulate is friable, the increase in velocity may cause more of the material to break up into the smaller size fraction.
- The total grain loadings decreased as the excess air increased, but more rapidly than straight dilutions would account for. This could indicate that there is more unburned carbon in the particulate at the lower excess air levels. Thus it appears that the effect of excess air is to lower the overall grain loading while concentrating more of the particulate in the respirable size fraction.

TABLE 4-9. PARTICULATE ANALYSES: EFFECT OF EXCESS AIR

Test No.	Excess Air (%)	%* RDF	Filter (gr/ft^3)	>10μ (gr/ft^3)	>3μ (gr/ft^3)	>1μ (gr/ft^3)	Total (gr/ft^3)
37	10	10	0.02287	0.39145	0.29222	0.08274	0.78930
% of Total			2.90	49.59	37.02	10.48	
38	20		0.04439	0.26900	0.22627	0.04422	0.58389
% of Total			7.60	46.07	38.75	7.87	
34	30		0.04833	0.25437	0.20814	0.03725	0.52276
% of Total			9.25	48.49	39.82	7.13	
32	10	20	0.05455	0.45018	0.39695	0.13290	1.03459
% of Total			5.27	43.51	38.37	12.85	
31	20		0.02583	0.13386	0.10736	0.01570	0.28276
% of Total			9.13	47.34	37.97	5.55	

*Fired with coal

4.5.3.3 RDF Concentration

The effect of refuse concentration, cofired with coal, is shown in Table 4-10. Results are listed for both 10 and 20 percent excess air levels. An even distribution again occurred in the larger than 1.0 micron (μ) size ranges. This table is merely a rearrangement of the previous table. The only point that needs to be reemphasized here is that it appears that the fraction in the less than 1 μ size cut increases with increasing percent RDF. However, these conclusions should be addressed with a bit of caution because the total grain loadings did not increase with percent RDF in all cases. The reason for this apparent data scatter is not clear at this time. However, it could be caused by holdup in the heat exchange sections of the furnace, by non-isokinetic sampling in the duct, or by the wall and probe effects in the small exhaust duct due to the standard large EPA method 5 sampling probe.

A summary curve of the data shown in the table is shown in Figure 4-28 as the cumulative percent less than a given particle size. This again shows the trend of a higher percentage in the less than 1 μ size cut as the percent of RDF increases.

4.5.3.4 Fuel Makeup

Table 4-11 compares the particulate loadings of the three fuel mixtures. These results are further illustrated in Figure 4-29 where particulate loading is plotted along with fuel ash content. The table illustrates that the fraction in the less than 1 μ size cut is increased when firing coal alone. This indicates that the RDF is contributing to this fraction and probably not agglomerating to the larger coal particles. The figure

TABLE 4-10. PARTICULATE ANALYSES: EFFECT OF PERCENT RDF

Test No.	Excess Air (%)	%* RDF	Filter (gr/ft^3)	>10μ (gr/ft^3)	>3μ (gr/ft^3)	>1μ (gr/ft^3)	Total (gr/ft)
37	10	10	0.02287	0.39145	0.29222	0.08274	0.78930
% of Total			2.90	49.59	37.02	10.48	
32		20	0.05455	0.45018	0.39695	0.13290	1.03459
% of Total			5.27	43.51	38.37	12.85	
38	20	10	0.04439	0.26900	0.22627	0.04422	0.58389
% of Total			7.60	46.07	38.75	7.57	
31	20	20	0.02583	0.13386	0.10736	0.01570	0.28276
% of Total			9.13	47.34	37.97	5.55	
35	20	30					

*Fired with coal

TABLE 4-11. PARTICULATE ANALYSES: COAL VS. 10% RDF + COAL VS. 10% RDF + GAS

Test No.	Excess Air (%)	% RDF + Fuel	Filter (gr/ft^3)	>10 (gr/ft^3)	>3 (gr/ft^3)	>1 (gr/ft^3)	Total (gr/ft^3)
40	20	Coal	0.02052	0.53895	0.34355	0.05465	0.97769
% of Total			2.14	56.28	35.87	5.71	
28		10% RDF + Coal	0.04439	0.26900	0.22627	0.04422	0.58389
% of Total			7.60	46.07	38.75	7.57	
11B		10% RDF + Gas	0.02445	0.00095	0.00036	0.00023	0.02600
% of Total			94.04	3.65	1.38	0.88	

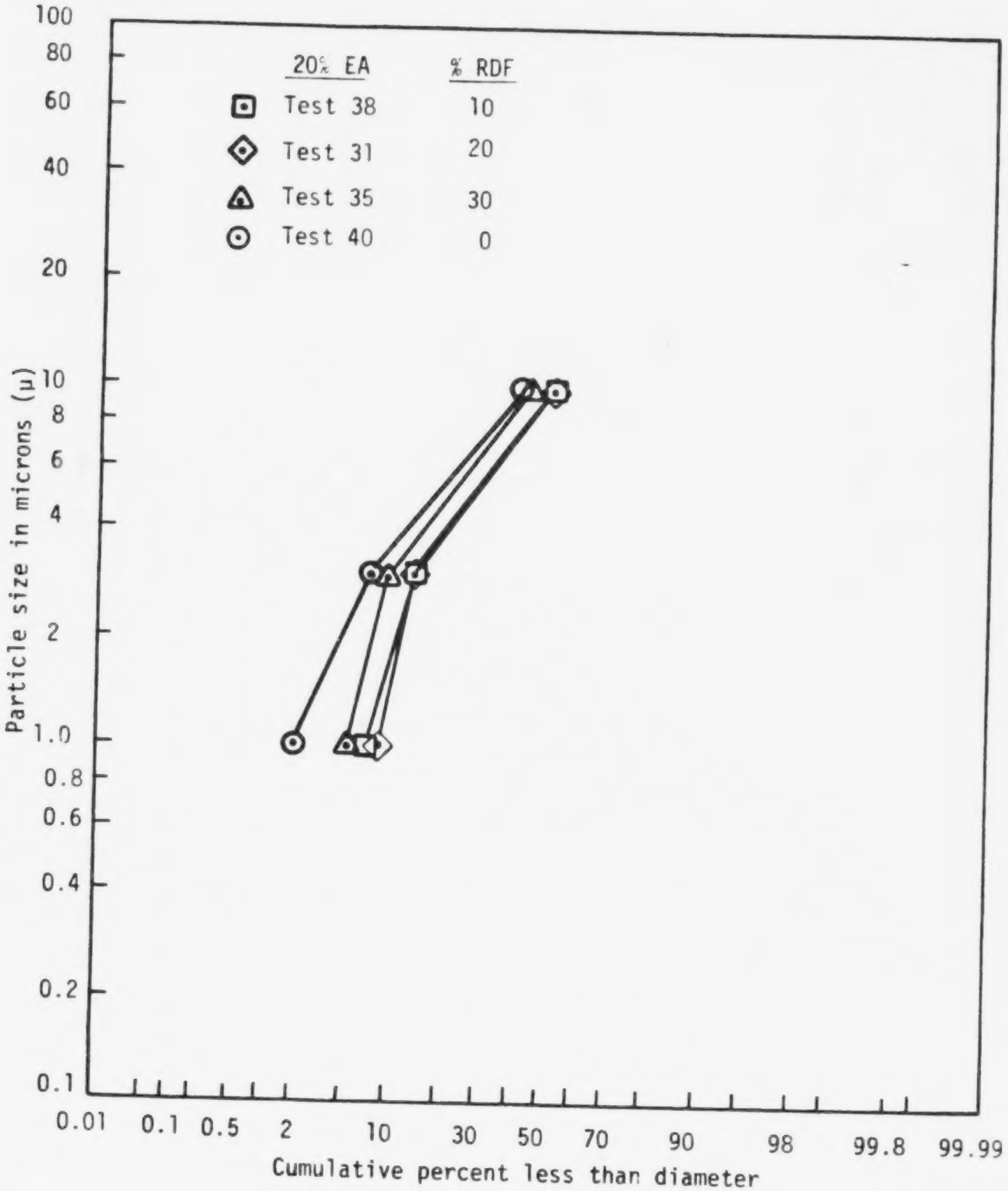

Figure 4-28. Stack gas particle size vs. cumulative percent less than diameter.

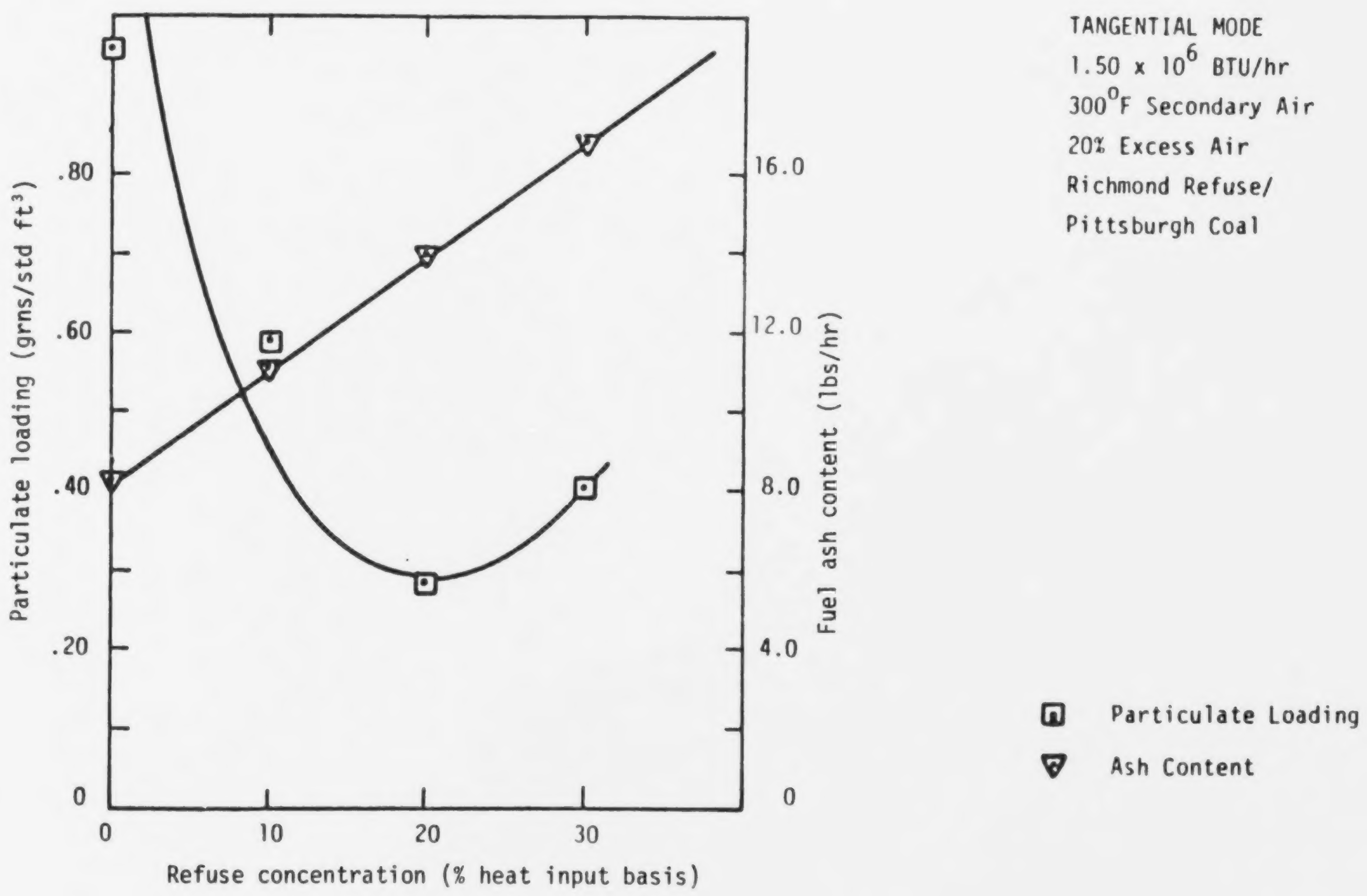

Figure 4-29. Particulate loading results.

indicates a rather strange effect, and that is that the grain loadings decrease with increasing percent RDF with a minimum at 20 percent RDF. Possible explanations for this include a greater hold up in the convective section, or more material reaching the ashpit or sticking to the walls of the furnace. It is possible that resultant ash properties or heat transfer conditions are changing such that more material is deposited either in the furnace or on the convective tubes. However, the duration of each of these tests was not sufficiently long to determine if this hypothesis is true. In addition, due to the refractory walls and dissimilar convective tubes compared to a full-scale boiler, it is rather speculative to say a similar effect would occur in the full-scale systems.

4.5.3.5 Percent Combustibles in Flyash

Table 4-12 lists the results of the analysis on percent combustibles as a function of percent excess air and percent refuse when cofired with coal. As was the case for CO and unburned hydrocarbons, these results indicate that the combustion efficiency is quite good in the pilot-scale facility when cofiring RDF with coal as long as the excess air is above 10 percent. There is an indication that even this facility does not operate quite as efficiently with the refuse as with coal alone. This certainly has been the case in full-scale units where considerable unburned material has found its way to the ashpit. The reference to the plugging of the ashpit in Section 4.2.5 is another indication of unique problems with the RDF materials.

However, it is possible that the additional shredding and/or the hot refractory walls aid in ignition and achieving complete combustion in

TABLE 4-12. COMBUSTIBLE CONTENT IN FLYASH

RDF CONCENTRATION (Heat Input Basis)		EXCESS AIR		
		10%	20%	30%
	0%		0.43%	
	10%	9.56%	1.37%	
	20%	8.15%	1.35%	
	30%		1.17%	3.46%

Tangential mode - 1.5 x 106 Btu/hr
Richmond refuse/Pitts #8 coal
300°F sec air

the pilot-scale facility. Perhaps boilers designed specifically to burn RDF cofired with coal will require a hotter radiative section. Of course, the resulting ashing problems associated with the coal would have to be taken into consideration.

4.5.4 Trace Metals

Concentrations of 11 trace metals were determined in the solid particulate and condensible vapors collected in the SASS impingers.

A summary of the total concentrations found on a μg/Btu basis is shown in Table 4-13 for all the coal plus RDF tests where the SASS train was used. A comparison is also made with the gas test using the same Richmond RDF. Although few conclusions can be drawn with regard to this limited sample, the following commments are in order:

- With a few exceptions, the order of magnitude of each of the trace elements does not vary greatly from test to test.
- Exceptions to this comment include the following:

Cu	Tests #37 and #40
Zn	Test #32
Pb	Test #40
Sn	Test #11b
As	Test #32

- There appears to be no clear trend on any of the elements with regard either to percent RDF or percent excess air.
- There does not appear to be much difference in the total trace metal concentrations when firing gas plus RDF or coal plus RDF (six approximately the same, one higher, and four lower).

This last comment leaves the validity of these measurements somewhat in question as it would have been expected that the trace metal concentrations when cofiring with natural gas would be considerably lower.

TABLE 4-13. TOTAL TRACE METAL LOADINGS (μg/Btu) – COAL COFIRING

Fuel	Coal	Coal	Coal	Coal	Coal	Coal	Gas
% EA	10	20	10	20	30	20	20
% RDF	10	10	20	20	30	0	10
Test No. / Element	#37	#38	#32	#31	#34	#40	#11B
Cu	<1.660		<0.309	<0.184	0.206	1.958	0.340
Zn	1.978		5.327	1.504	2.025	0.686	1.821
Mn	<0.207	<0.2693	<0.520	<0.3549	<0.3512	0.153	0.0209
Pb	0.697		1.319	<2.591	2.865	17.53	1.500
Cd	<0.0081		0.0126	<0.013	0.0037	0.009	0.0062
Be	0.004		<0.0009	<0.0108	0.0025	<0.0176	<0.0034
Ti	<1.125		<1.2525	<0.4379	<1.382	<1.7540	<0.0277
Sb	<0.0047	<0.0090	<0.0386	<0.0809	<0.010	<0.024	0.0333
Sn	<0.1101	<0.0913	0.1060	0.1508	<0.1481	0.130	<3.503
Hg	0.0274	<0.0173	<0.0293	<0.0058	0.0187	<0.0015	<0.0009
As	<0.0389	<0.0323	1.3839	<0.0408	<0.0402	<0.088	<0.0184

However, the nonhomogeneity of the material must be considered as well as the influence of the test furnace. First, it is possible that large concentrations of a particular trace metal can be present locally in the feed and find their way to the stack sampling equipment. Holdup of material in the heat exchange sections of the furnace system can also result in momentary high particulate concentrations if the material breaks loose from the heat exchange surfaces in large discrete clumps. Finally, metals in the furnace from the burners (particularly copper, lead, and Zn from cooling coils, silver solder and brazing compounds) may also find their way to the stack. Due to these factors, it will probably require a large data base at any given test condition to obtain a statistically meaningful result.

Table 4-14 lists the percentages of the total trace metals found as condensible vapors collected in the organic module and impinger sections of the SASS. Again, no clear trends are present although Hg, Cu, Mn, and Sn generally had high percentages in the vapor phase. Cd was usually split between the vapor and solid and As was almost always found with the particulate. The remaining trace metals had widely varying concentrations of the condensible material.

Table 4-15 presents the total trace metal concentration for the four RDF materials when cofired with natural gas. Again, there appears to be wide variations between the different RDF types. Similarly, Table 4-16 presents the percent vapor for each of these materials. Hg always appears in the vapor and As in the particulate. Be, Cu, Sn and Mn were also usually found in the vapor. Again, the heterogeneous nature of these materials must be considered.

TABLE 4-14. TRACE METAL CONCENTRATIONS (%) – COAL COFIRING

Fuel	Coal	Coal	Coal	Coal	Coal	Coal	Gas
% EA	10	20	10	20	30	20	20
% RDF	10	10	20	20	30	0	10
Test No. / Element	#37	#38	#32	#31	#34	#40	#11B
Cu	99.9		79.1	45.4	73.1	96.2	64.7
Zn	81.1		28.2	44.9	68.2	77.2	24.5
Mn	90.6	91.7	89.5	92.3	93.2	39.4	77
Pb	57.4		28.1	3.8	84.5	98	40.6
Cd	43.2		51.6	2.3	49.9	48.4	43.5
Be	90.0		11.1	41.7	23.0	73.9	82
Ti	1.1		0.9	30.0	2.0	25.1	64.1
Sb	17.0	1.1	76.9	61.8	28.7	3.3	7.2
Sn	74.8	63.9	68.5	49.5	87.6	65	99.6
Hg	31.0	91.3	97.6	100	81.3	80	100
As	3.9	10.2	0.3	3.7	9.3	18.2	9.2

TABLE 4-15. TOTAL TRACE METAL LOADINGS (μg/Btu) — GAS COFIRING

Fuel	Gas	Gas	Gas	Gas
%EA	20	20	20	20
% RDF	10	10	10	10

Test No. Element	11A Ames	11B Richmond	11C Americology	11D San Diego
Cu	0.653	0.340		4.11
Zn	2.972	1.821		13.58
Mn	0.0111	0.021	0.039	0.238
Pb	4.38	1.50		42.08
Cd	0.0119	0.006		0.0613
Be	0.0008	0.003		0.00027
Ti	0.088	0.028		0.281
Sb	0.118	0.033	0.222	0.0988
Sn	0.090	3.50	0.102	0.722
Hg	0.032	0.001	0.005	0.035
As	0.020	0.018	0.0095	0.319

TABLE 4-16. TRACE METAL CONCENTRATIONS AS VAPOR (%) — COAL COFIRING

Fuel	Gas	Gas	Gas	Gas
% EA	20	20	20	20
% RDF	10	10	10	10

Test No. / Element	11A Ames	11B Richmond	11C Americology	11C San Diego
Cu	80.2	64.7		86.8
Zn	21.7	24.5		8.7
Mn	78.4	77	48	92.3
Pb	7.5	40.6		10.7
Cd	5.9	43.5		98.2
Be	94.9	82		94.8
Ti	11.3	64.1		6.4
Sb	0.6	7.2	1.2	39.7
Sn	68.2	99.6	89	15.7
Hg	99.9	100	98.8	99.9
As	11.1	9.2	30.2	55.8

A comparison was also made between the trace metal concentrations in the particulate flyash found in these tests and data found in the literature for both coal and coal plus various RDF. These results are shown in Table 4-17 for each of the test conditions and for three sets of field data. The field data is from the St. Louis demonstration (Reference 12), Wright Patterson Air Force Base (Reference 13), and the Ames-Iowa facility (Reference 14). The data is presented in μg/grain of flyash for the solid particulate only. Again, wide variations in both the data developed on this program as well as the field data are seen. It should also be mentioned that the field data are average numbers and that there was considerable variation even from one site. From the field data, it appears the results generated here are within the same order of magnitude. However, trends as a function of either excess air or percent RDF still cannot be discerned.

Finally, two sets of particulate data were analyzed for each of the trace metals in each of the cyclone size cuts. This was done for the coal only test (#40) and for coal plus 20 percent RDF at 20 percent excess air, Test 31. Figures 4-30 through 4-40 show the charts of cumulative percent versus size cut for each trace metal. As before, this is plotted as the cumulative percent below and including a given size. The first cyclone catches all material >10 μ, and the filter catches everything less than 1 μ. Seven out of the 11 elements indicate that the presence of RDF results in a higher percentage in the smaller size cuts. Trace metals which have a reverse trend include As, Be, Mn, and Zn where the coal only has high concentrations of these elements in the finer sizes. However, in light of the randomness of much of the other trace metal data, caution should be exercised in drawing any definitive conclusions from these curves.

TABLE 4-17. TRACE METAL CONCENTRATIONS (μg/g OF FLYASH) — PILOT VS. FULL SCALE (PARTICULATE ONLY)

Fuel	Coal	Coal	Coal	Coal	Coal	Coal	Coal	Coal	Coal	Coal	Coal	Coal	Coal	Coal
% EA	10	20	10	20	30	20	--	--	--	--	--	--	--	--
% RDF	10	10	20	20	30	0	7	0	34	51	0	20	50	0
Test Element	#37	#38	#32	#31	#34	#40	St.Louis Ref 12	St. Louis Ref 12	WPAFB Ref 13	WPAFB Ref 14	WPAFB Ref 13	Ames Ref 14	Ames Ref 14	Ames Ref 14
Cu	1,508	--	--	4,611	126	1,304	430	236	--	--	--	472	379	153
Zn	506.8	--	4,799	28,927	1,465	2,516	2,534	1,102	11,433	27,563	902	29,211	25,211	8,373
Mn	26	76.5	69	619	54	600	--	--	--	--	--	414	360	628
Pb	402	--	1,190	118,475	1,010	5,519	1,681	598	9,880	21,290	493	31,684	22,815	6,733
Cd	6.2	--	7.6	515.4	4.1	42.9	44	35	--	--	--	--	--	--
Be	0.6	--	1.0	83.8	4.3	50.0	24.3	8.98	--	--	--	--	--	--
Ti	1,508	--	1,558	12,188	3,081	4,994	12,050	2,584	--	--	--	3,196	235,710	3,625
Sb	5.31	30.3	11.1	1415.7	16.2	29.8	17.3	1.82	--	--	--	--	--	--
Sn	<38	113	<42	4,042	4.2	596	--	--	--	--	--	--	--	--
Hg	25.5	5.1	8.5	1.4	8.0	1.1	13.04	6.42	--	--	--	--	--	--
As	50.6	99	55.9	1206.6	82.9	725.7	62	189	--	--	--	--	--	--

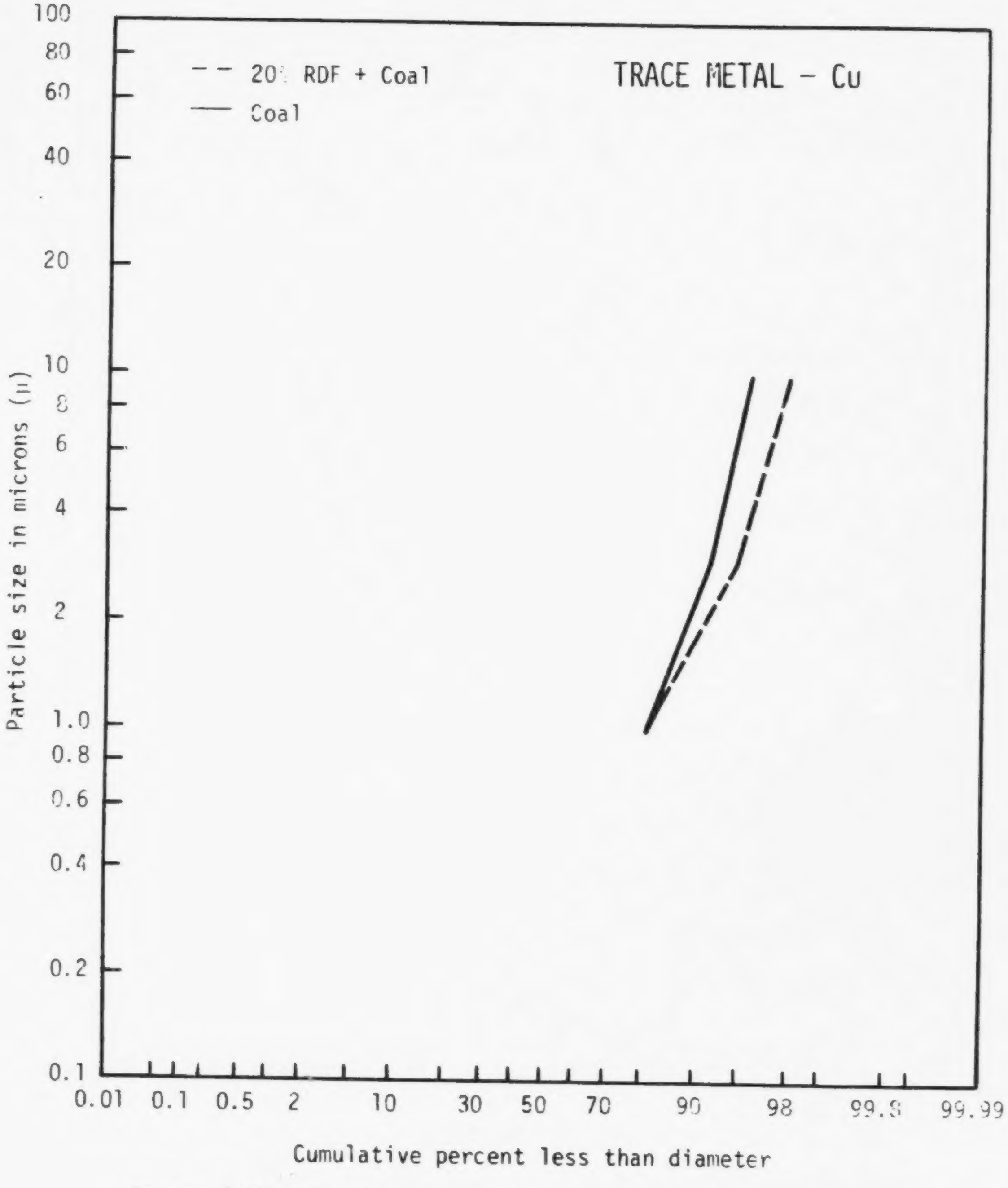

Figure 4-30. Stack gas particle size vs. cumulative percent less than diameter — trace metal Cu.

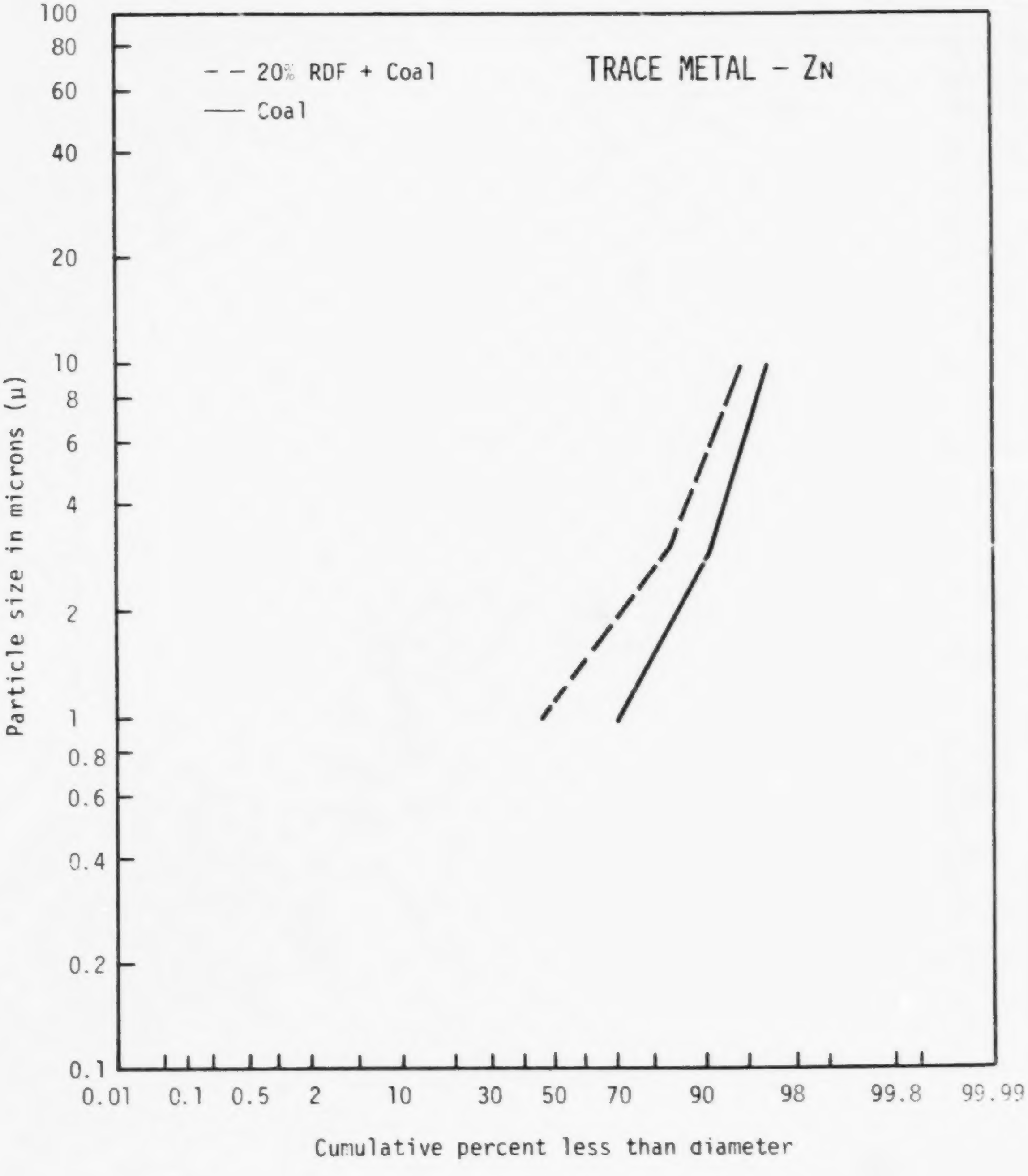

Figure 4-31. Stack gas particle size vs. cumulative percent less than diameter — trace metal Zn.

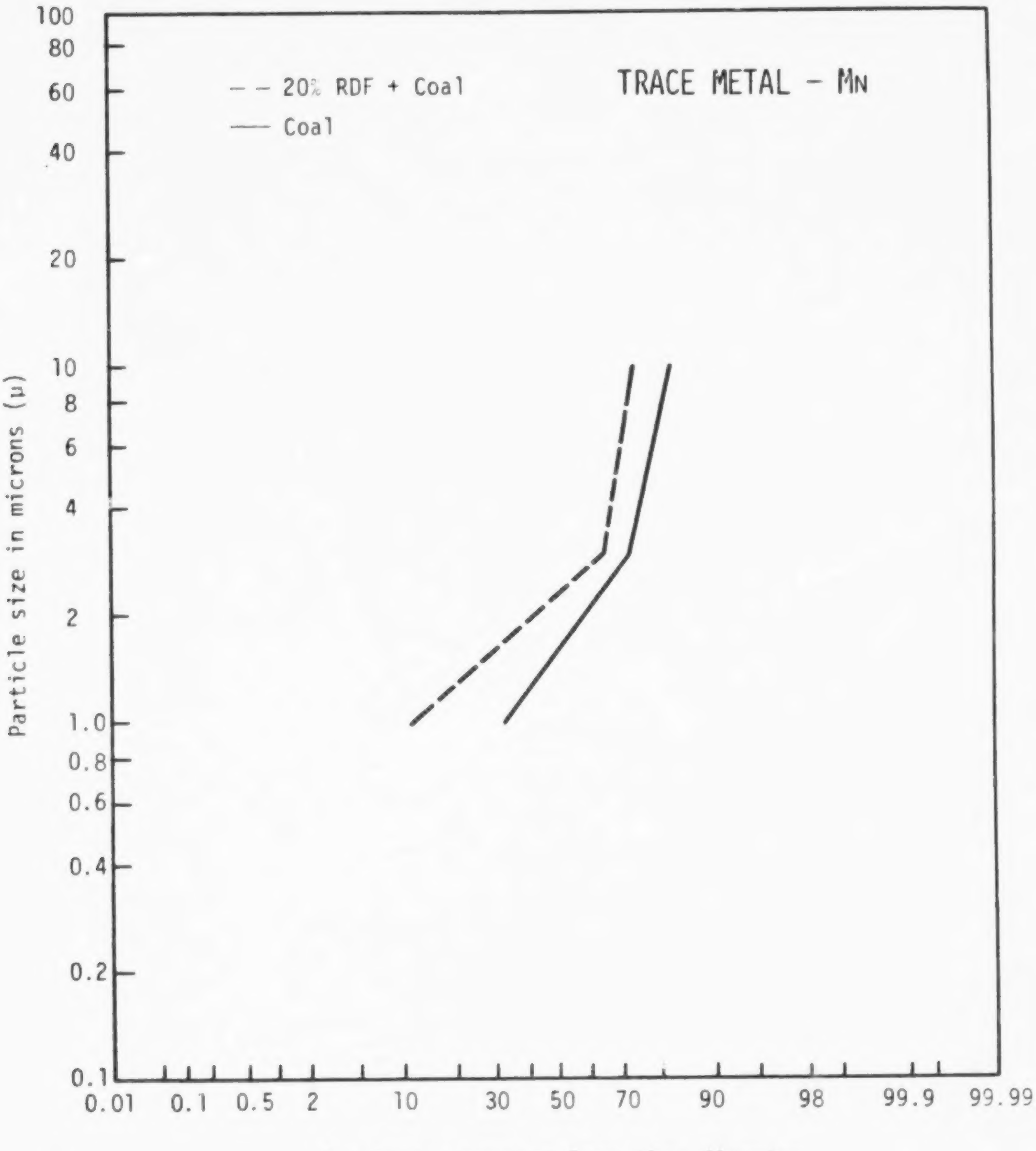

Figure 4-32. Stack gas particle size vs. cumulative percent less than diameter — trace metal Mn.

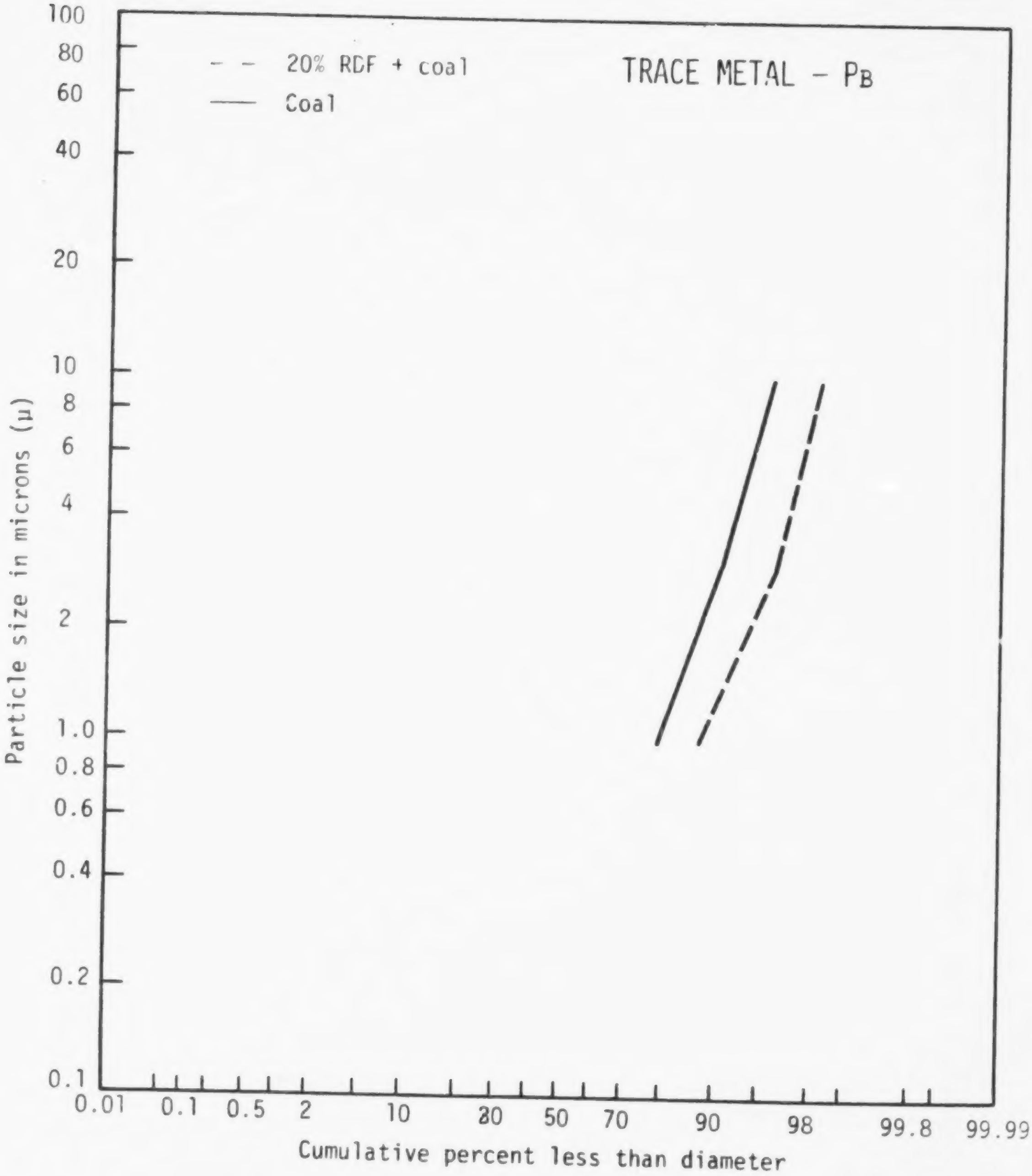

Figure 4-33. Stack gas particle size vs. cumulative percent less than diameter — trace metal Pb.

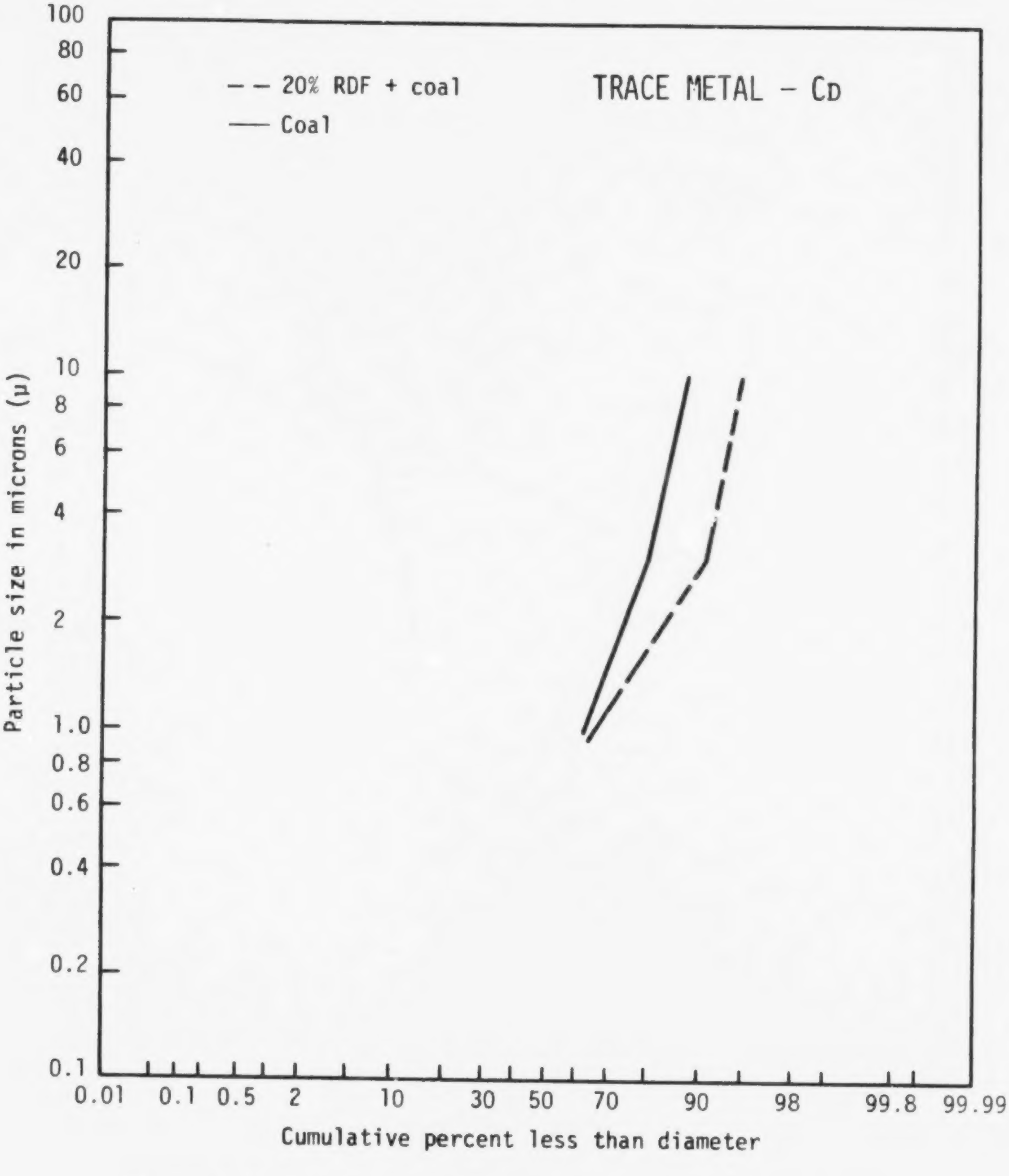

Figure 4-34. Stack gas particle size vs. cumulative percent less than diameter - trace metal Cd.

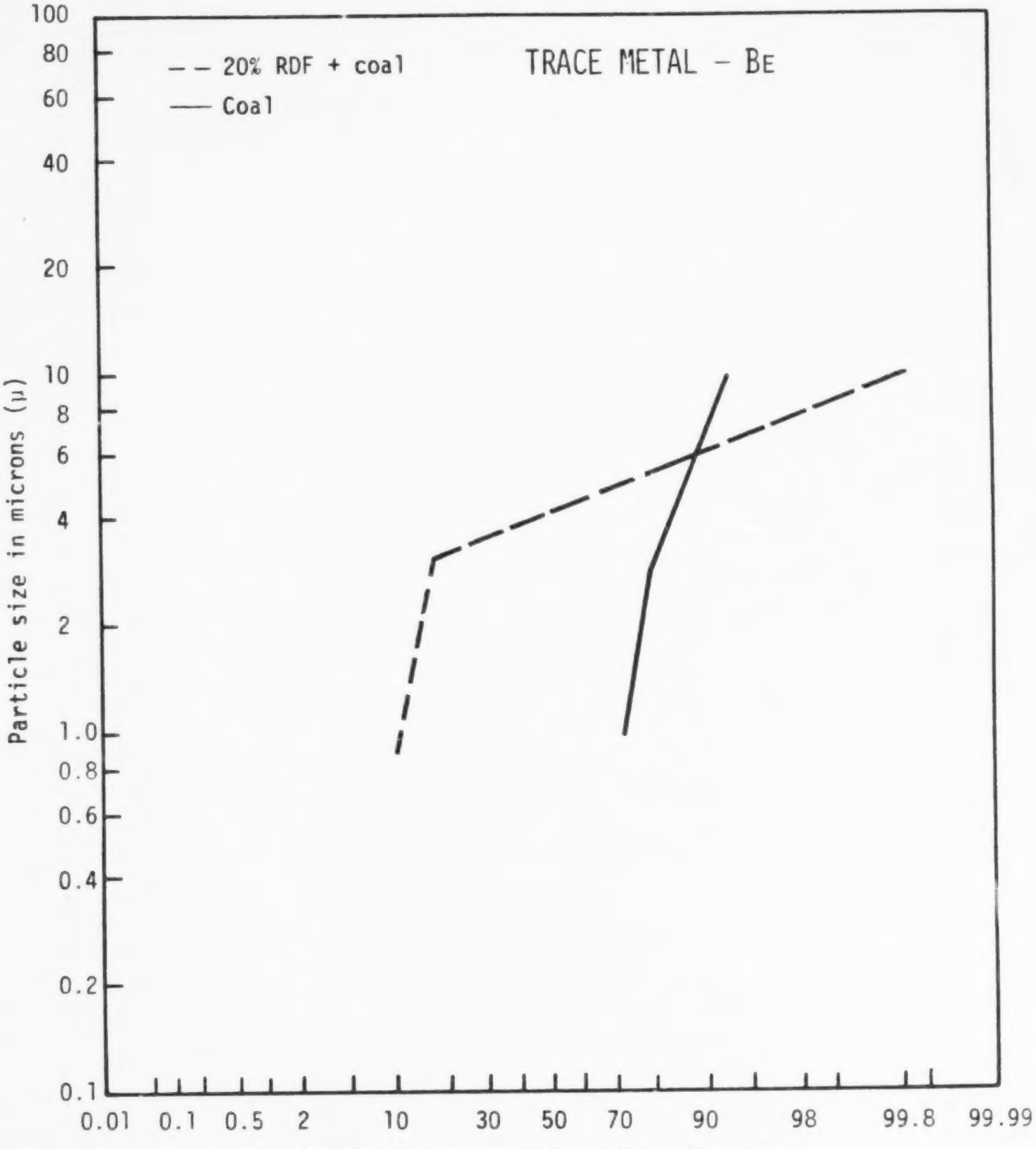

Figure 4-35. Stack gas particle size vs. cumulative percent less than diameter — trace metal Be.

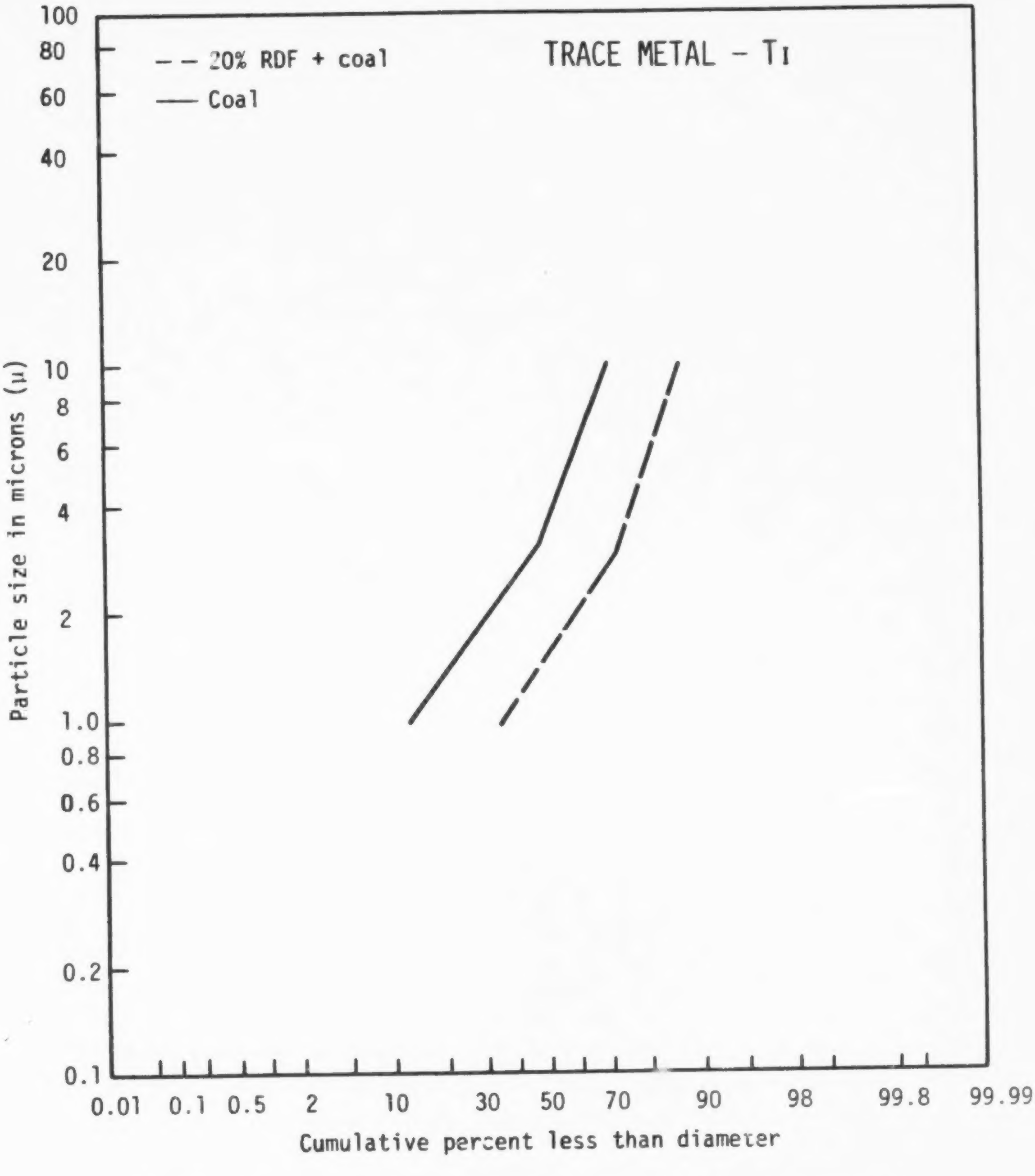

Figure 4-36. Stack gas particle size vs. cumulative percent less than diameter — trace metal Ti.

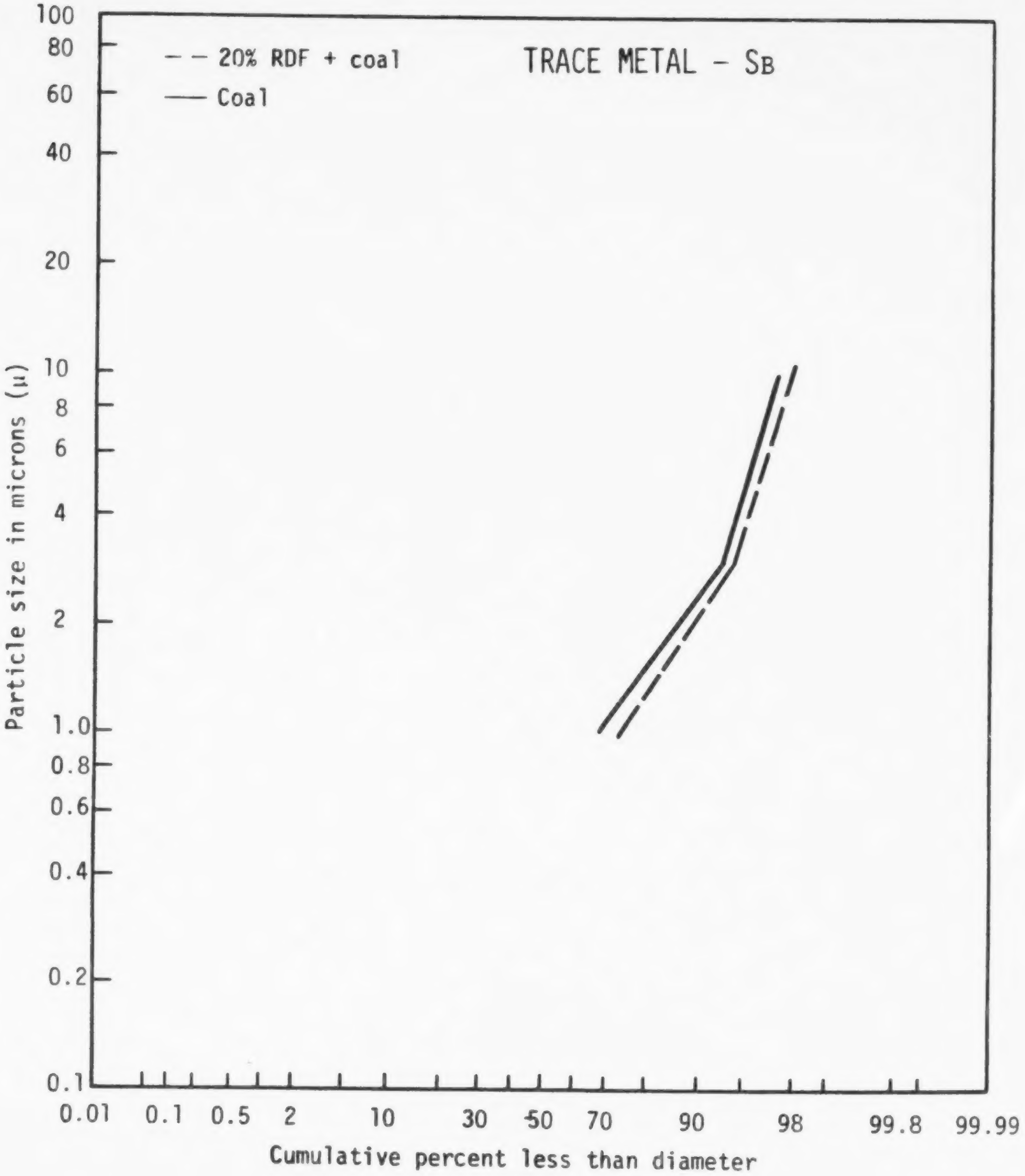

Figure 4-37. Stack gas particle size vs. cumulative percent less than diameter — trace metal Sb.

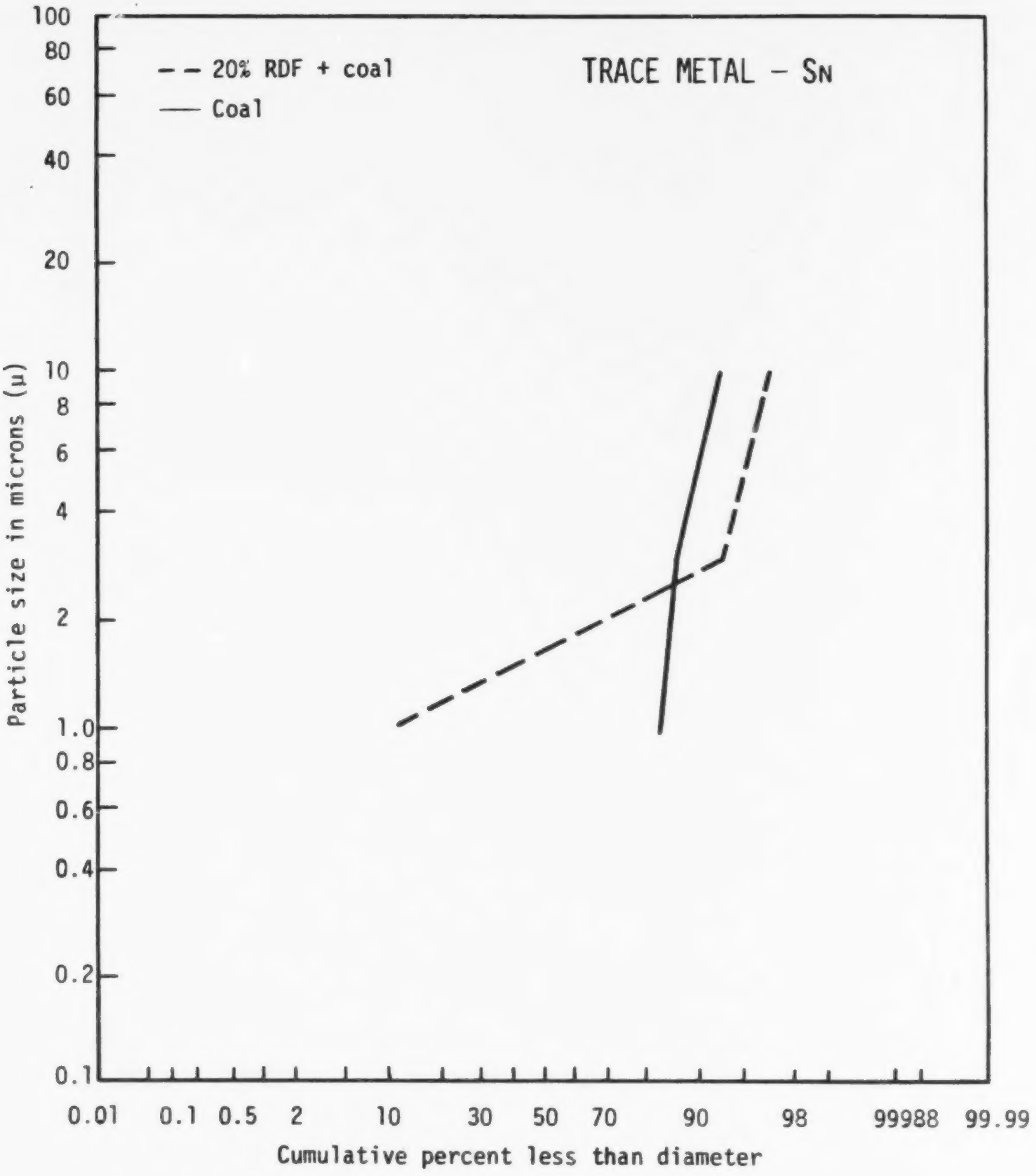

Figure 4-38. Stack gas particle size vs. cumulative percent less than diameter — trace metal Sn.

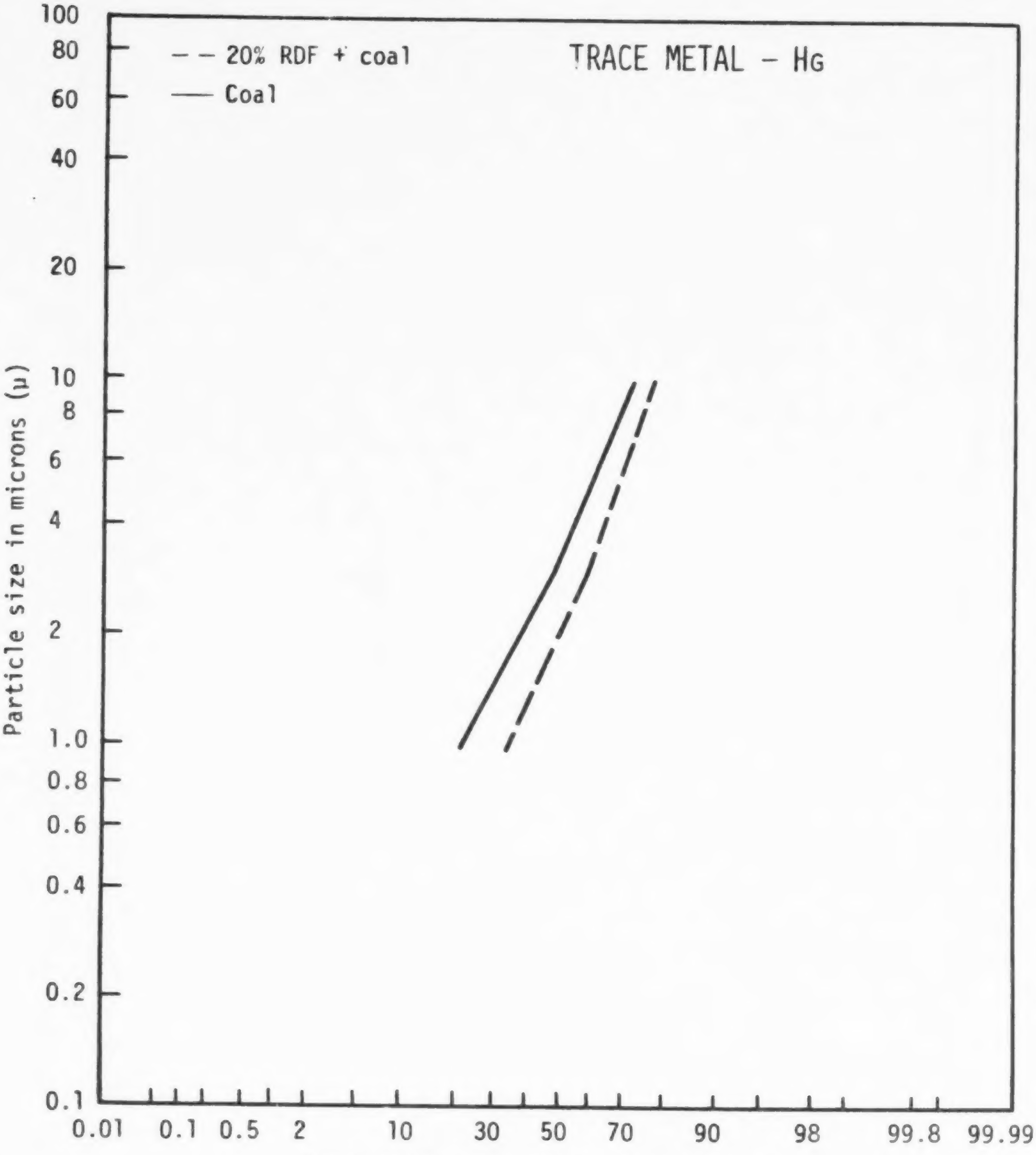

Figure 4-39. Stack gas particle size vs. cumulative percent less than diameter — trace metal Hg.

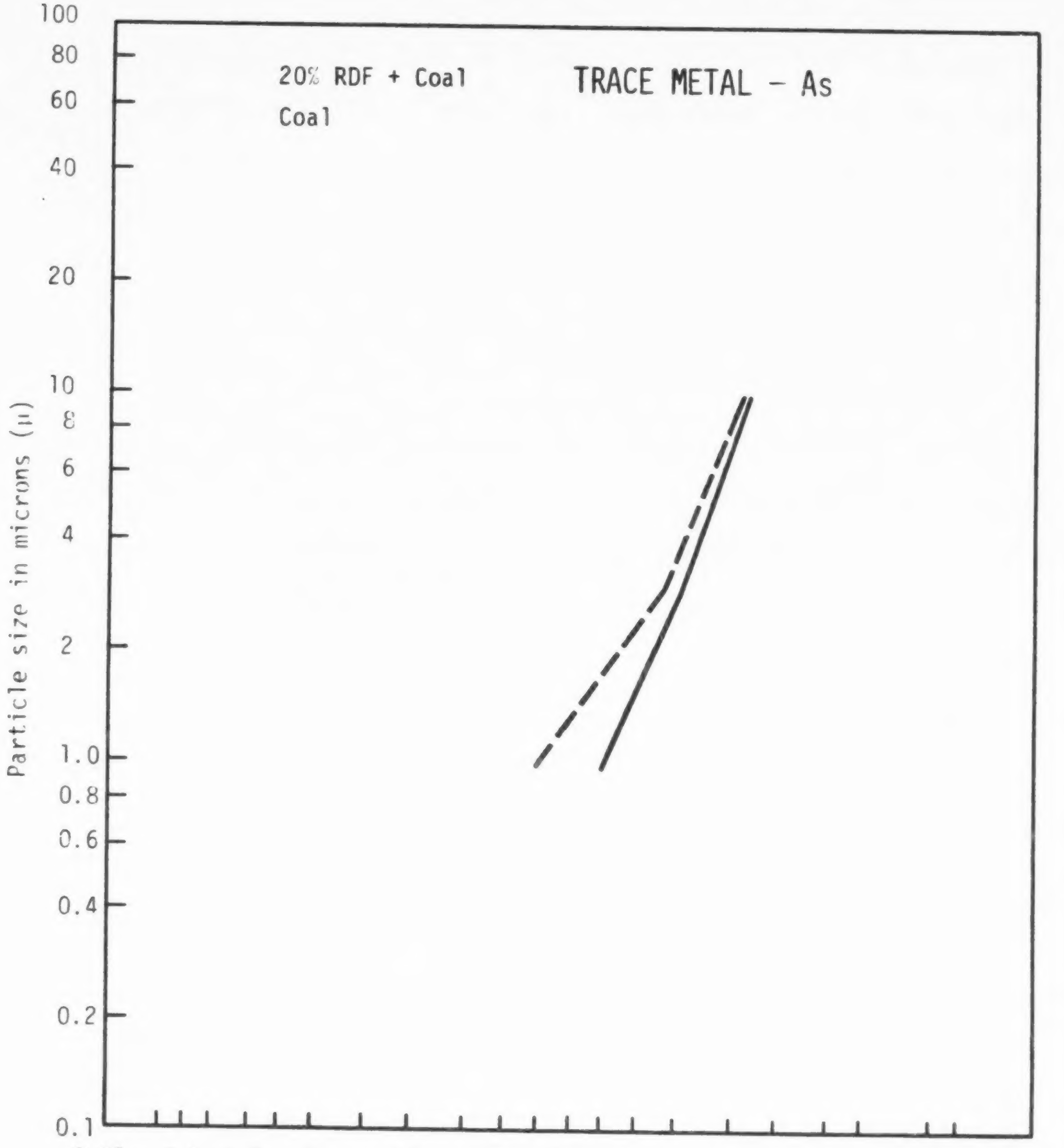

Figure 4-40. Stack gas particle size vs. cumulative percent less than diameter — trace metal As.

In summary, it appears that very little can be said about this data with regard to either the levels or trends of trace metals when cofiring RDF with either coal or natural gas. For future tests, it is recommended that at least five samples be collected at any given test condition in order to adequately determine the concentrations. In addition, background tests on gas only also need to be taken so that metals coming off the furnace can be taken into account.

4.5.5 Organics

As was mentioned in Section 4.4, the organic modules of the SASS train were analyzed by GC/MS for organic compounds. Tests 31, 32, 34, 37, and 40 contained no detectable organic compounds. Samples from Tests 38, 11A, 11B, and 11C contained polynuclear aromatic hydrocarbons and derivatives in the amounts indicated in Table 4-18. No PCBs were detected in any samples.

Two other compounds were detected in the RDF Test 11B sample. The mass spectra of these components were indicative of silicon containing compounds. They could not, however, be positively identified. The spectra of these compounds as well as the total ion current traces for the analyses are available if needed.

A final point involves the presence of medium weight polynuclear aromatic hydrocarbons in these stack samples. A large volume of literature indicates that combustion of hydrocarbon fuels gives rise to polynuclear aromatic hydrocarbons and also to highly polymerized species which are collectively known as "soot." The latter species are not readily analyzed, but the lower homologues are analyzed as the polynuclear aromatics. In these samples, the medium weight species such as pyrene, fluoranthene and

TABLE 4-18. ORGANICS FOUND

Test Condition	Organic	Amount
Gas Cofire 10% RDF 20% EA Ames Fuel	fluoranthene pyrene	0.0000102 µg/Btu 0.0003325 µg/Btu
Gas Cofire 10% RDF 20% EA Richmond Fuel	phenanthrene fluoranthene pyrene diphenyl ether biphenyl phenyl ether	0.0000641 µg/Btu 0.0001601 µg/Btu 0.0005765 µg/Btu 0.003395 µg/Btu 0.001697 µg/Btu
Gas Cofire 10% RDF 20% EA Americology Fuel	phenanthrene pyrene	0.0000593 µg/Btu 0.0010369 µg/Btu
Coal Cofire 10% RDF 20% EA	phenanthrene	0.0000981 µg/Btu

phenanthrene normally dominate with the higher molecular weight species (such as benzo(a) pyrene present also, but at concentrations lower by a factor of 10 to 100. If such were true with the RDF samples, then these carcinogenic compounds would be present, but at concentrations below the detection limit for these analyses.

In addition, it should be remembered that only two of the LC fractions were analyzed (LC 2,3). Tables 4-19 and 4-20 show the quantity and percent of the material found in all of the LC fractions for each of the tests where a SASS analysis was made. As can be seen from this table, considerable material was found in Fraction LC 1, 6 and 7 in many of the tests although these fractions were not analyzed. Table 4-21 gives a representative listing of the possible compounds that could make up each of these fractions and the MEG concentration limit. Thus, if the material in these fractions were made up of any one of these compounds, it could exceed the MEG criteria. For this reason alone, further analysis on these samples is warranted.

TABLE 4-19. LC COLUMN DATA

Test No.	mg/m^3						
	L_1	L_2	L_3	L_4	L_5	L_6	L_7
11A	0.10728	0.01314	0.08393	0.09414	0.08612	0.05692	1.14943
11B	0.49074	0.05708	0.24537	0.15677	0.26326	1.36317	0.84943
11C	0.16019	0.03620	0.08688	0.05249	0.10951	0.05068	1.11047
31	0.12811	0.00217	0.03908	0.03474	0.03908	0.01954	0.38144
32	0.91087	0.04315	0.12758	0.15572	0.15197	0.17448	1.77577
34	0.49676	0	0	0.04909	0.07034	0.02125	1.20453
37	0.38268	0.00656	0.02697	0.07070	0.09767	0.04155	1.25519
38	1.12582	0.02124	0.07379	0.13416	0.12522	0.09503	2.46853
40	0.21218	0.05378	0.06410	0.08767	0.14146	0.90547	3.79500

TABLE 4-20. LC COLUMN DATA

Test No.	L_1/L_T %	L_2/L_T %	L_3/L_T %	L_4/L_T %	L_5/L_T %	L_6/L_T %	L_7/L_T %
11A	6.74	0.83	5.27	5.92	5.41	3.58	72.25
11B	14.32	1.67	7.16	4.58	7.68	39.79	24.79
11C	9.97	2.25	5.41	3.27	6.82	3.15	69.13
31	19.89	0.34	6.07	5.39	6.07	3.03	59.21
32	27.28	1.29	3.82	4.66	4.55	5.22	53.17
34	26.97	0	0	2.67	3.82	1.15	65.39
37	20.34	0.35	1.43	3.76	5.19	2.21	66.72
38	27.84	0.53	1.82	3.32	3.10	2.35	61.05
40	4.03	1.02	1.22	1.67	2.69	17.22	72.15

TABLE 4-21. POSSIBLE COMPOUNDS IN LC FRACTIONS NOT ANALYZED

Test No.	Sample Fraction	Concentration (μg/m^3)	Sample Fraction	Concentration Limit (μg/m^3)
38	LC1	1125.82	Tetraethyllead	100.0
	LC7	2468.53	2,4,6-Trinitrophenol	100.0
			4,6-Dinitro-O-Cresol	200.0
			4,4'-Methylene-Bis-(2-Chloroaniline)	220.0
			Penthachlorophenol	500.0
			1-Aminonaphthalene	560.0
			Dinitro-P-Cresol	680.0
			Dinitrophenols	1400.0
40	LC1	212.18	Tetraethyllead	100.0
	LC6	905.47	2-Aminonaphthalene	170.0
			Dibenz (A,H) Acridine	220.0
			Dibenz (A,J) Acridine	250.0
			Anisidines	500.00
			Perchloromethanethiol	800.0
	LC7	3795.00	2,4,6-Trinitrophenol	100.0
			4,6-Dinitro-O-Cresol	200.0
			4,4'-Methylene-Bis-(2-Chloroaniline)	220.0
			Penthachlorophenol	500.0
			1-A[illegible]phthalene	560.0
			Di[illegible]Cresol	680.0
			Dini[illegible]enols	1400.0
118	LC1	490.74	Tetraethyllead	100.0
	LC6	1363.17	2-Aminonaphthalene	170.0
			Dibenz (A,H) Acridine	220.0
			Dibenz (A,J) Acridine	250.0
			Anisidines	500.0
			Perchloromethanethiol	800.0
			Dibenzo (C,D) Carbazole	1000.0
			Methylamine	1200.0
	LC7	849.32	2,4,6-Trinitrophenol	100.0
			4,6-Dinitro-O-Cresol	200.0
			4,4'-Methylene-Bis-(2-Chloroaniline)	220.0
			Penthachlorophenol	500.0
			1-Aminonaphthalene	560.0
			Dinitro-P-Cresol	680.0

REFERENCES

1. Brown R. A., Kelly, J. T., Neubauer, Peter, "Pilot Scale Evaluation of NO_x Combustion Control for Pulverized Coal, Phase II Final Report." EPA 600/7-79-132, June 1979.

2. Wendt, J. O. L., Lee, S. W., Pershing D. W., "Pollutant Control Through Staged Combustion of Pulverized Coal. Phase I -- Comprehensive Report. U.S. Dept. of Energy, Fe-1817-4, February 1978.

3. Johnson, S. A., Cioffi, P. L., McElroy, M. W., "Development of an Advanced Combustion System to Minimize NO_x Emissions from Coal-Fired Boilers." Presented to 1978 Joint Power Conference, Dallas, Texas, September 11, 1978.

4. Demeter, J. J., et al., "Combustion of Coal-Oil Slurry in a 100-HP Firetube Boiler," PERC/R1-77/8, Pittsburgh Energy Research Center, Pittsburgh, Pennsylvania, May 1977, pp. 3-8.

5. Beér, J. M., Combustion Aerodynamics, John Wiley and Sons, New York, N.Y., 1972.

6. Thompson, R. E., et al., "Effectiveness of Gas Recirculation and Staged Combustion of Reducing NO_x on a 560-MW Coal-Fired Boiler," EPRI FP-257, September 1976.

7. Heap, M. P., et al., "The Optimization of Burner Design Parameters to Control NO_x Formation in Pulverized Coal and Heavy Oil Flames," Proceedings of the Stationary Source Combustion Sumposium, Volume I, EPA-600/2-76-1526, June 1976.

8. England, G. C., et al., "The Control of Pollutant Formation in Fuel Oil Flames -- The Influence of Oil Properties and Spray Characteristics," Proceedings of the Third Stationary Source Combustion Symposium; Volume II. Advanced Processes and Special Topics, EPA-600/7-79-0506, February 1979, pp. 41-71.

9. Brown, R. A., "Pilot Scale Investigation of Combustion Modification Techniques for NO_x Control in Industrial and Utility Boilers," EPA-600/2-76-1526, Proceedings of the Stationary Source Combustion Symposium, Volume II, June 1976.

10. Wendt, J. O. L. and Ekmann, J. M., "Effect of Sulfur on NO_x -- Emissions from Premixed Flames," EPA-600/2-75-075, October 1975.

11. Wendt, J. O. L., et al., "Interactions Between Sulfur Oxides and Nitrogen Oxides in Combustion Processes," Proceedings of the Second Stationary Source Combustion Symposium, Vol. IV, EPA-600/7-77-073d, July 1977.

12. Gorman, et al., St. Louis Demonstration Project Final Report: "Power Plant Equipment, Facilities and Environmental Evaluations," EPA Contract 68-02-1871, Prepared for U.S. Environmental Protection Agency, Washington, D.C., by Midwest Research Institute, Kansas City, Missouri, July 1977, pp. 402.

13. Jackson, J. W., "A Bioenvironmental Study of Emissions from Refuse Derived Fuels," USAF Environmental Health Laboratory, McClellan, California, January 1976, pp. 113.

14. Hall, J. L., et al., "Evaluation of the Ames Solid Waste Resources -- An Energy Recovery System, Part III -- Environmental Evaluation of the Stoker-Fired Steam Generators at the City of Ames, Iowa, Prepared for U.S. Environmental Protection Agency, Cincinnati, Ohio, and Energy Research and Development Administration by Iowa State University, Midwest Research Institute, and Ames Laboratory, April 1977, pp. 133.

APPENDIX

DATA SUMMARY — DISTRIBUTED AIR
DATA SUMMARY — COAL/OIL MIXTURE
DATA SUMMARY — RDF TESTING
COM/DOE REPORT

TABLE A-1. DATA SUMMARY — DISTRIBUTED AIR

Test No.	Fuel	SR	EA %	Load x 10 Btu/hr	Preheat		Burners	SW/Int or Yaw	Prim. Stoich. %	Stg Air Mixing/ Location	Temperature		NO$_c$ ppm	Comments SR$_{1a}$
					sec °F	Stg °F					T$_{23}$ °F	T$_{24}$ °F		
209a	1	0.80	15	0.85	75	75	4 IFRF	4	12	Hor b	1910	1957	300	0.45
b		0.80		0.85	78	81				Hor b	2024	2010	310	0.30
c		0.80		0.85	79	82				Hor b	2048	2023	377	0.60
d		0.80		0.85	79	82				Hor a	2077	2014	299	0.60
e		0.80		0.85	79	82				Hor a	2104	2023	290	0.45
f		0.80		0.85	79	82				Hor a	2135	2059	257	0.30
g		0.80		0.85	79	82				Hor a	2149	2088	251	0.30
h		0.95		0.85	80	90				Hor a	2165	2088	424	0.45
i		0.95		0.85	600	--				Hor a	2227	2088	480	0.45
j		0.80		0.85	580	227				Hor a	2234	2103	262	0.30
k		0.80		0.85	580	269				Hor a	2185	2133	266	0.45
ℓ		0.80		0.85	550	276				Hor a	2176	2128	250	0.60
210a		0.95		1.7	600	350				HE-J	2146	2132	376	0.45
b		0.95		1.7	600	350				HE-J	2034	2562	451	0.30
c		0.95		1.7	600	350				HE-J	2108	2574	284	0.60
d		0.80		1.7	600	296				HE-J	--	2480	133	0.60
e		0.80		1.7	600	296				HE-J	--	2508	152	0.45
f		0.80		1.7	600	296				HE-J	--	2557	163	0.30
g		0.80		1.7	600	322				HE-J	--	2488	170	0.80
h		0.95		1.7	600	327				HE-J	--	2497	258	0.95
211a		0.80		1.7	600	323				HE-K	2362	2540	215	0.45
b		0.80		1.7	600	371				HE-K	2314	2529	260	0.30
c		0.80		1.7	600	381				HE-K	2394	2442	197	0.60
d		0.80		1.3	600	337				HE-K	2366	2338	185	0.45
e		0.80		1.3	600	336				HE-K	2374	2368	167	0.60
f		0.80		1.3	600	335				HE-K	2282	2473	224	0.30
g		0.95		1.3	580	288				HE-K	2261	2558	305	0.45
h		0.95		1.3	600	242				HE-K	2350	2548	252	0.60
i		0.95		1.3	550	230				HE-K	2325	2438	335	0.30
j		0.80		1.3	600	368				HE-H	2306	2384	289	0.30
k		0.80		1.3	580	422				HE-H	2256	2615	264	0.45
ℓ		0.80		1.3	600	443				HE-H	2364	2582	229	0.60
212a		0.80		0.85	500	256				HE-H	1877	1927	190	0.45
b		0.80		0.85	550	379				HE-H	1767	1978	219	0.30
c		0.80		0.85	550	409				HE-H	2429	1981	178	0.60
d		0.95		0.85	600	359				HE-H	2339	1966	222	0.60
e		0.95		0.85	575	334				HE-H	2621	2003	253	0.45
f		0.95		0.85	575	326				HE-H	2482	2036	296	0.30
g		0.95		1.3	635	330				HE-H	2621	2203	346	0.30
h		0.95		1.3	625	312				HE-H	2603	2266	289	0.45
i		0.95		1.3	650	305				HE-H	2577	2268	260	0.60

TABLE A-1. DATA SUMMARY – DISTRIBUTED AIR (CONCLUDED)

Test No.	Fuel	SR	EA %	Load $\times 10^6$ Btu/hr	Preheat		Burners	SW/Int or Yaw	Prim. Stoich. %	Stg Air Mixing/ Location	Temperature		NO_c ppm	Comments SR_{1a}
					sec °F	Stg °F					T_{23} °F	T_{24} °F		
212j	1	0.95	15	1.7	675	263	4 IFRF	4	12	HE-K	2878	2182	379	0.60
k		0.95		1.7	675	269				HE-K	2759	2396	375	0.45
ℓ		0.95		1.7	675	270				HE-K	2274	2515	480	0.30
213a		0.80		0.85	100	98				HE-E	2059	1830	190	0.45
b		0.80		0.85	98	---				HE-E	2089	1880	185	0.60
c		0.80		0.85	90	98				HE-E	2137	1905	215	0.30
d		0.95		0.85	90	103				HE-E	2161	1957	303	0.30
e		0.95		0.85	90	104				HE-E	2172	1974	287	0.45
f		0.95		0.85	90	104				HE-E	2188	1987	284	0.60
g		0.95		1.3	575	196				HE-E	2075	2296	305	0.60
h		0.95		1.3	600	250				HE-E	2381	2145	300	0.45
i		0.95		1.3	600	275				HE-E	1937	2258	466	0.30
j		0.80		1.3	600	282				HE-E	2017	2379	324	0.30
k		0.80		1.3	600	276				HE-E	1864	2372	305	0.45
ℓ		0.80		1.3	600	277				HE-E	1507	2376	281	0.60
m		0.80		1.3	620	302				HE-F	2233	2379	255	0.60
n		0.80		1.3	600	300				HE-F	1760	2433	244	0.45
o		0.80		1.3	600	---				HE-F	1890	2370	285	0.30
p		0.95		1.3	600	---				HE-F	1886	2432	348	0.30
q		0.95		1.3	---	---				HE-F	---	2456	300	0.45
r		0.95		1.3	---	---				HE-F	---	2427	312	0.60
s		0.80		1.7	---	---				HE-F	---	2460	346	0.45
t		0.80		1.7	---	---				HE-F	---	2482	311	0.60
u		0.80		1.7	---	---				HE-F	---	2597	397	0.30
v		0.95		1.7	600	366				HE-F	2507	2592	368	0.45
w		0.95		1.7	600	382				HE-F	2886	2572	405	0.60
x		0.95		1.7	600	385				HE-F	2572	2655	381	0.30
214a		0.95		1.7	625	264				HE-M	2220	1996	223	0.60
b		0.95		1.7	625	244				HE-M	2691	2085	230	0.70
c		0.80		1.7	620	294				HE-M	2855	2335	151	0.60
d		0.80		1.7	580	313				HE-M	3861	2083	163	0.70
e		0.80		1.7	600	100				HE-N	---	2235	116	0.70
f		0.80		1.7	620	335				HE-N	---	2566	122	0.60
g		0.95		1.7	620	310				HE-N	---	2596	201	0.60
h		0.95		1.7	670	314				HE-N	2532	2330	257	0.70

TABLE A-2. DATA SUMMARY – COAL/OIL MIXTURE

Test No.	Residence Time	Firing Rate (Btu/hr x 10^6)	Radiant Heat Transfer (Btu/hr x 10^6)	Excess Air	Coal Type (%)	Oil Type	Preheat Temp	Staged Air Preheat Temp	Nozzle Type
215a	S	1.8	0.558	20	0	Chevron	80		DeLavan
b			0.483	30			82		
c			0.571	40			77		
d			0.442	20			76		
216a			0.521	20			82		
b			0.429	30			83		
c			9.438	20			82		
d			0.471	40			83		
e			0.438	40		Penn	82		
f			0.438	30			82		
g			0.454	20			81		
h			0.492	20		Chevron	83		
i			0.463	40			83		
217a			0.250	30			300		Sonicore
b			0.238	20					
c			0.242	40					
d			0.254	40	30% W.Kty.	Penn			
e			0.254	30					
f			0.254	20					
g			0.254	20					
h			0.254	20					
i			0.254	20					
j			0.275	20					
k			0.304	20					
ℓ			0.304	20					
m			0.313	20					
n			0.313	20					
o			0.283	20					
218a			0.263	30	30% Va.	Chevron			
b			0.263	40					
c			0.313	20					
d			0.300	30					
e			0.296	40					
f			0.308	20				277	
g			0.263	20				277	
h			0.321	20				277	
i			0.342	20				290	
a			0.267	20	30% W.Kty.	Penn		216	
b			0.258	20				220	

TABLE A-2. DATA SUMMARY — COAL/OIL MIXTURE (CONTINUED)

Test No.	Residence Time	Firing Rate (Btu/hr x 10⁶)	Radiant Heat Transfer (Btu/hr x 10⁶)	Excess Air	Coal Type (%)	Oil Type	Preheat Temp	Staged Air Preheat Temp	Nozzle Type
219c	S	1.8	0.258	20	30% W.Kty.	Penn	300	225	Sonicore
d			0.258	20				228	
220e			0.304	20				251	
f			0.304	--	---	---	---	---	
g			0.267	20	30% Va.	Chevron	300	---	
h			0.267	20				---	
i			0.271	20				---	
j		1.7	0.263	20				---	
k		1.7	0.263	20				246	
ℓ		1.8	0.263	20				---	
221a			0.288	30	30% Mont.			---	
b			0.292	40				---	
c			0.292	20				---	
d			0.292	20				200	
e			0.292	20				238	
f	L		0.292	20	30% Va.			238	
g	S		0.292	20				261	
h	L		0.292	20				261	
i	S		0.321	20				267	
j			0.338	20				274	
k			0.338	20				275	
ℓ			0.267	20				275	
m			0.317	20				---	
n			0.279	20	30% Mont.	Penn		---	
o			0.275	20				---	
p			0.275	20				---	
q			0.275	30				---	
r			0.267	40				---	
222a			0.267	20		Chevron		---	
b			0.313	20				205	
c	L		0.304	20				205	
d	L		0.304	20				205	
e	S		0.296	20	0	Penn		---	
f			0.300	30	0			---	
g			0.275	40	0			---	
223a			0.292	20	30% Mont	Chevron		---	
b	L		0.292	20				220	
c	S		0.292	20				220	
d	S		0.292	20				261	

TABLE A-2. DATA SUMMARY — COAL/OIL MIXTURE (CONTINUED)

Test No.	Residence Time	Firing Rate (Btu/hr x 10^6)	Radiant Heat Transfer (Btu/hr x 10^6)	Excess Air	Coal Type (%)	Oil Type	Preheat Temp	Staged Air Preheat Temp	Nozzle Type
223e	L	1.8	0.292	20	30% Mont.	Chevron	300	261	Sonicore
f	S		0.292	20				---	
g			0.292	20				---	
h			0.292	20				---	
i			0.292	20				---	
j			0.292	20				213	
k			0.292	20				223	
ℓ	L		0.292	20				223	
m	S		0.292	20				229	
n	L		0.292	20				229	
o	S		0.288	20				229	
p	L		0.288	20				229	
q	S	1.2	0.288	20				---	
r			0.288	20				---	
224a			0.304	20				---	
b			0.304	20				224	
c	L		0.308	20				221	
d	S		0.304	20				250	
e			0.304	20				250	
f			0.304	20				268	
g			0.304	20				268	
h	L		0.304	20			276	282	
i	S		0.308	20			276	282	
j			0.308	20			320	---	
k			0.283	20			320	---	
ℓ			0.288	20			300	---	
225a		1.8	0.313	15	100% W.Kty.	---	350	---	
b			0.313	20		---	330	---	
c			0.313	30		---	330	---	
d			0.313	40		---	330	---	
226a			0.313	20	100% Mont.	---	320	---	
b			0.317	30		---		---	
c			0.300	40		---		---	
d			0.300	20		---		---	
e			0.288	20	100% Va.	---		---	
f			0.288	30		---		---	

TABLE A-2. DATA SUMMARY — COAL/OIL MIXTURE (CONTINUED)

Test No.	Burner Swirl	Atomized Air Flow	Atomized Air Pressure	Fuel Pressure	Fuel Temp	Stoich. Ratio (SR_1)	Stoich. Ratio (SR_{1a})	Dopant Type	Total Fuel Nitro/Sulfur (%)
215a	5	240	65	40	185	1.05			
b	4.5			44	190	1.30			
c				42	185	1.40			
d				42	185	1.20			
216a	4	72	71	--	---	1.25			
b		81	82	78	185	1.40			
c				78	185	1.30			
d				78	205	1.30			
e				78	200	1.40			
f				78	187	1.30			
g				79	196	1.20			
h				79	195	1.20			
i				79	195	1.40			
217a	0.5	200	26	25	220	1.30			
b				25	220	1.20			
c				25	220	1.40			
d				25	200	1.40			
e				25	200	1.30			
f				25	200	1.20			
g				25	200	0.95			
h				25	200	0.85			
i				25	200	0.75			
j				25	200	0.65			
k		185	25	32	200	1.20	0.85		
ℓ				32	210	1.20	---		
m				32	200	1.20	0.75		
n				32	200	1.20	0.65		
o			26	32	200	1.20	0.55		
218a		200	32	35	220	1.30	---		
b				35	220	1.40	---		
c		160	22	27	200	1.20	---		
d				27	200	1.30	---		
e				27	200	1.40	---		
f				27	200	0.95	---		
g				25	200	0.85	---		
h				25	200	0.75	---		
i				25	200	0.65	---		
219a	1.0	166		26	200	0.95	0.85		
b				26	200	0.95	0.75		

TABLE A-2. DATA SUMMARY — COAL/OIL MIXTURE (CONTINUED)

Test No.	Burner Swirl	Atomized Air Flow	Atomized Air Pressure	Fuel Pressure	Fuel Temp	Stoich. Ratio (SR_1)	Stoich. Ratio (SR_{1a})	Dopant Type	Total Fuel Nitro/Sulfur (%)
219c	1.0	166	22	26	200	0.95	0.65		
d	1.0	166	22	26	200	0.95	0.55		
220e	0.5	---	26	27	210	---	0.55		
f	---	---	--	--	---	---	---		
g	0.5	150	22	24	215	0.85	1.20		
h				27	210	0.75	1.20		
i				29	200	0.65	1.20		
j				29	210	0.55	1.20		
k				28	210	0.95	0.55		
ℓ				26	200	---	0.65		
221a				38	200	---	---		
b				38	200	---	---		
c				38	200	---	---		
d				38	200	0.95	---		
e				38	200	0.85	---		
f				38	200	0.85	---		
g				38	200	0.75	---		
h		143		38	200	0.75	---		
i			17	27	190	0.95	0.85		
j				27	200	0.95	0.75		
k				27	200	0.75	---	Thiophene	2.151 S
ℓ				27	200	0.95	0.65	---	---
m			14	27	210	---	---	Thiophene	2.148 S
n		125		27	220	---	---	---	---
o				26	210	---	---	Pyridene	0.965 N
p				26	210	---	---	Pyridene	0.796 N
q		110	12	25	210	---	---	---	---
r				25	200	---	---	---	---
222a		150	22	38	200	---	---	---	---
b				38	200	0.95	---	---	---
c				38	200	0.95	---	---	---
d				38	200	0.65	---	---	---
e		110	10	20	180	---	---	---	---
f				20	180	---	---	---	---
g				20	190	---	---	---	---
223a		150	22	38	200	---	---	---	---
b				38	200	0.85	---	---	---
c				38	200	0.85	---	---	---
d				38	200	0.65	---	---	---

TABLE A-2. DATA SUMMARY — COAL/OIL MIXTURE (CONTINUED)

Test No.	Burner Swirl	Atomized Air Flow	Atomized Air Pressure	Fuel Pressure	Fuel Temp	Stoich. Ratio (SR_1)	Stoich. Ratio (SR_{1a})	Dopant Type	Total Fuel Nitro/Sulfur (%)
223e	0.5	150	22	38	200	0.65	---		
f				38	200	---	0.85		
g				38	200	---	0.75		
h				38	200	---	0.65		
i				30	200	---	0.55		
j				30	200	0.95	0.55		
k				30	200	0.95	0.65		
ℓ				30	200	0.95	0.65		
m				30	200	0.95	0.75		
n				30	200	0.95	0.75		
o				12	200	0.95	0.85		
p				12	200	0.95	0.85		
q		110	12	22	190	---	---		
r		120	20	22	190	---	---		
224a		110	12	22	190	---	---		
b				22	190	---	---		
c				22	190	0.95	---		
d				22	180	0.85	---		
e			16	22	180	---	---		
f				22	180	---	---		
g				22	180	0.75	---		
h		120	18	22	180	0.65	---		
i				22	180	---	---		
j				22	180	---	---		
k				25	190	---	---		
ℓ				24	180	---	---		
225a	4.0	190	8.4	--	---	---	---		
b				--	---	---	---		
c				--	---	---	---		
d				--	---	---	---		
226a				--	---	---	---		
b				--	---	---	---		
c				--	---	---	---		
d				--	---	---	---		
e				--	---	---	---		
f				--	---	---	---		

TABLE A-2. DATA SUMMARY — COAL/OIL MIXTURE (CONTINUED)

Test No.	T_{25}	T_{26}	T_{27}	O_2	CO	CO_2	NO	SO	UHC
215a	---	---	---	3.6	----	----	649	---	---
b	2137	1723	788	5.0	8.5	----	831	542	2.6
c	2049	1811	834	6.3	14.5	----	890	562	0.4
d	1962	1651	775	---	17.5	----	833	574	0.0
216a	2099	1675	766	---	4.7	----	451	564	---
b	1779	1605	820	---	6.8	----	510	600	---
c	1732	1529	763	5.0	5.8	----	460	605	---
d	---	---	---	5.2	7.6	----	434	608	---
e	1730	1546	823	5.9	---	----	358	713	---
f	1706	1552	793	5.1	---	----	345	677	---
g	1682	1595	786	3.6	---	----	333	617	---
h	1790	1611	787	3.7	41.7	----	409	620	---
i	1819	1535	826	6.1	---	----	487	607	---
217a	1823	1595	823	5.2	12.6	13.2	622	568	---
b	1805	1644	801	3.7	4.8	15.9	508	610	---
c	1816	1580	846	6.4	16.0	12.5	683	661	---
d	1831	1676	872	5.8	45.6	12.8	385	1756	---
e	1730	1637	815	4.9	78.0	13.3	427	1917	---
f	1774	1635	801	3.8	77.1	13.9	380	1931	---
g	1899	1602	776	3.0	85.0	14.7	319	1991	---
h	1864	1532	722	3.4	70.0	14.3	328	2017	---
i	2042	1626	770	3.2	70.2	15.1	324	2088	---
j	2059	1531	706	3.4	38.2	15.3	265	2098	---
k	1834	1663	907	4.0	69.5	14.9	372	2063	---
l	1800	1610	835	---	---	15.6	364	---	---
m	1775	1609	839	3.4	62.5	15.2	331	1963	---
n	1816	1637	845	3.9	63.8	14.7	332	1987	---
o	1865	1578	793	3.5	91.5	14.8	204	2033	---
218a	1900	1685	880	5.4	125.7	11.8	760	691	---
b	1959	1639	886	6.6	119.8	10.8	812	843	---
c	1857	1748	899	3.6	123.0	13.7	688	548	---
d	1856	1732	930	4.9	191.0	13.2	732	739	---
e	1824	1777	967	6.1	271.0	12.2	763	786	---
f	1928	1758	862	3.4	139.0	14.4	627	790	---
g	2025	1680	822	3.9	142.0	14.1	571	780	---
h	2061	1678	825	3.6	95.0	14.5	510	786	---
i	2209	1620	786	3.4	91.0	14.6	416	790	---
219a	2085	1584	784	4.3	70.7	12.8	468	1725	---
b	1882	1529	767	4.1	70.4	12.9	422	1628	---

TABLE A-2. DATA SUMMARY — COAL/OIL MIXTURE (CONTINUED)

Test No.	T_{25}	T_{26}	T_{27}	O_2	CO	CO_2	NO	SO	UHC
219c	2014	1603	791	3.8	64.8	14.0	404	1554	
d	2025	1626	803	3.2	60.0	14.3	346	1525	
220e	2021	1637	831	3.3	47.0	14.0	389	1315	
f	----	----	---	2.8	----	----	---	----	
g	1871	1606	831	4.0	75.0	12.2	653	843	
h	----	----	---	---	----	11.6	623	----	
i	1960	1560	806	3.6	73.0	12.4	504	921	
j	1898	1553	817	3.6	66.0	12.4	413	913	
k	2040	1691	832	3.6	83.0	12.2	606	838	
l	----	----	---	---	----	----	---	----	
221a	1799	1626	885	4.9	113.4	12.3	705	538	
b	1850	1627	932	6.3	99.9	12.7	782	643	
c	1835	1674	909	3.8	83.5	14.6	622	701	
d	1918	1602	836	3.3	82.3	15.0	668	776	
e	1996	1625	832	3.0	166.5	15.1	580	735	
f	2001	1524	776	3.5	105.3	14.6	233	841	
g	1917	1648	835	3.3	132.2	15.0	600	771	
h	----	----	---	4.1	1869.0	14.2	228	830	
i	1887	1615	804	4.7	63.0	14.0	606	596	
j	1929	1615	790	3.4	54.0	14.9	581	732	
k	1977	1620	796	4.0	53.0	14.6	541	1022	
l	1995	1599	781	5.9	91.0	13.7	563	754	
m	1883	1632	834	6.0	107.0	13.0	607	1336	
n	1806	1666	850	3.9	85.0	14.7	397	1409	
o	1834	1695	862	5.4	106.0	13.9	622	1568	
p	1847	1684	862	3.2	79.0	15.2	603	1524	
q	1786	1639	855	5.9	131.0	13.2	471	1480	
r	1680	1497	836	9.3	268.0	11.0	---	1704	
222a	----	----	----	----	----	----	653	----	
b	----	----	----	3.3	39.2	14.3	533	809	
c	1947	1588	807	3.9	98.5	13.9	307	741	
d	----	----	----	----	----	----	226	----	
e	1824	1669	867	3.6	76.9	13.3	370	977	
f	1780	1648	879	5.2	95.0	12.1	399	1240	
g	1730	1637	915	6.2	160.0	11.5	427	1522	
223a	1922	1668	872	4.2	179.6	13.9	630	599	
b	1964	1677	815	3.2	356.7	14.7	285	774	
c	2096	1601	806	3.3	110.3	14.7	566	700	
d	1917	1637	790	3.3	138.6	14.8	418	708	
e	1925	1531	749	3.7	1147.0	14.6	280	689	
f	1972	1631	823	3.9	125.7	14.6	588	695	

TABLE A-2. DATA SUMMARY – COAL/OIL MIXTURE (CONCLUDED)

Test No.	T_{25}	T_{26}	T_{27}	O_2	CO	CO_2	NO	SO_2	UHC
223g	2003	1611	792	3.9	1156.6	14.4	219	716	
h	2038	1661	819	3.3	122.7	14.9	234	726	
i	2082	1582	812	3.9	87.1	14.4	256	728	
j	2067	1631	778	3.7	625.3	14.1	221	724	
k	1979	1592	805	3.2	161.8	14.7	221	717	
l	1934	1509	772	3.9	426.1	14.1	611	729	
m	1955	1540	777	3.6	123.1	14.2	336	689	
n	1963	1489	759	3.8	116.8	14.0	712	700	
o	1843	1617	799	4.1	229.0	13.7	524	694	
p	1879	1587	789	3.4	190.9	13.9	733	712	
q	1807	1574	712	3.5	68.0	14.5	547	683	
r	----	----	---	----	----	----	----	---	
224a	1923	1553	719	3.3	84.0	14.6	581	691	
b	1842	1549	682	3.6	131.0	14.2	568	764	
c	2134	1472	626	2.8	687.0	14.6	246	911	
d	2194	1458	629	2.9	----	13.9	168	794	
e	2138	1552	681	3.6	134.1	14.2	381	792	
f	2087	1551	671	3.2	96.7	14.3	480	781	
g	2196	1458	629	4.1	----	----	210	832	
h	2115	1595	669	3.6	----	13.8	205	726	
i	2129	1507	676	3.1	169.8	14.3	427	827	
j	----	----	---	---	----	----	---	---	
k	2041	1400	670	3.8	87.0	14.8	238	783	
l	1852	1274	595	7.6	119.7	11.1	---	883	
225a	----	1664	895	4.0	95.2	15.4	---	2552	
b	----	1669	924	3.7	109.0	15.6	1092	2536	
c	----	1664	960	4.5	136.7	14.9	1159	2553	
d	----	----	---	---	----	----	1226	----	
226a	2216	1783	995	3.7	138.9	13.4	1156	1695	
b	2189	1754	1014	5.1	136.5	12.7	1199	1479	
c	2168	1754	1040	6.2	194.8	11.9	1266	1446	
d	2223	1806	998	3.5	64.0	13.6	1158	1350	
e	2277	1844	987	3.8	74.0	13.3	1152	1403	
f	2222	1807	1010	4.9	121.0	12.6	1237	1298	

TABLE A-3. DATA SUMMARY – RDF TESTING

Test No.	Load (Btu/hr x 10^6)	Excess Air	Primary Fuel	Refuse* No.	Refuse Concen.	Preheat Temp	Yaw	Level of Stack Testing
227a	1.5	5	Nat. Gas	1	5	290	+6	
b		10		1	5	300		
c		30		1	5	310		
d		5		1	10	310		
e		10		1	10	315		
f		30		1	10	315		
g		30		1	20	310		
h		10		1	20	315		
i		5		1	20	300		
228a	1.0	20		1	10	300		
b	1.5	5		2	5	300		
c		10		2	5	300		
d		30		2	5	300		
e		5		2	10	300		
f		10		2	10	300		
g		30		2	10	300		
h		30		2	20	300		
i		10		2	20	303		
j		5		2	20	300		
229a	1.0	20		2	10	290		
b	1.0	20		3	10	310		
c	1.5	5		3	10	310		
d		10		3	10	316		
e		30		3	10	313		
f		30		3	20	317		
g		10		3	20	310		
230a	1.0	20		4	10	304		
b	1.5	30		4	10	305		
c		10		4	10	313		
d		5		4	10	313		
e		30		4	20	314		
f		10		4	20	319		
g		5		4	20	319		
231a		5		2	5	470		
b		10		2	5	560		
232a		20		2	10	300		3
b		20		2	20	300		2
233a		20		2	20	302		2
234a		20		1	20	302		2
235a		20		1	20	302		2
b		20		3	20	309		2
236a		20		4	20	300		2
237a		20		4	10	317		3
238a		20		3	10	319		3
239a		20		1	10	319		3
240a		20	Coal	2	20	309		3
241a		20		2	20	304		3
b		30		2	20	300		-
c		10		2	30	300		-
d		20		2	30	300		2
242a		30		2	30	300		3
243a		10		2	20	300		3
244a		20		2	10	300		3
245a		10		2	10	317		3
b		20		-	--	315		3

*1 = Ames
2 = Richmond
3 = Americology
4 = San Diego

TABLE A-3. DATA SUMMARY – RDF TESTING (CONCLUDED)

Test No.	T_{25}	T_{26}	T_{27}	Emission Level					
				CO (ppm)	CO_2 (ppm)	NO (ppm)	SO (ppm)	UHC (ppm)	O_2 (%)
227a	2066	1802	2092	47.8	9.4	80			3.8
b	2107	1843	2162	39	11.3	81			2.0
c	2149	1885	2217	66	9.6	116	59.7		4.4
d	2223	1927	2285	147.	12.5	85	168.7		1.2
e	2172	1892	2262	31.2	11.9	100	169.6		2.2
f	2229	1955	2333	50.8	9.7	143	167.2		5.6
g	2200	1958	2298	88.9	9.9	163	165.5		5.2
h	2277	2011	2350	----	----	117	---		---
i	2334	2049	2396	972.3	13.0	112	183.2		1.0
228a	1977	1721	2102	29.4	10.5	90	3.1		3.5
b	2231	1956	2344	53.7	11.0	88	9.8	1.0	1.4
c	2228	1956	2350	715	11.4	104	9.8	5.0	1.8
d	2251	1969	2370	42.4	8.8	144	14.8	8.0	5.2
e	2251	1969	2374	1068	12.2	108	22	4.0	1.1
f	2301	2011	2411	34.6	10.8	116	24.9	5.0	2.1
g	2273	1999	2395	45.6	9.3	193	30.7	4.0	5.0
h	2155	1920	2302	66.3	9.8	135	8.4	6.0	5.4
i	2282	2007	2368	65.8	11.2	110	34.7	6.0	2.1
j	2320	2047	2426	350	12.1	106	54	6.0	1.1
229a	1904	1663	2018	104	10.2	82	7.4	---	3.8
b	2055	1795	2195	102	10.3	99	6.1	---	3.7
c	2245	1971	2334	107	11.4	102	13.7	---	1.3
d	2281	2006	2381	114.1	10.8	114	13.1	---	2.0
e	2253	2002	2363	154.5	9.2	144	15.1	---	5.1
f	2257	2022	2360	160.1	9.7	189	23.0	---	5.1
g	2296	2041	2386	123.6	11.7	147	34.1	---	2.1
230a	1987	1750	2081	0.6	9.5	93	10.5	---	3.9
b	2087	1850	2160	4.5	8.7	150	10.7	4.0	5.3
c	2093	1858	2175	5.4	9.9	111	19.0	3.8	2.3
d	2293	1989	2368	6.4	10.9	98	19.9	4.5	1.1
e	2269	2000	2351	19.1	8.5	182	34.9	4.0	5.2
f	2303	2015	2377	32.9	10.5	129	29.1	4.0	1.8
g	2326	2034	2395	10.0	10.7	115	23.5	3.8	1.1
231a	2157	1904	2340	145.1	17.7	348	2123.5	---	1.2
b	2304	2014	2460	94.0	17.8	458	1902	---	1.9
232a	2231	1919	2318	24	10.8	123	6.6	---	3.5
b	2311	1966	2429	19	11.5	134	---	---	---
233a	2320	1977	2386	21	12.9	117	18.6	---	3.9
234a	2054	1751	2039	11	11.5	130	22.1	---	3.8
235a	1915	1653	1958	12	9.7	122	22.1	---	3.8
b	----	----	----	12	11.0	215	----	---	---
236a	2035	1759	2050	5	11.3	161	34.8	---	---
237a	2078	1801	2110	9	11.4	185	35.9	0.5	3.8
238a	1976	1757	1995	5	10.6	188	51.4	11.2	3.8
239a	1982	1766	1928	6	11.3	129	18.1	0.4	3.8
240a	2139	1931	2117	---	----	410	1358.6	1.3	3.6
241a	2082	1898	2059	18	15.0	405	1321.1	---	3.5
b	----	----	----	18	14.9	456	1321.1	---	3.5
c	2017	1831	2068	90.4	15.9	334	1243	---	2.1
d	2052	1817	2138	56.6	15.8	383	1487	---	3.2
242a	2066	1865	2165	66	13.8	427	1575.3	---	5.2
243a	2289	1972	2175	90	16.0	289	1508.6	436	1.9
244a	2196	1720	1964	85	15.3	381	1148.6	---	4.0
245a	1996	1861	2088	112	16.6	348	1565.9	---	2.0
b	3452	1995	2328	16	14.4	493	1692.8	---	3.7

COAL/OIL MIXTURE (COM) SUBSCALE COMBUSTION TEST RESULTS CONDUCTED IN THE EPA/ACUREX MULTIFUEL FURNACE FACILITY

INTRODUCTION

Subscale combustion tests with coal/oil mixtures as fuel were performed by Acurex in the EPA Multifuel Furnace Facility to provide design support for the planned full-scale COM facility at Lorillard Division, Loew's Theaters, Inc., Danville, Virginia. The test objectives were as follows:

- Determination of emissions for 30 to 50 percent coal in No. 6 oil using identical fuels as anticipated for use at the Lorillard demonstration site
- Identification of fouling, piping, and pumping problems resulting from fuel handling and combustion
- Determination of suitability of the Carbonoyl, Inc., COM additive planned for use in the full-scale demonstration program

The subscale combustion tests consisted of two major activities:

- Fuel preparation
- Combustion tests

These activities are described in the following sections.

1. FUELS AND FUEL PREPARATION

COM fuels for combustion testing were prepared with the coal and oil identical to those anticipated for use at the Lorillard demonstration site. No. 6 oil which meets Lorillard specifications and is identical to that which is presently in use was obtained from Amerada Hess Corporation. The high volatile bituminous coal which was determined to have the most desirable properties for wet grinding (from subscale wet grinding tests at Colorado School of Mines Research Institute) and which will be used during demonstration testing was obtained from Maryland Coal and Coke Company. Specifications and chemical analyses of the oil and coal are presented in Tables 1 and 2.

Although a wet grinding ball mill will be used for demonstration fuel preparation, dry grinding and subsequent mixing were used for the test fuels. This preparation scheme was chosen because a suitable wet grinding system was not available. Pulverized coal prepared by C$MRI was blended

TABLE 1. NO. 6 OIL ANALYSES

Specifications[a]		Ultimate (% Wt)[a]	
API gravity	15.3	Carbon	84.71
Sulfur (% Wt)	2.22	Hydrogen	10.75
Flash point (PMCC °F)	204.0	Nitrogen	0.36
Viscosity (SSF @ 122°F)	247.0	Oxygen	1.93
Pour point (F)	+50.0	Sulfur	2.22
BS&W (% Vol)	0.4	Ash	0.03

[a] Supplied by Amerada Hess Corporation

TABLE 2. COAL ANALYSES

Proximate (% Wt)[a]		Ultimate (% Wt)[b]	
Moisture	4.2	Carbon	79.0
Volatiles	33.0	Hydrogen	5.0
Fixed carbon	54.0	Nitrogen	1.5
Ash	8.9	Sulfur	0.9
Ash fusion temp (F)	2700.0	Oxygen	13.4
Hardgrove grindability	68.0		
Btu per pound	13368.0 As Rec'd 13954.0 Dry		
Origin: Clintwood seam, Conoway, Virginia			

[a] Supplied by Maryland Coal and Coke Company
[b] EPA-650/2-75-046, May 1975

with No. 6 oil and the Carbonoyl additive in a high turbulence batch mixer supplied by Littleford Brothers. The grind distribution of the coal was approximately 80 percent passing 200 mesh and 100 percent passing 48 mesh. The additive was prepared in a 50-percent aqueous solution and constituted 3.75 percent by weight of the COM independent of coal fraction.

The blending procedure was as follows:

1. Place premeasured No. 6 oil in the Littleford Brothers batch mixer (Model FM 13100 20-gallon capacity). The mixer is maintained in the "on" position. Mixer is steam jacketed and mixture is maintained at about 140°F.
2. Add premeasured additive solution to oil
3. Add premeasured pulverized coal to oil and additive and allow to mix for 10 minutes
4. Discharge into 55-gallon storage drum

Fuel mixing occurred between July 11 and July 22, 1977. Approximately 1500 total gallons of 50-, 40-, and 30-percent COM were prepared. No unexpected difficulties arose. Those problems which did occur were related to handling of the fuels, particularly the pulverized coal. None of the handling problems, however, are related to full-scale operation.

The COM was stored at ambient temperatures (minimum approximately 50°F) for up to 24 days before use. About 3 hours prior to use, the storage drum was wrapped with electrical resistance heating blankets and a mixer with a 6-inch propellor was immersed in the mixture. During this period, the mixture temperature rose to about 140 to 150°F. A homogeneous mixture was observed at about 100°F. The mixture was pumped into tanks located within the facility. The empty storage drums were examined for signs of pulverized coal which had settled in the mixture during storage and failed to reentrain during the mixing cycle. In all cases, no deposits of pulverized coal were found.

2. SUBSCALE COMBUSTION TESTS

Subscale combustion testing occurred between July 27 and August 11 at the EPA/Acurex facility. The test facility, shown in Figure 1, is

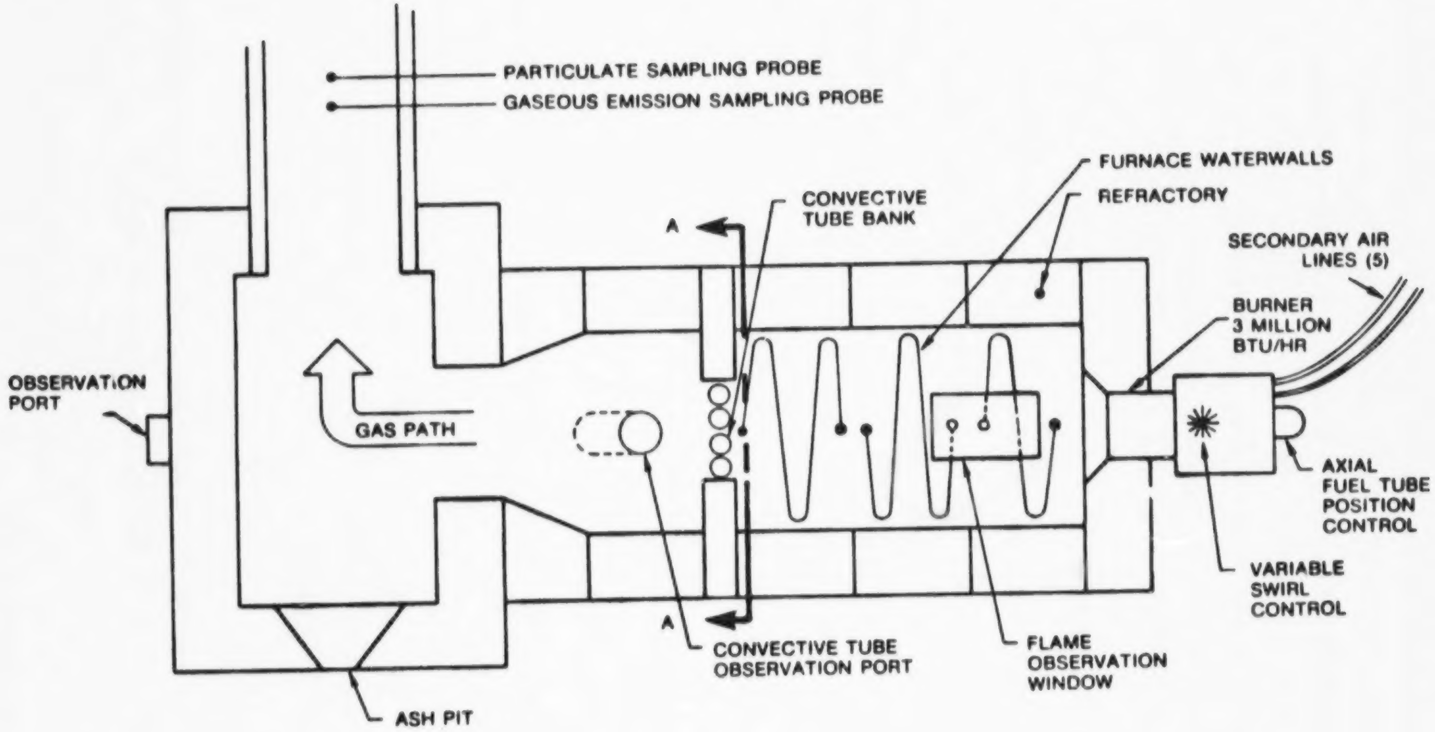
PARTICULATE SAMPLING PROBE
GASEOUS EMISSION SAMPLING PROBE
FURNACE WATERWALLS
REFRACTORY
CONVECTIVE TUBE BANK
A
SECONDARY AIR LINES (5)
BURNER 3 MILLION BTU/HR
OBSERVATION PORT
GAS PATH
AXIAL FUEL TUBE POSITION CONTROL
VARIABLE SWIRL CONTROL
A
CONVECTIVE TUBE OBSERVATION PORT
FLAME OBSERVATION WINDOW
ASH PIT

Figure A-1. EPA/Acurex Multifuel Furnace Test Facility — 3 million Btu/hr capability — side view. (See Figure 2 for Section A-A) sponsored by the Environmental Protection Agency to investigate advanced emission control concepts for utility and industrial boilers. The configuration additions indicated on the sketch were made to more closely simulate industrial boiler operating conditions. One important addition to these tests was the steam-cooled tube bank across the path of the combustor gases. The purpose of these tubes was to model the convective section of a boiler and thereby provide information regarding tube fouling. Water-cooled tubes spiralled around the combustion chamber were added to simulate the water-walled combustion chamber of industrial watertube boilers.

2.1 FACILITY MODIFICATIONS

2.1.1 Convective Tubes (Slagging Probes)

A bank of four tubes mounted across the gas flow was designed to simulate the entrance plane of the convective tube banks of the demonstration boiler with the primary objective of gaining qualitative information regarding the fouling tendencies of the Lorillard fuels. The tube configuration is shown in Figure 2. The tube sizing and spacing were selected to duplicate the velocity through the tubes of the demonstration unit. Cooling was provided to maintain the tubes below 600°F, the factory estimated temperature of the convective tubes.

2.1.2 Combustion Chamber Waterwalls

As shown in Figure 1, the combustion chamber preceeding the convective tube section was lined with several loops of copper tubing for radiant cooling. This cooling reduced the bulk gas temperature to below 2300°F which is the factory estimate of gas temperature entering the convective section of the demonstration boiler. The cooling loops were in the three horizontal extension sections.

2.1.3 Fuel Supply System

The fuel supply system is shown schematically in Figure 3. The item numbers shown are described in an equipment list in Table 3.

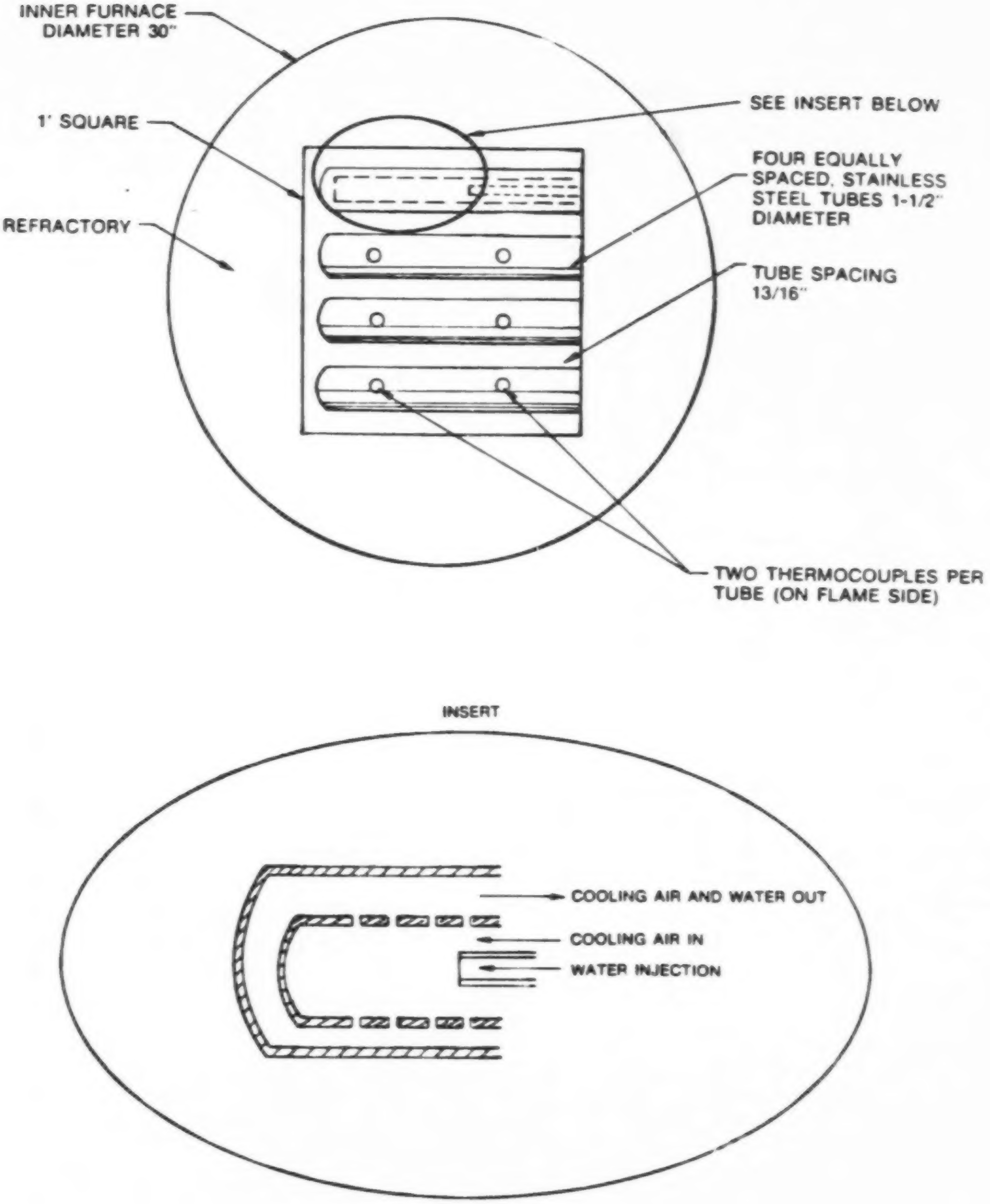
INNER FURNACE DIAMETER 30"
1' SQUARE
REFRACTORY
SEE INSERT BELOW
FOUR EQUALLY SPACED, STAINLESS STEEL TUBES 1-1/2" DIAMETER
TUBE SPACING 13/16"
TWO THERMOCOUPLES PER TUBE (ON FLAME SIDE)
INSERT
COOLING AIR AND WATER OUT
COOLING AIR IN
WATER INJECTION

Figure A-2. Convection tube bank.
(Section A-A from Figure A-1)

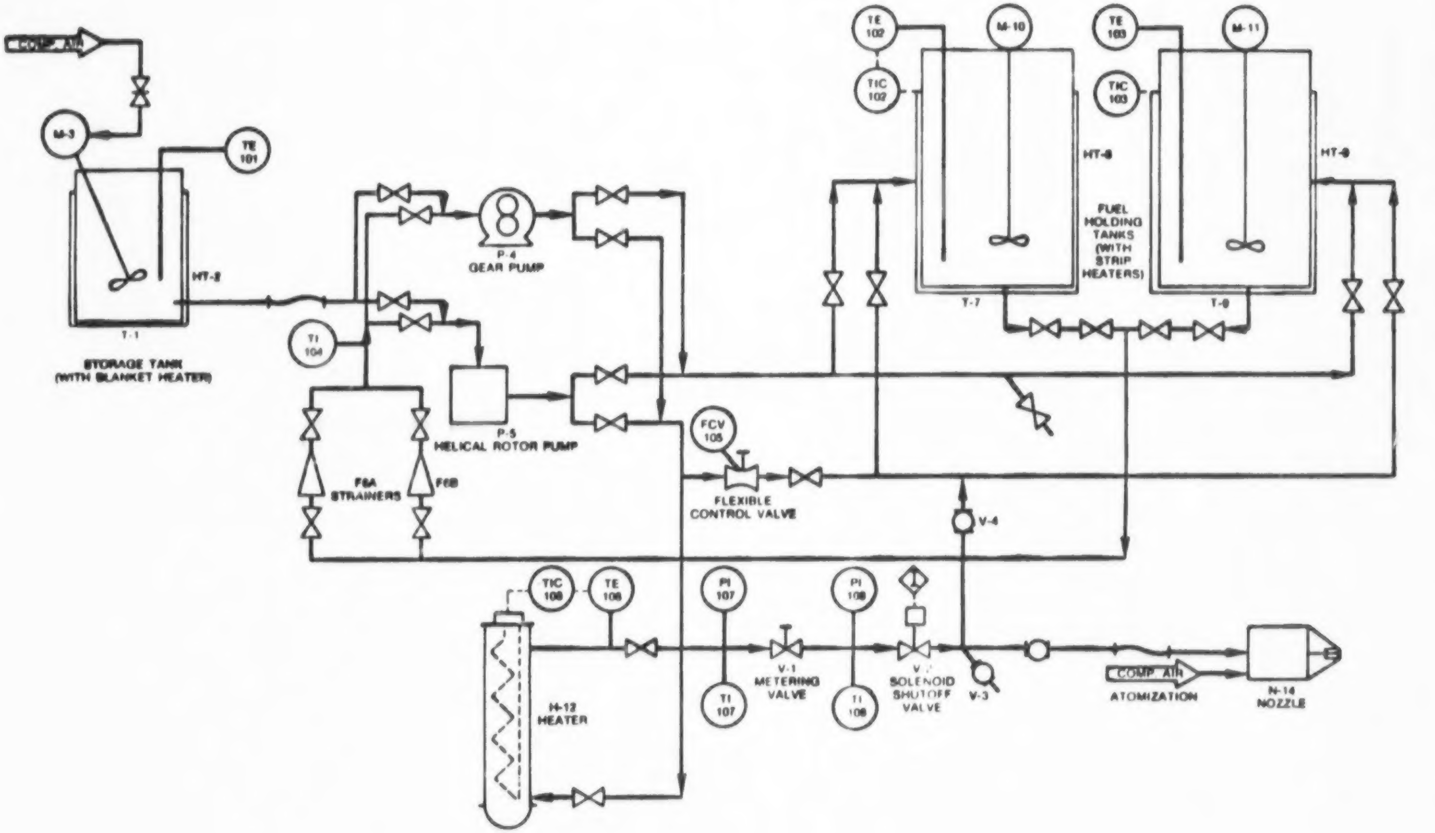
COMP. AIR
M-3
TE 101
HT-2
T-1
STORAGE TANK (WITH BLANKET HEATER)
TI 104
P-4 GEAR PUMP
P-5 HELICAL ROTOR PUMP
F6A STRAINERS
F6B
TE 102
TIC 102
M-10
HT-8
T-7
FUEL HOLDING TANKS (WITH STRIP HEATERS)
TE 103
TIC 103
M-11
HT-9
T-9
FCV 105
FLEXIBLE CONTROL VALVE
V-4
TIC 106
TE 106
H-12 HEATER
PI 107
TI 107
V-1 METERING VALVE
PI 108
TI 108
V-2 SOLENOID SHUTOFF VALVE
V-3
COMP. AIR
ATOMIZATION
N-14 NOZZLE

Figure A-3. Fuel supply system schematic.

TABLE 3. FUEL SUPPLY SYSTEM EQUIPMENT LIST

Item	Description	Comments
T-1	Fuel storage tank	55-gal drum
T-7	Fuel holding tank	135-gal
T-9	Fuel holding tank	135-gal
M-3	Pneumatic mixer, propeller type	1.3 hp, variable speed
M-10	Pneumatic mixer, propeller type	1.0 hp, variable speed
M-11	Pneumatic mixer, propeller type	1.0 hp, variable speed
HT-2	Heating blanket	1200 W
HT-8	Strip heaters	8 per tank, 500 W each
HT-9	Strip heaters	8 per tank, 500 W each
TE-101	Temperature element	
TE-102	Temperature element	
TE-103	Temperature element	
TE-106	Temperature element	
P-4	Gear pump	1.0 hp, 450 RPM
P-5	Helical rotor pump	0.75 hp, 1200 RPM
TIC-102	Temp indicating controller	70 to 250°F
TIC-103	Temp indicating controller	70 to 250°F
TIC-106	Temp indicating controller	70 to 250°F
F6A	Strainers	1/16" perforations
F6B	Strainers	1/16" perforations
TI-104	Temperature indicator	60 to 260°F
TI-107	Temperature indicator	60 to 260°F
TI-108	Temperature indicator	60 to 260°F
H-12	Circulation heater	3000 W
PI-107	Pressure indicator	0 to 160 psi
PI-108	Pressure indicator	0 to 160 psi
V-1	Metering valve	Self cleaning
V-2	Solenoid valve	Flame safety
V-3	Ball valve	Sampling port
V-4	Ball valve	Nozzle flow recirc
N-14	Nozzle	
FCV-105	Flexible control valve	Regulates recirculation

For transfer of fuel into the holding tanks, (Item T1, Table 3) a COM storage drum is preheated using electrical resistance heaters (Item HT-2) and agitated with a pneumatically driven shaft mixer (Item M-3). The drum is connected by flexible hose to the system inlet where the mixture is pumped through either the gas pump (Item P-4) or the helical rotor pump (Item P-5) (or both pumps) to holding tank 1 or 2 (Items T-7 and T-9).

During furnace operation, COM is pumped from either holding tank through one of two parallel strainers (Items F6A or F6B) by either or both pumps. The flow then splits into a recirculation line and a nozzle line. The recirculation line returns excess flow to the holding tank. A flexible pinch valve (Item FCV-105) regulates the recirculation flow and as a result acts as a coarse adjustment for flow into the nozzle. COM flow to the nozzle is directed through a circulation heater (Item H-12). The fine adjustment on flowrate is done with a self-cleaning metering valve (Item V-1). Temperatures and pressures are monitored on either side of this valve (Items TI-107 and TI-108, PI-107 and PI-108). A solenoid valve (Item V-2) is wired to the furnace flame safety system. Flow progresses from the system outlet through flexible hose to the nozzle (Item N-14). Fuel samples may be drawn at any time (Item V-3). Prior to light-off, nozzle flow may be redirected into the recirculation line (Item V-4).

Several other flow options are available. COM may be transferred from either of the holding tanks to the other holding tank or to the original storage drum. Fuel may be delivered to the nozzle directly from the storage drum. This operation requires that both pumps be employed, however. The circulation heater (Item 38) may be used to augment holding tank heaters prior to startup.

The entire system was electrically heat traced and insulated to maintain COM temperatures to at least 140°F. Temperature was controlled by five individual thermostats covering the storage tank to delivery system inlet line; the holding tanks, system piping and the circulation heater. These on-off type thermostats were capable of controlling fluid temperature from 60°F to 250°F with a 7°F tolerance.

A duplex pumping arrangement was chosen such that system shutdown would be prevented in case one pump failed and also to compare operation of the two pumps on COM. The fuel flow through each pump was approximately 8 gpm yielding fluid velocities in the 3/4-inch lines of approximately 5 ft/second.

2.1.4 Atomization Air System

Standard shop air at 150 psig at flowrates up to 30 scfm was used for fuel atomization. The pressure and flowrate at the nozzle were controlled by appropriate pressure regulators and flowmeters.

2.2 EMISSION MONITORING EQUIPMENT

Continuous monitors were used to collect emission data. Table 4 lists the instrumentation used and the principle of operation of each device.

Calibration was performed prior to, during, and at the end of each test period. Correction in the emission data due to calibration shifts, whenever present, were taken into account in the calculation of reported NO and CO levels.

2.3 CHECKOUT TESTING

Prior to actual testing, several hours of system checkout and equipment evaluation were conducted.

During operation on natural gas, it was discovered that the convective tube bank was not adequately cooled by air alone, and a water injection system was added (see Figure 2). The goal was to maintain the tubes at about 600°F, but the coarse control afforded by the water injection provided temperatures of about 400°F. Also, the water in the tubes caused differential expansion between the top and bottom of each tube. As a result, tube-to-tube and tube-to-wall spacing changed during the test run.

Two nozzle configurations were evaluated on No. 6 oil and 30-percent COM during checkout. A Delavan Corporation swirl air nozzle and a Sonic Development Corporation Sonicore nozzle were tested. The Delavan nozzle, designed for 60 gph maximum flow with a 70-degree spray angle performed well with moderate burner secondary air swirl. No flame

TABLE 4. EMISSION MONITORING INSTRUMENTATION

Pollutant	Type of Operation	Manufacturer	Models	Instrument Range
NO	Chemiluminescence	Ethyl Intertech	Air Monitoring	0-5 ppm 0-10 0-100 0-250 0-1000 0-5000
SO_2	Pulsed Fluorescent	Thermoelectron	Teco Model 40	0-50 ppm 0-100 0-500 0-1000 0-5000
CO	Nondispersive Infrared (NDIR)	Ethyl Intertech	Uras 2T	0-500 ppm 0-2000
CO_2	Nondispersive Infrared (NDIR)	Ethyl Intertech	Uras 2T	0-5% 0-20%
O_2	Paramagnetic	Ethyl Intertech	Magnos 5A	0-5% 0-21%
Particulate Loading	Cyclone and Filtration	Acurex Corp	HVSS	0-3 μm Minimum

impingement on the furnace walls was observed. Fuel pressure of about 40 psi delivered the desired 10 to 15 gph. An atomization air pressure of 40 psi and a flowrate of 1000 scfh adequately atomized the 180 to 200°F fuel. When the fuel temperature was greater than about 200°F, pulsations in the flame were observed. These pulsations, thought to be due to the vaporization of water in the fuel, stopped when the fuel temperature was lowered. Since atomization was adequate at 180 to 190°F, the remainder of the tests were run in this temperature range. Following approximately three hours of operation on 30-percent COM, extensive erosion was observed on the nozzle tip. Figure 4 shows the nozzle and the areas where erosion occurred. The erosion was probably a result of the high fuel-air mixture velocities (600 to 1000 feet per second) necessary for proper atomization. Although the part was supplied as stainless steel, it was discovered later to be carbon steel. A stainless steel metering nut with a tungsten carbide pintle was then obtained to minimize erosion.

Figure 5 shows a diagram of the Sonicore nozzle. Designed for flowrates up to 60 gph, it was operated at fuel pressures of 0 to 5 psig at the nozzle and atomization air pressure and flowrate of 35 psig and 1500 scfh, respectively. Initial nozzle operation at moderate and low secondary air swirl resulted in clinker formation at the nozzle tip within 15 minutes of light-off. This condition was eliminated at a zero swirl setting, but the flame was unstable. Following approximately 3 hours of operation on 30-percent COM at various swirl levels, examination of the nozzle did not reveal any erosion. A decision was made to use the Delavan nozzle. Even though the Sonicore nozzle was more erosion resistant, the Delavan nozzle provided superior flame characteristics.

During the checkout tests, a thermocouple mounted adjacent to the furnace wall just prior to the convective tube bank was used to estimate combustion gas temperatures when the suction pyrometer failed. Also, a proportional controller was used to minimize fluctuations in fuel flowrate caused by the "on-off" characteristic of the circulation heater thermostat. The flow variation resulted from the temperature-induced change in the viscosity.

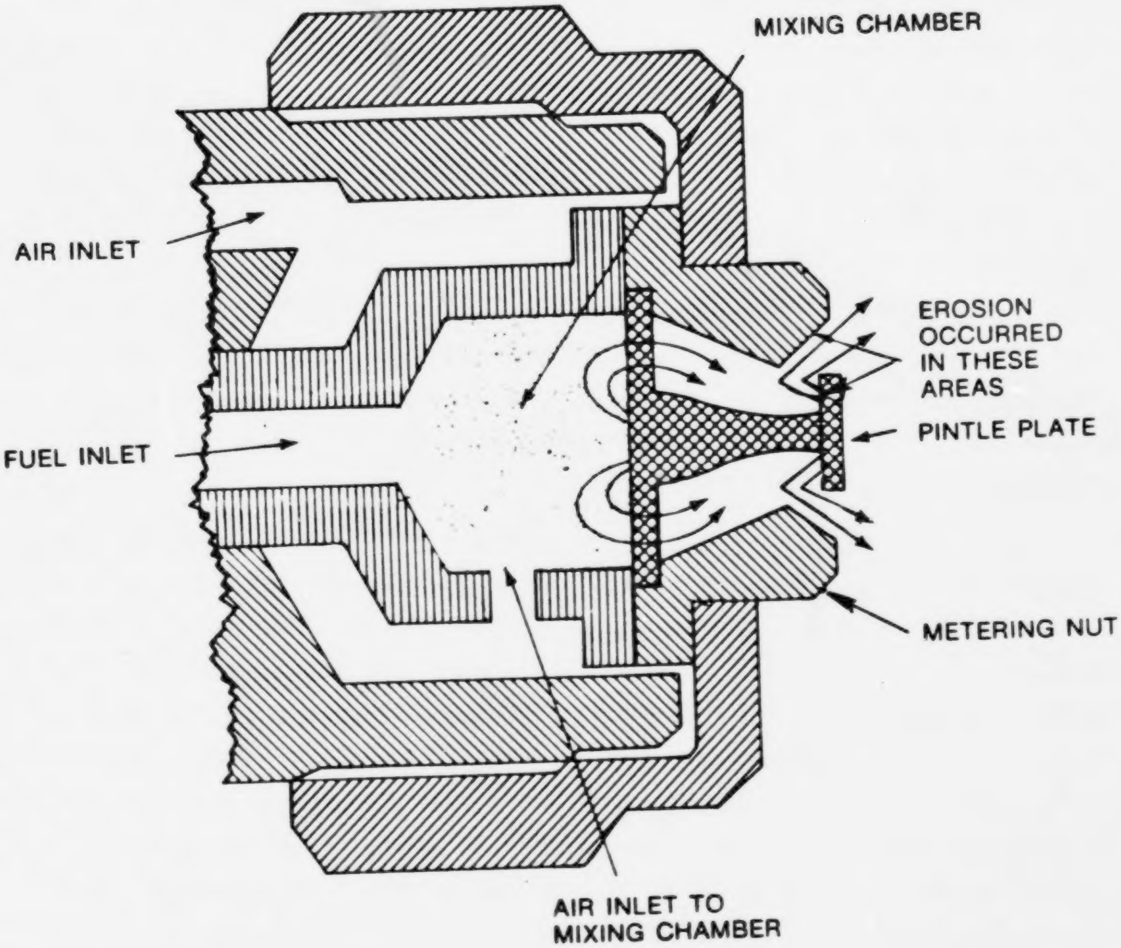
MIXING CHAMBER
AIR INLET
EROSION OCCURRED IN THESE AREAS
PINTLE PLATE
FUEL INLET
METERING NUT
AIR INLET TO MIXING CHAMBER

Figure A-4. Delavan swirl-air nozzle.

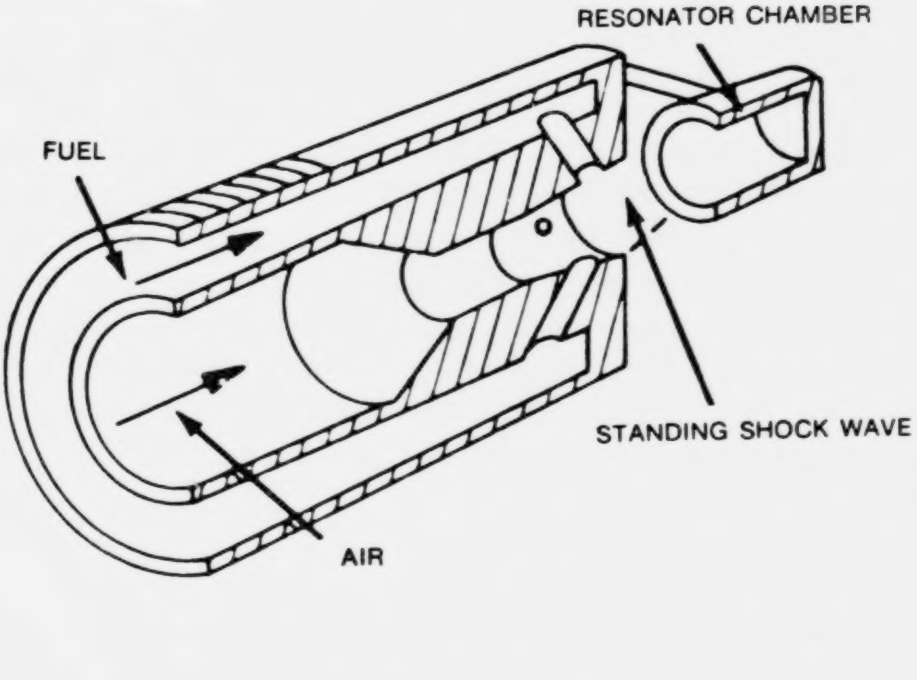
RESONATOR CHAMBER
FUEL
STANDING SHOCK WAVE
AIR

Figure A-5. Sonic Corporation Sonicore nozzle.

2.4 TESTING

The test points completed are shown in the matrix of Table 5.

TABLE 5. COM TEST MATRIX

% Coal / % Excess Air	1.8 Million Btu/hr					1.35 Million Btu/hr				
	0	30	40	50	100	0	30	40	50	100
20	X	X	X	X	X					
30	X	X	X	X	X	X	X		X	X
40	X	X	X	X	X	X				

For a furnace load of 1.8 million Btu/hr corresponding to the heat release rate of the demonstration boiler at full load (80,000 pph), three coal-oil mixtures were burned for a range of excess air. To provide reference points, 100-percent No. 6 oil and 100-percent pulverized coal were fired at the same conditions. Additional data was taken at a reduced load of 1.35 million Btu/hr corresponding to 60,000 pph for full-scale. Test conditions at 40 percent of full-scale load (0.72 million Btu/hr) were planned but eliminated because of the limited range of burner secondary air control.

2.4.1 Test Narrative

Tests were first performed with 100 percent pulverized coal at a firing rate of 1.8 million Btu/hr. Following nearly 3 hours of operation, approximately 50 percent of the convective passages were blocked by ash deposits. The hard, porous deposit was removed mechanically.

A case hardened (R_C = 58 to 0.03 inches) Delavan nozzle was used to obtain test points on No. 6 oil. This was a higher capacity nozzle (100 gph) than had been used in the checkout runs, but no differences were observed either in flame shape or in emission levels. After 3 to 5 hours of testing, inspection of the nozzle showed no signs of erosion. Also, no ash deposition on the convective tube bank was noted.

A 30-percent COM was tested next using the case-hardened nozzle used on the No. 6 oil. After about 3 hours of operation, significant deterioration of the flame shape suggested nozzle tip erosion which was confirmed by inspection. The erosion pattern was similar to the first eroded nozzle (see Figure 4); substantial erosion occurred on the pintle plate with slight but definite erosion occurring on the metering nut. The nozzle life was unaffected by the case hardening process. A new nozzle with tungsten carbide pintle and stainless steel metering nut was used to complete the tests. This 60 gph nozzle was compared with the larger nozzle by taking two duplicate points; no difference was observed in the two nozzles. After approximately 2-1/2 to 3 hours, the nozzle was inspected and significant erosion was observed. In this case, only the stainless steel metering nut had eroded and the tungsten carbide pintle remained unchanged.

The convective tubes showed some fouling but this was minimal compared to the pulverized coal.

A 50-percent COM was tested next. A high capacity (150 gph) Delavan nozzle was chosen to minimize velocities through the nozzle tip. Test data was taken prior to flame deterioration at the 3-hour point when erosion was again observed. At this point, approximately 10 percent of the total convective passage was occluded by ash deposition. Factors contributing to this high rate of deposition were probably the volumetric heat release (0.75×10^6 Btu/hr-ft^3) and the hot refractory wall of the furnace.

The 40-percent COM was the last fuel tested. Equipment problems arose after about 1 hour of testing. First, the helical rotor pump failed. Subsequent inspection revealed that the rotor was extensively galled. The gear pump was used for the remainder of the tests. Second, plugging of the fuel metering valve was experienced. The valve was removed and cleaned twice without success.

After flushing the entire system with No. 6 oil, a second attempt at 40-percent COM was made. Similar valve plugging was experienced. The valve was replaced with a conventional needle valve and data points were taken. Erosion of the nozzle was observed following these tests, but it was less than that leading to eratic flame patterns. Fouling was less than with

50-percent COM but greater than with 30-percent COM. Again, the high volumetric heat release and the hot-wall effect probably contributed to the high rate of deposition.

2.4.2 Emission Tests

Pollutant emissions for each fuel were measured at excess air levels of 20-, 30-, and 40-percent. For these measurements, the furnace load was maintained at 1.8×10^6 Btu/hr. This load corresponds to a volumetric heat release of 0.75×10^6 Btu/hr-ft^3, which is approximately the same as the demonstration boiler at full load.

2.4.2.1 Nitric Oxide (NO) Emissions

Figures 6 through 10 show NO levels as a function of stoichiometric ratio for No. 6 oil, 30-, 40-, and 50-percent COM, and pulverized coal. In Figure 8, the data taken in test 201a is believed to be most representative as it was taken prior to plugging problems experienced with the fuel supply system. The data recorded in tests 201b, c, and d, are questionable since partial fuel supply blockage occurred during these tests. As expected, NO emissions increased with stoichiometric ratio for each fuel. This was probably due to increased oxidation of fuel nitrogen with each increase in excess air. The rate of increase of NO with excess air was greater for coal and coal-oil mixtures than for oil alone. This is attributed to the increased emissions of fuel NO for the coal-containing fuels. Fuel NO is generally more sensitive to excess air levels than thermal NO which predominates with oil combustion. Table 6 lists general properties of the five fuels tested. Note that fuel nitrogen increases as coal content of the fuel (mixture) increases.

The effect of coal content on NO emissions is shown in Figure 11. The upper curve represents NO levels recorded at 40 percent excess air, and the lower curve represents data taken at 20 percent excess air. NO emissions from COM combustion were slightly lower than levels expected from a straight proportional weighting of emissions according to weight percentage of coal and oil.

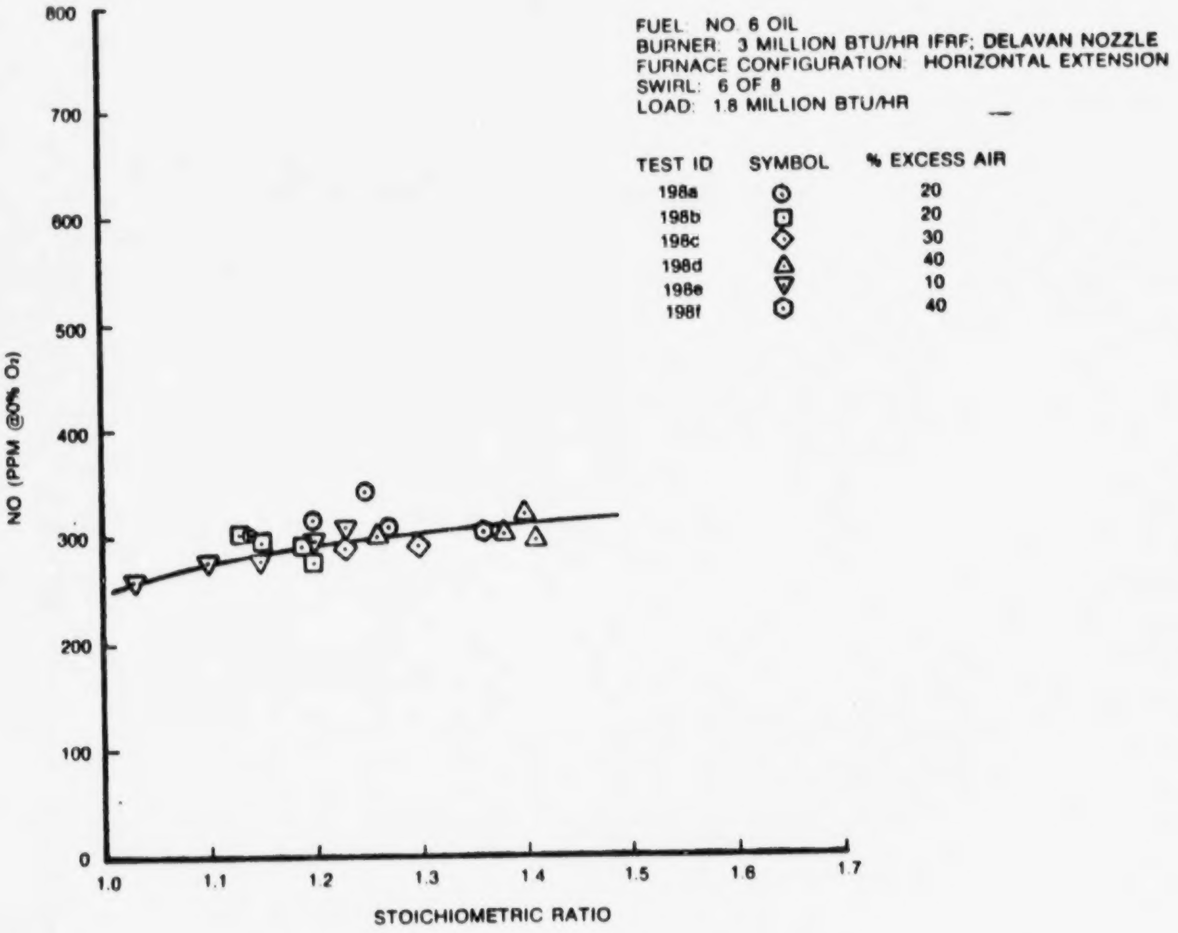

Figure A-6. Nitric oxide (NO) versus stoichiometric ratio: No. 6 oil.

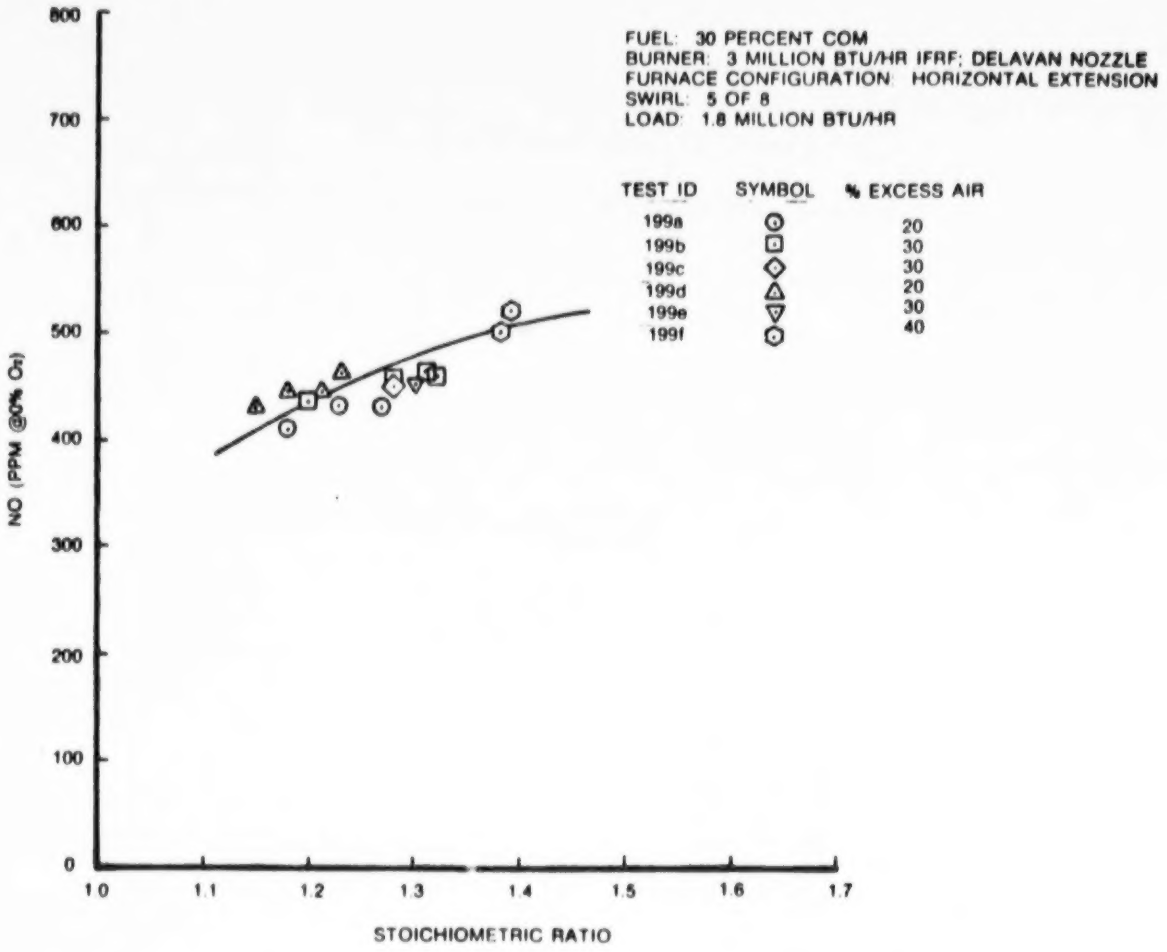

Figure A-7. Nitric oxide (NO versus stoichiometric ratio: 30-percent COM.

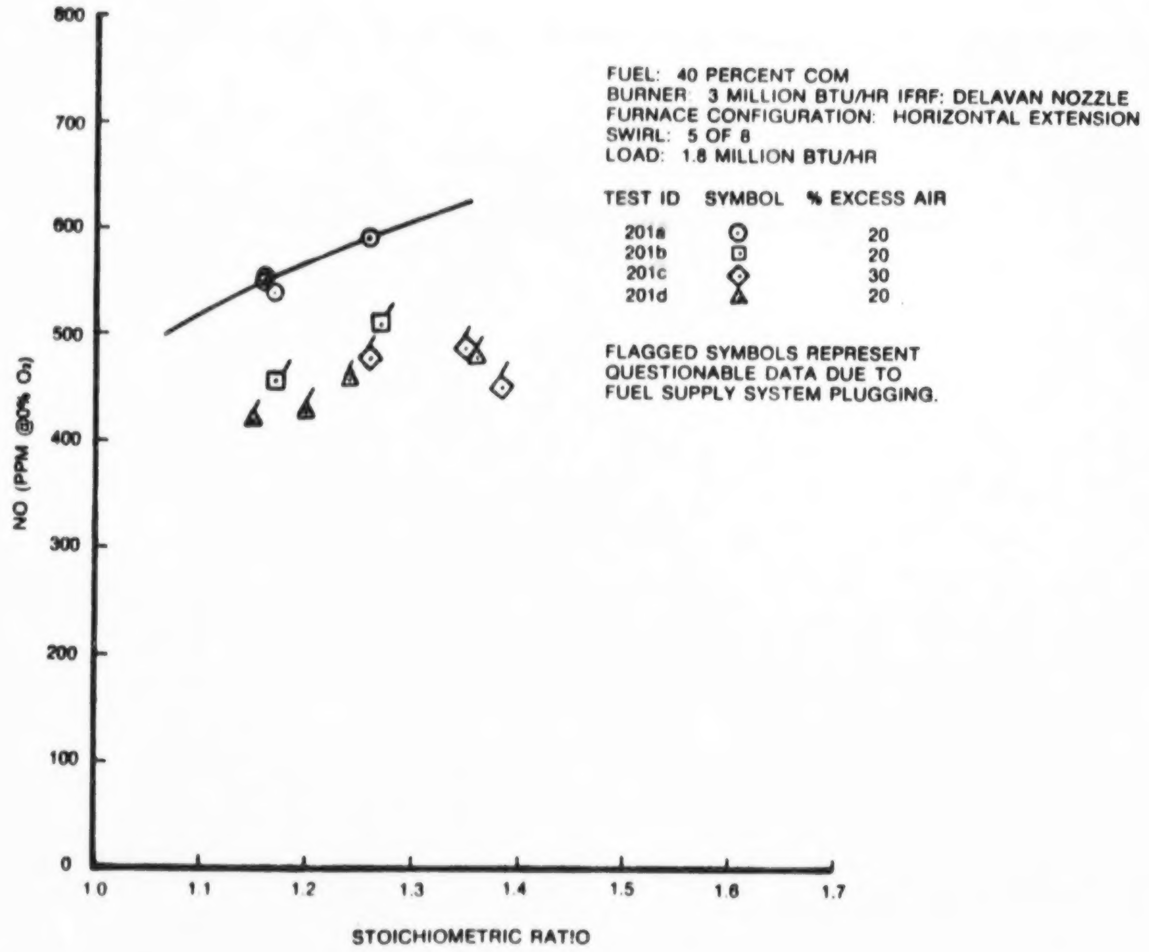

Figure A-8. Nitric oxide (NO) versus stoichiometric ratio: 40-percent COM.

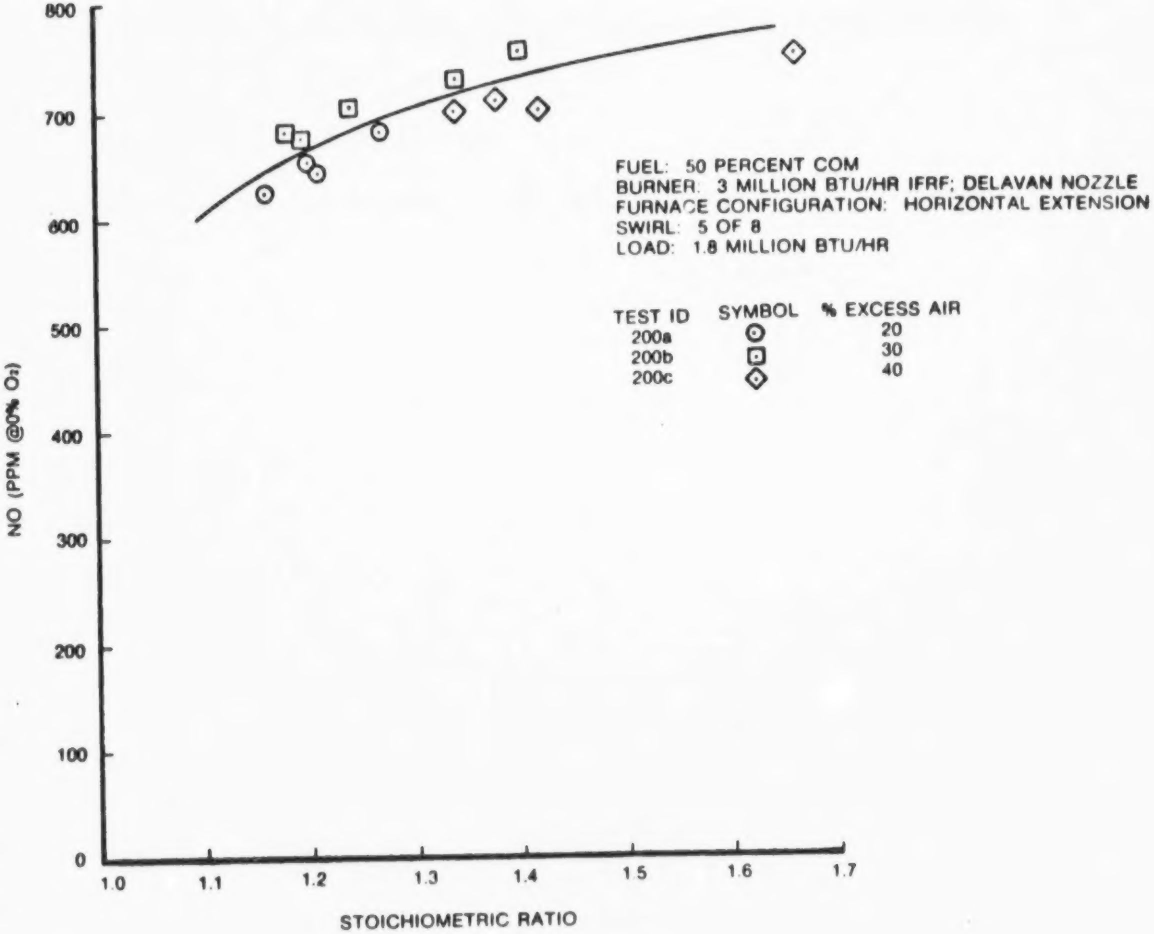

Figure A-9. Nitric oxide (NO) versus stoichiometric ratio: 50-percent COM.

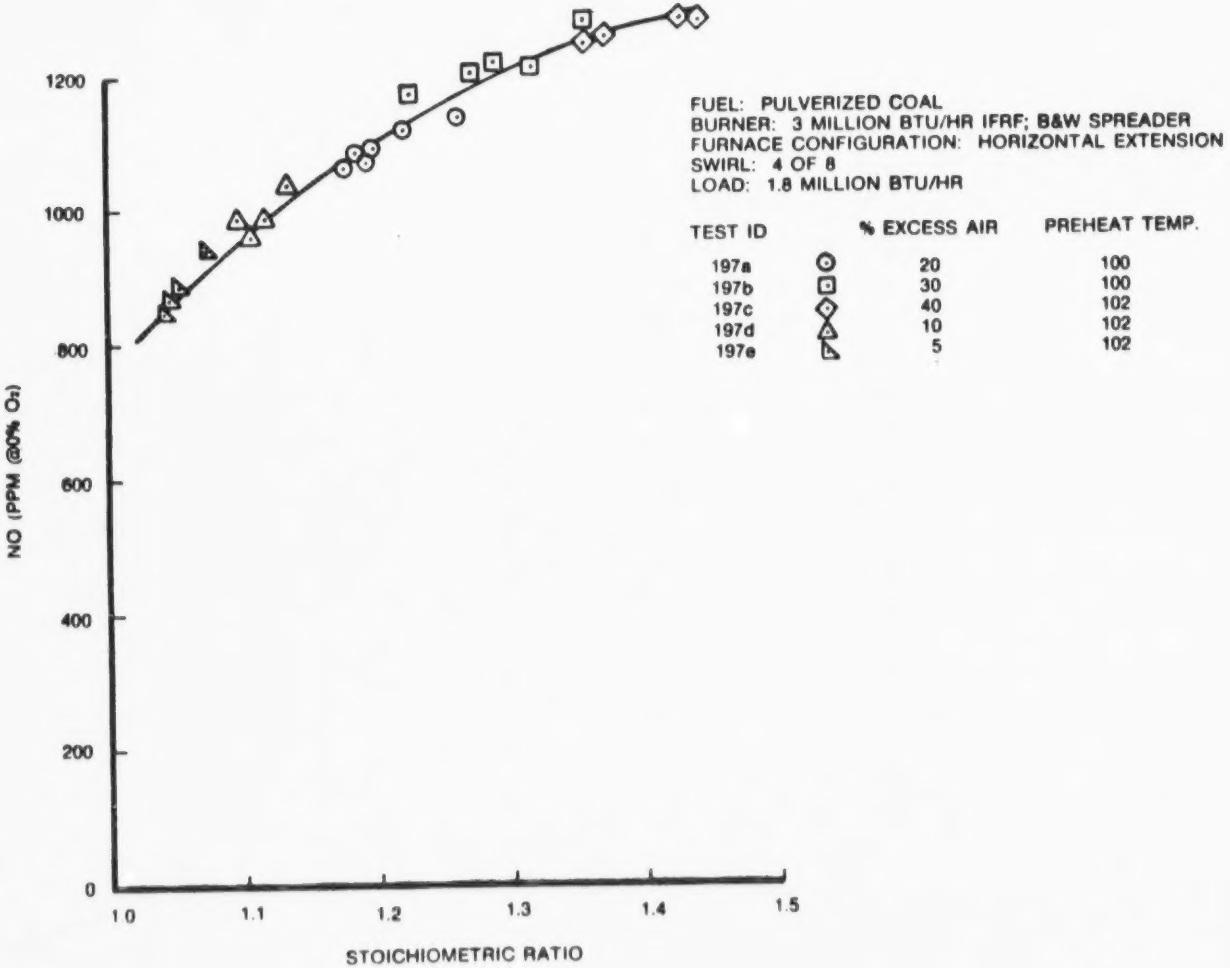

Figure A-10. Nitric oxide (NO) versus stoichiometric ratio: pulverized coal.

TABLE 6. FUEL PROPERTIES

Fuel Type	% N By Weight	% S By Weight	% Water By Weight[a]	% O_2 By Weight	HHV Btu/lb
No. 6 oil	0.36	2.22	0.0	0.0	18,800
30% COM	0.70	1.82	4.82	2.67	17,170
40% COM	0.82	1.69	5.24	3.56	16,627
50% COM	0.93	1.56	5.66	4.45	16,084
100% Coal	1.5	0.9	4.2	8.9	13,368

[a] Includes 3.56 percent of fuel by weight due to fuel additive.

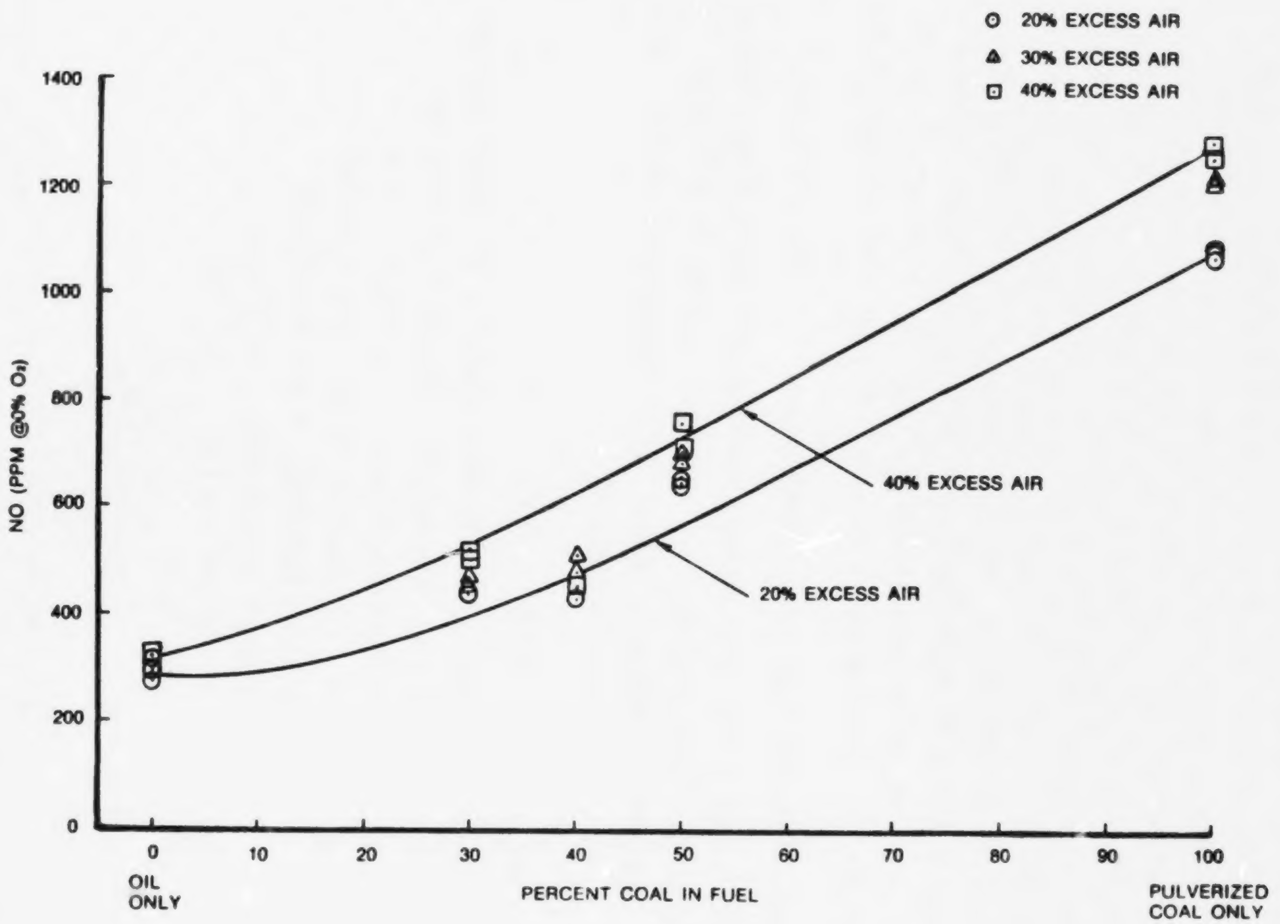

Figure A-11. Nitric oxide (NO) versus percent coal in fuel.

The lower NO emissions of the COM fuels could have been caused by the water content of the additive, or the shielding of coal by the oil spray. Water content in the fuel has been found to reduce NO emissions. During some studies of water emulsions with distillate and residual oils the NO levels were reduced an average of 100 ppm when approximately 5-percent water was added to the fuel oil.* In the COM tests the water content of the fuels attributed to the additive were 3.56 percent by weight. Accounting for this water content, on the basis of the emulsion tests cited above, yields NO levels which conform more closely to proportional levels based on No. 6 oil and pulverized coal NO emissions. The second factor which may have affected NO emissions during these tests results from the layer of oil surrounding each coal particle. This oil layer delays oxygen diffusion to the coal and suppresses oxidation of coal fuel nitrogen to NO.

2.4.2.2 Carbon Monoxide (CO) and Unburned Hydrocarbon (UHC) Emissions

Carbon monoxide (CO) and unburned hydrocarbon emissions were nearly zero for all COM, oil and coal tests. CO emissions were insignificant even though the excess air levels were reduced to 10 percent on occasion. UHC emissions were undetectable during all tests.

2.4.2.3 Particulate Mass Loading

Particulate stack sampling tests were conducted for the 50-percent coal and pulverized coal fuels. The results indicate that very low fractions of the ash contained in the fuel went out the stack. Based on the relatively small amounts of ash remaining in the furnace (compared to the amount of fuel fired), the stack test results are in question. The test results are also contradicted by more extensive testing at General Motors† where nearly 100 percent of the ash appeared in the flue gas.

---

*G.B. Martin, "Evaluation of NO_x Emission Characteristics of Alcohol Fuels in Stationary Combustion Systems," presented at the Joint Meeting Western and Central States Sections, The Combustion Institute, San Antonio, Texas, April 21 to 22, 1975.

†Brown, A, "First Report of the General Motors Corporation Powdered Coal-In-Oil Mixtures Program," ERDA Contract E(49-18)-2267, December 1976.

2.4.3 Discussion

Pumping of the COM resulted in the failure of the helical rotor pump after approxiamtely 50 hours of operation. On disassembly, no damage was observed to the BUNA-N stator. However, significant galling was seen on the lobes of the rotor. Two possible explanations for this failure are: the pump should have operated at 400 to 500 rpm but instead operated close-coupled to a 1200 rpm motor; the pump operated in a dry state for short periods. The transfer of COM from the storage tank to the system feed tank was probably responsible for the dry operation of the pump. For the transfer operation, the helical rotor pump was actuated as soon as the mixture was thought pumpable. This resulted in dry pump operation if the mixture was not flowing.

The Viking gear pump did not fail, but developed leaks in the packing. When disassembled after test completion, hardened or congealed fuel was detected between the shaft and the packing resulting in leakage. This problem could probably be remedied by the use of mechanical seals. Inspection of the pump components susceptible to wear showed no indication of abrasion after about 50 hours of operation.

Metering problems resulted primarily from the very low flowrates associated with test conditions. The self-cleaning micrometering valve had a maximum fuel passage dimension of about 0.125 inches. Operation was found to be most effective if the valve metering position was between 75 and 100 percent open. Operation in this range was possible by controlling the amount of recirculation by adjusting the flexible valve. While the valve performed satisfactorily with both 30- to 50-percent COM, excessive plugging occurred with the 40-percent COM. For the 40-percent COM, however, operation was impossible even in the 100-percent open position. The plugging occurred upstream of the metering groove where the self-cleaning feature was ineffective and where plugging would not be suspect because of its larger dimensions (approximately 0.25-inch).

No explanation can be given for the failure of the metering valve on the 40-percent COM while not on the 50-percent COM. Subsequent analysis of fuel samples indicated a ±2 percent tolerance on the total solids content of the fuels indicating that the difficulty was not in improperly prepared fuel.

Although the exact cause of the failure is not known, two definite possibilities exist.

- Insufficient additive in the fuel resulted in particle agglomeration leading to eventual plugging
- Following each COM fuel, the entire system was flushed with No. 6 oil stored in the second holding tank. Continued flushings resulted in a mixture of No. 6 and the coal in the second holding tank and in the system lines. In standing for any period of time, this coal would settle onto the walls of the pipes. Settlement occurred because the dilution of the additive rendered it ineffective. Agglomerated coal particles would then reentrain from the pipe walls when flow occurred.

Of these two failure modes, the second is the most suspect since each drum of fuel required two and a half batches of fuel preparation. Carbonoyl Company has stated that little difference in fuel characteristics would be observed if the additive was not included in one of these batches. Also, it is highly improbable that three consecutive batches would have been made without additive. The second failure mode is supported by the fact that plugging was the result of agglomerated coal particles. The packing of these particles was very similar to that observed when unstabilized coal is removed from a sample after settling.

Significant erosion of the Delavan nozzle was experienced. At the time, this occurrence was viewed as a major problem but further investigation indicated that a change in nozzle design would probably remedy the problem. The Delavan nozzle uses an impingement type internal-mix atomization scheme which, by design, is highly susceptible to erosion. A recommendation for future use of air atomizing nozzles are the external-mix type where atomization takes place after the fuel and air have left the nozzle. Several types under this general design are available.

Fouling of the convective tube bank was observed for all coal-containing fuels. Deposition was greatest, as would be expected, for the pulverized coal and least for the 30-percent COM. For the pulverized coal, about half of the convective flow passages were occluded. Deposition associated with the 50-percent COM was less obvious. Due to the displacement of the convective tubes, some tube-to-tube and tube-to-wall spacings were reduced. Increased deposition was noted for these spacings while generally no fouling occurred in spacings which remained equal to or wider than planned.

Two existing conditions which probably contributed substantially to tube fouling were the volumetric heat release rate of the test points and the loss of radiant cooling in the combustion chamber. The volumetric heat rate of the tests corresponded to that of the demonstration boiler at full load. Since the initial tests were made at this load, fouling had already occurred when the load was reduced to 1.35 x 10^6 Btu/hr and any subsequent slagging went unobserved. The loss of coolant tubes during checkout probably contributed to slagging as well. The radiating refractory was sufficiently hot to melt the impinging ash particles. Slag thickness averaged about 0.25 inch at the completion of the test program. These slagging results indicate that tube fouling is a possibility at full-scale operation, but firm conclusions are inappropriate at this time due to the variation in results at both GM and PERC (Pittsburgh Energy Research Center).

ACUREX
Corporation

additional routing

INTEROFFICE

to: Craig Derbidge

from: Allen Shimizu

date: September 15, 1977

subject: COM Viscosity

The viscosity tests on the Lorillard fuels have been completed, although their validity is in question. Doubt arises from the exceedingly high viscosities of the 50% slurries. This indicates either improper measurement procedure or extremely high viscosities. A study of the literature for operation of the Brookfield viscometer did not reveal any error in procedure. In addition, prior to the viscosity measurements, the instrument was calibrated with two standard liquids. This all points to a highly viscous mixture at 50%.

Figure 1 shows viscosities for the following fuels:

- GM oil: 47% coal weight COM
- Lorillard oil: 50% COM
- Chevron oil & Ptsbg. #8 oil: 30, 35, 40, 50% COM
- PERC oil: 20, 40% COM

Note that the PERC and GM oils are substantially less viscous than the Lorillard and Chevron oils. Also note that the slurries made with the GM and PERC oils are far less viscous than those made with the Chevron oil. This leads one to believe that the viscosity of the mixture may be a strong function of the oil viscosity. Figure 2 plots the ratio of the mixture viscosity to the oil viscosity versus the % coal in the mixture. This figure indicates that the "normalized viscosities" as a function of coal fraction at 150°F are similar for the PERC 20 and 40% COM, the GM 47% and the Chevron 30. 35. and 40% COM. The two points at 50% seem to be extremely high, but this may be due to the coal fraction. According to Brown at GM, the viscosities of the mixtures increased significantly as the coal fraction approached and exceeded 50%. His comments are reflected in the Chevron/Ptsbg. #8 tests showing the 30, 35 and 40% viscosities with uniformly increasing values, while the 50% COM exhibits anomolously high values.

Also shown on Figure 1 are viscosities of the GM oil and Marathon oil mixtures made with the petrolite additive. The GM oil and -200 mesh coal is denoted by PGM 30 and PGM 50 for 30 and 50% COM. The Marathon oil, which is similar in viscosity to the Chevron oil, is denoted MAR 30 and MAR 50. These were also made with -200 mesh coal. Those marked with FN indicate -325 mesh coal. This shows a slight viscosity increase with finer particles.

Conclusions:

- Our viscosity measurements were correct
- Mixture viscosity is a strong function of oil viscosity
- Viscosity of the mixture increases significantly as the coal fraction approaches and exceeds 50%
- Although decreasing particle size increases viscosity, viscosity appears to be only a weak function of particle size
- GM used a #6 oil that was particularly fluid
- The GM 46.6% COM should be questioned

ABS:mmcL

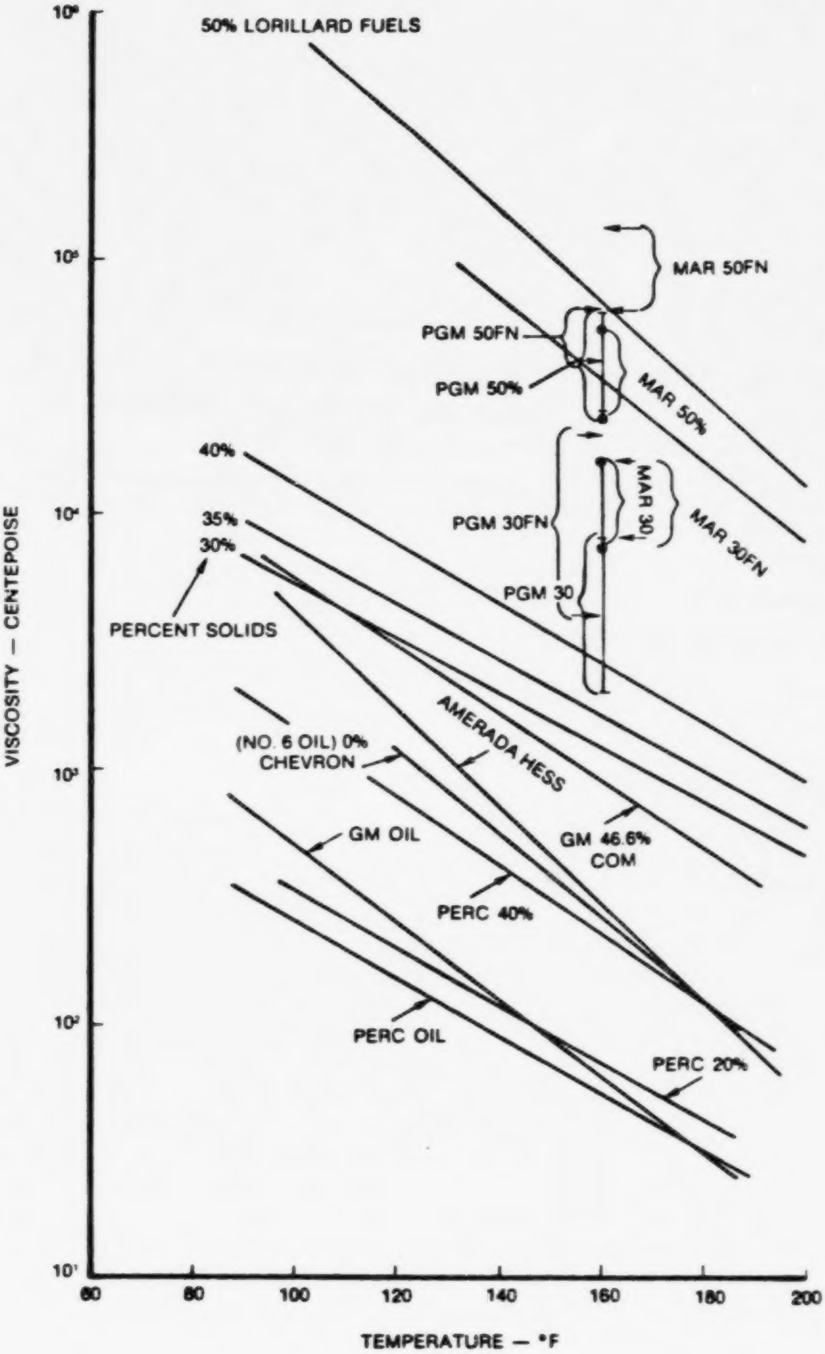

Figure 1. Viscosity of various COM fuels.

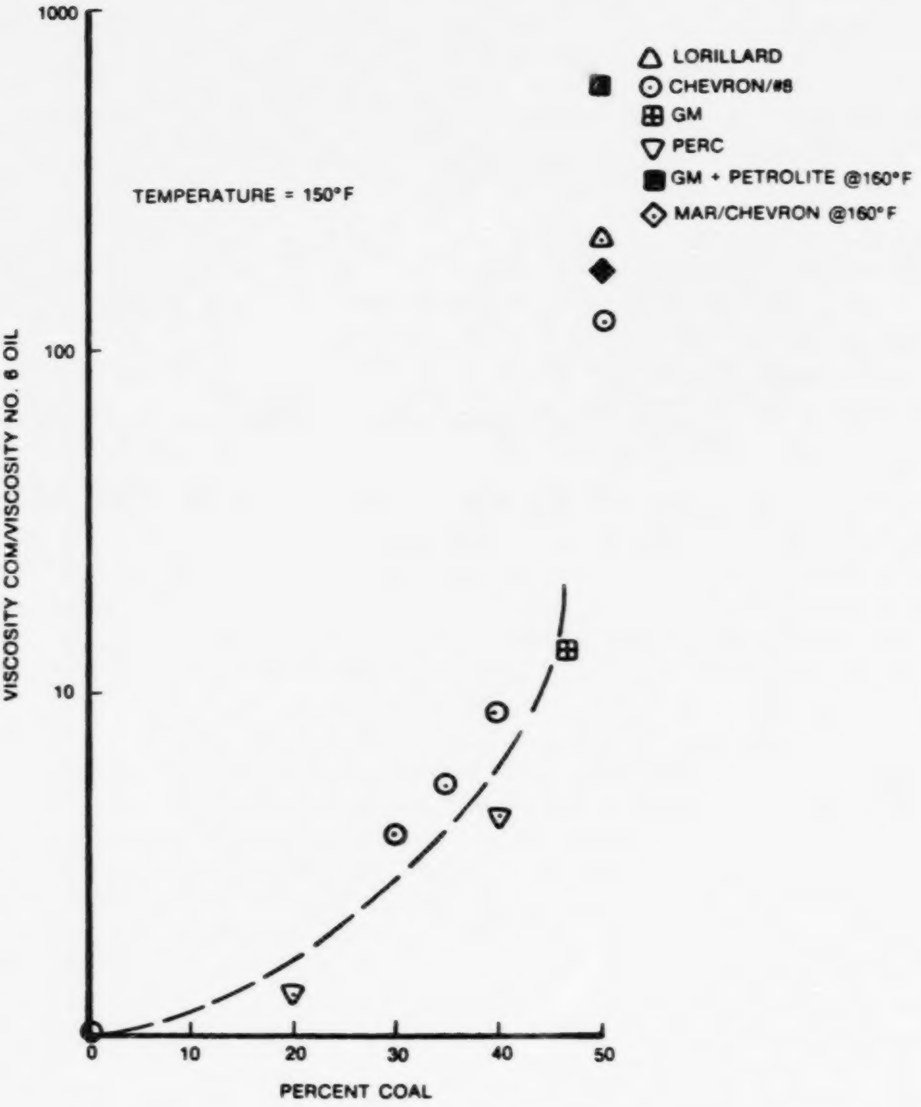

Figure 2. Relative COM viscosity versus coal mixture ratio (percent by weight).